FINITE ELEMENT METHOD FOR
THE STRESS ANALYSIS OF SAW BLADES

THE FINITE ELEMENT METHOD USED FOR THE STRESS ANALYSIS OF A DIAMOND IMPREGNATED CIRCULAR SAW BLADE

by

Moosa Mahomed, B.Sc.(Eng.)

A Thesis
Submitted to the School of Graduate Studies
in Partial Fulfillment of the Requirements
for the Degree
Master of Engineering

McMaster University

July, 1971

MASTER OF ENGINEERING (1971) (Mechanical Engineering)

McMASTER UNIVERSITY Hamilton, Ontario

TITLE: The Finite Element Method Used for the Stress Analysis of a Diamond Impregnated Segmented Circular Saw Blade.

AUTHOR: Moosa Mahomed, B.Sc.(Eng.),(Witwatersrand)

SUPERVISOR: Professor M.C. de Malherbe

NUMBER OF PAGES: vii, 238

SCOPE AND CONTENTS:

Much attention is devoted to the development and testing of four plane stress/strain finite element programs. Two basic programs use three nodal and six nodal triangular elements in conjunction with the method of partitions. Centrifugal force discretization is incorporated in the program. To aid in the study of the stress field contour plots are drawn by computer. Problems of increasing degrees of sophistication are solved using these programs. The problem of special interest is the fatigue stress analysis of a slotted circular saw blade. A theory for the cutting force distribution is developed, and a program for automatic mesh generation is described. Two different slot shapes that may improve the fatigue life of the saw blade are found.

ACKNOWLEDGEMENTS

The author wishes to express his sincere thanks to the following people:

Dr. M.C. de Malherbe for his guidance and supervision,

Dr. B. Young of the Boart Research Laboratory of South Africa for suggesting the problem,

Richie Peppin for his assistance and moral support,

Suzanne Chatland for intelligent typing of the manuscript,

Dr. M.A. Dokainish for his advice, and

the McMaster Computer Center for providing the computing facilities.

TABLE OF CONTENTS

APPENDICES

CHAPTER 1

INTRODUCTION

The finite element method has been used to solve many varied and complex engineering problems. By this method a continuous body is idealized by a number of discrete elements, continous forces are discretized and the problem is then solved by the methods of structural analysis.

The method is especially useful for stress analysis problems which cannot be solved by classical theory. One such problem which is of special interest in this report, concerns the planar stress analysis of a diamond impregnated segmented (or slotted) circular saw blade which is used for the cutting of stone. A detailed description of the saw blade and other factors concerned with stone cutting are provided in Appendix J.

The problem encountered with slotted circular saw blades is that the blades fail due to fatigue cracking at the bases of the slots after prolonged usage. The slot shapes commonly used consist of parallel sides with a semi-circular base. This shape is responsible for high stress concentration.

The aims of this report are two-fold:

(i) To develop a finite element program for plane stress/strain which would have the capacity to solve problems containing large numbers of finite elements, and to adapt the program for use in solving the above problem.

(ii) To perform a qualitative study of the effect of varying slot shapes on the fatigue characteristics of a slotted saw blade, by means of the finite element method. A slot shape that would improve the fatigue life of a saw blade is to be determined.

CHAPTER 2

GENERAL DISCUSSION ON STRESS ANALYSES WITH SPECIAL REFERENCE TO THE FINITE ELEMENT METHOD

2.1. Classical Theory:

It is generally known that classical elastic theory for the solution of displacement and stress field problems is limited only to very simple structures. These are available in close form solutions to the governing differential equations. Unfortunately, the majority of practical design problems do not fall into the categories of these simplified problems because of irregular boundaries and complex boundary conditions.

The traditional approach is then to establish a simplified and idealized model of the real structure, for which a closed solution is available, and apply the solution with proper interpretation. It is obvious that the traditional methods are highly inaccurate, and where safety and efficiency are important a more accurate method has to be found.

Apparently, the design of slotted circular saw blades follow this traditional approach, which relies on the experience of the designer. A greater accuracy is, however, required because of the need to establish the fatique strength levels of the saw. Therefore, it is necessary to use a method of stress analysis capable of predicting the stress concentrations accurately so that fatique failures may be countermanded.

Methods that meet the above requirements are the matrix methods.

2.2. Matrix Methods:

These are numerical methods and can be divided into two types: (i) numerical solutions of differential equations for displacements or stresses, and (ii) matrix methods based on discrete-element idealization.

The Finite Difference Methods fall into the first category and the Finite Element Methods into the second category.

In both types of methods, the field to be analysed is sub-divided by a mesh into finite sized elements and a simple law of variation of the values of characteristic parameters from node to node is assumed. In both cases, again, the results are obtained by solving a large set of linear equations by matrix methods.[1]

The basic equations are, in the case of Solid Mechanics, the equations of equilibrium, compatibility and stress-strain (or force-deformation).

In Finite Difference Methods the basic equations are applied to an infinitesimal element yielding a system of partial differential equations which hold for the whole field. These are subsequently replaced by finite difference approximations relating to the mesh. Thus, the approximations are essentially of a mathematical nature and arise from the truncation of a series.

In the Finite Element Method the basic equations are applied directly to each element and the approximations have a simple physical interpretation. This results in two advantages:

a. The engineer can keep close contact with the physical aspects of the problem and has greater control over the degree of accuracy required of the solution.

b. Each element can, theoretically, have different properties. The Finite Element Method can handle with relative ease non-homogeneous or mixed regime (e.g., elastic-plastic) fields. In the Finite Difference Methods discontinuities across boundaries of different regions would normally raise difficult computational problems.

Experience has shown that the Finite Element Method converges more rapidly than the Finite Difference Methods, i.e. the Finite Element Method can yield fairly accurate results when the mesh is still quite coarse. This is an important economic consideration.

2.3. The Finite Element Methods:

There are two Finite Element Methods:

(i) the displacement method (or stiffness method) where displacements are chosen as the basic unknowns, and

(ii) the force method (or flexibility method) where forces are the basic unknowns.

In reference [6], Argyris has developed the general theory with both forces and displacements as unknowns. The striking feature which emerges is that the two methods are completely analogous. Knowing the equations in either of the two procedures, one can write down, by a translation process, the equations of the other procedure. There does exist, however, significant differences in the detailed application of the methods.

Much of the early work on aircraft structures [5] was devoted to the first method, probably as a result of the extensive work of Argyris [6,10]. Taig and Kerr [7] have shown that displacement techniques are particularly well suited to the analysis of multicell box structures. In their application to plate and shell problems, research workers, in general, choose to exploit the displacement method. It has been shown by Hassel [8], however, that linear static plate and shell problems can be analysed successfully by the force method which is the technique adopted by Denke [9] in his analysis of non-linear static problems. The displacement method is used in this dissertation, and any reference to the Finite Element Method implies the displacement method.

A body, such as a plate, may be thought of as an internally statically indeterminate structure with infinite degrees of freedom. The first step in the Finite Element Method is to idealize the actual continuous body to a discrete-element mathematical model, which consequently has a finite number of degrees of freedom.

The model is obtained by replacing the body by a number of triangular (or otherwise) shaped elements. This model closely resembles the original body. The elements are separated by fictitious boundaries and adjacent elements are connected at common points at the vertices, which are called "nodal points" or "nodes". The elements do not interact along the fictitious boundaries and behave like members of a truss. In the case of plane stress/strain a node has two degrees of freedom, namely, the two orthogonal displacements.

The idealized model is then analysed in a manner which is in principle identical to the well-known displacement method (or slope deflection method) of frame analysis.

The Finite Element Method requires the solution of the following two main problems:

a. the element analysis, and

b. the system analysis.

The element analysis involves:

(i) The selection of functions which uniquely describe the displacements within the elements in terms of the nodal point displacements.

The displacement function thus defines uniquely the state of strain within an element in terms of the nodal displacements.

(ii) Knowing the elastic properties of the material the state of stress throughout an element can be found.

(iii) The derivation of fictitious nodal point forces which equilibrate the distributed boundary stresses and/or distributed loads.

The element analysis provides a relation between nodal point forces and nodal point displacements, expressed in terms of an element stiffness matrix. This matrix defines the properties of the element.

For elements to be conforming* the displacement function must be chosen such that compatibility is maintained along the entire length of the common boundary between adjacent elements.

In order to find the properties of the whole structure, the properties of the individual elements are assembled such that overall equilibrium of the structure is satisfied. The assembled matrix is known as the 'overall stiffness matrix'. By the reciprocal theorem, this matrix should be symmetric. The nodal forces are related to the nodal displacements by the overall stiffness matrix.

The conditions of equilibrium of the nodes may be shown to yield a displacement field corresponding to minimum potential energy for the selected displacement pattern. As in

---

* Elements which do not give rise to discontinuities between displacements of adjacent elements. Conforming elements give a lower bound to the strain energy.

the Ritz method the solution will generally be approximate. The analysis tends to yield a structure which is stiffer than the real one, due to the restraints which are introduced when selecting the displacement pattersn inside the elements. (This is true only for conforming elements).

2.4. Structural Idealization:

It is apparent at this stage that the closer the finite element idealization fits the real structure, the closer the solution will be to the real solution.

In areas where high stress gradients occur, it is necessary to use a much finer mesh because a series of piecewise displacement functions would approximate a steep gradient better than just one. Usually these high stress gradients occur due to stress concentrations and would anyway necessitate a finer mesh to fit the physical boundary.

2.5. Boundary Conditions:

It is possible to load the structure at the nodal points by concentrated loads. Equivalent nodal forces are calculated to equilibrate any distributed boundary loads or body forces (such as centrifugal forces) using the virtual work theorem. More details are given in Chapters 4 and 5.

It is also possible to apply prescribed displacements. As a matter of fact, it is necessary to have enough prescribed displacements to prevent rigid body rotation and translation. The basic overall stiffness matrix is singular and a number of rows and columns have to be eliminated for the system of equations to be solved.

2.6. Element Types for Plane Stress:

The element that has hitherto been in vogue is the three nodal plane stress triangle, commonly known as the TRIM3 element.

This element has the following properties:

(i) linear displacement distribution within element

(ii) constant stress within element

(iii) a total of six degrees of freedom, i.e., two displacements at each node.

For this type of element there is displacement continuity from element to element, but there is a discontinuity of stress from element to element, with the result that the actual stress field is approximated by a series of steps, like a histogram. It is evident that in cases of steep stress gradients this element is only useful if the region is covered by a very fine mesh of elements.

In such cases, it may be better to resort to improved elements. Holand [2] describes a number of improved plane stress elements which are obtained either by increasing the number of degrees of freedom per node, or by increasing the number of nodes per element.

The element of interest is the 6-nodal plane stress triangular element, commonly known as the TRIM6 element. This element has a node on each side in addition to the nodes at the vertices. The additional nodes are stationed mid-way between vertices so that they may be generated by computer. This element has a total of twelve degrees of freedom and the displacement distribution within an element is a second degree polynomial. This polynomial satisfies compatibility across the element boundaries.

This element is superior to the TRIM3 element in that the stress distribution within an element is now linear, meaning that the stress field is now approximated by a series of linear functions. However, stresses are still discontinuous at the element boundaries, but the discontinuity is less severe than the TRIM3 element.

CHAPTER 3

MATHEMATICAL BACKGROUND

3.1. General:

The mathematics of both the TRIM3 and TRIM6 elements are developed in this chapter. The TRIM3 element is explained in previous references [2,3,4,11] and for completeness the theory will be developed in section 3.3. with particular reference to the problem at hand and to the subsequent computer programs. The TRIM6 element was introduced by Argyris [12] and is discussed by Zienkiewicz [3] and Holand [2]. However, not much attention is devoted to the mathematics in these references. The mathematics of this element is developed in section 3.4. In the next section, a general formula for the element stiffness matrix is derived in matrix notation, and is applicable to any plane stress or plane strain element.

Sections 3.3. and 3.4. constitute the element analysis. The system analysis, in which the element stiffness mttrices are assembled, is done in section 3.5. A rectangular cartesian co-ordinate system is used throughout.

3.2. General Formulation for Element Stiffness:

Let the displacements at a point within an element e be defined as a column vector $\{f\}$, and $\{\delta\}$ be a column vector representing nodal displacements. The displacements of the internal point can be interpolated from the nodal displacements of the element as follows:

$$\{f\} = [N]\{\delta\}^e \tag{3.1}$$

where matrix N is known as the interpolation matrix and superscript e denotes displacements of element e. For plane stress,

$$\{f\} = \begin{Bmatrix} u \\ v \end{Bmatrix} \tag{3.2}$$

where u and v are the displacement components in the x and y directions, respectively. Matrix N is dependent only on the nodal co-ordinates of element e.

For a TRIM3 element,

$$\{\delta\}^e = [\delta_i|\delta_j|\delta_m]^* = [u_iv_i|u_jv_j|u_mv_m] \tag{3.3}$$

where δ_i is the displacement of node i.

For a TRIM6 element,

$$\{\delta\}e = [\delta_i|\delta_j|\delta_k|\delta_l|\delta_m|\delta_n] \tag{3.4}$$

The subscripts denote the nodes of the element.

Strains at the internal point referred to in equation (3.1) can be obtained from the linear strain-displacement relations.

$$\{\varepsilon\} = [\varepsilon_x|\varepsilon_y|\varepsilon_{xy}] = [\frac{\partial u}{\partial x} | \frac{\partial v}{\partial y} | \frac{\partial u}{\partial y} + \frac{\partial v}{\partial x}] \tag{3.5}$$

By differentiating equation (3.1) as required by equation (3.5),

---

* In order to save space, a column vector is written as a row matrix with square brackets.

the following can be written,

$$\{\varepsilon\} = [B]\ \{\delta\}^e \tag{3.6}$$

where B is called the strain-displacement matrix.

Knowing the material properties, stresses at the interior point can now be related to the strains. The stress-strain relation is

$$\{\sigma\} = [D]\ \{\varepsilon\} \tag{3.7}$$

where $\{\sigma\} = [\sigma_x | \sigma_y | \tau_{xy}]$ and D is the elasticity matrix, obtained from the basic stress-strain relations of elasticity,

$$[D] = \frac{E}{1 - \nu^2} \begin{bmatrix} 1 & \nu & 0 \\ \nu & 1 & 0 \\ 0 & 0 & (1-\nu)/2 \end{bmatrix} \tag{3.8}$$

E is Young's modulus and ν is Poisson's ratio. Equation (3.8) holds for an isotropic material in plane stress.

Let column vector F represent equivalent forces on the nodes of element e. These forces are fictitious forces set up to equilibrate internal stresses and/or body forces distributed over the element. This 'discretization' of the distributed loading is a necessary feature of the finite element method, and it is here that the infinite degrees of freedom of a continuous system is reduced to a finite number of degrees of freedom. It may be visualized that as the number of finite elements approach infinity the continuity of the system is restored.

For the TRIM3 element the force vector is,

$$\{F\}^e = [F_i | F_j | F_m] \tag{3.9a}$$

and for the TRIM6 element the vector is,

$$\{F\}^e = [F_i | F_j | F_k | F_l | F_m | F_n] \tag{3.9b}$$

Here $$\{F_i\} = \begin{Bmatrix} F_{ix} \\ F_{iy} \end{Bmatrix} = \begin{Bmatrix} \text{Force in x-direction at node i} \\ \text{Force in y-direction at node i} \end{Bmatrix} \tag{3.9c}$$

Let $\{p\} = \begin{Bmatrix} p_x \\ p_y \end{Bmatrix}$ be the body forces per unit volume of material acting on the system. These may be either centrifugal forces or gravity forces or both.

The equivalent nodal forces may be found by isolating an element (e) as a free body as in Fig. 3.1 and satisfying the equations of equilibrium. It is well known that the theorem of virtual work is an indirect statement of equilibrium and is easy to apply to the equilibrium of an element.

If a virtual displacement is applied at the element nodes, then by the virtual work theorem:

Work done by nodal forces + work done by distributed loads = work done by internal stresses

For the TRIM3 element, the virtual displacements are written vectorially as,

$$\{\delta^v\}^e = [\delta_i^v | \delta_j^v | \delta_m^v]$$

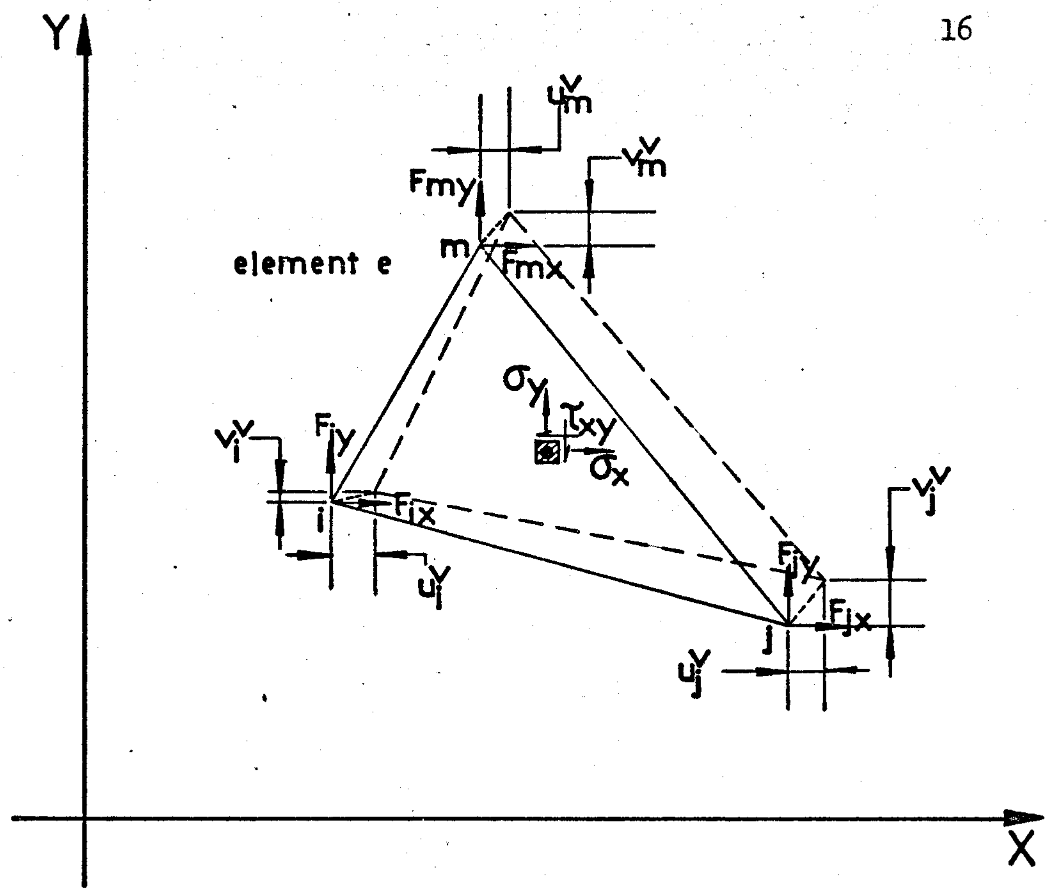

FIG. 3.1 Displacements of a TRIM3 Element Due to Virtual Dispalcements and Internal Stresses.

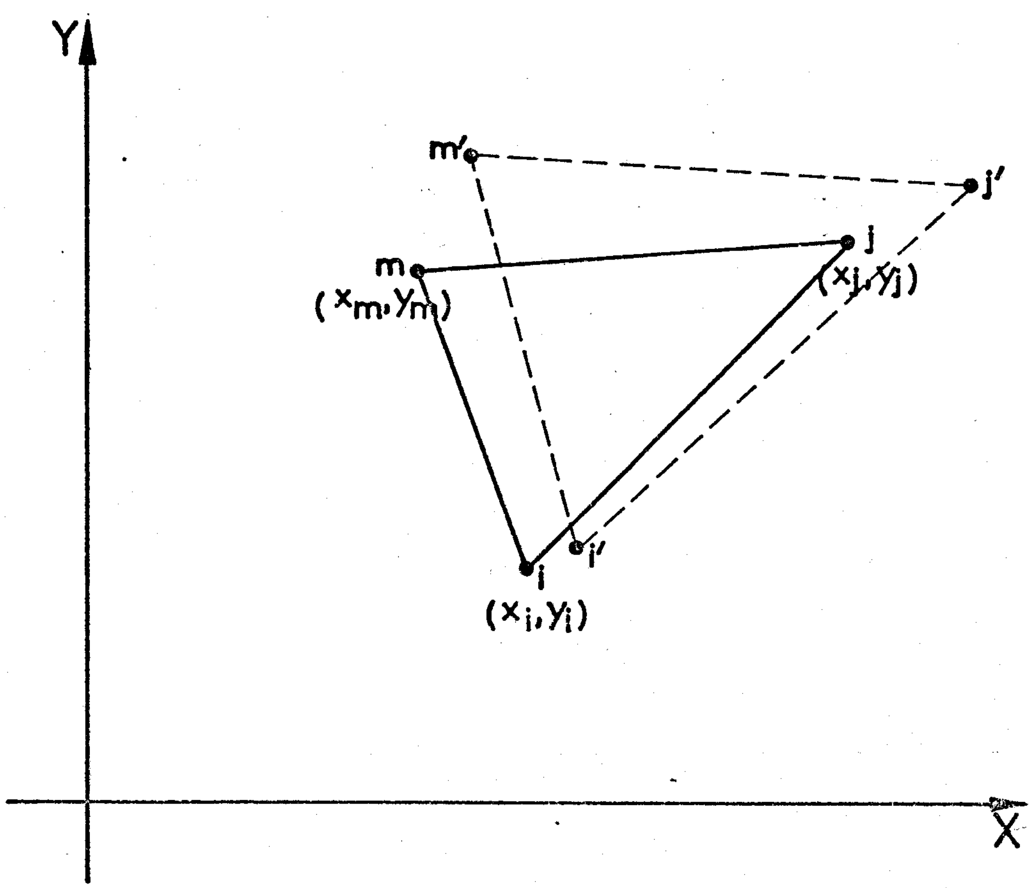

FIG. 3.2 TRIM3 Plane Stress/Strain Element and Allowed Deformation Pattern.

The virtual displacements, nodal forces and stresses at some internal point are shown in Fig. 3.1.

The work done by the nodal forces due to the virtual displacements is,

$$W_E = \{\delta^v\}^{e^T} \cdot \{F\}^e \qquad (3.10)$$

The work done per unit volume by the distributed loading is,

$$dW_D = \{f^v\}^T \cdot \{p\}$$

$$= \{\delta^v\}^{e^T} [N]^T \{p\} \quad \text{from equation (3.1)} \qquad (3.11)$$

The total work done by the distributed loading is, by integration,

$$W_D = \int_{vol} \{\delta^v\}^{e^T} [N]^T \{p\}.d(Vol)$$

$$= \{\delta^v\}^{e^T} \int_{vol} [N]^T \{p\} \, t \, dxdy \qquad (3.12)$$

for a 2-dimensional system, where t is the element thickness, and (t dx dy) is the element volume. Since δ^v is not a function of x and y it is factored out.

The work done per unit volume by the internal stresses is,

$$dW_I = \{\varepsilon^v\}^T \{\sigma\}$$

$$= \{\sigma^v\}^{e^T} [B]^T \{\sigma\} \quad \text{from equation (3.6)} \qquad (3.13)$$

and, therefore, total work done by internal stresses is,

$$W_I = \{\sigma^v\}^{e^T} \int_{vol} [B]^T \{\sigma\} \, t \, dx \, dy \qquad (3.14)$$

By the theorem of virtual work

$$W_E + W_D = W_I$$

The common factor $\{\delta^v\}^{e^T}$ may be eliminated from equations (3.10), (3.12) and (3.14) and the above relation becomes,

$$\{F\}^e + \int [N]^T \{p\} \, t \, dx \, dy$$

$$= \int [B]^T \{\sigma\} \, t \, dx \, dy \qquad (3.16)$$

(from equations (3.7) and (3.6))

Thus equation (3.16) reads as,

$$\{F\}^e = \left(\int [B]^T [D][B] \, t \, dx \, dy \right) \{\delta\}^e - \int [N]^T \{p\} \, t \, dx \, dy$$

or,

$$\{F\}^e = [k]^e \{\delta\}^e + \{F\}_p^e \qquad (3.17)$$

where the element stiffness matrix is defined as

$$[k]^e = \int [B]^T [D][B] \, t \, dx \, dy \qquad (3.18)$$

The equivalent nodal forces due to the distributed loading are,

$$\{F\}_p^e = - \int [N]^T \{p\} \, t \, dx \, dy \qquad (3.19)$$

Notes:

(i) Equation (3.19) is a consistent method of discretizing distributed loads.

(ii) Virtual displacements applied at the nodes are different from nodal displacements, because nodal displacements are as a result of the interaction of all the elements which in turn react to the applied loading. In equation (3.15) nodal displacements are used because the element e (Fig. 3.1) is isolated with an already-existent stress which is related to the nodal displacements by this equation.

(iii) Equation (3.17) satisfies equilibrium of an element. To satisfy overall equilibrium of the system, the fictitious forces defined by this equation are to be summed over all elements and equated to the external loading at the nodes. The overall stiffness matrix is obtained in this way, and the procedure is known as the system analysis.

3.3. Element Analysis of the TRIM3 Element:

3.3.1. Displacement Function

Having two degrees of freedom per node, the TRIM3 element has a total of 6 degrees of freedom. If the displacements in the two directions are denoted by u and v respectively, then two polynomials having three constants each may be assumed for u and v respectively, namely,

$$u = \alpha_1 + \alpha_2 x + \alpha_3 y \tag{3.20}$$

$$v = \alpha_4 + \alpha_5 x + \alpha_6 y \tag{3.21}$$

These are linear functions of x and y and it means that the straight edges of the triangle remain straight after deformation. The deformation pattern implied is shown in Fig. 3.2.

The interpolation matrix of equation (3.1) is obtained by substituting the nodal displacements and co-ordinates of the three nodes in the above equations and solving for the α's in terms of the nodal displacements. Zienkiewicz [3] does a manual manipulation of the equations and obtains the following relation for N in submatrix notation,

$$[N] = [\mathrm{IN}_i' | \mathrm{IN}_j' | \mathrm{IN}_m'] \tag{3.22}$$

where I is a (2 x 2) identity matrix and

$$N_i' = (a_i + b_i x + c_i y)/2\Delta$$

$$N_j' = (a_j + b_j x + c_j y)/2\Delta \qquad (3.23)$$

$$N_m' = (a_m + b_m x + c_m y)/2\Delta$$

$$a_i = x_j y_m - x_m y_j \quad ; \quad a_j = x_m y_i - x_i y_m \quad ; \quad a_m = x_i y_j - x_j y_i$$

$$b_i = y_j - y_m \quad ; \quad b_j = y_m - y_i \quad ; \quad b_m = y_i - y_j$$

$$c_i = x_m - x_j \quad ; \quad c_j = x_i - x_m \quad ; \quad c_m = x_j - x_i \qquad (3.24)$$

$$\Delta = \frac{1}{2}\begin{vmatrix} 1 & x_i & y_i \\ 1 & x_j & y_j \\ 1 & x_m & y_m \end{vmatrix} = \text{area of triangle} \qquad (3.25)$$

If the local co-ordinate system is located at the element centroid, then

$$x_i + x_j + x_m = 0$$

$$y_i + y_j + y_m = 0 \qquad (3.26)$$

$$a_i = a_j = a_m = 2\Delta/3$$

For the displacement functions assumed compatibility between adjacent elements is always satisfied because the displacements vary linearly along any side of a triangle and, with identical displacements imposed at the nodes, the same displacement will clearly exist all along an interface.

3.3.2. Strain-displacement Matrix

Equations (3.5) and (3.6) define the strain-displacement matrix B. By differentiating equation (3.22) as required by equation (3.5) the matrix B is found to be

$$[B] = \frac{1}{2\Delta} \begin{bmatrix} b_i & 0 & b_j & 0 & b_m & 0 \\ 0 & c_i & 0 & c_j & 0 & c_m \\ c_i & b_i & c_j & b_j & c_m & b_m \end{bmatrix} \quad (3.27)$$

In submatrix notation,

$$[B] = [B_i | B_j | B_m] \quad (3.28)$$

The submatrices may be inferred from equation (3.27).

All the terms in the strain-displacement matrix are constant, meaning that the strains within an element are constant.

The stress matrix is defined by equation (3.15) and since D is constant, stresses with an element are constant. Since stresses differ from element to element in general, the stress field is approximated by a series of jumps.

3.3.3. Element Stiffness Matrix for TRIM3 Element

Basically,

$$[k]^e = \int [B]^T [D][B] \, t \, dx \, dy$$

Since D and B are constant matrices they may be factored from the integral sign. Then,

$$[k]^e = [B]^T[D][B]\ t \int dxdy = [B]^T[D][B]\ t\ \Delta \qquad (3.29)$$

where is the area of the element found by equation (3.25).

In submatrix notation, the element stiffness matrix is written as,

$$[k]^e = \begin{bmatrix} k_{ii} & k_{ij} & k_{im} \\ k_{ji} & k_{jj} & k_{jm} \\ k_{mi} & k_{mj} & k_{mm} \end{bmatrix} \qquad (3.30)$$

The subscripts i,j,m are the nodal numbers of the triangle. (see Fig. 3.2). Each of the k terms is a (2 x 2) submatrix. Hence, the element stiffness matrix is a (6 x 6) matrix.

An individual (2 x 2) submatrix may be obtained from the following formula,

$$k_{ln} = B_l^T \quad D \quad B_n$$

$$l = i,j,m \qquad (3.31)$$

$$n = k,j,m$$

A description of the finite element program using TRIM3 elements is given in Chapter 6 and a program listing is given in Appendix E.

3.4. Element Analysis of the TRIM6 Element:

3.4.1. Displacement Function

The TRIM6 triangular element has three nodes stationed on each side in addition to the three nodes at the vertices of the triangle. The former may be anywhere along the sides, but are assumed to be midside for this analysis. This assumption facilitates input data to the computer program as only the co-ordinates of the vertices are necessary. For this reason, too, the nodes are numbered as shown in Fig. 3.3, i.e. in the form of a counter-clockwise spiral starting at the vertices.

The displacements of a point within an element are written in terms of the displacements of six nodes. This allows the choice of a higher order polynomial in x and y to approximate the displacement field.

In total there are twelve degrees of freedom per element. The u and v displacements can each be written in terms of six constants, hence a full quadratic expansion in x and y can be used. The displacement functions are:

$$u = \alpha_1 + \alpha_2 x + \alpha_3 y + \alpha_4 x^2 + \alpha_5 xy + \alpha_6 y^2 \qquad (3.32)$$

$$v = \alpha_7 + \alpha_8 x + \alpha_9 y + \alpha_{10} x^2 + \alpha_{11} xy + \alpha_{12} y^2 \qquad (3.33)$$

Fig. 3.3 shows the original and deformed shape of the element; it can be seen that the additional degrees of freedom allow the element to deform in a more realistic manner. Along a side such as ilk in Fig. 3.3 y is a function of x. Say,

$$y = ax + b \tag{3.34}$$

Thus, the variation of u along ilk is found by the substitution of equation (3.34) in equation (3.32),

$$u = (\alpha_1 + \alpha_3 b + 2\alpha_6 ab + \alpha_6 b^2)$$

$$+ (\alpha_2 + \alpha_3 a + \alpha_5 b)x + (\alpha_4 + \alpha_5 a + \alpha_6 a^2)x^2$$

By lumping the constants, the above equation reads as

$$u = c + dx + ex^2 \tag{3.35}$$

Equation (3.35) shows that displacements vary parabolically along a side. The constants c,d and e in equation (3.35) may be found by substitution of the x-co-ordinates of the three nodes on the side ilk. Since the nodes of the adjacent elements are coincident on this side, the same parabola is defined by both the adjacent elements. Compatibility is thus always satisfied, and adjacent elements never separate during deformation according to the assumed displacement function.

Since the variation of stress within an element is one degree less than the degree of the displacement function, stress varies linearly within an element.

In matrix notation, equations (3.32) and (3.33) are:

$$\{f\} = \begin{Bmatrix} u \\ v \end{Bmatrix} = \begin{bmatrix} 1 & x & y & x^2 & xy & y^2 & 0 & 0 & 0 & 0 & 0 & 0 \\ 0 & 0 & 0 & 0 & 0 & 0 & 1 & x & y & x^2 & xy & y^2 \end{bmatrix} \begin{Bmatrix} \alpha_1 \\ \alpha_2 \\ \alpha_3 \\ , \\ , \\ \alpha_{12} \end{Bmatrix} \tag{3.36}$$

of

$$\{f\}^e = [R]\ \{\alpha\}^e \tag{3.37}$$

A relation between the coefficients, α, and the element nodal displacements is obtained by substituting the nodal displacements and co-ordinates in equations (3.32) and (3.33). This yields, in matrix notation:

$$
\begin{Bmatrix} u_i \\ v_i \\ u_j \\ v_j \\ u_k \\ v_k \\ u_l \\ v_l \\ u_m \\ v_m \\ u_n \\ v_n \end{Bmatrix}
=
\begin{bmatrix}
1 & x_i & y_i & x_i^2 & x_iy_i & y_i^2 & 0 & 0 & 0 & 0 & 0 & 0 \\
0 & 0 & 0 & 0 & 0 & 0 & 1 & x_i & y_i & x_i^2 & x_iy_i & y_i^2 \\
1 & x_j & y_j & x_j^2 & x_jy_j & y_j^2 & 0 & 0 & 0 & 0 & 0 & 0 \\
0 & 0 & 0 & 0 & 0 & 0 & 1 & x_j & y_j & x_j^2 & x_jy_j & y_j^2 \\
1 & x_k & y_k & x_k^2 & x_ky_k & y_k^2 & 0 & 0 & 0 & 0 & 0 & 0 \\
0 & 0 & 0 & 0 & 0 & 0 & 1 & x_k & y_k & x_k^2 & x_ky_k & y_k^2 \\
1 & x_l & y_l & x_l^2 & x_ly_l & y_l^2 & 0 & 0 & 0 & 0 & 0 & 0 \\
0 & 0 & 0 & 0 & 0 & 0 & 1 & x_l & y_l & x_l^2 & x_ly_l & y_l^2 \\
1 & x_m & y_m & x_m^2 & x_my_m & y_m^2 & 0 & 0 & 0 & 0 & 0 & 0 \\
0 & 0 & 0 & 0 & 0 & 0 & 1 & x_m & y_m & x_m^2 & x_my_m & y_m^2 \\
1 & x_n & y_n & x_n^2 & x_ny_n & y_n^2 & 0 & 0 & 0 & 0 & 0 & 0 \\
0 & 0 & 0 & 0 & 0 & 0 & 1 & x_n & y_n & x_n^2 & x_ny_n & y_n^2
\end{bmatrix}
\begin{Bmatrix} \alpha_1 \\ \alpha_2 \\ \alpha_3 \\ \alpha_4 \\ \alpha_5 \\ \alpha_6 \\ \alpha_7 \\ \alpha_8 \\ \alpha_9 \\ \alpha_{10} \\ \alpha_{11} \\ \alpha_{12} \end{Bmatrix}
\tag{3.38}
$$

By naming the (12 x 12) matrix C_T, the above equation is condensed to:

$$\{\delta\}^e = [C_T]\ \{\alpha\}^e \tag{3.39}$$

With the aid of equations (3.37) and (3.39) it is now possible to find the interpolation matrix N.

The coefficients, α, are determined by inversion,

$$\{\alpha\}^e = [C_T]^{-1}\ \{\delta\}^e \tag{3.40}$$

Substituting this into equation (3.37) yields,

$$\{f\} = [R][C_T]^{-1}\ \{\delta\}^e \tag{3.41}$$

and by comparison with equation (3.1) N is seen to be equal to the pre-multiple of δ, i.e.

$$[N] = [R][C_T]^{-1} \tag{3.42}$$

Matrix C_T is a (12 x 12) matrix, but in order to save computational effort of inverting the full matrix, it may be modified so that the inversion of only a (6 x 6) matrix is necessary. Because of the similarity of the sets of equations for u and v (see equation 3.38), the equations for u and v are separated as follows,

$$\{u\} = [c]\ \{\alpha_u\} \tag{3.43}$$

where

$$[C] = \begin{bmatrix} 1 & x_1 & y_1 & x_1^2 & x_1y_1 & y_1^2 \\ 1 & x_2 & y_2 & \text{etc.} & & \\ 1 & \text{etc.} & & & & \\ 1 & & & & & \\ 1 & & & & & \\ 1 & & & & & \end{bmatrix} \quad \text{and } \{\alpha_u\} = \begin{matrix} \alpha_1 \\ \alpha_2 \\ \cdot \\ \cdot \\ \cdot \\ \alpha_6 \end{matrix} \qquad (3.43a)$$

It is seen that the same matrix C applies to the u-displacements, viz,

$$\{v\} = [C]\{\alpha_v\} \qquad \text{where} \qquad \{\alpha_v\} = [\alpha_7, \alpha_8, \ldots \alpha_{12}]$$

By proper manipulation of the terms in the inverse of C, the inverse of C_T is found. The correspondence is as follows:

$$[C_T]^{-1} = \left[\begin{array}{cc|cc|cc|cc|cc|cc}
C^{-1}_{11} & 0 & C^{-1}_{12} & 0 & C^{-1}_{13} & 0 & C^{-1}_{14} & 0 & C^{-1}_{15} & 0 & C^{-1}_{16} & 0 \\
C^{-1}_{21} & 0 & C^{-1}_{22} & 0 & C^{-1}_{23} & 0 & C^{-1}_{24} & 0 & C^{-1}_{25} & 0 & C^{-1}_{26} & 0 \\
C^{-1}_{31} & 0 & C^{-1}_{32} & 0 & C^{-1}_{33} & 0 & C^{-1}_{34} & 0 & C^{-1}_{35} & 0 & C^{-1}_{36} & 0 \\
C^{-1}_{41} & 0 & C^{-1}_{42} & 0 & C^{-1}_{43} & 0 & C^{-1}_{44} & 0 & C^{-1}_{45} & 0 & C^{-1}_{46} & 0 \\
C^{-1}_{51} & 0 & C^{-1}_{52} & 0 & C^{-1}_{53} & 0 & C^{-1}_{54} & 0 & C^{-1}_{55} & 0 & C^{-1}_{56} & 0 \\
C^{-1}_{61} & 0 & C^{-1}_{62} & 0 & C^{-1}_{63} & 0 & C^{-1}_{64} & 0 & C^{-1}_{65} & 0 & C^{-1}_{66} & 0 \\
\hline
0 & C^{-1}_{11} & & & & & & & & & & \\
0 & C^{-1}_{21} & & & & & & & & & & \\
0 & C^{-1}_{31} & & & \multicolumn{6}{c}{\text{(analogous to above terms)}} & & \\
0 & C^{-1}_{41} & & & & & & & & & & \\
0 & C^{-1}_{51} & & & & & & & & & & \\
0 & C^{-1}_{61} & & & & & & & & & &
\end{array}\right] \tag{3.44}$$

The matrix may be sectioned into submatrices so that,

$$[C_T]^{-1} = [C_1, C_2, C_3, C_4, C_5, C_6]$$

where C_r is a (12 x 2) submatrix. The negative one superscript in equation (3.44) signifies the terms of C inverse.

3.4.2. Strain-displacement Matrix

Strains are functions of the partial derivatives of the displacement functions as defined by equation (3.5). The implied differentiations yield,

$$\{\varepsilon\} = \begin{Bmatrix} \varepsilon_x \\ \varepsilon_y \\ \varepsilon_{xy} \end{Bmatrix} = \begin{bmatrix} 0 & 1 & 0 & 2x & y & 0 & 0 & 0 & 0 & 0 & 0 & 0 \\ 0 & 0 & 0 & 0 & 0 & 0 & 0 & 0 & 1 & 0 & x & 2y \\ 0 & 0 & 1 & 0 & x & 2y & 0 & 1 & 0 & 2x & y & 0 \end{bmatrix} \begin{Bmatrix} \alpha_1 \\ \alpha_2 \\ \alpha_3 \\ \vdots \\ \alpha_{12} \end{Bmatrix} \qquad (3.45)$$

Condensing,

$$\{\varepsilon\} = [Q]\ \{\alpha\} \qquad (3.46)$$

and by substitution of α from equation (3.40) the required strain-displacement relation is found:

$$\{\varepsilon\} = [Q]\ [C_T^{-1}]\ \{\delta\}^e \qquad (3.47)$$

and by comparison with equation (3.6), the strain-displacement matrix is,

$$[B] = [Q][C_T^{-1}] \qquad (3.48)$$

Note:

While C_T^{-1} is a constant matrix, Q contains linear functions of x and y. From equation (3.47) it can be concluded that strains within an element are linearly proportional to the nodal displacements of the element. Also, for an elastic medium, stresses are linear within an element.

3.4.3. Element Stiffness Matrix for TRIM6 Element

In general, the stiffness matrix of an element is defined as,

$$[k] = \int [B]^T [D][B] \; t \; dx \; dy \qquad (3.18)$$

Matrix B is a linear function of x and y and may not be removed from the integral sign, as was the case with the TRIM3 element. Manual multiplication of the matrices and subsequent explicit integration is thus necessary.

Substitution for B in equation(3.18) from equation (3.48) gives,

$$[k] = \int [C_T^{-1}][Q]^T[D][Q][C_T^{-1}] \; t \; dx \; dy \qquad (3.49)$$

By factoring the coefficient matrices, k is written as,

$$[k] = [C_T^{-1}][P][C_T^{-1}] \qquad (3.50)$$

where

$$[P] = \int [Q]^T[D][Q] \; t \; dx \; dy \qquad (3.51)$$

Manual miltiplication of the triple product under the integral sign yields a (12 x 12) symmetric matrix, the lower triangle of which is written below,

[P] = integral over element volume of

$$
\begin{bmatrix}
0 & & & & & & & & & & & \\
0 & D_{11} & & & & & & & & & & \\
0 & D_{31} & D_{33} & & & & & & & & & \\
0 & 2D_{11}x & 2D_{13}x & 4D_{11}x^2 & & & & & & \text{(SYMMETRIC)} & & \\
0 & D_{11}y+D_{31}x & D_{13}y+D_{33}x & 2D_{11}xy+2D_{31}x^2 & D_{11}y^2+D_{33}x^2+2D_{31}xy & & & & & & & \\
0 & 2D_{31}y & 2D_{33}y & 4D_{31}xy & 2D_{31}y^2+2D_{33}xy & 4D_{33}y^2 & & & & & & \\
0 & 0 & 0 & 0 & 0 & 0 & 0 & & & & & \\
0 & D_{31} & D_{33} & 2D_{31}x & D_{31}y+D_{33}x & 2D_{33}y & 0 & D_{33} & & & & \\
0 & D_{21} & D_{23} & 2D_{21}x & D_{21}y+D_{23}x & 2D_{23}y & 0 & D_{23} & D_{22} & & & \\
0 & 2D_{31}x & 2D_{33}x & 4D_{31}x^2 & 2D_{31}xy+2D_{33}x^2 & 4D_{33}xy & 0 & 2D_{33}x & 2D_{32}x & 4D_{33}x^2 & & \\
0 & D_{21}x+D_{31}y & D_{23}x+D_{33}y & 2D_{21}x^2+2D_{31}xy & D_{23}x^2+D_{31}y^2+(D_{21}+D_{33})xy & 2D_{23}xy+D_{33}y^2 & 0 & D_{23}x+D_{33}y & D_{22}x+D_{32}y & 2D_{23}x^2+2D_{33}xy & D_{22}x^3+D_{33}y^2+2D_{23}xy & \\
0 & 2D_{21}y & 2D_{23}y & 4D_{21}xy & 2D_{21}y^2+2D_{23}xy & 4D_{23}y^2 & 0 & 2D_{23}y & 2D_{22}y & 4D_{23}xy & 2D_{22}xy+2D_{23}y^2 & 4D_{22}y^2
\end{bmatrix}
\qquad (3.53)
$$

An explicit integration over the element area has to be performed on all the terms of the above matrix. (Area integration is implied as the thickness is assumed constant for an element). If the local system of co-ordinates* is chosen at the centroid of the element then the following area integral fomulae may be used, as cited from reference [3].

$$\int x \, dx \, dy = \int y \, dx \, dy = 0$$
$$\int dx \, dy = \Delta = \text{area of triangle}$$
$$\int x^2 \, dx \, dy = \Delta(x_i^2 + x_j^2 + x_k^2)/12 \qquad (3.54)$$
$$\int y^2 \, dx \, dy = \Delta(y_i^2 + y_j^2 + y_k^2)/12$$
$$\int xy \, dx \, dy = \Delta(x_i y_i + x_j y_j + x_m y_m)/12$$

where subscipts i,j and k** refer to the numbers of nodes stationed at the element vertices. Under the centroidal system, all terms with the first power of x or y disappear. In submatrix notation, the element stiffness matrix of a TRIM6 element is,

---

* Once the stiffness matrix is obtained with reference to the local co-ordinate system it is not necessary to transform to the global system, as translation of the co-ordinate areas does not alter the stiffness matrix.

** Subscript k not to be confused with stiffness matrix k.

$$[k]^e = \begin{bmatrix} k_{ii} & k_{ij} & k_{ik} & k_{il} & k_{im} & k_{in} \\ k_{ji} & k_{jj} & k_{jk} & k_{jl} & k_{jm} & k_{jn} \\ k_{ki} & k_{kj} & k_{kk} & k_{kl} & k_{km} & k_{kn} \\ k_{li} & k_{lj} & k_{lk} & k_{ll} & k_{lm} & k_{ln} \\ k_{mi} & k_{mj} & k_{mk} & k_{ml} & k_{mm} & k_{mn} \\ k_{ni} & k_{nj} & k_{nk} & k_{nl} & k_{nm} & k_{nn} \end{bmatrix} \qquad (3.55)$$

As in the TRIM3 element, each of the terms in k is a (2 x 2) submatrix. The submatrices of k may be obtained individually by following through the relevant equations in submatrix notation. Briefly,

$$[B] = [B_1, B_2, \ldots . B_r \ldots . B_6] \qquad (3.56)$$

$$[C_r]^{-1} = [C_1, C_2, \ldots C_r \ldots C_6] \qquad (3.57)$$

$$[B_r] = [Q][C_r] \qquad (r = 1,6) \qquad (3.58)$$

$$[k_{rs}] = [C_r]^T[P][C_s] \qquad \begin{pmatrix} r = 1,6 \\ s = 1,6 \end{pmatrix} \qquad (3.59)$$

A description of the finite element program using TRIM6 elements is provided in Chapter 6 and a program listing in Appendix E. The method of partitioning as applied to the TRIM6 element is described in Chapter 7, together with a computer program listing.

3.4.4. Stresses

By definition,

$$\{\sigma\} = [D][B]\{\delta\}^e$$

$$= [D][Q][C_T]^{-1}\{\delta\}^e \qquad (3.60)$$

As mentioned previously, this results in a linear-stress distribution within an element. Matrices D and C_T are constant. Matrix Q contains linear functions of x and y. This means that stresses at all points within an element differ in general, and it is necessary to define the co-ordinates of the point at which the stress is required. Usually, the stress is required at the element nodes. Because stress continuity at the element boundaries is not achieved, an average nodal stress is obtained by considering all the elements connected at the node examined.

Fig. 3.4 shows three elements extracted from a test case in which the stress at node a is required. The stresses as found by the three elements are discontinuous at point a, but the discontinuity is not very serious. The average stress at point a in this case would be 150.4 psi.

3.5. System Analysis:

The system analysis involves the assembly of individual stiffness matrix which describes the deformation behaviour of the system or body under load.

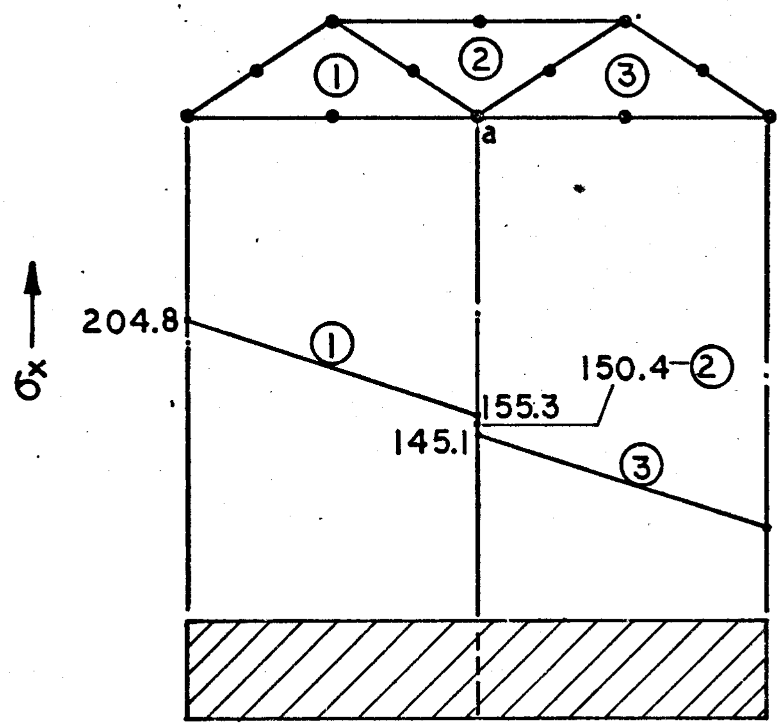

FIG. 3.4 Stress Discontinuity at TRIM6 Element Boundary.

As can be recalled, the equilibrium of an element is satisfied by replacing the effect of internal stresses and/or body forces by a set of equivalent nodal forces. The assembly is done by satisfying overall equilibirum of the entire system of nodes. Considering one node, this means that the sum of the equivalent nodal forces due to all elements attached to the node must equal the external force at the node. If R is a column vector containing the external (reactive) forces at all the nodes in the system then the above statement may be generalized as follows:

$$\{R_i\} = \Sigma F_i \qquad i - 1, \text{number of nodes.}$$

After assembly of element stiffness matrices, an overall system of linear equations of the following form is obtained.

$$\{F\} = [K]\{\delta\} + \{F_p\} \tag{3.61}$$

where F now stands for the column of external reactive forces (change of notation is for convenience of computing). Matrix K is the overall stiffness matrix and F_p is a column of body forces.

Note that equation (3.61) holds for both the TRIM3 and TRIM6 elements. Once the element stiffness matrices are obtained for either of the element types, the assembly is similar.

The steps leading to equation (3.61) are best explained by a simple example.

Fig. 3.5(a) shows a finite element idealization of 3-nodal elements for a plate under uniform tension. Node 2 is fixed while nodes 1 and 3 are placed on rollers so that they are free to move in the y-direction. The uniform loading is discretized to concentrated nodal forces. The origin of the global system is assumed to be at node 3. There are no body forces.

Since there are 9 nodes, the overall stiffness relation in submatrix notation is of the following form,

$$\begin{Bmatrix} F_1 \\ F_2 \\ F_3 \\ F_4 \\ F_5 \\ F_6 \\ F_7 \\ F_8 \\ F_9 \end{Bmatrix} = \begin{bmatrix} K_{11} & K_{12} & 0 & K_{14} & 0 & 0 & & & \\ K_{21} & K_{22} & K_{23} & K_{24} & K_{25} & 0 & 0 & & \\ 0 & K_{32} & K_{33} & 0 & K_{35} & K_{36} & 0 & 0 & \\ K_{41} & K_{42} & 0 & K_{44} & K_{45} & 0 & K_{47} & 0 & 0 \\ 0 & K_{52} & K_{53} & K_{54} & K_{55} & K_{56} & K_{57} & K_{58} & 0 \\ 0 & 0 & K_{63} & 0 & K_{65} & K_{66} & 0 & K_{68} & K_{69} \\ 0 & 0 & 0 & K_{75} & K_{75} & 0 & K_{77} & K_{78} & 0 \\ 0 & 0 & 0 & 0 & K_{85} & K_{86} & K_{87} & K_{88} & K_{89} \\ 0 & 0 & 0 & 0 & 0 & K_{96} & 0 & K_{98} & K_{99} \end{bmatrix} \begin{Bmatrix} \delta_1 \\ \delta_2 \\ \delta_3 \\ \delta_4 \\ \delta_5 \\ \delta_6 \\ \delta_7 \\ \delta_8 \\ \delta_9 \end{Bmatrix} \tag{3.62}$$

Submatrix notation of equation (3.62) is helpful, conceptually, but in the actual computer program it is necessary to revert to complete matrices. The entire stiffness matrix is thus (18 x 18).

In practice K is obtained by considering one element at a time. Assume elements 5 and 6 are to be assembled.

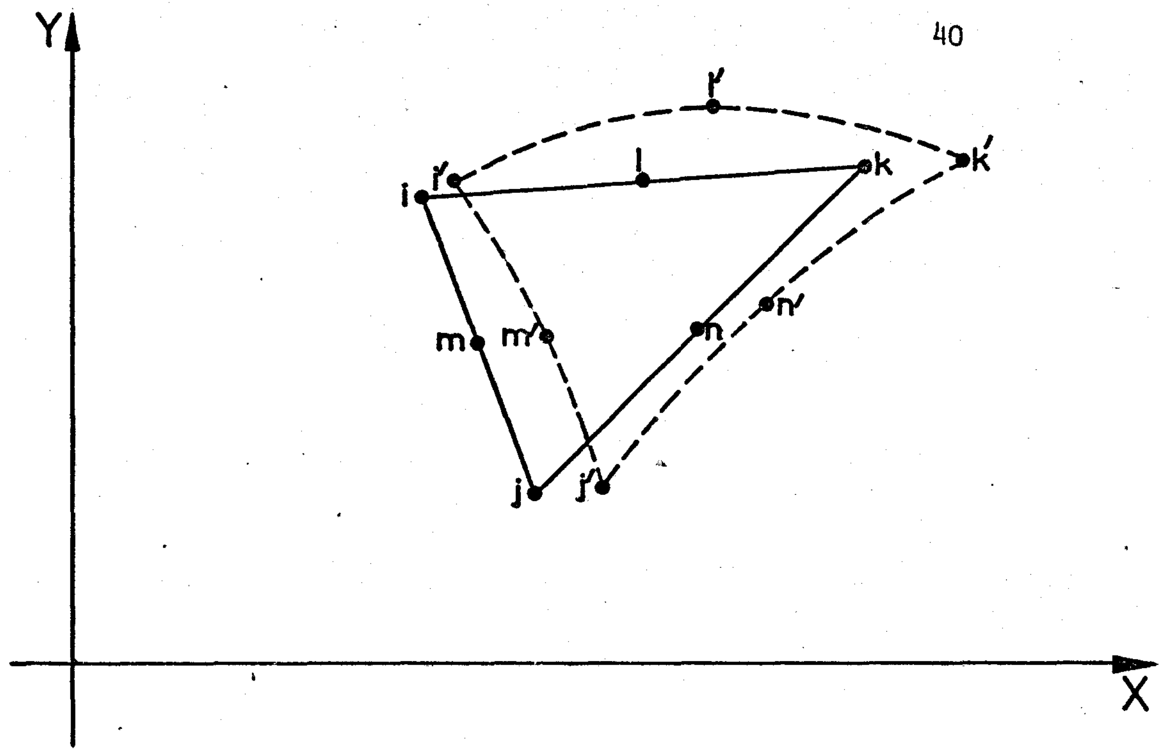

FIG. 3.3 TRIM6 Plane Stress/Strain Element and Allowed Deformation Pattern.

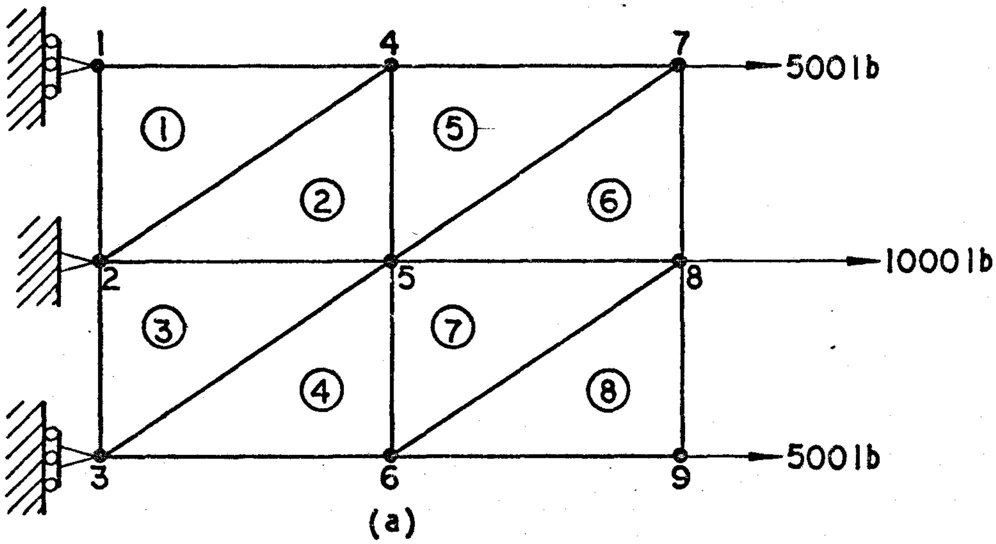

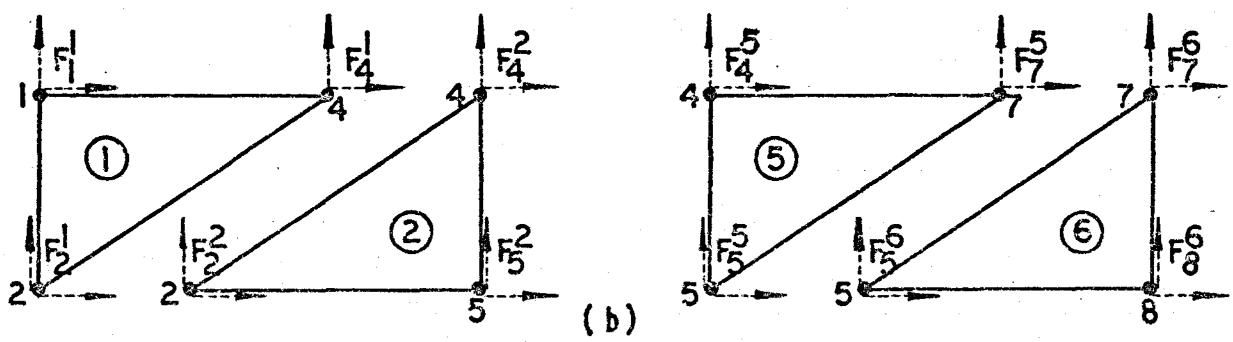

FIG. 3.5 (a) Plate Divided into 8 TRIM3 Elements. (b) Free Body Diagrams of Elements 1, 2, 5 and 6.

The stiffness relations for the two elements are:

$$\begin{Bmatrix} F_4^5 \\ F_5^5 \\ F_7^5 \end{Bmatrix} = \begin{bmatrix} k_{44}^5 & k_{45}^5 & k_{46}^5 \\ k_{54}^5 & k_{55}^5 & k_{56}^5 \\ k_{74}^5 & k_{75}^5 & k_{76}^5 \end{bmatrix} \begin{Bmatrix} \delta_4 \\ \delta_5 \\ \delta_7 \end{Bmatrix} \tag{3.63}$$

$$\begin{Bmatrix} F_5^6 \\ F_8^6 \\ F_7^6 \end{Bmatrix} = \begin{bmatrix} k_{55}^6 & k_{58}^6 & k_{57}^6 \\ k_{85}^6 & k_{88}^6 & k_{87}^6 \\ k_{75}^6 & k_{78}^6 & k_{77}^6 \end{bmatrix} \begin{Bmatrix} \delta_5 \\ \delta_8 \\ \delta_7 \end{Bmatrix} \tag{3.64}$$

The superscripts in the above two equations reference the element number. Fig. 3.5(b) show the elements isolated as free bodies in order to demonstrate the interaction of the nodal forces.

Considering the equilibrium of node 7, the contributions by elements 5 and 6 are (from equations 3.63 and 3.64),

$$F_7^5 = k_{74}^5\ \delta_4 + k_{75}^5\ \delta_5 + k_{77}^5\ \delta_7 \tag{3.65}$$

$$F_7^6 = k_{75}^6\ \delta_5 + k_{78}^6\ \delta_8 + k_{77}^6\ \delta_7 \tag{3.66}$$

For equilibrium to be satisfied at node 7, the sum of the above two forces must equal the external forces at node 7. The external force at node 7 is F_7 (without superscript) and is equal to 500#. Thus,

$$F_7 = k_{74}^5\ \delta_4 + (k_{75}^5 + k_{75}^6)\delta_5 + (k_{77}^5 + k_{77}^6)\delta_7 + K_{78}^6\ \delta_8 \tag{3.67}$$

Equation (3.67) is seen to be row 7 in equation (3.62). By comparison,

$$K_{74} = k_{74}^5$$

$$K_{75} = k_{75}^5 + k_{75}^6$$

$$K_{77} = k_{77}^5 + k_{77}^6$$

$$K_{78} = k_{78}^6$$

The other terms in row 7 are zeros as node 7 is not connected to nodes 1,2,3,6 and 9. The subscripts of the terms in the element stiffness matrices are imaginary and are obtained from the element nodal numbers. This numbering system facilitates immediate storage of the k's into the over stiffness matrix. In the actual program these local subscripts are transformed to global subscripts. In the complete stiffness matrix odd number rows refer to the x-direction and even numbered rows to the y-direction.

The discretization and superposition of centrifugal forces is dealt with in Chapter 5.

3.6. Boundary Conditions:

Either the reactive force or the displacement of all the nodes of the system must be known. Unless concentrated loads are applied, internal nodes are presumed to have zero reactive force. However, if body forces exist, they are added to the force column. The finite element method presupposes that forces are concentrated, and distributed boundary loads have to be lumped on the nodes in some way. In Chapter 4 a consistent way of doing this is described.

As mentioned previously, enough displacements must be prescribed in order to prevent rigid body tranlations and rotation. By prescribing a displacement, it means that one of the unknown displacements may be written in terms of the other unknowns.

In order to prevent the added work of reorganizing the stiffness matrix to account for prescribed displacements, an artifice is used whereby the diagonal term of the row to be eliminated is multiplied by a large number which makes the off-diagonal terms insignificant. The corresponding term in the force column is replaced by the product of the new diagonal term and the prescribed displacement. In the example of Fig. 3.5, node 3 has a prescribed displacement of d(equal to zero) in the x-direction. The row in the complete stiffness matrix to be eliminated is row 5. After modification this now reads,

$$10^{15}K_{55}d = K_{51}U_1 + K_{52}U_2 + \ldots + 10^{15}K_{55}U_5 + \ldots K_{5,18}U_{18} \qquad (3.68)$$

or
$$10^{15}K_{55}U_5 \doteq 10^{15}K_{55}d$$

$$U_5 \doteq d$$

Equation (3.68) is thus an indirect statement that U_5 is a prescribed displacement equal to d. Matrix U is a column vector of displacements, odd terms being x-displacements, etc.

3.7. SOLUTION OF LINEAR SYSTEM OF EQUATIONS:

If the column vector containing the body forces in equation (3.61) are summed into the force column vector F, then the following system of linear equations remain to be solved,

$$\{F\} = [K]\{\delta\} \qquad (3.69)$$

Presumably, equation (3.69) has been modified to include boundary conditions.

One way of solving for the unknown displacements is by inversion. However, the fact that the stiffness matrix is symmetric and banded is used in order to save computer storage and execution time. The largest matrix that can be stored in the CDC 6400 computer is approximately of the size of 30,000 words, or (180 x 180). If the entire matrix is stored, the largest number of nodes one can have is 90.

From the example in the previous section it can be seen that the stiffness matrix in equation (3.62) is banded, i.e. the non-zero terms are close to the main diagonal. Also, the stiffness matrix is symmetric. It is thus only necessary to store the upper band of the matrix, which has been shaded in equation (3.62). In the basic TRIM3 and TRIM6 programs of

Chapter 7, the upper band is stored row-wise. The stiffness matrix of equation (3.62) is hence stored as follows:

$$\begin{array}{l} \text{MAIN DIAGONAL} \\ \text{1st SUPER DIAG.} \\ \text{2nd SUPER DIAG.} \\ \text{3rd SUPER DIAG.} \end{array} \begin{bmatrix} K_{11} & K_{22} & K_{33} & K_{44} & K_{55} & K_{66} & K_{77} & K_{88} & K_{99} \\ K_{12} & K_{23} & 0 & K_{45} & K_{56} & 0 & K_{78} & K_{89} & \\ 0 & K_{24} & K_{35} & 0 & K_{57} & K_{68} & 0 & & \\ K_{14} & K_{25} & K_{36} & K_{47} & K_{58} & K_{69} & & & \end{bmatrix} = [K]_{BANDED} \quad (3.70)$$

The saving in computer storage is substantial. If the bandwidth is 30 then a total of 500 nodes are possible. It is apparent that in this method of storage, the bandwidth is a critical parameter. It is defined as the total number of diagonals in the upper band of the stiffness matrix, and is dependent on the maximum amount by which the nodal numbers of an element differ. Mathematically,

$$\text{bandwidth} = n(n + 1) \qquad (3.71)$$

where n = maximum difference between element nodal numbers. In Fig. 3.5, n = 4 - 1 = 3

$$\text{bandwidth} = 2(3 + 1) = 8 \qquad \text{(see equation 3.70)}$$

It is evident, therefore, to keep the nodal numbers of an element as close to each other as possible.

In the computer programs of Chapter 6, the Cholesky Method is used for the solution of the total system of equilibrium equations as it was assumed that this method would give good accuracy for the type of problems considered.

In the Choleski method the stiffness matrix of the system, K, is expressed as the product of a lower triangular matrix and an upper triangular matrix, i.e.

$$[K] = [R_L][R_u] \tag{3.72}$$

The lower triangular form is obtainable from the upper triangular form as the stiffness matrix is real symmetric and positive definite, viz,

$$[K] = [R_u]^T[R_u] \tag{3.73}$$

The matrix $[R_u]$ has a band structure similar to the stiffness matrix and the bandwidth is equal to that of the upper band of the stiffness matrix.

If

$$[K]\{U\} = \{F\} \text{ it follows that}$$

$$[R_u]^T[R_u]\{U\} = \{F\} \tag{3.74}$$

This equation may be written as two matrix equations by introducing an auxiliary vector Z such that

$$[R_u]^T\{Z\} = \{F\} \tag{3.75}$$

and

$$[R_u]\{U\} = \{Z\} \tag{3.76}$$

It is thus necessary to solve first the lower triangular form for Z, and then the upper triangular for U. This is similar to the Gaussian elimination technique where solution is achieved by backward substitution.

CHAPTER 4

CONSISTENT APPROACH TO DISTRIBUTED BOUNDARY LOADS

4.1. General Formula for Discretization:

Often reasonable answers are obtained by lumping the distributed loads on neighbouring nodes simply by physical intuition. This, however, does not always work, especially with the TRIM6 element. A formula for consistent nodal forces is set up in this section by using the principle of virtual work. The theory is developed with the TRIM6 element as example, but is applicable to a general planar element.

Consider a boundary element e which is loaded by distributed laod g, as in Fig. 4.1. For any point within the TRIM6 element the displacements are defined by equation (3.36) or

$$\{f\} = [R]\{\alpha\}$$

However, on the boundary side of element e, y is a linear function of x, namely

$$x = b_1 y + b_2 \qquad (4.1)$$

By substitution of equation (4.1) into (3.36), the displacements of a point such as m along the boundary side of element e is obtained in terms of a new set of coefficients.

$$\{f\} = \begin{Bmatrix} u \\ v \end{Bmatrix} = \begin{bmatrix} 1 & y & y_2 & 0 & 0 & 0 \\ 0 & 0 & 0 & 1 & y & y^2 \end{bmatrix} \begin{Bmatrix} a_1 \\ a_2 \\ a_3 \\ a_4 \\ a_5 \\ a_6 \end{Bmatrix} \quad (3.2)$$

or $\{f\} = [R_r]\{a_r\}$ (4.3)

where subscript r simply denotes 'reduced'.

The 'a' coefficients are found in terms of the displacements of the three boundary nodes of the element as follows

$$\{\delta_r\}^e = \begin{Bmatrix} u_i \\ v_i \\ u_j \\ v_j \\ u_k \\ v_k \end{Bmatrix} = \begin{bmatrix} 1 & y_i & y_i^2 & 0 & 0 & 0 \\ 0 & 0 & 0 & 1 & y_i & y_i^2 \\ 1 & y_j & y_j^2 & 0 & 0 & 0 \\ 0 & 0 & 0 & 1 & y_j & y_j^2 \\ 1 & y_k & y_k^2 & 0 & 0 & 0 \\ 0 & 0 & 0 & 1 & y_k & y_k^2 \end{bmatrix} \begin{Bmatrix} a_1 \\ a_2 \\ a_3 \\ a_4 \\ a_5 \\ a_6 \end{Bmatrix} \quad (4.4)$$

or $\{\delta_r\}^e = [C_r]\{a_r\}$ (4.5)

and $\{a_r\} = [C_r^{-1}]\{\delta_r\}^e$ (4.6)

Substituting in equation (4.3)

$$\{f\} = [R_r][C_r^{-1}]\ \{\delta_r\}^e \tag{4.7}$$

or

$$\{f\} = [N_r]\{\delta_r\}^e \tag{4.8}$$

where $[N_r] = [R_r][C_r^{-1}]$ is the reduced interpolation matrix. (4.9)

Let the nodal forces on the boundary nodes of element e be expressed as a column F,

$$\{F\}^e = \begin{Bmatrix} F_i \\ F_j \\ F_k \end{Bmatrix} \tag{4.10}$$

and assume a virtual displacement δ^v is applied at the boundary nodes,

$$\{\delta^v\} = \begin{Bmatrix} \delta_i^v \\ \delta_j^v \\ \delta_k^v \end{Bmatrix} \tag{4.11}$$

The work done by the nodal forces due to the applied virtual displacement is,

$$W_n = \{\delta^v\}^T\ \{F\}^e \tag{4.12}$$

The displacement of a point along the boundary side due to the virtual displacement is, by equation (4.8),

$$\{f\} = [N_r]\{\delta^v\}^e \tag{4.13}$$

The total work done by the distributed load g is,

$$W_d = \int \{f\}^T \cdot \{g\} \; ds \tag{4.14}$$

or

$$W_d = \{\delta^v\}^T \int [N_r] \, \{g\} \; ds \tag{4.15}$$

By the virtual work theorem W_n equals W_d. The pre-multiples in equations (4.12) and (4.15) cancel and the result is

$$\{F\}^e = \int [N_r]^T \{g\} \, ds \tag{4.16}$$

Hence, for an element such as e, equation (4.16) discretizes the distributed load to concentrated nodal forces. For a node such as i in Fig. 4.1 there is a contribution due to both elements d and e, and have to be summed to find the net forces on the node.

4.2. Special Cases:

4.2.1. Case 1: TRIM3 element, uniform load in x-direction

See Fig. 4.2(a). By analogy to Sec. 4.1, the governing equations are:

$$[R_r] = \begin{bmatrix} 1 & y & 0 & 0 \\ 0 & 0 & 1 & y \end{bmatrix} \tag{4.17}$$

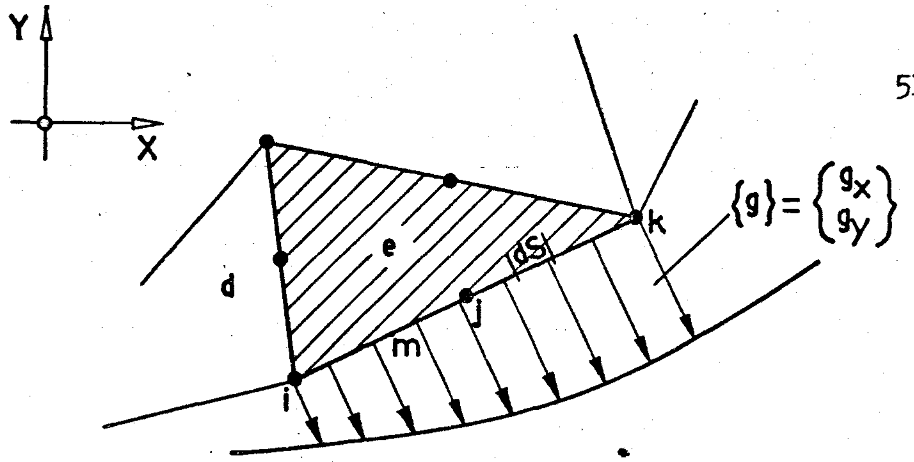

FIG. 4.1 Distributed Load g lbs per Unit Length on a TRIM6 Boundary Element e.

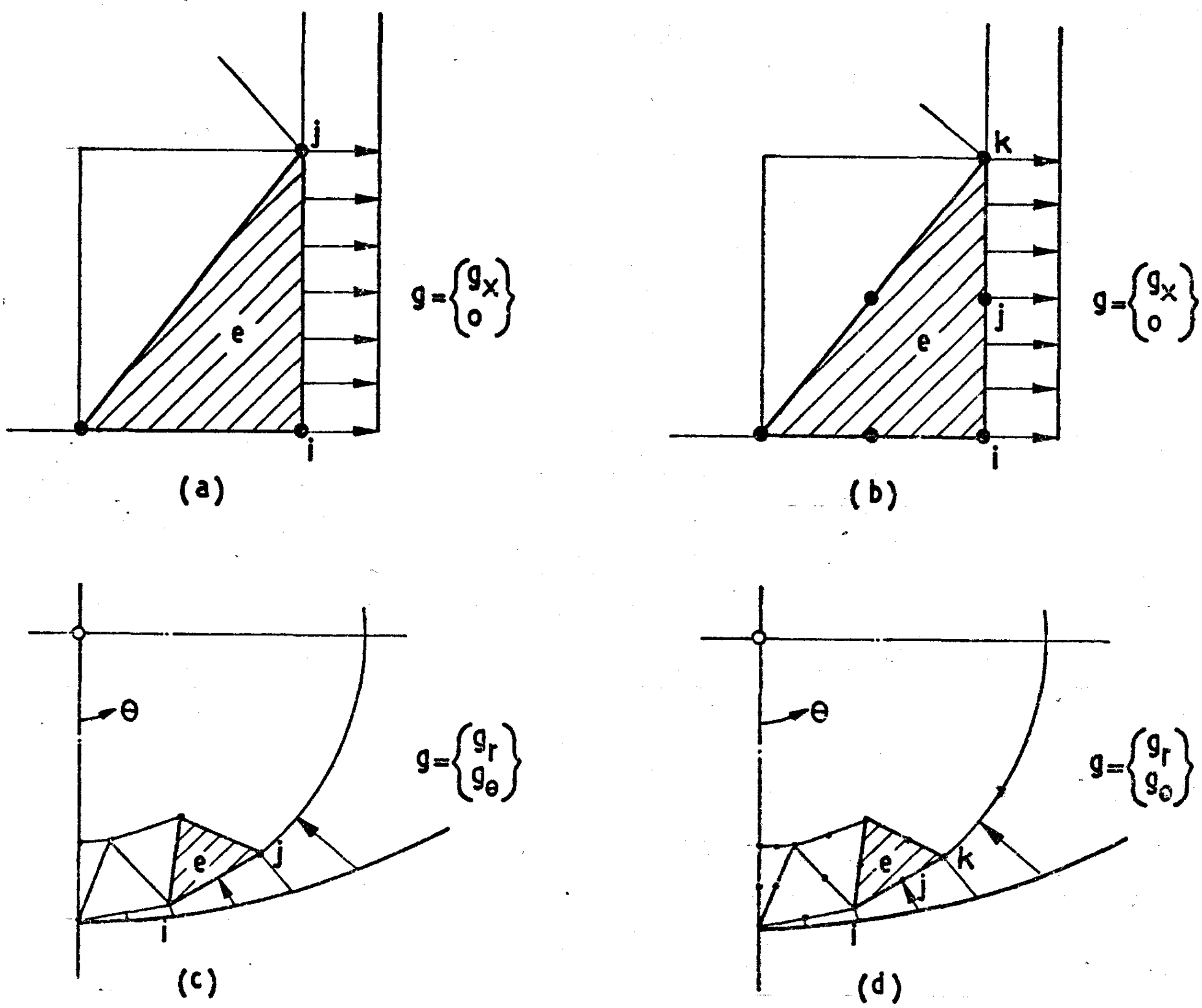

FIG. 4.2 Two Types of Distributed Loadings as Applied to TRIM3 and TRIM6 Boundary Elements.

$$[C_r] = \begin{bmatrix} 1 & y_i & 0 & 0 \\ 0 & 0 & 1 & y_i \\ 1 & y_j & 0 & 0 \\ 0 & 0 & 1 & y_j \end{bmatrix} \tag{4.18}$$

$$\{g\} = \begin{Bmatrix} g_x \\ 0 \end{Bmatrix} \quad \text{(per unit length in y-direction)} \tag{4.19}$$

By equation (4.16)

$$\begin{Bmatrix} F_{ix} \\ F_{iy} \\ F_{jx} \\ F_{jy} \end{Bmatrix} = [C_r^{-1}]^T \int_{y_i}^{y_j} \begin{bmatrix} 1 & 0 \\ y & 0 \\ 0 & 1 \\ 0 & y \end{bmatrix} \begin{Bmatrix} g_x \\ 0 \end{Bmatrix} dy$$

$$= g_x [C_r^{-1}]^T \begin{Bmatrix} (y_j - y_i) \\ (y_j^2 - y_i^2)/2 \\ 0 \\ 0 \end{Bmatrix} \tag{4.20}$$

Having $y_i = 2.0$, $y_j = 3.0$, $g_x = 1000$ lb/in,

equation (4.20) yields

$$\begin{Bmatrix} F_{ix} \\ F_{iy} \\ F_{jx} \\ F_{jy} \end{Bmatrix} = \begin{Bmatrix} 500.0 \\ 0.0 \\ 500.0 \\ 0.0 \end{Bmatrix}$$

These results are coincident with the static method of lumping half the total load on the triangular element equally on the two nodes. Hence, either approach is acceptable for the TRIM3 element under uniform load.

4.2.2. Case 2: TRIM6 element with uniform load in x-direction

See Fig. 4.2(b). The governing equations for the TRIM6 element have been derived in section 4.1. Matrix C_r is defined by equation (4.4) and matrix R_r is defined by equation (4.2). The distributed loading is

$$\{g\} = \begin{Bmatrix} g_x \\ 0 \end{Bmatrix} \text{ lb/in}$$

After manually performing the product $[R_r]^T\{g\}$, the force equation yields

$$\begin{Bmatrix} F_{ix} \\ F_{iy} \\ F_{jx} \\ F_{jy} \\ F_{kx} \\ F_{ky} \end{Bmatrix} = g_x[C_r^{-1}]^T \int_{y_i}^{y_k} \begin{Bmatrix} 1 \\ y \\ y^2 \\ 0 \\ 0 \\ 0 \end{Bmatrix} dy$$

$$= g_x[C_r^{-1}]^T \begin{Bmatrix} (y_k - y_i) \\ (y_k^2 - y_i^2)/2 \\ (y_k^3 - y_i^3)/3 \\ 0 \\ 0 \\ 0 \end{Bmatrix} \qquad (4.21)$$

Having $y_i = 2.0$, $y_j = 2.5$, $y_k = 3.0$, $g_x = 1000$ lb/in, equation (4.21) gives the following results,

$$\begin{Bmatrix} F_{ix} \\ F_{iy} \\ F_{jx} \\ F_{jy} \\ F_{kx} \\ F_{ky} \end{Bmatrix} = \begin{Bmatrix} 166.67 \\ 0.0 \\ 666.67 \\ 0.0 \\ 166.67 \\ 0.0 \end{Bmatrix}$$

From these results it can be concluded that for a uniform load, 1/6th of the total load on an element is concentrated on each of the outer nodes while 2/3 of the total load is concentrated on the midside node. Obviously, this differs from the static approach.

4.2.3. Case 3: Circumferential loading on TRIM3 element

See Fig. 4.2(c). Assume the loading is a function of the angle measured from the vertical, as,

$$\{g\} = \begin{Bmatrix} g_r \\ g_\theta \end{Bmatrix} = \begin{Bmatrix} g_r(\theta) \\ g_\theta(\theta) \end{Bmatrix} \text{ load per unit angle} \qquad (4.22)$$

If the radius is held constant equal to the radius of the outer boundary, the governing equations in polar co-ordinates*

---

* See Note at end of section.

are:

$$[R_r] = \begin{bmatrix} 1 & \theta & 0 & 0 \\ 0 & 0 & 1 & \theta \end{bmatrix} \tag{4.23}$$

$$[C_r] = \begin{bmatrix} 1 & \theta_i & 0 & 0 \\ 0 & 0 & 1 & \theta_i \\ 1 & \theta_j & 0 & 0 \\ 0 & 0 & 1 & \theta_j \end{bmatrix} \tag{4.24}$$

where θ_i is the angle at node i measured from the vertical.

Nodal forces are subsequently,

$$\{F\} = [C_r^{-1}]^T \int_{\theta_i}^{\theta_j} \begin{Bmatrix} g_r \\ \theta g_r \\ g_\theta \\ \theta g_\theta \end{Bmatrix} d\theta \tag{4.25}$$

In Chapter 11 it is shown that a feasible loading distribution as a result of cutting forces on a diamond circular saw blade is

$$\begin{Bmatrix} g_r \\ g_\theta \end{Bmatrix} = \begin{Bmatrix} a\ C_n\ \theta \\ C_f\ g_r \end{Bmatrix} \tag{4.26}$$

For this distribution equation (4.24) gives

$$\{F\} = a\ C_n [C_r^{-1}]^T \int_{\theta_i}^{\theta_j} \begin{Bmatrix} \theta \\ \theta^2 \\ C_f \theta \\ C_f \theta^2 \end{Bmatrix} d\theta$$

By integration,

$$\begin{Bmatrix} F_{ir} \\ F_{i\theta} \\ F_{jr} \\ F_{j\theta} \end{Bmatrix} = a\, C_n\, [C_r^{-1}]^T \begin{Bmatrix} (\theta_j^2 - \theta_i^2)/2 \\ (\theta_j^3 - \theta_i^3)/3 \\ C_f(\theta_j^2 - \theta_i^2)/2 \\ C_f(\theta_j^3 - \theta_i^3)/3 \end{Bmatrix} \quad (4.27)$$

Forces in the cartesian system are obtained by a simple transformation. A listing of the program used for this case is included in Appendix F. Results pertaining to the actual finite element idealization of the saw blade (Chapter 12) are shown in Table 4.1, in which the cartesian components of forces are cited. A comparison is made with the static method, and good agreement is observed.

TABLE 4.1. Results of example for case 3.

NODE	CONSISTENT APPROACH		STATIC APPROACH	
	F_x lb.	F_y lb.	F_x lb.	F_y lb.
4	-0.078	0.390	-0.062	0.292
14	-1.572	6.161	-1.439	5.641
23	-7.944	19.766	-7.945	19.767
35	-10.711	18.943	-10.994	19.442
50	-6.972	11.073	-6.944	11.164
102	-3.911	6.002	-3.878	5.950
101	-19.902	27.917	-19.570	27.450
80	-20.088	21.486	-20.521	21.948

Note:

By using the polar co-ordinate system, it is assumed that the boundary side is an arc of a circle. In reality, the sides are straight and this introduces some error. However, the error is acceptable.

4.2.3. Case 4: Circumferential loading on TRIM6 element

See Fig. 4.2(d). Making the same assumptions as for Case 3, the governing equations are,

$$[R_r] = \begin{bmatrix} 1 & \theta & \theta^2 & 0 & 0 & 0 \\ 0 & 0 & 0 & 1 & \theta & \theta^2 \end{bmatrix} \tag{4.28}$$

$$[C_r] = \begin{bmatrix} 1 & \theta_i & \theta_i^2 & 0 & 0 & 0 \\ 0 & 0 & 0 & 1 & \theta_i & \theta_i^2 \\ 1 & \theta_j & \theta_j^2 & 0 & 0 & 0 \\ 0 & 0 & 0 & 1 & \theta_j & \theta_j^2 \\ 1 & \theta_k & \theta_k^2 & 0 & 0 & 0 \\ 0 & 0 & 0 & 1 & \theta_k & \theta_k^2 \end{bmatrix} \tag{4.29}$$

Assume the loading is,

$$\{g\} = \begin{Bmatrix} g_r \\ g_\theta \end{Bmatrix} = \begin{Bmatrix} k_1\theta \\ k_2\theta \end{Bmatrix} \tag{4.30}$$

Then

$$\{F\} = [C_r^{-1}]^T \int_{\theta_i}^{\theta_k} \begin{Bmatrix} k_1\theta \\ k_1\theta^2 \\ k_1\theta^3 \\ k_2\theta \\ k_2\theta^2 \\ k_2\theta^3 \end{Bmatrix} d\theta \qquad (4.31)$$

By integration,

$$\{F\} = \begin{Bmatrix} F_{ir} \\ F_{i\theta} \\ F_{jr} \\ F_{j\theta} \\ F_{kr} \\ F_{k\theta} \end{Bmatrix} = [C^{-1}]^T \begin{Bmatrix} k_1(\theta_K^2 - \theta_i^2)/2 \\ k_1(\theta_K^3 - \theta_i^3)/3 \\ k_1(\theta_K^4 - \theta_i^4)/4 \\ k_2(\theta_K^2 - \theta_i^2)/2 \\ k_2(\theta_K^3 - \theta_i^3)3 \\ k_2(\theta_K^4 - \theta_i^4)/4 \end{Bmatrix} \qquad (4.32)$$

Again, the forces in the rectangular cartesian system are obtained by a simple transformation. In Appendix F a computer program is listed for this case as used in Chapter 12 to calculate boundary forces on TRIM6 element meshes.

CHAPTER 5

CENTRIFUGAL FORCES

5.1. General Formula to Find Equivalent Nodal Forces:

Centrifugal forces exist in all rotating bodies. For instance, in a rotating disk, centrifugal forces vary in proportion to the radius. In the Finite Element Method, this type of problem is basically treated as a static problem and the effect of the centrifugal forces is accounted for by applying equivalent forces to all the nodes of the system (D'Alembert's Principle). One approach is to treat each individual element as a mass concentrated at the element centroid, rotating independently of the other elements. The centrifugal force obtained by this idealization is then distributed equally to the nodes of the element. Although simple in its application, this method is inconsistent in that no consideration is given to the shape of the element.

In Chapter 3 a formula (equation 3.19) was derived with which body forces can be discretised. This formula is applicable to centrifugal forces. Reiterating equation (3.19),

$$\{F\}_p^e = - \int [N]^T \{p\}\ t\ dx\ dy \qquad (5.1)$$

Here matrix [N], the interpolation matrix, is a function of the element nodal co-ordinates and gives some 'weighting' to the actual position of the nodes. If matrix N was absent from equation (5.1), or if it was constant and could be factored out, then what remains is simply a summation of the forces acting over the element, and that is what the inconsistent method does in essence. It is thus concluded that equation (5.1) is a consistent discretization method.

The problem now is to define the centrifugal forces in terms of a vector {p}. Figs. 5.1(a) and (b) illustrate a rotating body from which a triangular finite element is isolated. From basic mechanics it is recalled that the radial force per unit volume acting at a point distance r from the centre of rotation is defined as,

$$F_r = m\,r\omega^2 = \frac{w}{g}\,r\,\omega^2 \quad \underline{\text{(force per unit volume)}}$$

where w = weight density lbs/cubic in, and

ω = angular velocity rads/sec

From Fig. 5.1(b), the infinitesimal force acting on an infinitesimal element (shaded in the figure), is given by $d\,F_r = \frac{w}{g}\,\omega^2\,r\,t\,dx\,dy$ in the radial direction.

Taking rectangular components

$$d\,F_x = \frac{w}{g}\,\omega^2\,r\cos\theta \quad t\,dx\,dy \tag{5.2}$$

$$d\,F_y = \frac{w}{g}\,\omega^2\,r\sin\theta \quad t\,dx\,dy$$

(dx = dX)

or

$$\{d\,F_r\} = \begin{Bmatrix} d\,F_x \\ d\,F_y \end{Bmatrix} = \frac{w}{g}\,\omega^2\,t \begin{Bmatrix} X \\ Y \end{Bmatrix} dx\,dy \tag{5.3}$$

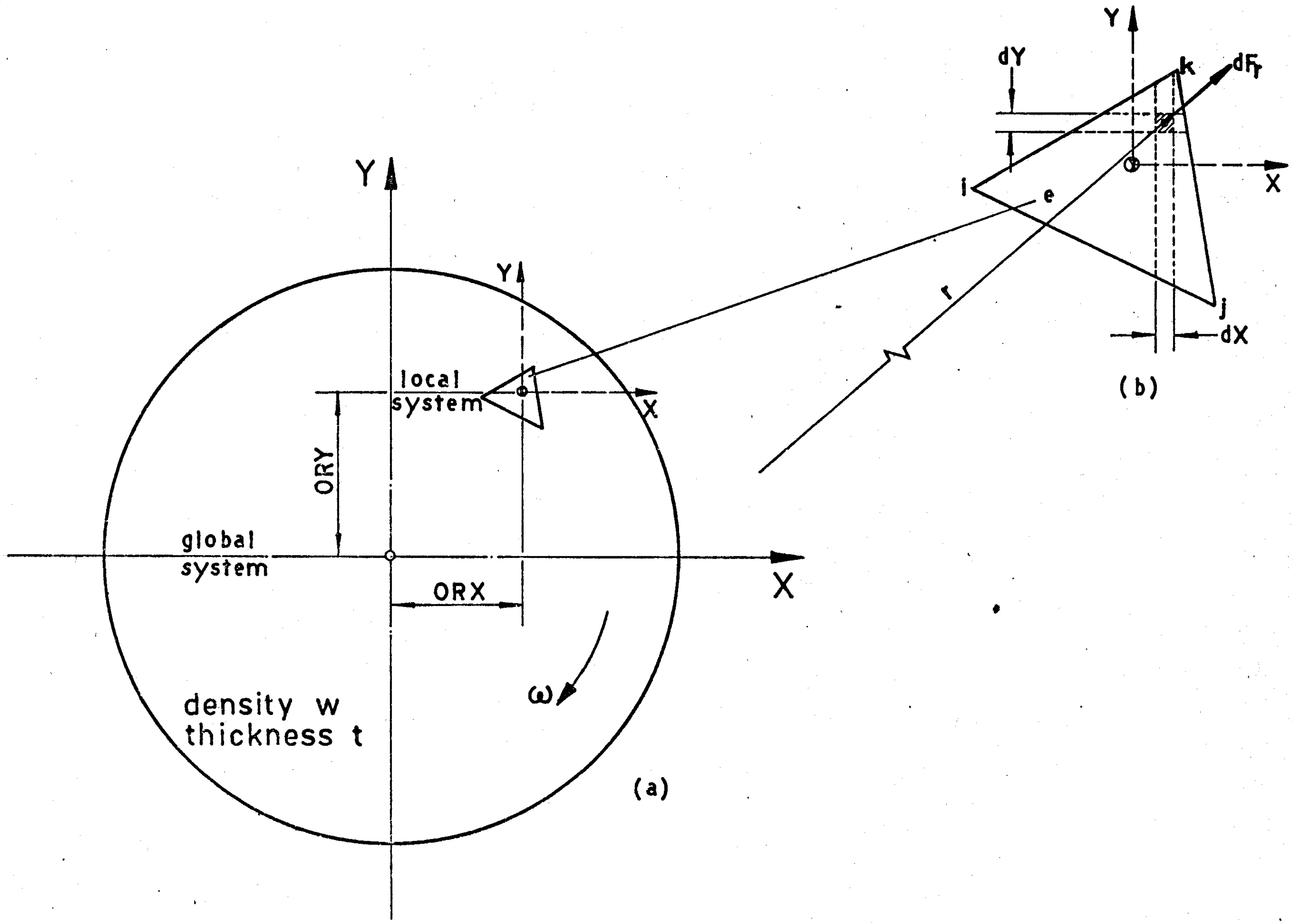

FIG. 5.1 (a) A Triangular Element (e) Isolated from a Body Rotating at ω rads/sec.

(b) An Enlarged View of Element e Showing Infinitesimal Centrifugal Force Acting on an Infinitesimal Element.

Integration of equation (5.3) would give the net force acting over the element. However, if equation (5.3) were pre-multiplied by N before integration, the effect would be as required by equation (5.1). Thus by analogy between (5.3) and (5.1),

$$\{p\} = \frac{w}{g}\,\omega^2 \begin{Bmatrix} X \\ Y \end{Bmatrix} \quad \text{centrifugal force per unit volume} \qquad (5.4)$$

Because of the simplification of the area integrals if a local co-ordinate system is chosen at element centroids, equations (5.4) and (5.1) are modified for this system,

$$\{p\} = \frac{w}{g}\,\omega^2 \begin{Bmatrix} ORX + x \\ ORY + y \end{Bmatrix} \qquad (5.5)$$

where (ORX, ORY) are co-ordinates of the centroid of the element with respect to the global system.

(X,Y) are co-ordinates of a general point with respect

(x,y) are co-ordinates of the general point with respect to the local system.

Equation (5.1) is modified as,

$$\{F\}_p^e = -\frac{w}{g}\omega^2 t \left[\int [N]^T \, dx\, dy\right] \begin{Bmatrix} ORX \\ ORY \end{Bmatrix}$$

$$-\frac{w}{g}\omega^2 t \int [N]^T \begin{Bmatrix} x \\ y \end{Bmatrix} dx\, dy$$

or

$$\{F\}_p^e = \{F_1\} + \{F_2\} \tag{5.6}$$

5.2. Centrifugal Forces for TRIM3 Element:

The interpolation matrix for a TRIM3 element is defined by equation (3.22). Matrix F_1 in equation (5.6) becomes,

$$\{F_1\} = \begin{Bmatrix} F_{1i} \\ F_{1j} \\ F_{1k} \end{Bmatrix} = -\frac{w}{g}\omega^2 t \int \begin{bmatrix} IN_i \\ IN_j \\ IN_k \end{bmatrix} dx\, dy \quad \text{(local co-ordinate system)}$$

I is a (2 x 2) identity matrix and N_i, N_j, N_m are defined in equation (3.23). By using the integration formulae given in equation (3.54), the above equation reduces to,

$$\{F_{1j}\} = \{F_{1j}\} = \{F_{1k}\} = -\frac{w}{g}\omega^2 t \frac{\Delta}{3} \begin{Bmatrix} ORX \\ ORY \end{Bmatrix} \tag{5.7}$$

The forces above are, of course, submatrices having an x and a y component.

Matrix F_2 of equation (5.6) becomes,

$$\{F_2\} = \begin{Bmatrix} F_{2i} \\ F_{2j} \\ F_{2k} \end{Bmatrix} = -\frac{w}{g}\omega^2 t \int \begin{bmatrix} IN_i \\ IN_j \\ IN_m \end{bmatrix} \begin{Bmatrix} x \\ y \end{Bmatrix} dx\, dy \qquad (5.8)$$

from which,

$$\{F_{2i}\} = -\frac{w}{g}\omega^2 t/2\Delta \int \begin{Bmatrix} b_i x^2 + c_i xy \\ b_i xy + c_i y^2 \end{Bmatrix} dx\, dy \qquad (5.9)$$

Terms F_{2j} and F_{2j} are obtained from equation (5.9) by a counter-clockwise permutation of the subscripts. Coefficients b and c are defined in equation (3.24).

Note:

By splitting the force vector into two vectors, the argument concerning lumping of the forces becomes clearer. Term F_1 effectively allocates 1/3 of the total force equally to the nodes while term F_2 is the actual 'weighting' term.

5.3. Centrifugal Forces for TRIM6 Element:

The interpolation matrix N for the TRIM6 element is defined by equation (3.42). The transpose of N is,

$$[N]^T = [C_r^{-1}]^T[R]^T \qquad (5.10)$$

(In the computer program of Chapter 6 the inverse of matrix C_r is calculated when finding the stiffness matrix of each element and is stored on mass storage area for use in calculating the centrifugal forces).

The local co-ordinate system is again assumed at the element centroid. Matrix F_1 of equation (5.6) becomes,

$$\{F_1\} = -\frac{w}{g}\omega^2 t\,[C_r^{-1}]^T \int \begin{bmatrix} 1 & 0 \\ x & 0 \\ y & 0 \\ x^2 & 0 \\ xy & 0 \\ y^2 & 0 \\ 0 & 1 \\ 0 & x \\ 0 & y \\ 0 & x^2 \\ 0 & xy \\ 0 & y^2 \end{bmatrix} \begin{matrix} (ORX) \\ (ORY) \end{matrix} \, dx\,dy \quad (5.11)$$

After performing the product under the integral sign and integrating formally, the following is obtained for F_1

$$\begin{Bmatrix} F_{1i} \\ F_{1j} \\ F_{1k} \\ F_{1l} \\ F_{1m} \\ F_{1n} \end{Bmatrix} = -\frac{w}{g}\omega^2 t[C_r^{-1}]^T \begin{bmatrix} ORX*\Delta \\ 0 \\ 0 \\ ORX*Ix \\ ORX*Ixy \\ ORX*Iy \\ ORY*\Delta \\ 0 \\ 0 \\ ORY*Ix \\ ORY*Ixy \\ ORY*Iy \end{bmatrix} \quad (5.12)$$

where Ix, Iy and Ixy are the three moments of area.

Term F_2 of equation (5.6) yields,

$$\{F_2\} = -\frac{w}{g}\,\omega^2\, t\, [C_T^{-1}]^T \int \begin{bmatrix} x \\ x^2 \\ xy \\ x^3 \\ x^2y \\ xy^2 \\ y \\ xy \\ y^2 \\ x^2y \\ xy^2 \\ y^3 \end{bmatrix} dx\, dy \qquad (5.13)$$

or

$$\{F_2\} = -\frac{w}{g}\,\omega^2\, t\, [C_r^{-1}]^T \begin{bmatrix} 0 \\ X2 \\ XY \\ X3 \\ X2Y \\ XY2 \\ 0 \\ XY \\ Y2 \\ X2Y \\ XY2 \\ Y3 \end{bmatrix} \qquad (5.14)$$

In equation (5.14) X2, Y2 and XY are respectively equal to Ix, Iy and Ixy, the area moments. The area integrals of the higher order terms, named X3, X2Y, etc., are more complicated.

One way of finding these integrals is by a numerical method described in Appendix A which divides the element into a number of sub-elements and sums the contribution of the sub-elements. A program listing of the method is also given in the appendix and the accuracies with which the integrals are obtained are demonstrated. Though not exact, this method has the advantage that integration of any powers of x and y may be performed, including negative powers.

Another method of obtaining these integrals is by manual integration which unfortunately becomes cumbersome for orders higher than 3. In Appendix B integrals for the 3rd degree obtained in this way are provided (in part). The formulae are not completely followed through as they are easily calculated by computer after the stages completed.

Calculation of centrifugal forces is incorporated in the finite element programs which follow.

CHAPTER 6

DESCRIPTION OF BASIC COMPUTER PROGRAMS FOR TRIM3 AND TRIM6 ELEMENTS

In this chapter the finite element programs using the two types of elements is described. In Chapter 7 the method of partitions as applied to the same two element types is described. They are grouped in this way as the procedures within each group are similar. In Table 6.1 a list of the important variables as used in the programs are listed together with their meanings. This table includes variables contained in all of the four programs, and an indication is given in brackets to show in which program the variable is used. For example, 'TRIM3 Sub' means the program using the method of substructures (or partitions) and the TRIM3 element.

The finite element procedure is divided into a number of sections each of which is diverted to a subroutine. The main differences between the two programs described here occur in the calculation of the element stiffness matrices and the calculation of centrifugal nodal forces.

Other differences are due to the difference in nodal numbering. Fig. 6.1 shows the basic flow of the programs and the subroutines to which the flow is diverted.

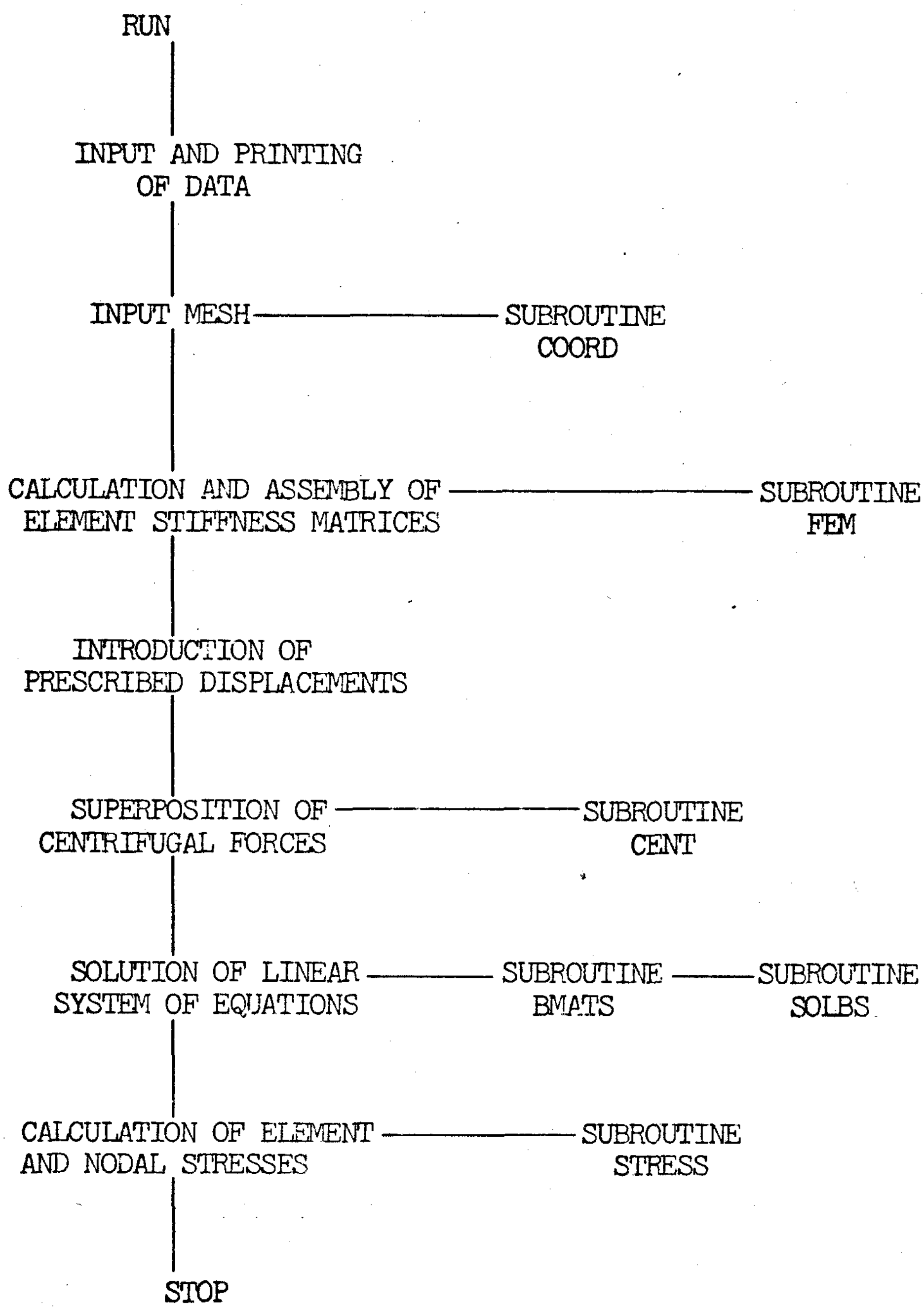

Fig. 6.1 Flow diagram of TRIM3 and TRIM6 finite element programs.

TABLE 6.1 Dictionary of Fortran Variables

Fortran Variables	Equivalent Symbol	Significance
NPOIN		Total number of nodal points in system
NELEM		Total number of finite elements in system
NON		Total number of nodes having concentrated nodal forces
NBOUN		Total number of nodes having prescribed displacements
IWATE		Number of elements connected at a node below which Wilson's method is used to find weighted nodal stresses (TRIM3, TRIM3 Sub)
NCENT		Centrifugal force option = 0 no centrifugal forces present = 1 centrifugal forces present
NCOLN		Number of force columns (TRIM3, TRIM3 Sub, TRIM6 Sub)
NTHICK		Number of variations in elements thicknesses in system
E	E	Young's modulus (psi)
P	ν	Poisson's ratio
DENS	w	Weight density of material (lb/cubic inch)
RPM	N	Speed of rotation in (revs/min)
T(I)	t_i	Thickness for Ith thickness variation (inches)
IT(I)		Flag on Ith element defining thickness from T(I) to be used for element (TRIM3, TRIM6)

NOD(I,J)	i,j,m	Nodal numbers for TRIM3 element
	i,j,k,l,m,n	Nodal numbers for TRIM6 element
Z(I,J)	x_i, y_i	J = 1, x co-ordinate of ith node J = 2, y co-ordinate of ith node
F(I)	F_i	Net force on ith node (include body forces)(TRIM3, TRIM6)
SK(I,J)	[K]	Banded overall stiffness matrix (TRIM3, TRIM6)
IBAN		Bandwidth of upper band of stiffness matrix
NF(I)		Array containing nodal numbers of nodes having prescribed displacements
NB(I,J)		Flag denoting direction of Ith prescribed displacement NB(I,1) = 0 Disp. in x-direction prescribed NB(I,2) = 0 Disp. in y-direction prescribed NB(I,1) = 1 Disp. in x-direction not prescribed NB(I,2) = 1 Disp. in y-direction not prescribed
BV(I,J)		BV(I,1) = value of Ith prescribed displacement in x-direction BV(I,2) = value in y-direction
(ORX,ORY)		Centroidal co-ordinates of element
D(I,J)		(3 x 3) elasticity matrix
DELTA	Δ	Element area
U(I)	$u_i v_i$	Column vector of displacements. Odd terms are x-displacements, even terms are y-discplacement

TAPE1,TAPE2 TAPE3,TAPE4		Mass storage area
GRAVITY	g	Gravitational acceleration 32.2*12 in/sec^2
B(I,J)	[B]	(3 x 6) strain-displacement matrix (TRIM3)
CK(I,J)	[k]	Element stiffness matrix
DB(I,J)	[DB]	(3 x 6) stress matrix (TRIM3) (3 x 12) stress matrix (TRIM6)
S(I,J) J = 1,3	σ_x, σ_y τ_{xy}	Element stresses/Nodal stresses (TRIM3, TRIM6)
S1,S2	σ_1, σ_2	Principle stresses
THETA	θ	Principle angle
SR,ST,SRT	$\sigma_r, \sigma_t, \sigma_{rt}$	Stresses in polar system
X1,Y1		Nodal co-ordinates with respect to local system
NODE		Nodal numbers for one element
C	$[C_T]$ in part	(6 x 6) coefficient matrix (TRIM6, TRIM6 Sub)
P		(12 x 12) matrix subsidiary to element stiffness matrix (TRIM6, TRIM6 Sub)
NCOORD		Number of nodes stationed at element vertices (TRIM6, TRIM6 Sub)
NPUNCH		Punch option.Punch output of displacements nodal stresses and polar stresses provided if NPUNCH greater than zero
Q		(3 x 12) matrix subsidiary to stress matrix (TRIM6, TRIM6 Sub)

NPART		Number of partitions (TRIM3 Sub TRIM6 Sub)
NCONC		Number of nodes having concentrated forces
THICK	t	Element thickness
NSTART(I)		First element of ith partition
NEND(I)		Last element of ith partition
NFIRST(I)		First node of ith partition
NLAST(I)		Last node of ith partition
U		Force column / displacement column (TRIM3 Sub, TRIM6 Sub)
ST/AM	[K]	Submatrix of overall stiffness matrix (TRIM3 Sub, TRIM6 Sub)
BM	[C]	Connectivity matrix (TRIM3, TRIM6 Sub)

6.1. Description of TRIM3 Finite Element Program:

MAIN PROGRAM

Function: Reads input data and co-ordinates subprograms.
Flow: MAIN calls COORD, FEM, CENT and STRESS.

Discussion: Input data includes NPOIN, NELEM, etc. which is easily deduced from the listing. The input mesh is diverted to subroutine COORD so that the mesh may be generated in some special cases. Elements may have different thicknesses and the various thicknesses are stored in matrix T. While reading the element nodal numbers, a 'tag' is placed on each element in the form of an integer which indicates in which class of thickness each element falls into. The matrix in which these 'tags' are stored is IT. The 'tags' start from zero in steps of unity. If the structure has just one thickness, the space is left blank on the data cards, and is hence read as zero.

The elasticity matrix D is calculated for an isotropic material in plane stress. The program can be used for plane strain simply by changing the D matrix for that of plane strain. Only the upper band of the stiffness matrix is stored in accordance with the discussion presented in Sec. 3.7. Prescribed displacements are handled by the method described in Sec. 3.6. Centrifugal forces, if desired, are calculated element by element and are superposed on the reactive force column F.

The system of linear equations are solved by the Choleski method which is described in Sec. 3.7 and subroutine

BMATS and SOLBS are called in that order to achieve this.

Subroutine STRESS, among other things, calculates nodal forces by a weighted averaging method.

The program may be used to solve a problem with a number of sets of applied forces simply by specifying in NCOLN the number of sets, and supplying these as additional data.

An added facility of this program is that all nodes that are rigidly fixed may be numbered zero(0). The zero numbered nodes are overlooked during assembly. This artifice saves storage space.

A search technique to used in the initial stages of the program to find the bandwidth. (see Sec. 3.7). The program included occupies 2/3 of the available storage space and can have 200 nodes and a bandwidth of 30.

SUBROUTINE FEM

Function: (1) FEM finds an element stiffness matrix, and

(2) assembles the overall stiffness matrix.

Flow: FEM is called by MAIN. Calls BMAT to find the strain-displacement matrix.

Discussion: The (6 x 6) element stiffness matrix is called OK and is calculated according to equation (3.29). The product DB, which is the stress matrix, is calculated and stored on TAPE1 for later use in calculating stresses.

The assembly of the element stiffness matrix into the 'banded' overall matrix is done by finding the global storage locations as if the entire overall matrix were to be formed.

These global locations are then transformed to the new locations in the banded structure by the use of a simple formula obtained below.

Assuming a (2 x 2) submatrix k_{ij} of an element stiffness matrix has to be assembled. The global storage locations of the submatrix are:

$$[k_{ij}] \text{ stored as } \longrightarrow \begin{array}{c c} & \begin{array}{cc} (2j-1) & (2j) \end{array} \\ \begin{array}{c} (2i-1) \\ (2i) \end{array} & \left[\begin{array}{c|c} K_{11} & K_{12} \\ \hline K_{21} & K_{22} \end{array}\right] \end{array} \tag{6.1}$$

where the K's are the elements of the submatrix.

Term K_{21} is supposedly to be stored in row $m = 2i$ and column $n = 2j - 1$.

In the banded matrix K_{21} is stored as follows,

row = n - m + 1

column = m

(The diagonals are stored row-wise).

SUBROUTINE STRESS

Function: Calculates element and nodal stresses.

Flow: STRESS is called by MAIN, and calls PRINCE to find principal stresses.

Discussion: TAPE1, on which stress matrices DB for each element has been written in subroutine FEM, is rewound. The stress matrix of each element is read in turn and the stress calculated as by equation (3.15). This, however, yields a single constant value for the entire element.

Appendix C describes a method developed by Wilson [12] which finds nodal stresses by 'weighting' the stresses of all elements connected to the node. A search is performed for each node to find the elements connected to it, and stresses found using the formulae of Appendix C. At internal nodes stresses by these formulae almost equal the normal average of the element stresses, but differ greatly at the boundaries.

Principal stresses and angle are found at each node by subroutine PRINCE. The principal angle returned is the angle between S1 and the y-axis measured counter-clockwise positive.

The nodal point stresses are then transformed to the polar system by the formulae given in Appendix D.

SUBROUTINE BMATS

Function: To decompose a banded symmetric matrix into a product of lower triangular and upper triangular matrices.

Flow: BMATS is called by the MAIN program.

Discussion: Only the upper triangular banded coefficients of the stiffness matrix SK are input to BMATS through array BAND. BMATS decomposes, remaining within the bandwidth, and returns only the upper triangular form in array BAND. Subroutine SOLBS uses this upper triangular form to solve for the unknown quantities.

SUBROUTINE SOLBS

Function: To solve the equation $(R_L R_U)x = B$ for X, given R_U and B, and $A = R_L R_U$ is symmetric.

Flow: SOLBS is called from the MAIN program after BMATS had been called.

Discussion: Input to SOLBS is the upper triangular decomposition R_U of A and the constant column B. If $Z = R_U X$, then $R_L Z = B$ is solved for Z by first determining R_L from R_U (since A is symmetric) then using direct substitution. $R_U X = Z$ is then solved for X by backward substitution. R_U is input to SOLBS in banded form.

6.2. Description of TRIM6 Finite Element Program

The theory concerning the TRIM6 element is developed in Chapter 3. The sequence of operations in this program is as shown in the flow diagram of Fig. 6.1. It has already been mentioned that the main program differs slightly from the TRIM3 main program but the subprograms change completely. The method of assembly is the same as in the previous program though the element stiffness matrix size is doubled. Also, the basic character of the overall stiffness matrix is the same and the system of linear equations are solved by the same method.

The subroutines that change are: FEM, CENT and STRESS. These are described as follows.

SUBROUTINE FEM

Function: (1) To find element stiffness matrix

(2) To assemble element stiffness matrix in overall stiffness matrix.

Flow: FEM is called by MAIN for each element. Uses library subroutine INVMAT to invert matrix C. Uses a function subprogram CR.

Discussion: A local co-ordinate system located at the element centroid is used. The co-ordinates of the midside nodes are generated from the vertex nodes, and the six co-ordinates are transformed to the local system.

The (6 x 6) coefficient matirx C is found as defined by equation (3.43a), and inverted by subroutine INUMAT. The inverted matrix C^{-1} is stored on TAPE2 for later use in finding centrifugal forces and in stress calculations.

The elements of the lower triangle of matrix P (equation 3.53) are calculated and stored row by row in a column vector, each row ending at the diagonal element. All the first order terms in this matrix vanish (upon integration) because of the choice of co-ordinate system.

The submatrix formulation of equation (3.59) is used to find the (2 x 2) submatrices of the element stiffness matrix. Only the submatrices that are located in the upper triangle of the overall matrix are calculated and directly superposed. Because storage location is only a function of the nodal numbers, this portion is identical to the TRIM3 case, except that the loop is done 6 times instead of 3.

C_r and C_s are (12 x 12) submatrices of C_T^{-1} (see equations 3.57 and 3.44) and FUNCTION CR returns the elements of these submatrices by proper correlation of the elements* of C^{-1} and C_T^{-1}.

SUBROUTINE STRESS

Function: Calculation of centroidal, nodal, polar and principal stresses.

Flow: STRESS is called from MAIN. STRESS calls subroutines SIGMA and PRINCE.

Discussion: Equation (3.60) is used by subroutine SIGMA which returns three stresses at a point given the co-ordinates of the point with respect to the local system and the constant matrix C^{-1} of the element which contains the point.

Centroidal stresses are first calculated for each element. Mass storage TAPE2 is recalled to obtain C^{-1} and the nodal quantities which had previously been calculated in subroutine FEM. Principle stresses at the centroids are calculated by subroutine PRINCE.

As mentioned in Chapter 3, there is a discontinuity

* The term "elements", depending on the context in which it is used, may either mean finite elements or terms in a matrix.

in stress between adjacent element. In order to find nodal stress, the trick used in this program is to conduct a search to find all elements connected to the node in question, and to take an average of the stresses which each respective element yields. Again, principal stresses and principal angles at the nodes are calculated by subroutine PRINCE.

Finally, radial and tangenital stresses with respect to the polar system are calculated at the nodes by the transformations given in Appendix D.

SUBROUTINE SIGMA

Function: SIGMA finds stresses at a point, given the co-ordinates of the point with respect to the local co-ordinate system at the centroid of the element which contains the point, and the constant matrix $[C^{-1}]$ of the element.

Flow: SIGMA is called by STRESS which is called by MAIN. SIGMA calls QMAT and QCMAT.

Discussion: The formula used is (3.60). Matrix Q, defined in equation (3.45), is first found by subroutine QMAT. Q is a function of the co-ordinate of the point at which the stresses are wanted. The product of Q and C_T^{-1} is then formed by subroutine QCMAT, which uses FUNCTION CR to correlate C^{-1} to C_T^{-1}.

The three stresses are yielded by premultiplying QC by the elasticity matrix D.

SUBROUTINES BMAT and SOLBS

These are the same as in the TRIM3 program.

CHAPTER 7

METHOD OF SUBSTRUCTURES OR PARTITIONS

7.1. General Formulation of Method:

In this method the basic overall stiffness matrix of a system is partitioned into a number of submatrices in such a way that these form a tridiagonal system of submatrices. This does not alter the character of the stiffness matrix but allows the solution of the system of equations to be done part by part. Storage space of only one partition has to be maintained, with the result that it is possible to have as many partitions as desired depending on computer time allowed. The method is explained by means of an example.

Fig. 7.1 shows a finite element idealization (using TRIM3 elements) of a plate in uniform tension. Fig. 7.2 shows a skeleton of the overall stiffness matrix for the problem. The hatched portion signifies the bandwidth beyond which the terms are all zero. The matrix is arbitrarily partitioned into submatrices as indicated by the solid-lined rectangles. These are named K_I, C_I, K_{II}, C_{II} etc. It is seen that the K's are symmetric. Also C^T can be obtained from C and does not have to be stored.

The physical meaning of partitioning the stiffness matrix into these submatrices is seen by referring to Fig. 7.1. Since submatrix K_I is of size (44 x 44), it includes the first 22 nodes sectioned off by partition line I. Submatrix K_{II} includes

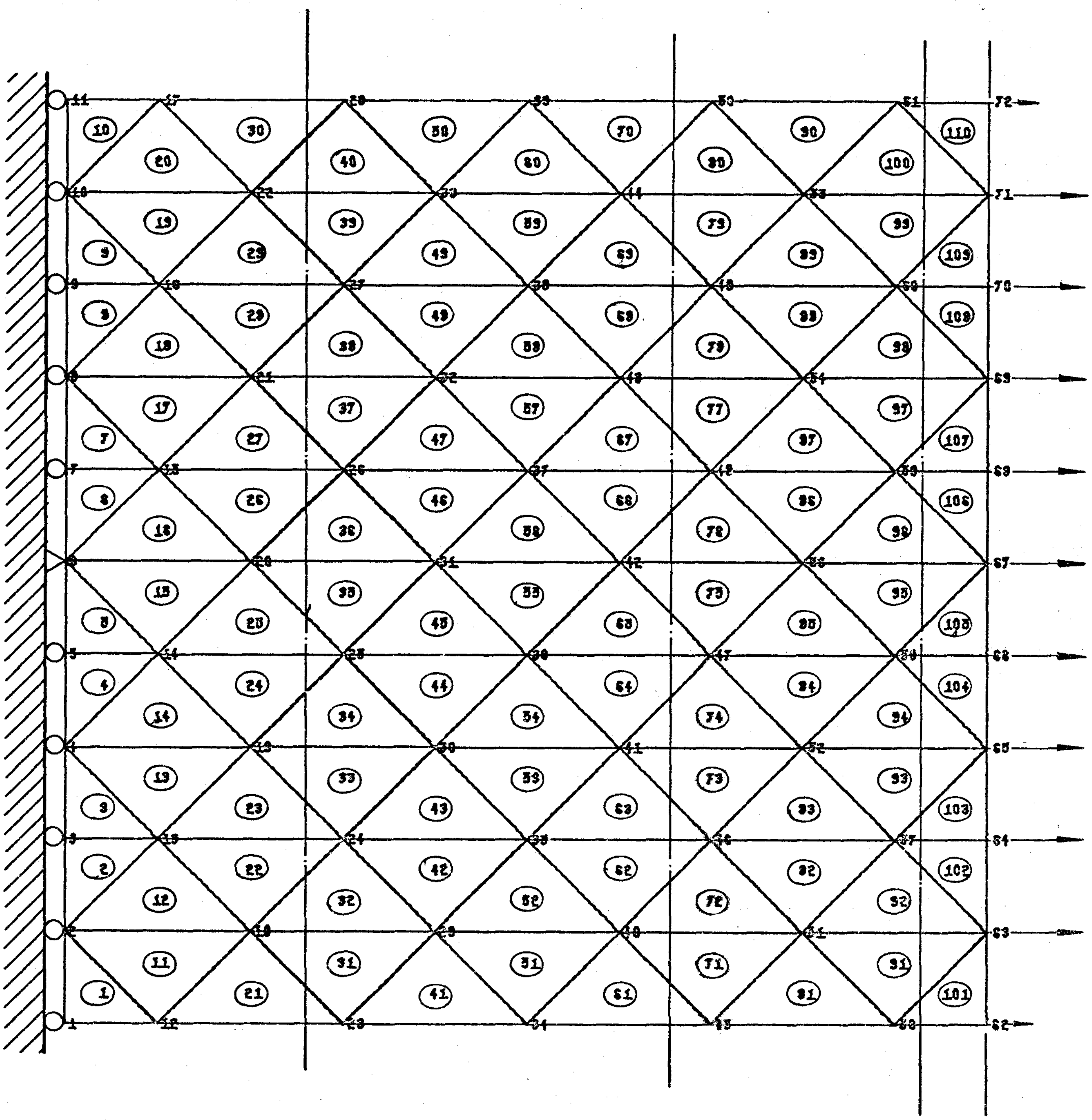

FIG. 7.1 TRIM3 Finite Element Idealization of a Square Plate With Uniform Loading in x-direction Showing Physical Partitioning Lines.

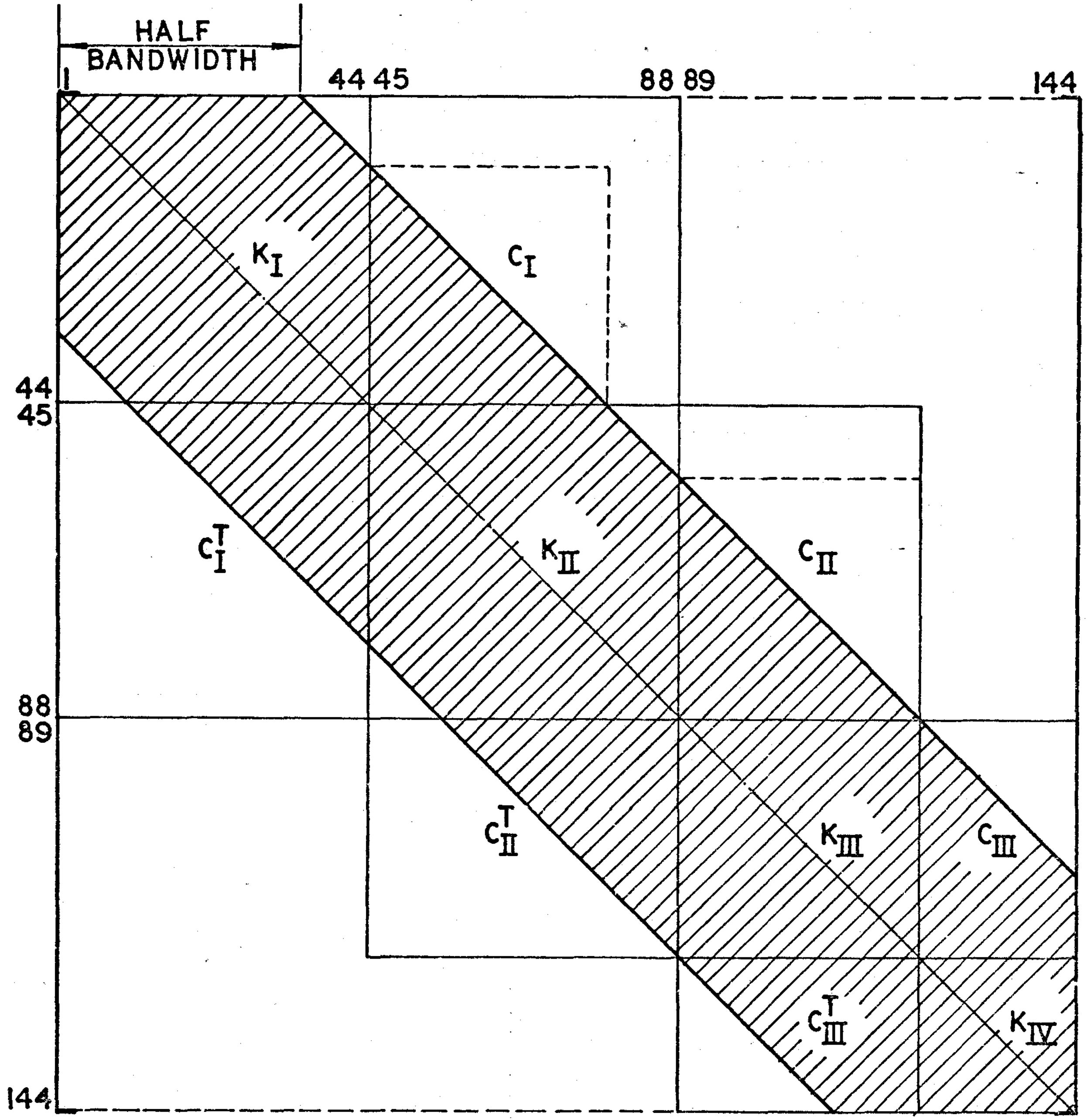

FIG. 7.2 Overall Stiffness Matrix for the Problem Shown in Fig. 7.1, Partitioned Into Submatrices.

nodes 23 to 44, i.e. the section of the structure between lines I and II. The partitioning lines effectively divide the structure into 'substructures'. The connection between the substructures is achieved mathematically by the 'connectivity' matrices C. For example, the last term in K_I is stiffness $K_{44,44}$ (stiffness of node 22); node 25 falls into the second substructure and the relative stiffness between nodes 24 and 25 ($K_{44,45}$) is contained in C_I.

In this example, the submatrices were formed first, then the partitioning lines. In practice, one sections off the structure first.

7.2. Solution of Equations:

The displacement and force columns are partitioned into submatrices in the same manner in which the stiffness matrix is partitioned. The sizes of these submatrices are determined by the number of nodes in the respective partitions, for example, the displacements of nodes 1 to 22 are included in submatrix δ_I in the example of sec. 7.1.

For this example, the stiffness relation in 'tridiagonalized' partitions is,

$$\begin{bmatrix} K_I & C_I & 0 & 0 \\ C_I^T & K_{II} & C_{II} & 0 \\ 0 & C_{II}^T & K_{III} & C_{III} \\ 0 & 0 & C_{III}^T & K_{IV} \end{bmatrix} \begin{Bmatrix} \delta_I \\ \delta_{II} \\ \delta_{III} \\ \delta_{IV} \end{Bmatrix} = \begin{Bmatrix} F_I \\ F_{II} \\ F_{III} \\ F_{IV} \end{Bmatrix} \qquad (7.1)$$

The first two matrix equations can be written out in full as,

$$[K_I]\ \{\delta_I\} + [C_I]\ \{\delta_{II}\} = \{F_I\}$$

$$[C_I]^T\ \{\delta_I\} + [K_{II}]\ \{\delta_{II}\} + [C_{II}]\ \{\delta_{III}\} = \{F_{II}\}$$

Solving for δ_I in the first equation,

$$\{\delta_I\} = [K_I]^{-1}\ F_I - [K_I]^{-1}[C_I]\ \{\delta_{II}\} \qquad (7.2)$$

Substituting this in the second equation,

$$([K_{II}] - [C_I]^T[K_I]^{-1}[C_I])\{\delta_{II}\} + [C_{II}]\ \{\delta_{III}\}$$

$$= \{F_{II}\} - [C_I]^T[K_I]^{-1}\{F_I\} \qquad (7.3)$$

Or, by defining new symbols

$$[K_{II}] = ([K_{II}] - [C_I]^T[K_I]^{-1}[C_I]) \qquad (7.3a)$$

$$[F_{II}] = \{F_{II}\} - [C_I]^T[K_I]^{-1}\{F_I\} \qquad (7.3b)$$

equation (7.3) may be written as,

$$[K_{II}]\{\delta_{II}\} + [C_{II}]\{\delta_{III}\} = \{F_{II}\} \qquad (7.4)$$

From equation (7.4) δ_{II} can be solved for and substituted in the next row equation to give modified K_{III} and F_{III}. Such a process of substitution and elimination is continued to the last row equation, which yields

$$[K_{IV}]\{\delta_{IV}\} = \{F_{IV}\} \qquad (7.5)$$

whence a direct inversion yields δ_{IV}. In general, for N submatrix rows, the last equation reads,

$$[K_N]\{\delta_N\} = \{F_N\} \tag{7.6}$$

The other displacement submatrices are obtained by backward substitution.

Notes:

With reference to Fig. 7.2, it is noticed that K_I, K_{II} etc. are symmetric and it is thus necessary only to store the symmetric parts of the matrices.

Also, with regard to the connectivity matrices C, it is necessary only to store the elements blocked off by dotted lines.

These observations are used to effect in the computer programs using the method of partitions. This involves an additional amount of book-keeping because it is necessary to keep track of the new storage locations in relation to what they should be in reality. However, this pays off in substantial storage saved.

7.3. Description of Program for Method of Partitions Using the TRIM3 Element.

The calculations of the element stiffness matrices, the centrifugal forces and the nodal stresses are done in the same way as the basic TRIM3 program as the basic formulae are the same.

The step by step method, however, necessitates a different sequence in the Main Program, and also a different method of solution. Appendix E has a listing of the entire program, but only the Main Program and Subroutine Solve are described in this section.

The significance of the Fortran variables are described in Table 6.1. Fig. 7.3 shows a flow diagram of operations for the Main Program.

MAIN PROGRAM

Function: Reads input data and co-ordinates subroutines.

Flow: MAIN calls COORD, CENT, FEM, SOLVE and STRESS.

Discussion: The input of data is best described by means of sample output on the next page. This output pertains to the example in Sec. 7.1.

Elements through which a sectioning line pass are included twice, once at the end of one partition and again at the beginning of the next partition. The reason for this will be clear if the first two partitions in Fig. 7.2 are considered. The first time round the elements through which section line I passes are required to calculate elements in C_I, and the second time round to calculate elements in K_{II}. The two nested DO loops shown in Fig. 7.3 perform the crux of the main program. By means of a search the size of connectivity matrix BM is found. (see note in Sec. 7.2).

Fig. 7.3. Flow diagram for finite element program using method on partitions

RUN

READ AND PRINT
INPUT DATA

INPUT MESH — SUBROUTINE COORD

SUPERPOSITION OF CENTRIFUGAL FORCES — SUBROUTINE CENT

OUTER LOOP INCREASES
PARTITION NUMBER

SEARCH FOR FINDING
SIZE OF CONNECTIVITY MATRIX

INNER LOOP INCREASES
ELEMENT NUMBER

FORMATION OF ELEMENT STIFFNESS MATRIX — SUBROUTINE FEM

ASSEMBLY OF OVERALL STIFFNESS
MATRIX AND CONNECTIVITY MATRIX

INTRODUCTION OF
PRESCRIBED DISPLACEMENTS

SOLUTION OF SYSTEM OF EQUATIONS — SUBROUTINE SOLVE

CALCULATION OF STRESSES — SUBROUTINE STRESS

STOP

For each partition, the stiffness submatrix, connectivity matrix and force submatrix are stored on TAPE4 and later used in SOLVE for the solution of the tridiagonal system of submatrix equations.

Subroutine STRESS finds element stresses, average nodal stresses and polar stresses.

SUBROUTINE SOLVE

Function: Solves tridiagonal system of matrix equations by elimination and backward substitution.

Flow: Called by MAIN which transfers stiffness and connectivity submatrices of all partitions on TAPE4.

Discussion : Basically, this subroutine consists of two DO loops. The first loop does the elimination and the second loop the backward substitution.

For each partition, 'modified' stiffness and force submatrices are calculated using the following formulae.

$$[K_N] = [K_N] - [YM_{N-1}] \tag{7.7}$$

where

$$[YM_{N-1}] = [C_{N-1}]^T[K_{N-1}]^{-1}[C_{N-1}] \tag{7.8}$$

$$\{F_N\} = \{F_N\} - \{TF_{N-1}\} \tag{7.9}$$

where

$$\{TF_{N-1}\} = [C_{N-1}]^T[K_{N-1}]^{-1}\{F_{N-1}\} \tag{7.10}$$

N is the partition number. Matrices YM and TF are initialized (when N = 1) to zero. Also,

$$K = AM$$

$$C = BM$$

As mentioned earlier, only parts of K and C are stored. The parts stored are clarified in Fig. 7.4 which is the first row of the system of matrix equations. Fig. 7.4 also indicates the meanings of the relevant variables.

The inversion of the K matrices (equation 7.8) is done by library subroutine INUSYM which inverts symmetric matrices.

Given row and column numbers, FUNCTION BMAT returns the correct elements of C by extracting the proper element from the portion stored. BMAT is a 'bookkeeping' subprogram.

The triple product in equation (7.8) is performed as shown in Fig. 7.5. The program is organized so that YM uses the storage area of PYM. Matrices K^{-1} and C^{-1} are written on TAPE2 for use in the backward substitution.

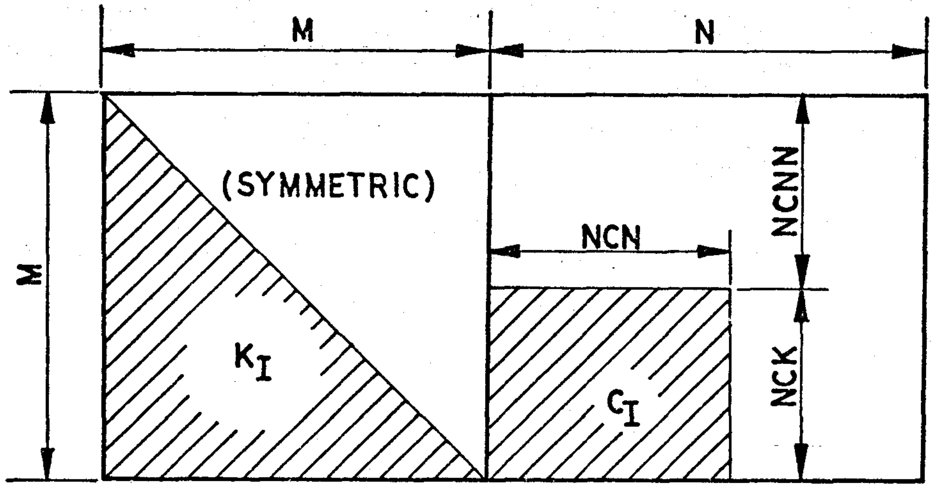

FIG. 7.4 First Submatrix Row of Stiffness Matrix. Only the Shaded Parts are Stored.

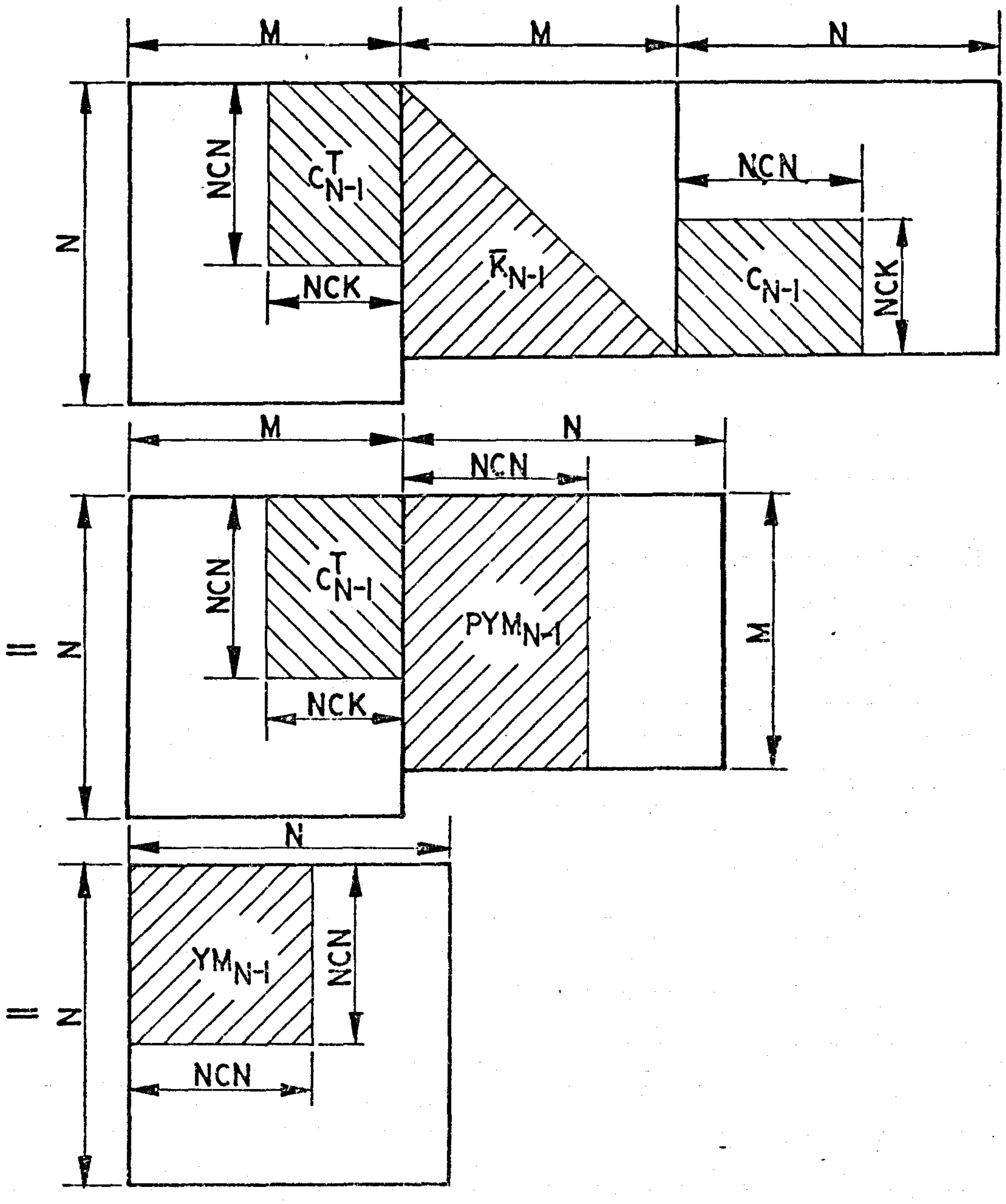

FIG. 7.5 Matrix Triple Product of Equation (7.8). The Shaded Areas Show the Computer Storage Areas Maintained.

INPUT DATA

TOTAL NUMBER OF PARTITIONS-NPART=	4
TOTAL NUMBER OF NODAL POINTS-NPOIN=	72
TOTAL NUMBER OF ELEMENTS-NELEM=	110
TOTAL NUMBER OF NODAL POINTS WITH PRESCRIBED DISPLACEMENTS-NBOUN=	11
TOTAL NUMBER OF LOAD VECOTRS-NCOLN=	1
NUMBER OF POINTS WITH CONCENTRATED LOADS=	11
PLANE THICKNESS-THICK=	1.0000000E+00

PARTITION	1ST ELEMENT	LAST ELEMENT	1ST NODE	LAST NODE
1	1	40	1	22
2	21	80	23	44
3	61	110	45	61
4	91	110	62	72

PRESCRIBED DISPLACEMENTS

NODE	X-DISPLACEMENT	Y-DISPLACEMENT
1	-0.	
2	-0.	
3	-0.	
4	-0.	
5	-0.	
6	-0.	-0.
7	-0.	
8.	-0.	
9	-0.	
10	-0.	
11	-0.	

PRESCRIBED FORCES

NODE	X-FORCE	Y-FORCE
62	1.0000000E+03	-0.
63	2.0000000E+03	-0.
64	2.0000000E+03	-0.
65	2.0000000E+03	-0.
66	2.0000000E+03	-0.
67	2.0000000E+03	-0.
68	2.0000000E+03	-0.
69	2.0000000E+03	-0.
70	2.0000000E+03	-0.
71	2.0000000E+03	-0.
72	1.0000000E+03	-0.

7.4. Description of Program for Method of Partitions Using the TRIM6 Element:

The theory for the method of partitions developed in sections 7.1 and 7.2 applies to a general finite element, and hence also to the TRIM6 element. The general procedure of this program is similar to the TRIM3 program and the flow diagram of Fig. 7.3 also applies here. Solution of equations is again achieved in Subroutine SOLVE. However, the element stiffness matrix and stress matrix is adapted for the TRIM6 element from the basic program. Assembly of the overall stiffness matrix differs in the respect that stiffness with respect to 6 nodes is catered for. Centrifugal forces are calculated by the same subroutine as in the basic TRIM6 program.

With this program large structural problems can be solved and has the added advantage of an improved element. Again, there is the proviso that the structure must be simply connected.

CHAPTER 8

TEST CASES FOR FINITE ELEMENT PROGRAMS

Many test cases were run in order to check the programs and to get familiar with the method. The finite element program returns large sets of numbers which describe variations at scattered points, called nodes, and experience with the method is necessary in order to correctly interpret the results. The two aims mentioned above are achieved by solving certain problems to which exact solutions are available using the theory of elasticity. Some of them are discussed below.

Each test case was run for both TRIM3 and TRIM6 element types. Although not discussed below, the same test cases were run on the programs using the method of partitions. The results were found to be identical in each class (of element type).

8.1. Case 1: Square Plate in Plane Stress. TRIM3 Element

Description: Figs. 8.1(a) and (b) show 8 elements idealizations of the plate under two types of loading conditions. The uniform loads shown in dotted lines were discretized to concentrated forces on the nodes. The displacement boundary conditions were chosen to prevent rigid body motion and to allow uniform displacements (node 1 and 3 on rollers in y-direction).

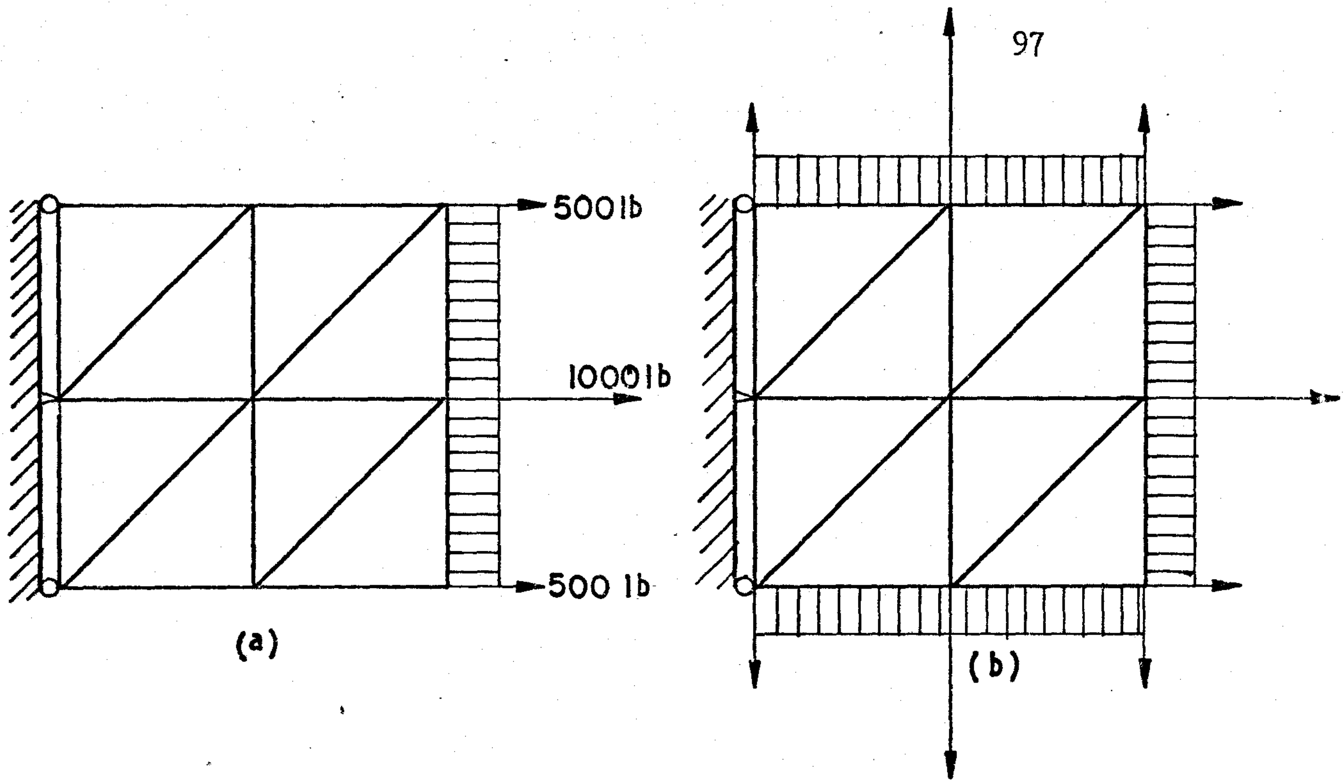

FIG. 8.1(a) Uniform Tension and (b) Hydrostatic Tension of Square Plate.

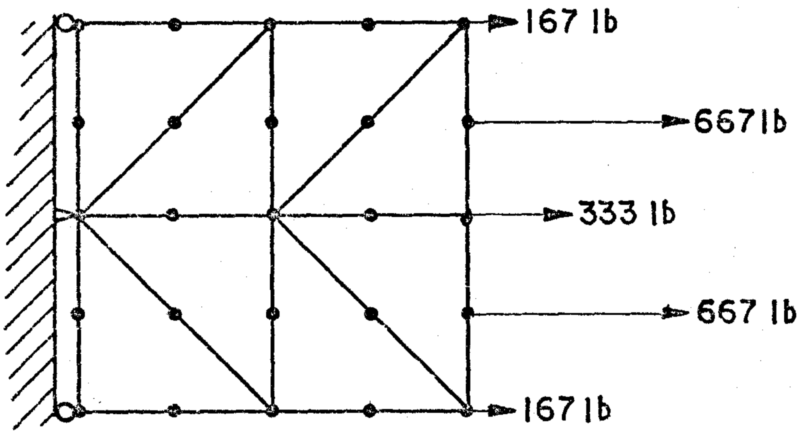

FIG. 8.2 TRIM6 Idealization of a Plate in Uniform Tension.

Discussion:

The displacements obtained show that the sides of the plate remain traight after deformation. Also, the displacements are symmetric about the center-line of the plate. For case 1(a) Poisson's ratio effect checks out as defined by the formula:

$$\frac{\text{Net lateral shrinkage}}{\text{Net longitudinal elongation}} = \frac{4.0\ \text{E} - 5}{1.33\ \text{E} - 4} = 0.3$$

This ratio is the Poisson's ratio assumed for steel.

From the element and nodal stresses it can be seen that constant stress conditions are achieved throughout the plate. The reactive forces are equal to, and opposite to, the applied forces, showing that numerical errors in computation are minimal. The stresses of case 1(b) checks the fact that hydrostatic tension produces zero shear.

8.2 Case 2: Square Plate in Plane Stress. TRIM6 Element:

Description: Fig. 8.2 shows an 8 element idealization of the same plate as in Case 1, using TRIM6 elements. The uniform load was discretized to nodal force by the consistent method described in Chapter 4. One node on the left side was fixed and the others were placed on rollers to allow freedom of motion in the y-direction.

Discussion:

Again a constant stress condition exists throughout the plate. According to the displacement, sides remain straight after deformation. The net displacement of the plate in the x-direction is 1.33 E - 4, which is exactly the same value obtained by the formula $u = PL/AE$.

8.3. Case 3: Uniform Tension of a Plate with a Control Hole TRIM3 Element

Description: See Fig. 101(a). Because of geometric and loading symmetry about both axes, it was necessary only to analyse a quarter of the plate. This section measured 5 in x 5 in x 1 in, with a hole radius of 1/4 in. A uniform load of 1000 psi was applied in the x-direction. The sides on the axes were placed on rollers as shown in the diagram.

Discussion:

Rigid fixing of nodes is not necessary as the displacement boundary conditions prevent rigid body motion.

The concentrated loads applied were again found by the consistent method. The break-up consists of 89 TRIM3 elements.

Stresses at the nodes were obtained by Wilson's weighted averaging method discussed in Appendix C. Fig. 8.3 shows a comparison of the normal stress in the x-direction with

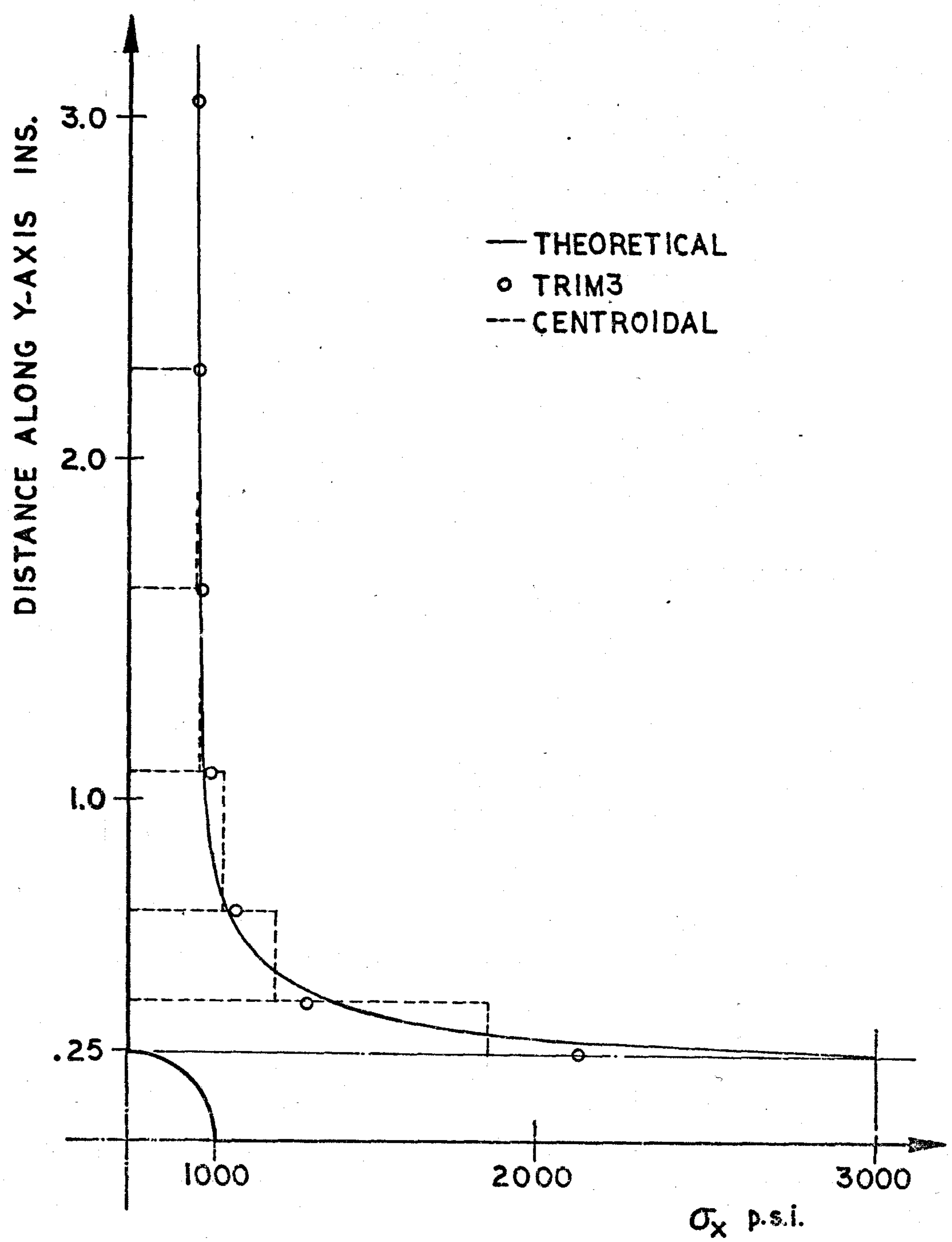

FIG 8.3 Comparison of TRIM3 Finite Element Solution with Theory for the Case of a Plate with a Central Hole Under Uniform Tension.

the theoretical stress (ref. [13]) along the y-axis in the vicinity of the hole. The circled points are nodal stresses obtained by the finite element method. A 'histogram' of elememt stresses is inscribed in Fig. 8.3 with dotted lines. Each step extends over one interval of element sub-division, and the stress pertaining to each step was found by taking an average of two elements which form a quadrilateral on that interval. A fair picture of the stress distribution would be obtained if a line was passed through the center of each step. However, a histogram of this type cannot be drawn to use in the interior of the structure.

It is obseverd, from the nodal point stresses, that the TRIM3 element is not very effective in the region of the steep stress gradient. The maximum error (at the hole edge) is 29.3 percent.

8.4. Case 4: Uniform Tension of a Plate with Central Hole TRIM6 element

Description: Fig. 8.4 shows the TRIM6 element idealization of 1/4 of a square plate having a 1/2 in central hole. The other dimensions were the same as in Case 3. The loading was again 1000 psi.

Discussion:

The plate was divided into 70 TRIM6 elements. The nodes on the axes were placed on rollers as shown in Fig. 8.4

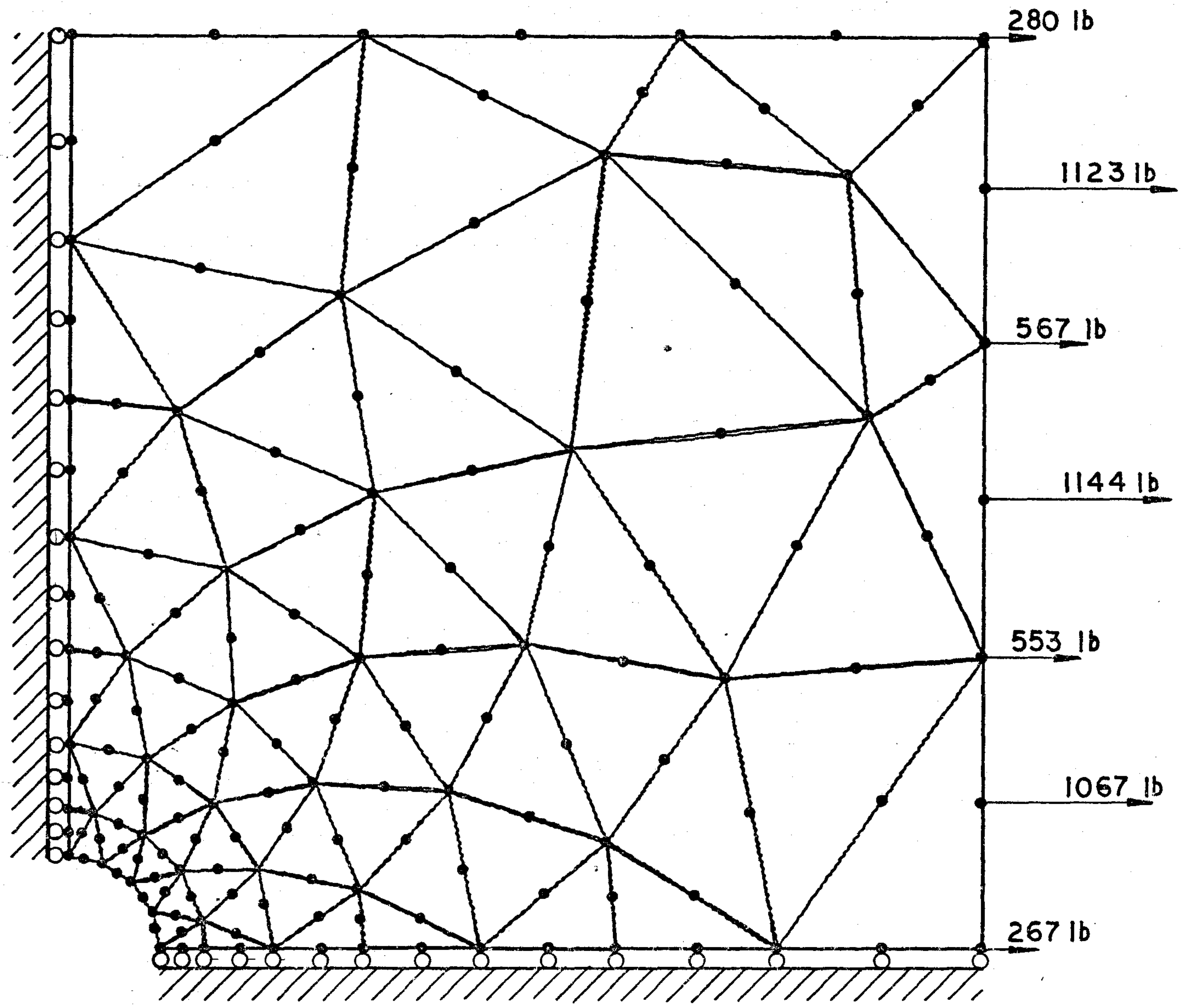

FIG. 8.4 Seventy TRIM6 Element Idealizations of 1/4 of a Square Plate with a Central 1/2 in Dia. Hole. (165 Nodes).

and concentrated nodal forces were calculated by the consistent method. Fig. 8.5 shows a comparison of the theoretical (ref. [13]) and finite element solutions of the normal stress along the y-axis in the region of the hole.

As can be seen, the TRIM6 element behaves very favourably in the region of the high stress gradient. A maximum error of 9.3 percent occurs at the hole edge.

8.5. Cases 5 and 6: Rotating Hollow Disk. TRIM3 and TRIM6

Description: This problem was solved using both element types, Case 5 using the TRIM3 element and Case 6 using the TRIM6 element. The dimension of the disk were as follows:

inner radius	1/2 in
outer radius	3 in
disk thickness	1/2 in

The rotational speed of the disk was 1000 rpm.

Discussion:

These two cases were run in order to check the theory of Chapter 5 in which equivalent nodal forces to replace centrifugal forces is discussed.

No forces other than centrifugal forces act on the disk. Because the geometric shape and the centrifugal force distribution is symmetric about both axes, only a quarter of the disk was analysed.

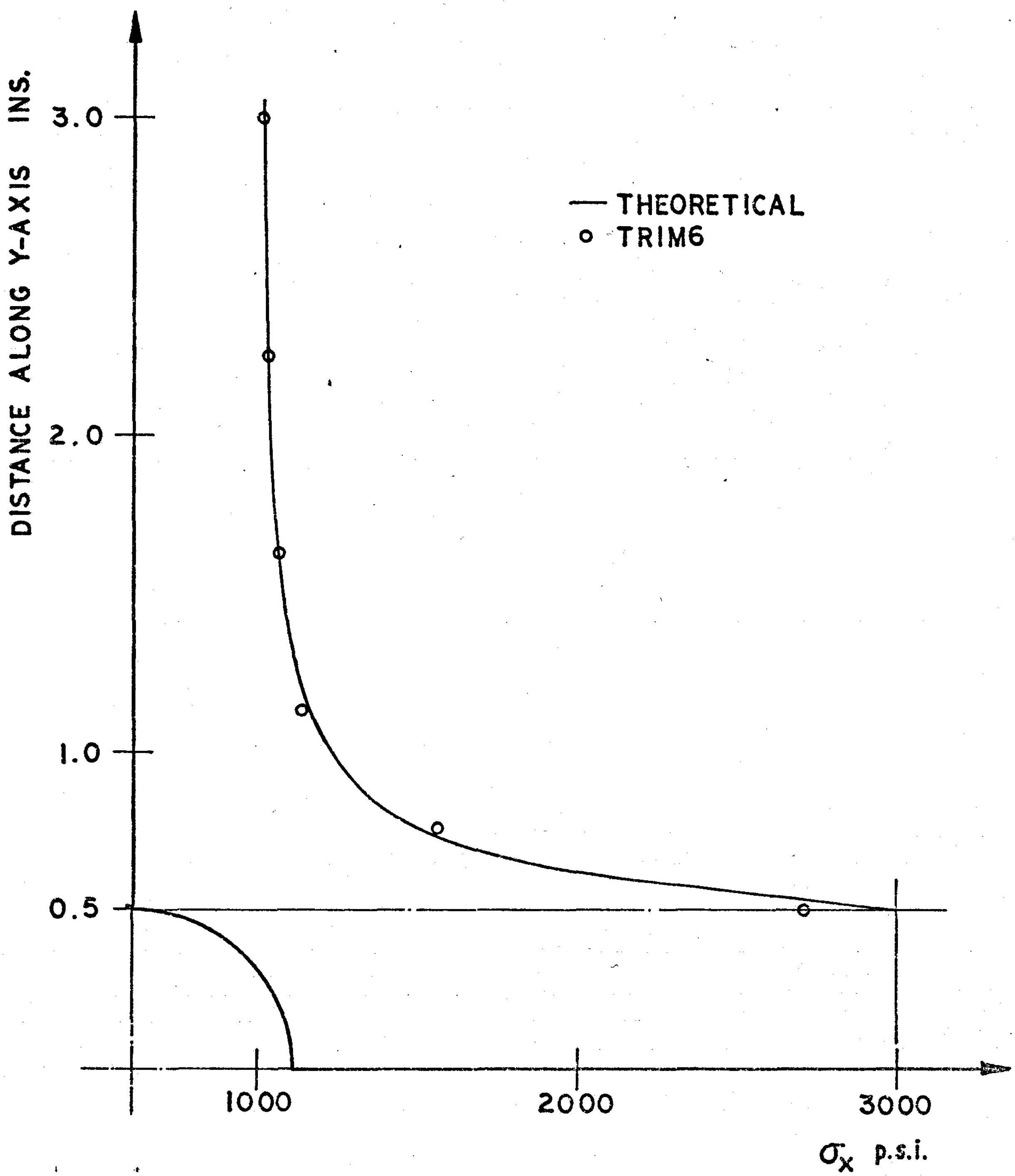

FIG. 8.5 Comparison of TRIM6 Finite Element Solution with Theoretical Solution for Stresses Along Center-line of a Holed-Plate in Uniform Tension.

The disk was basically treated as a static problem and centrifugal forces calculated by SUBROUTINE CENT were superposed on each of the nodes.

The finite element idealizations of the 1/4 disk are shown in Figs. 8.6 and 8.7 for the respective element types. The mesh sizes are as follows:

TRIM3 idealization, 168 elements, 104 nodes

TRIM6 idealization, 45 elements, 110 nodes.

Because of the symmetry discussed above, radial lines lying along the x and y axes will not distort. Therefore, nodes lying on these radial lines were placed on rollers to allow freedom of motion in the respective directions, as shown in Figs. 8.6 and 8.7.

An exact solution to this problem exists in many texts on the theory of elasticity and is shown in Fig. 8.8 together with the finite element solutions. The points indicated are average stresses at the nodal points. The agreement of the finite element solutions with the exact so ution is seen to be very good. Because the stress gradients are not great, the solution by the TRIM3 element does not differ by much from the exact, except the number of nodes had been made approximately equal in the two finite element solutions. The number of elements, however, are much less in the TRIM6 case. This points to the one disadvantage of the TRIM6 element, which is the error

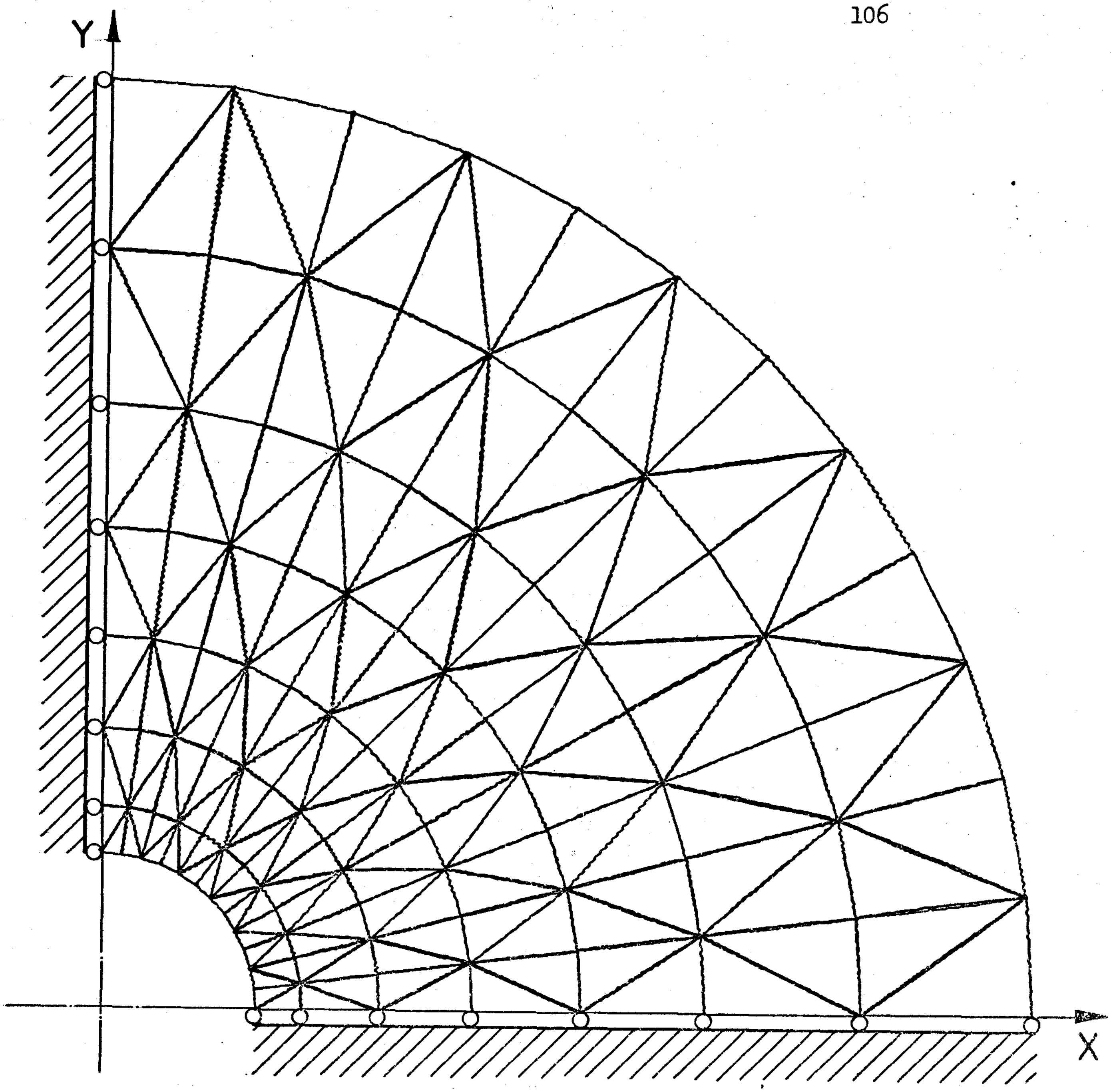

FIG. 8.6 TRIM3 Element Idealization of Quarter Section of a Hollow Disk Loaded by Centrifugal Forces Only.

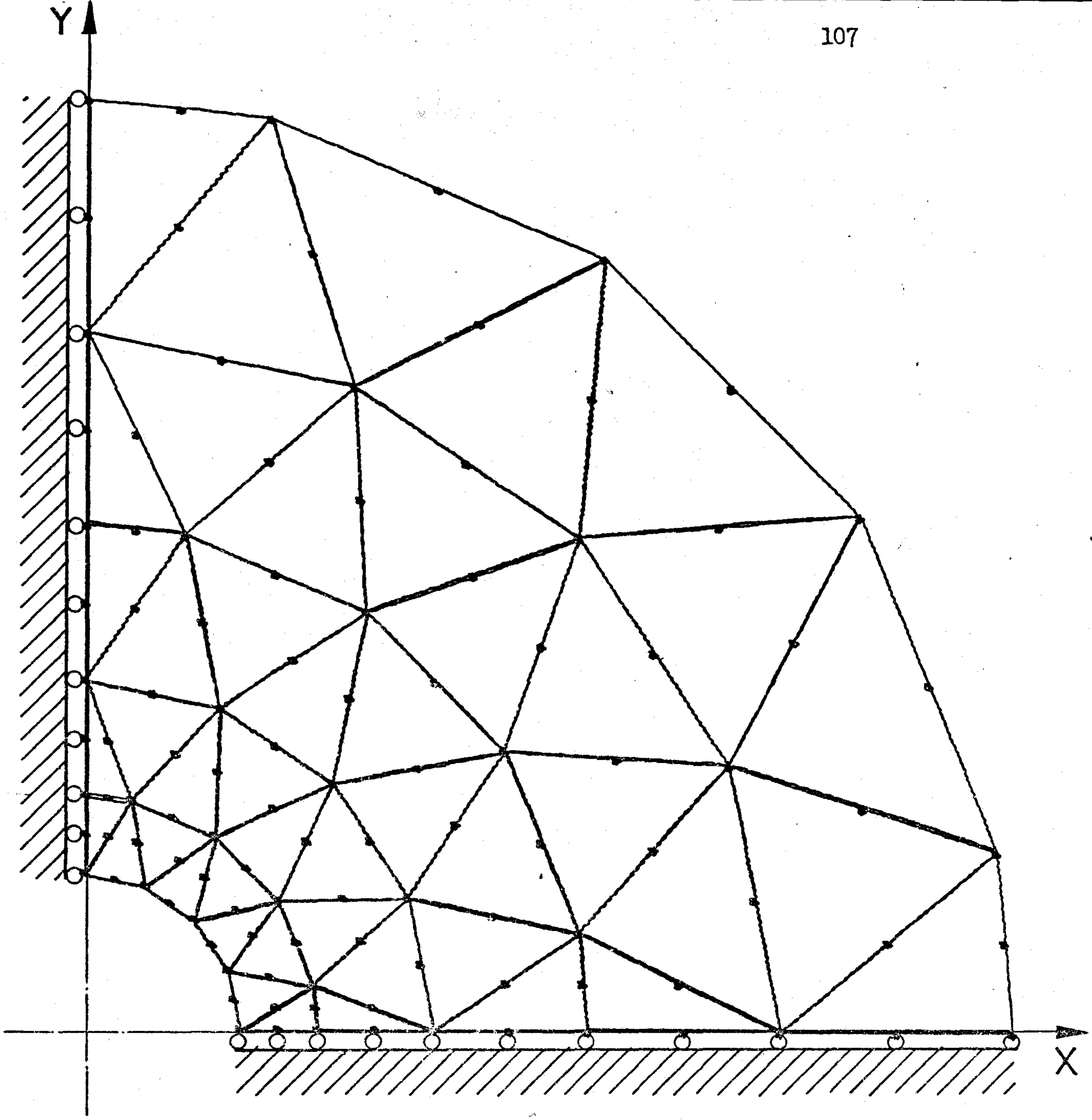

FIG. 8.7 TRIM6 Element Idealization of a Quarter Section of a Hollow Disk Under Centrifugal Forces.

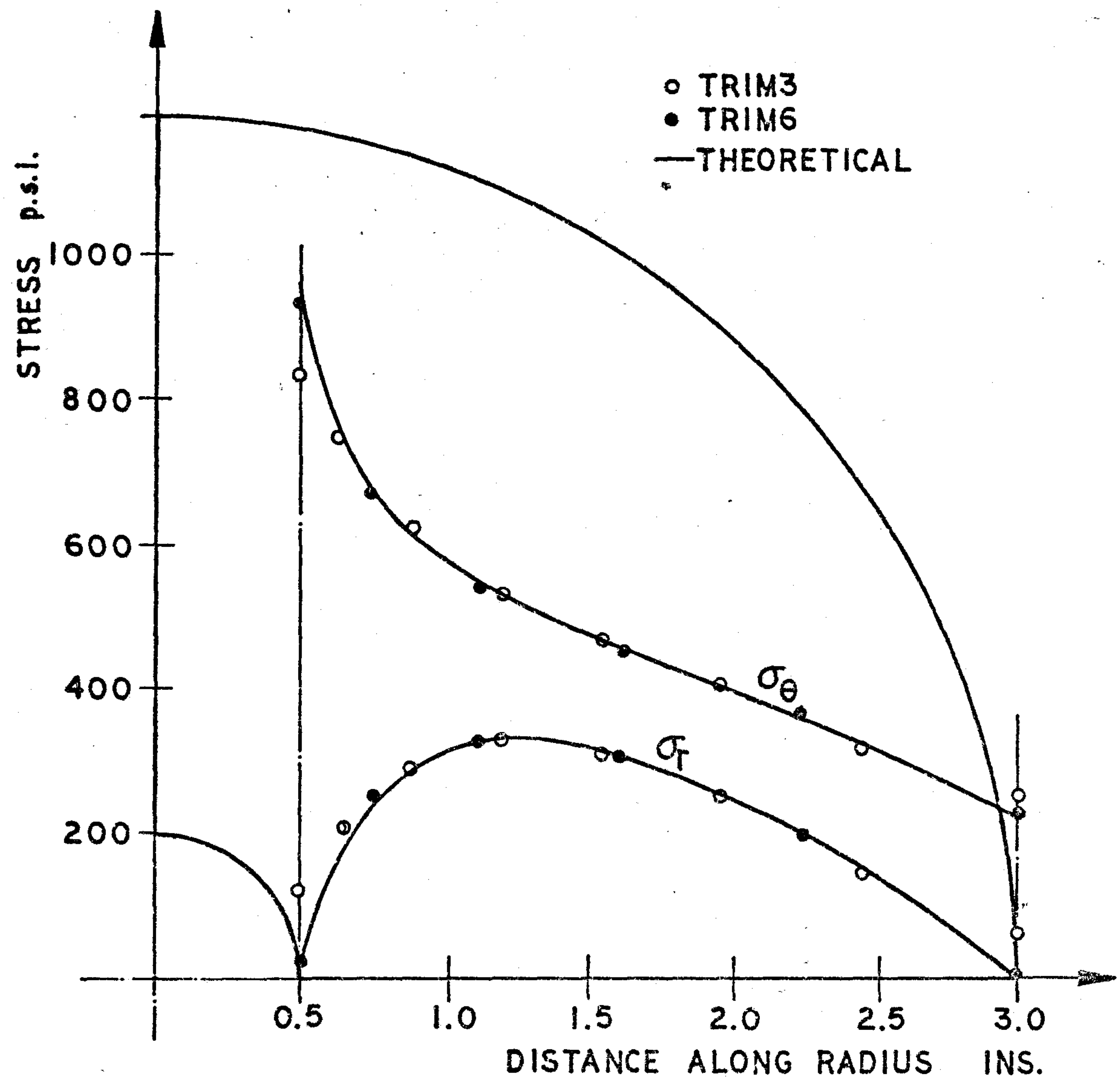

FIG. 8.8 Radial and Tangential Stresses Found by the Finite Element Method TRIM3 and TRIM6 Idealizations Compared with Theoretical Stresses.

due to the physical approximation of the boundary. For the same number of boundary nodes, the TRIM3 elements fit the boundary better than the TRIM6 elements. Nevertheless, this drawback of the TRIM6 element is more than sufficiently compensated for by the improved stress distribution within the elements.

8.6. Cases 7 and 8: Cantilever Beam in Bending. TRIM3 and TRIM6 Element

Description: A square section cantilever of length 10 in and depth 1 in was solved using the two element types in order to compare displacements. The inset on Fig. 8.9 shows the mesh break-up of the beam for the two cases. A shear load of 5 lb was applied at the free end.

Discussion:

The nodes were kept approximately the same for the two cases. The nodes at the built-in end of the cantilever were rigidly fixed.

Fig. 8.9 also shows the deflection of the beam along its length for the two cases as compared with beam theory. Although the mesh using the TRIM3 elements is much finer, the approximation is very poor. Theoretically, displacements vary with the cube of the length, whereas the TRIM3 element interpolates with linear functions. The higher order displacement function for the TRIM6 element is indeed superior for this case.

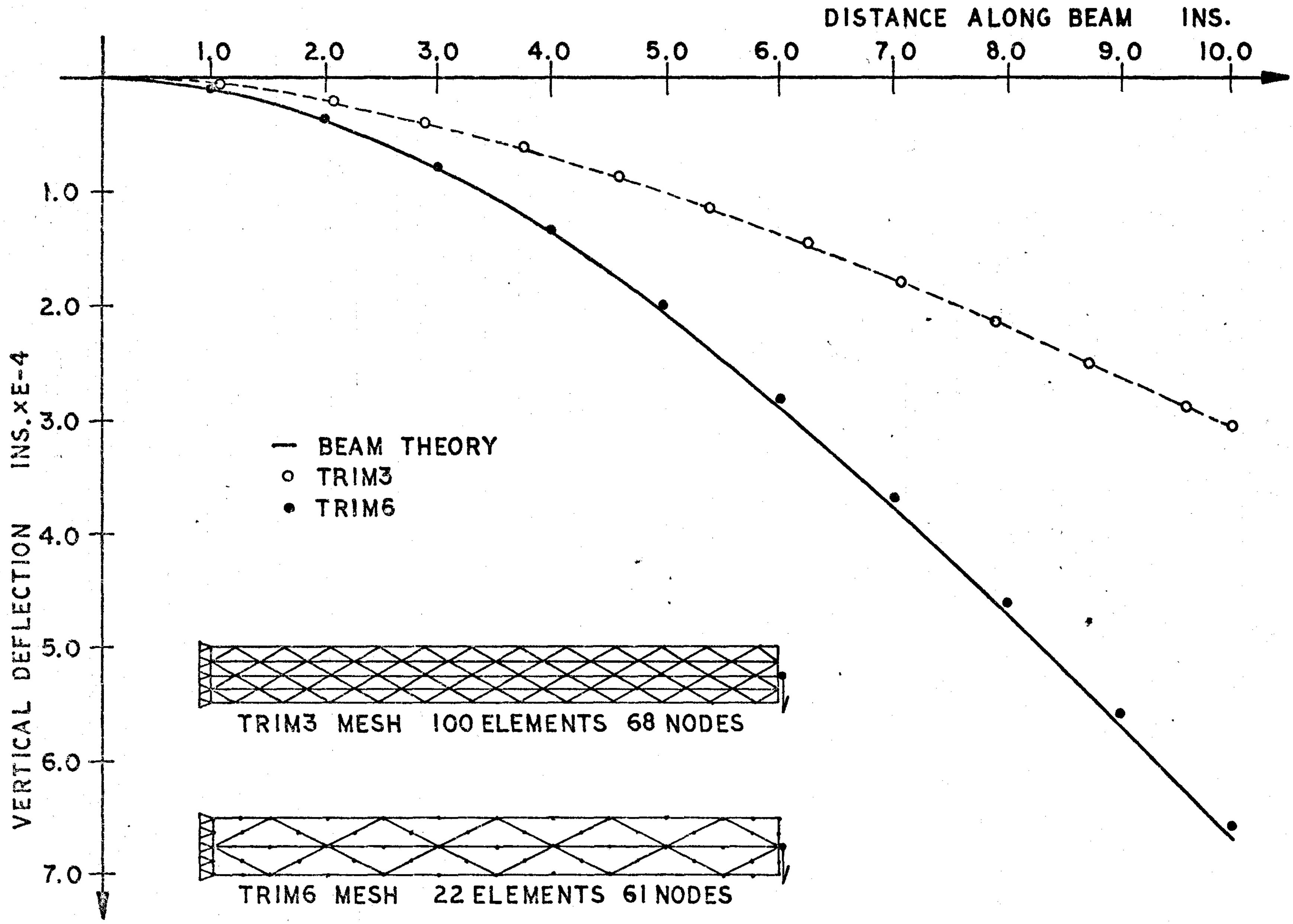

FIG. 8.9 Displacement Solutions by TRIM3 and TRIM6 Finite Element Idealizations Compared with Beam Theory for a Cantilever Loaded by a Shear Load of 5 lb.

8.7. General Discussion of Test Cases:

(i) One of the criteria for convergence is that 'if nodal displacements are compatible with a constant strain condition such constant strain will in fact be obtained'. Cases 1 and 2 are typical of cases that check if this criterion is satisfied. From these test cases and the above criteria, it can be concluded that the finer the mesh size the closer the solution will approach the real solution. This conclusion applied to all the finite element programs discussed in Chapters 6 and 7.

(ii) A mesh having long thin elements as shown Fig. 8.10 are usually bad for idealizing a body. The most desirable mesh is one having triangles close to isosceles, as shown alongside. Fig. 8.11 also shows the regions covered by the two element shapes. For the TRIM3 element, the long thin element has a constant stress over a larger region. Having a long thin TRIM6 element, however, is not as bad because stress within the element is linearly distributed.

(iii) For a given number of nodes, the TRIM6 element generally gives a better representation of true stress and displacement than would be obtained with the same number of nodes using a much finer sub-division with the TRIM3 elements.

(iv) Boundary values that are required in the displacement finite element method are displacements and forces only, and stress boundary conditions cannot be predetermined. The stresses obtained on the boundary by the method may be checked to see if

NODE	x in	y in	F_x lb	F_y lb
1	0.	0.	-0.1971	-0.0392
2	2.0000	0.	0.1103	-0.0392
3	1.8478	0.7654	0.0870	0.0784
4	0.9239	0.3827	1.1670	0.3137
5	1.0000	0.	1.1980	0.1568
6	1.9239	0.3827	1.5770	0.3137
F			3.9422	0.7842
RESULTANT			4.0194	

TABLE 8.1

Fig. 8.10

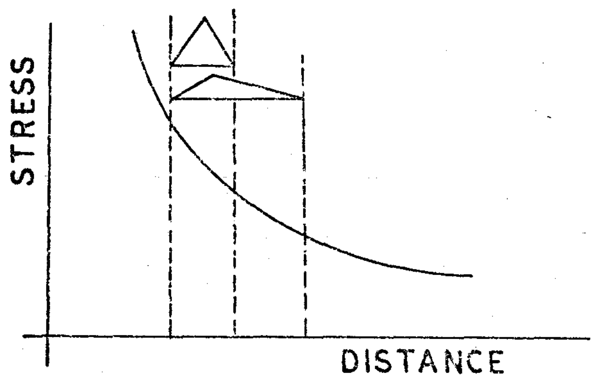

Fig. 8.11

the stress boundary conditions are actually achieved. For example, in the case of the rotating disk (Cases 5 and 6) radial stresses on the boundary are zero. Fig. 8.9 shows that this boundary condition is closely satisfied.

(v) The theory related to discretization of centrifugal forces (Chapter 5) is justified by Test Cases 5 and 6. Table 8.1 shows the forces on the 6 nodes of a representative TRIM6 element by using this theory. As can be seen from this table, the midside nodes are given more weighting. A vectorial summation of these forces yields a net force of 4.02 lb (see table). An identical value is obtained by lumping the mass of the element at its centroid and calculating the centrifugal force due to rotation of this mass, by the formula,

$$F_r = m\,r\,\omega^2$$

It is also observed that lumping of a sixth of the net force on each of the nodes would be incorrect.

(vi) The errors in the results obtained using a finite element approximation may be separated into two types, the discretization error and the rounding error. The rounding error is the error associated with the accuracy with which the numbers are manipulated in the computations. The discretization error, which occurs irrespective of the accuracy of numerical calculations, is a consequence of approximating a continuum, which has an infinite number of degrees of freedom, with a model having a finite number of degrees of freedom.

Ramstad [13] does a detailed analysis of the two types of errors and derives formulae for the range of these errors. He divides the finite element method into various stages and finds the numerical errors in each stage.

(vii) Although computer storage saving techniques were used there still is a limitation to the size of problem that can be solved by the basic finite element programs. By the method of partitions, however, one can solve a very large problem if it is simply connected, because the method uses a step-wise sequence. This method is not feasible for a multiply connected system.

CHAPTER 9

SUBREGIONS: ISOLATION OF AREAS OF HIGH STRESS GRADIENTS

Often, in bodies in which stress concentrations exist, it is necessary to perform a critical study of the stress distribution in regions of high stress gradients. In this chapter a technique is discussed in which the finite element method of stress analysis is used in a step-wise manner in order to 'home-in' on the regions of interest. An example is given to justify the method.

It is known that regions of high stress gradients necessitate a finer finite element mesh than the other regions of the body. This gives rise to the following two major difficulties:

(i) there will be a great variation in element size resulting in great variations in the terms of the stiffness matrix. This causes computational errors such as rounding errors.

(ii) because of limitations on computer memory size, the mesh cannot be made as fine as desired.

An answer to these difficulties is a sequential analysis. Using the finite element method, a first approximation is made by performing a course analysis of the structure without particular attention to the geometrical shape of the region of high concentration. A fair sized region around the concentration is then isolated from the main structure and a refined mesh applied to the isolated region, which is termed a 'subregion'. The subregion is now treated as a separate problem and the boundary displacements applied to it are those obtained from the previous solution. The refined analysis gives a more detailed picture of the stress distribution in the area under special consideration. If the solution by the first subregion is not as detailed as desired, a second subregion can be isolated from the first subregion. A number of subregions may be isolated successively in this manner until convergence occurs or until a desired accuracy is attained.

The series of steps in Fig. 9.1 shows how the approximation to the stress at a point in the region of high concentration converges to the exact solution with each successive subregion analysed.

Whether the subregion isolated is large enough can only be determined by trial, the criterion being that the stresses near the boundary in one subregion should not differ significantly from the stresses in the previous subregion.

Although this method of isolating subregions is intuitively justified, the method is an application of St. Venant's Principle, which states that changes in a small area of a body will cause considerable changes in the local stress distribution, but the effect on the stresses at distances large compared with the area under consideration will be negligible. It has been

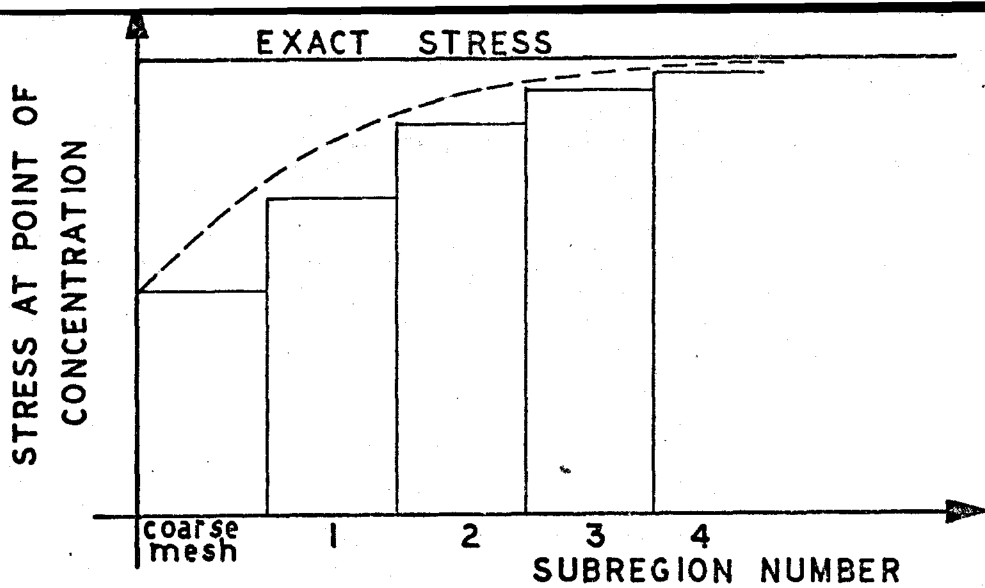

FIG. 9.1 Convergence to Exact Solution by Sequential Isolation of Subregions.

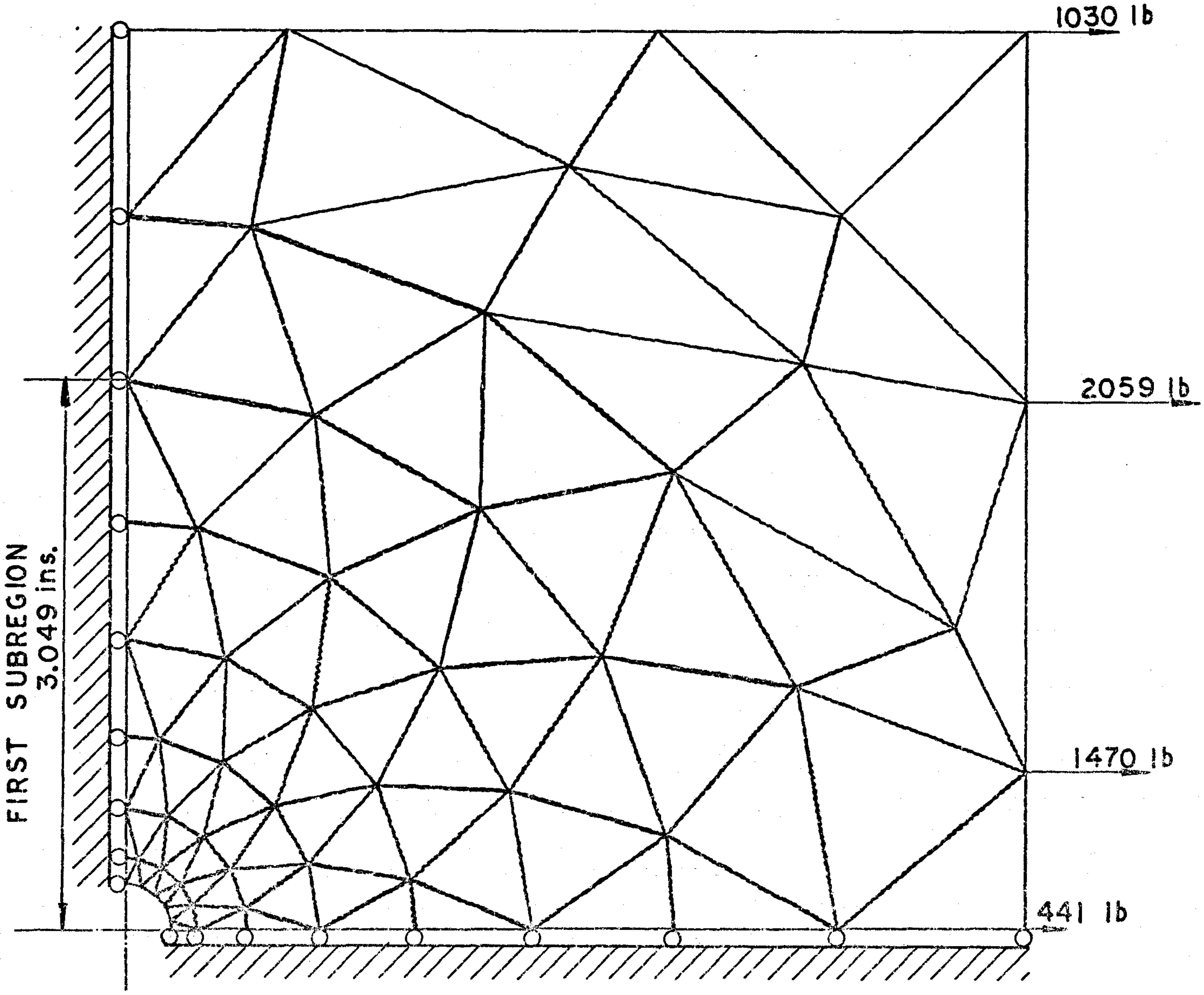

FIG. 9.2(a) TRIM3 Finite Element Idialization of 1/4 of a Plate with a Central Hole Under a Uniform Load of 1000 psi.

shown [23] that, for a case such as a circular notched bar in tension, the stress distribution is unaffected at a distance of between one and two diameters from the edges of the discontinuity.

To prove that convergence occurs with this method a test case was run on a 10 in x 10 in x 1/2 in plate having a 1/2 in diameter central hole, and acted upon by a uniformly distributed tensile load. The finite element mesh of the first approximation is shown in Fig. 9.2(a). Because of symmetry about both axes only 1/4 of the plate was analysed. The region of high concentration is near the hole and two successive subregions were taken here. The finite element meshes corresponding to these two subregions are shown in Figs. 9.2(b) and (c). The displacement boundary values for each subregion were obtained from the previous analysis.

Figs. 9.3 and 9.4 show how the stresses and displacements approach the theoretical solutions [13] with each successive approximation. These figures show that convergence occurred after three approximations. It can be seen that if the mesh of Fig. 9.2(c) were applied to the entire plate, the problem would be beyond the scope of the computer memory size.

It is apparent that this method is useful for the analysis of the circular saw blade in which an improved slot shape is sought. According to the hypothesis a region

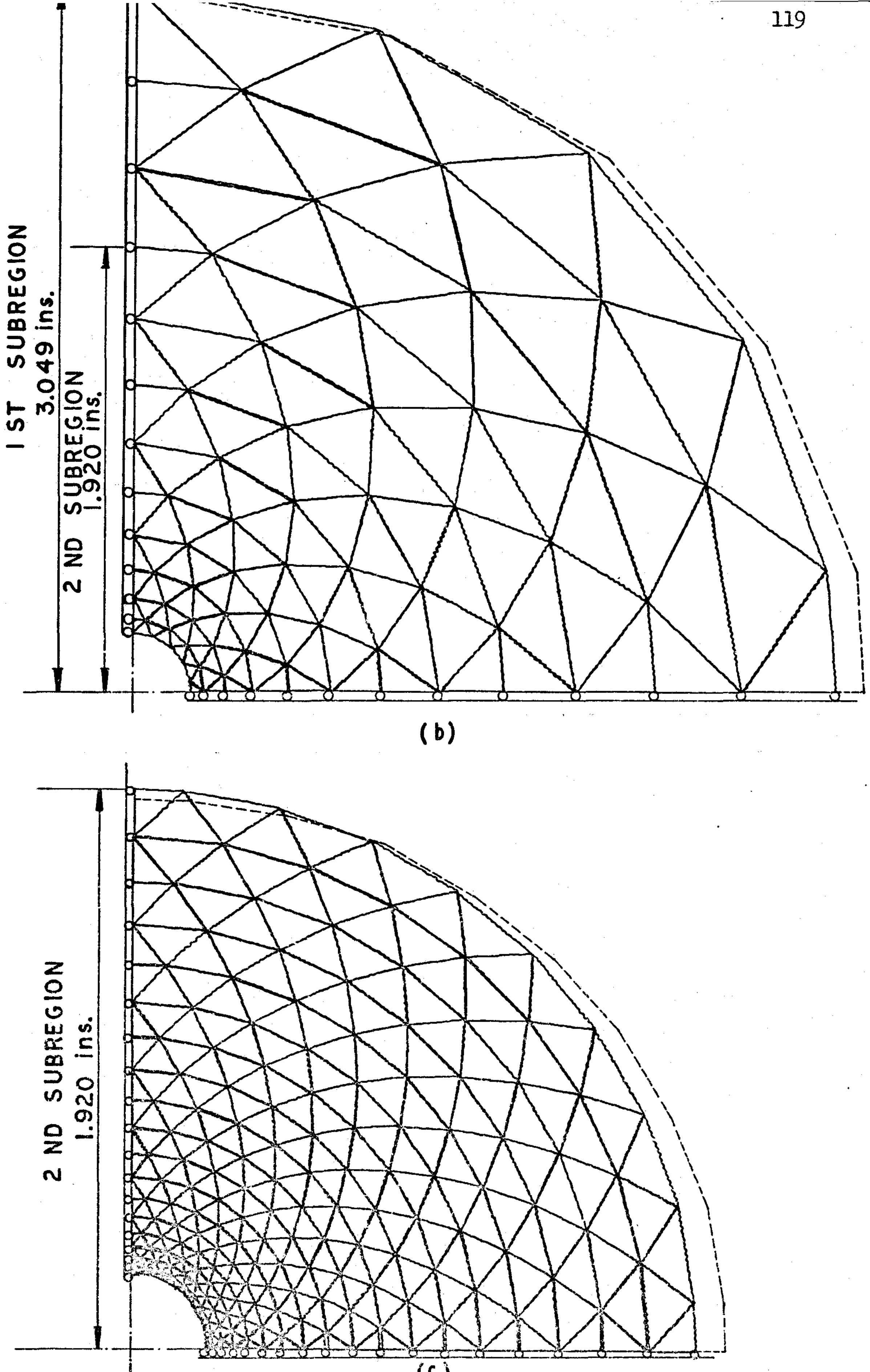

FIG. 9.2(b) 1st Subregion Isolated from Figure (a), Showing Extent of 2nd Subregion (c) 2nd Subregion Isolated from Figure (b).

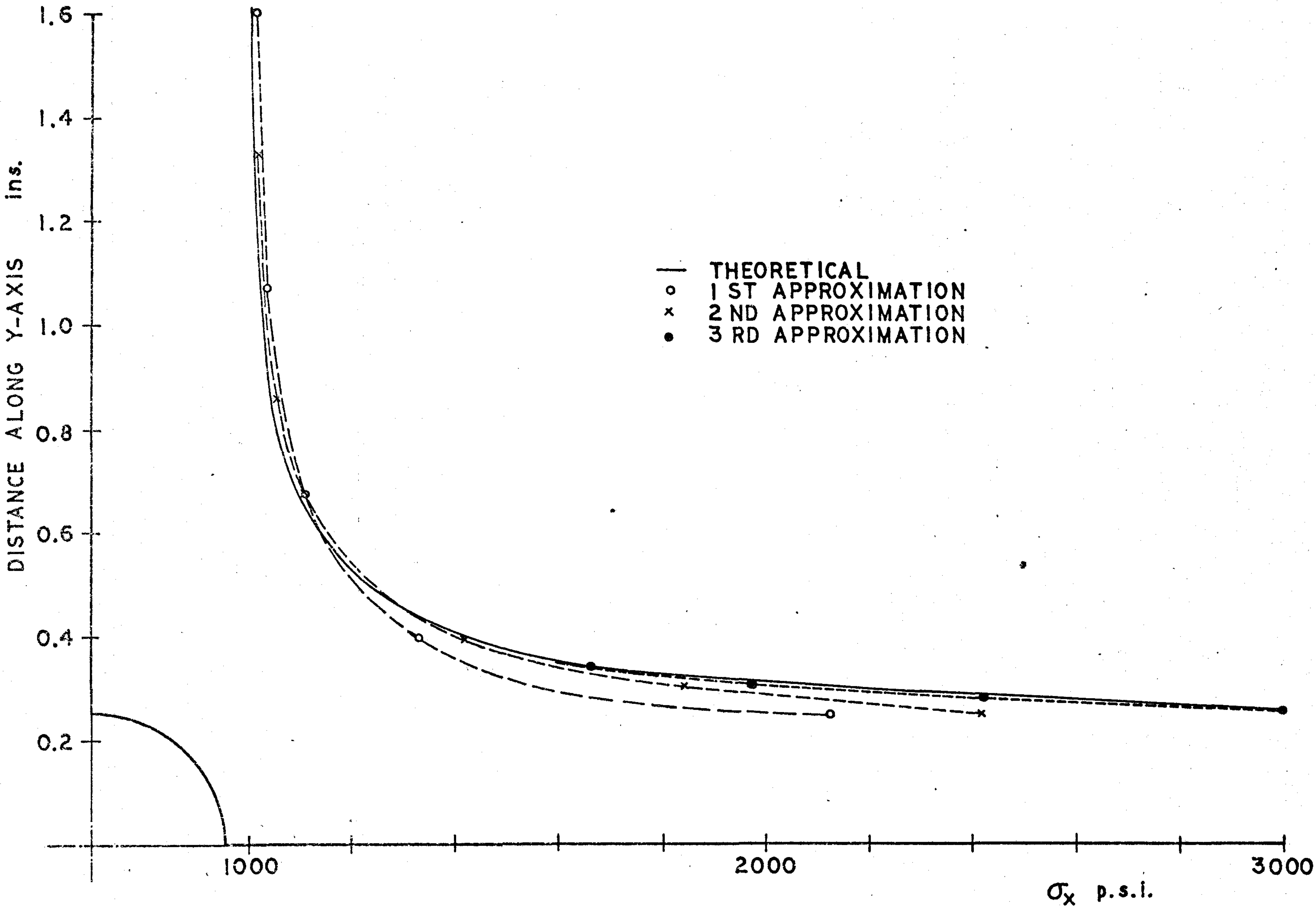

FIG. 9.3 Convergence of σ_x Stresses Along y-axis Solved by Three Successive Finite Element Approximations to Exact Stresses.

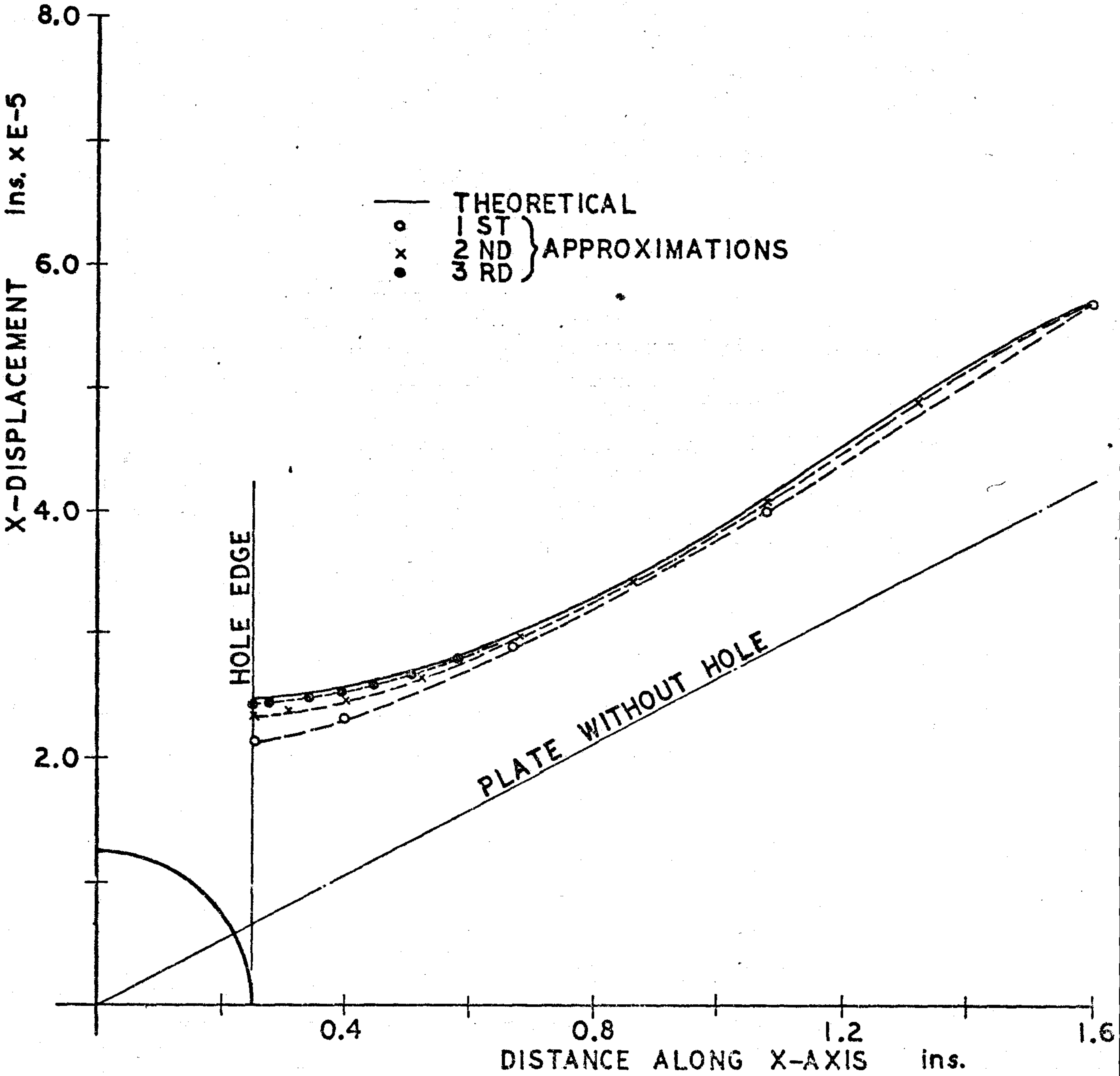

FIG. 9.4 Convergence of x-displacements to Exact Solution by Three Successive Finite Element Approximations (Two Subregions).

surrounding the slot may be isolated and the shape of the slot may be altered without affecting the stresses in the main body of the blade. The sectioning-off of the subregions is described later (Chapter 12).

CHAPTER 10

PLOTTING OF DATA

10.1. Stress Plotting:

10.1.1. General

Stress analysis by the finite element method has the drawback that stresses are obtained at a great many discrete points which makes the task of reading results very difficult. In order to study the stresses in a two-dimensional stress system, a number of graphical methods may be used to give a visual interpretation of the various aspects of the computed data. Some of these methods are:

(i) Isoclinic lines, or lines of constant principal angle.

(ii) Stress trajectories, which are the loci of the directions of constant principal stresses.

(iii) Isostress lines or stress contours which are the loci of algebraically equal principal stresses, regardless of their sense.

(iv) A principal stress plot, in which the two principal stresses are represented as vectors at chosen points.

(v) Isometric stress plot, in which a stress 'surface' is plotted in isometric view.

When regions of high stress gradients are of interest, then the countour plot is the most informative. On a stress surface plot, where stress is plotted as a function of x and y, these regions appear as peaks, the stress contours are essentially projections of 'slices' of the surface projected onto the xy-plane. Regions of high stress gradients are easily recognizable as contour lines that bunch together.

In whatever method of stress presentation chosen, manual plotting of the data is still arduous and error prone. Fortunately, stress plotting can be done by computer on an automatic device known as the 'plotter'. The computer converts numeric data to signals which are written on magnetic tapes which, when mounted on the plotter, are translated to digital motion of a pen point. However, all the user is required to do is correctly program the computer by means of a number of user-oriented Fortran subroutines.

In this chapter, a contour plotting program for use on data computed by the finite element method is discussed and a program listing is given in Appendix G. The program uses only the basic plotting subroutine called PLOT to draw the contours. The program had been successfully used on the Benson-Lehner and the Calcomp plotters. For labelling purposes a subroutine called LETTER is used, the equivalent of which is available on most plotters.

10.1.2. Basic Concept Used to Draw Contours

The basic idea used in the contour plotting program is best explained by means of an example. Fig. 10.1 shows

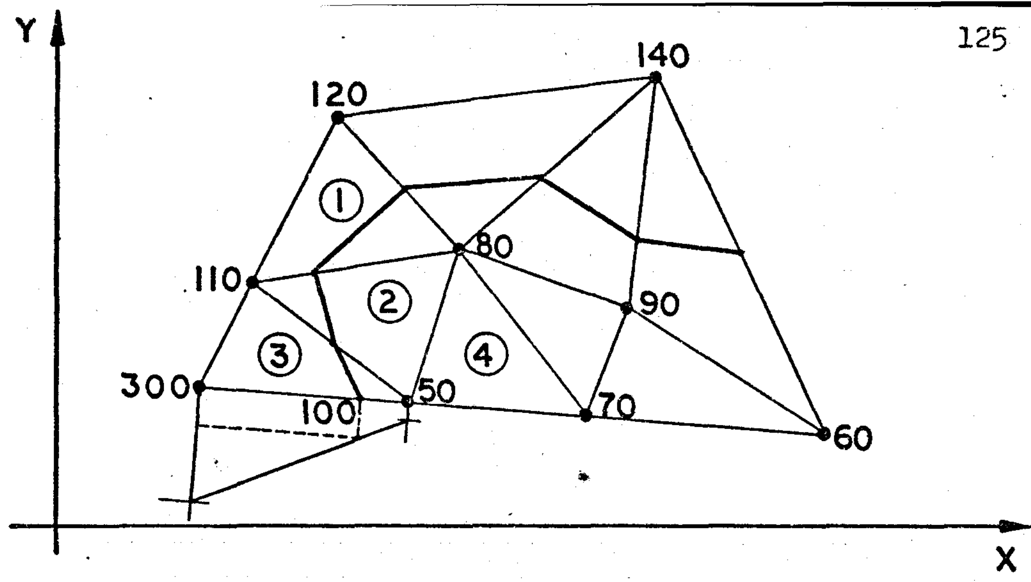

FIG. 10.1 Simple Mesh to Illustrate Basic Concept Used in Contour Plotting Program.

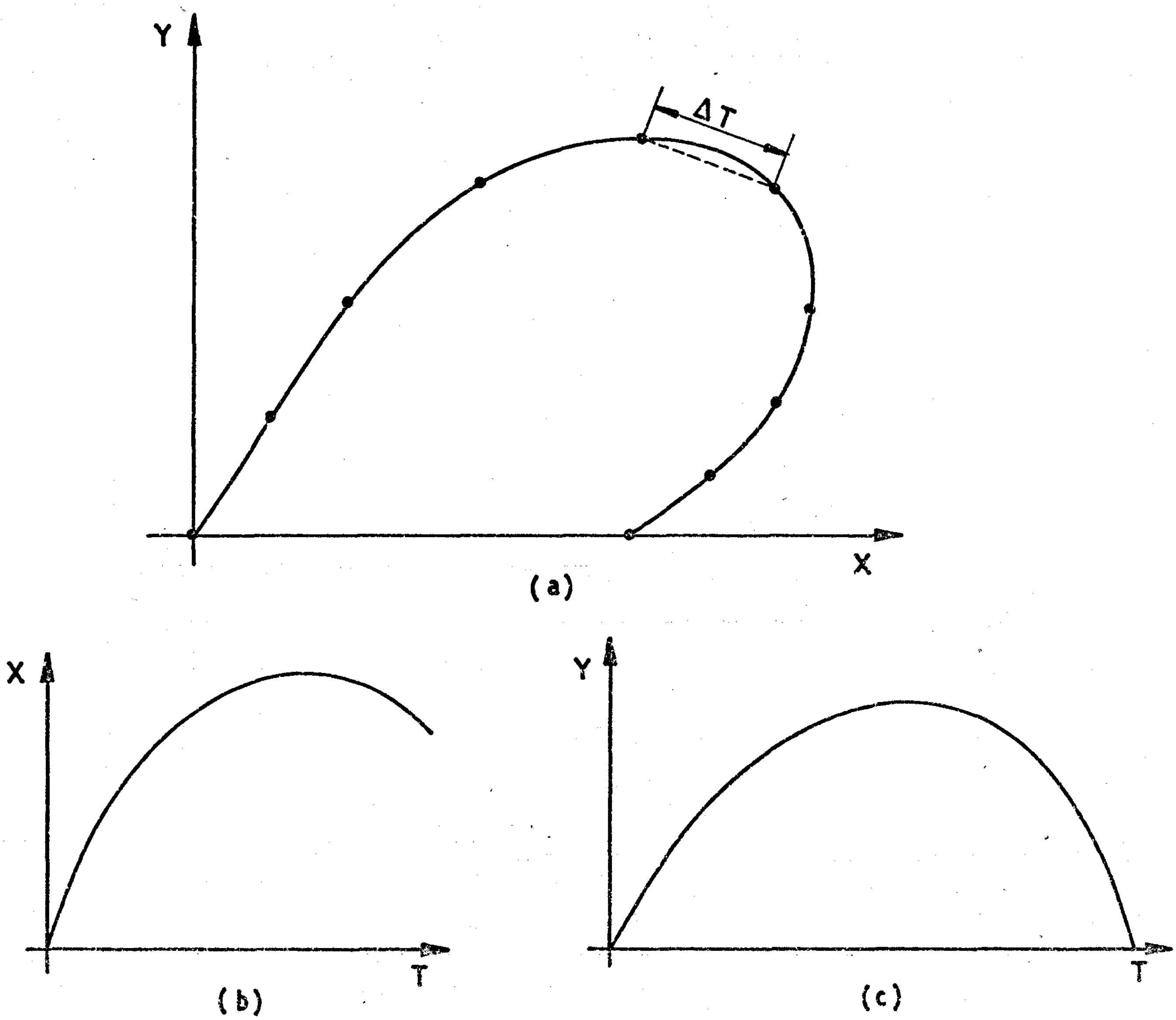

FIG. 10.2 (a) Multi-valued Contour in x and y Drawn Parametrically against Variable T in (b) and (c). (Not to scale).

stresses at nodal points for a simple finite mesh of TRIM3 elements. Assuming a 100 psi contour was required, then an element by element search is performed by computer to establish whether the contour passes through the element. If a contour does pass through an element it has to intersect two of the sides. The two intersection points on the sides are found by linear interpolation, as done for one side on element 3. The simplest way of drawing the contour would then be to join the two points by a straight line, and continue the search on the next element. If this procedure is adopted then the contour will take the shape of a series of piecewise continuous straight lines, as shown in Fig. 10.1.

In the computer program, a sophisticated method is used to smooth the contour. Since elements are numbered randomly, the line increments mentioned above are ordered so that they follow each other. The center-points of these lines are then used as data points in a cubic spline curve fitting program discussed in the next section.

10.1.3. Cubic Spline Fit

The x and y co-ordinates of the points defining the contour are stored in two arrays. In theory, the smoothing is done by joining each consecutive pair of points by a cubic in such a manner that the resulting composite curve has continuous first and second derivatives.

The relevant theory for the method is included in Appendix H. The method is known as the cubic spline method of interpolation and smoothing. The method ensures that, although the contour is composed of piecewise cubics, there are no kinks in the contour.

In the program the intervals in x values between points defining the contour are subdivided into smaller intervals and the y values are interpolated using the spline method. These subintervals are then connected by straight lines, and because they are so close they give the appearance of a smooth curve. A difficulty arises when the contour is a multi-valued function in x (Fig. 10.2(a), because cubics cannot be fitted to such a curve. This difficulty is overcome in the program by fitting both x and y parametrically against cumulative chord length T. The meaning of an increment in the parameter is indicated in Fig. 10.2(a). This artifice results in two curves shown in Fig. 10.2(b) and (c), both single-valued in the parameter. The spline fit is done on two curves now and, when plotting, subintervals in T are taken instead of x and values of x and y are interpolated from the cubic splines. This method is also useful when nearly sharp corners appear in the contour.

Notes:

The search technique employed in the program ensures that all contours having the same value are plotted. Since plots of contours of both principal stresses are usually required for one finite element mesh, a sample main program is also included in Appendix G to show how the contour plotting subroutine CONPLOT may be used for this purpose.

Fig. 10.3 shows the plot drawn when using subrouting CONPLOT on the example of Fig. 8.4. The subroutine was used for more involved contour plots in Chapter 12.

Subroutine CONPLOT can be used with either TRIM3 or TRIM6 elements because linear interpolation is done by using only the stresses of nodes on the vertices of the triangular elements. Ignoring the midside nodes in the TRIM6 elements is allowable as stresses along the sides of the elements are in fact linear by hypothesis.

10.2. Input Mesh Plotting:

From experience it was found that the greatest number of errors committed in a finite element analysis are due to errors in the data of the input mesh. Subroutine MESH2 was written for use on the plotter in order to obtain a quick visual check of the input mesh. A program listing of the subroutine is given in Appendix G.

This subroutine can be used to plot meshes having either TRIM3 or TRIM6 elements. A number of options are allowed and are explained in the comments. For TRIM6 elements only the co-ordinates of the vertices need to be defined, the midside nodal co-ordinates are generated by computer.

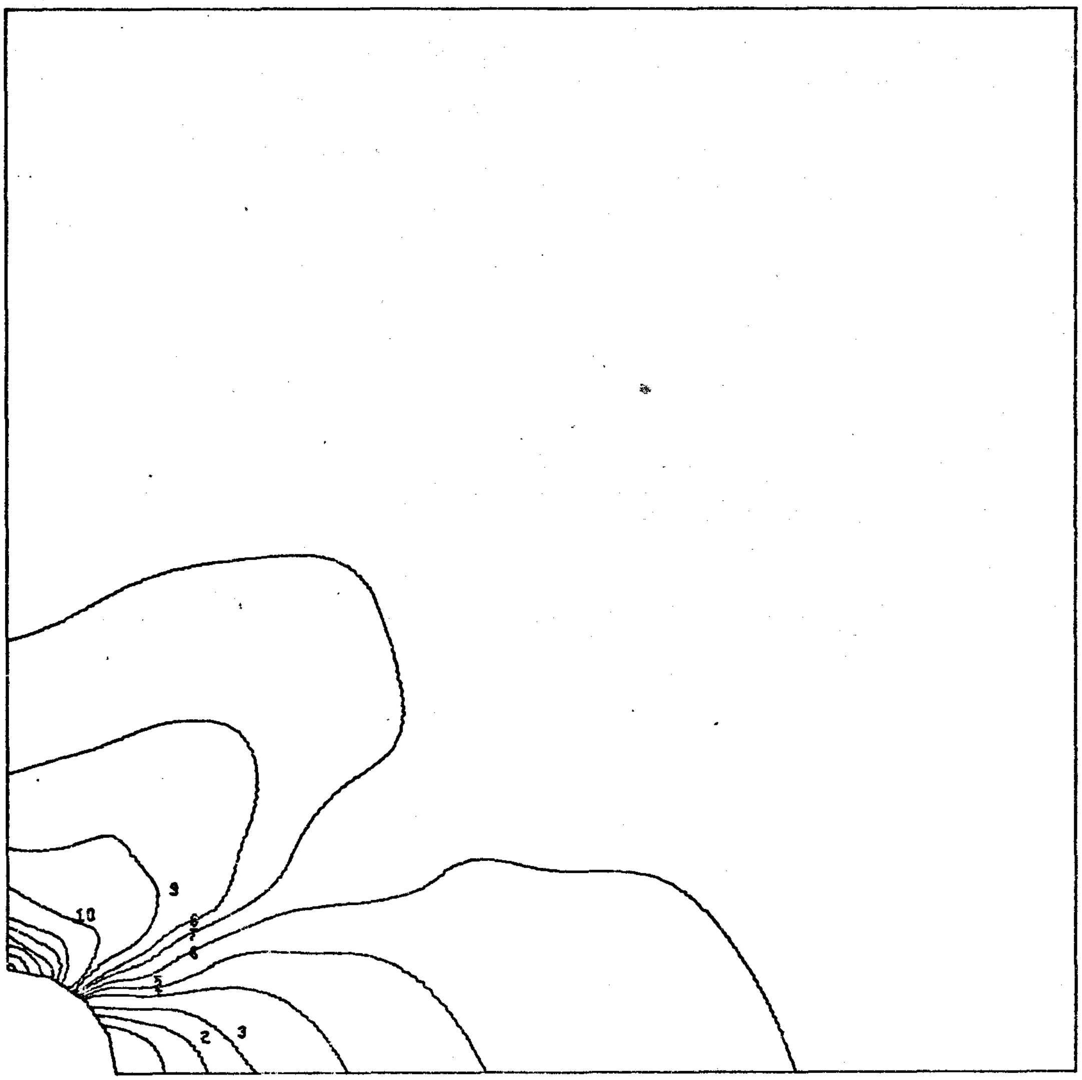

FIG. 10.3 Stress Contour Plot of σ_x Stresses for a Quarter-Section of a Plate with a Central Hole. Contours Labelled by Number.

This program's usefulness is evidenced in many diagrams of this thesis.

CHAPTER 11

APPROXIMATE FORCE DISTRIBUTION ON DIAMOND CIRCULAR SAW BLADE

11.1. General:

The economics of stone-cutting with diamond circular saws is well represented in the literature [31-35]. However, almost no studies of the cutting forces set up during cutting have been reported. In the field of grinding, theories have been developed by some authors [24-29] who relate the grinding forces to the 'undeformed' chip thickness. An analogy can be drawn between the cutting mechanism of a grinding wheel and diamond circular saw if one considers that both the tools remove material by an abrasive action. The analogy is used in this chapter in order to find an approximate cutting force distribution over the cutting region of a saw blade.

The following assumptions are made for the sawing process:

(i) If T and R are the tangential and radial forces respectively as measured by a force dynamometer, then the general shapes of the curves of T and R versus depth of cut will be the same as in grinding.

(ii) The undeformed chip shape will be the same as in grinding.

(iii) Because the cutting is achieved by incremental circular movements, the slots in the periphery of the saw affect neither the cutting process nor the chip shape (if the slots are not too wide).

Curves of normal and tangential cutting forces with respect to wheel depth of cut for the surface grinding of steel have been obtained by Marshall and Shaw [2] by means of a force dynamometer. Representative curves are reproduced in Fig. 11.1 to obtain an idea of their shapes.

11.2. The 'Undeformed' Chip:

The formation and shape of a mean chip is outlined in Figs. 11.2(a) and (b). Although actual chips vary along their lengths rather than having a constant width,b, a statistically mean chip with constant width is assumed.

An 'up-cutting' process is assumed as opposed to the 'down-cutting' process. In up-cutting a wedge-shaped chip is produced ideally starting at the thin end of the wedge and incr asing in thickness up to a maximum, when it rapidly diminishes in thickness up to the breaking out point. In down-cutting the chip starts at its big end and proceeds towards its thin end.

The undeformed chip thickness is defined as the thickness perpendicular to the chip length l. The maximum chip thickness is the length EG in Fig. 11.2(a) and is designated as t.

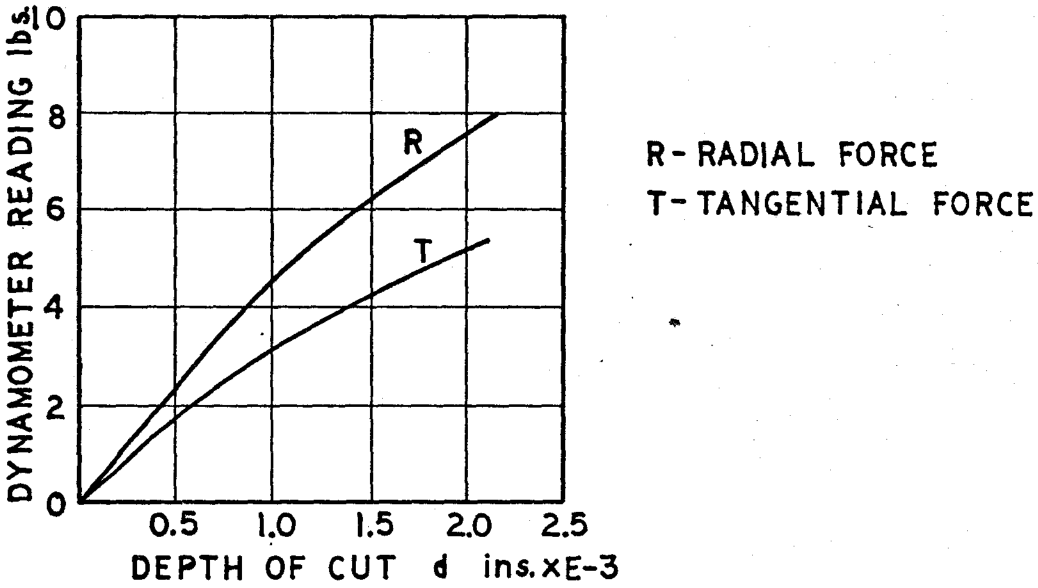

FIG. 11.1 Grinding Force Curves for Steel.

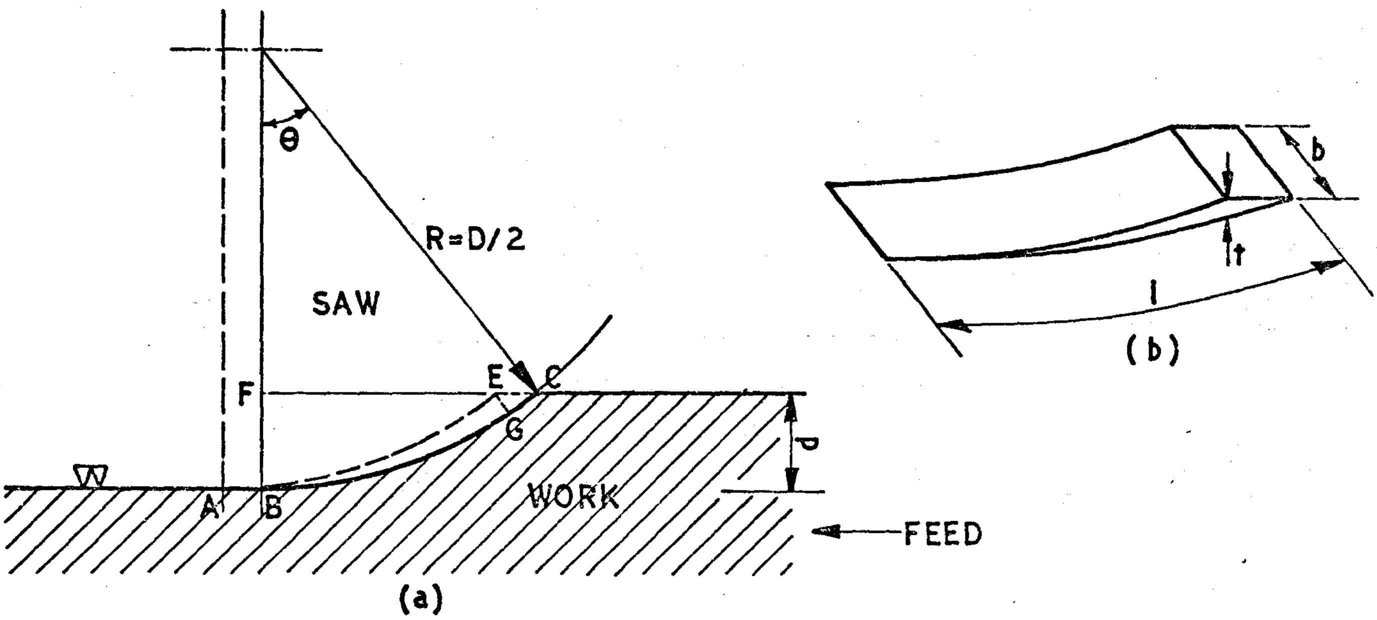

FIG. 11.2 (a) Formation of Chip During Cutting.
(b) Mean Undeformed Chip Shape.

11.3. Formula for Maximum Chip Thickness:

The chip length extends from A to C (Fig. 11.2a) but can be approximated by length BC since,

$$\frac{AB}{BC} = \frac{\nu}{V}$$

where ν = feed rate, V = wheel speed and $\nu << V$. Hence, $AB << BC$.

$$\text{Chip length } l = R\theta \qquad (11.1a)$$

from geometry $\cos\theta = (R - d)/R = 1 - d/R$

$$\approx 1 - \theta^2/2$$

$$\theta = 2\sqrt{d/D} \qquad (11.1b)$$

Substituting in equation (11.1)

$$l = \sqrt{dD} \qquad (11.2)$$

Maximum chip thickness

$$t = CE \ \sin\theta = CE(CF/R) \qquad (11.3)$$

From geometry

$$CF^2 = (D/2)^2 - (OF)^2$$

$$= (D/2)^2 - (D/2 - d)$$

$$CF = \sqrt{d(D - d)}$$

Substituting in equation (11.3)

$$t = 2\ CE/D\sqrt{d(D - d)}$$

If K is the mean number of grits on a complete circumferential line on the saw surface, then CE is the distance the table advances during the time it takes the wheel to make 1/K revolution.

$$CE = \frac{12\nu}{KN}$$

where N = wheel speed in rpm, and

= feedrate in in/min

$$t = \frac{24\nu}{KN}\sqrt{\frac{d(D-d)}{D^2}}$$

or approximately,

$$t = \frac{24\nu}{KN}\sqrt{\frac{d}{D}} \qquad (11.4)$$

11.4. Cutting Force Distribution:

At this stage it is necessary to differentiate between DYNAMOMETER MEAN FORCE and ACTUAL MEAN FORCE. If the cutting wheel had just one cutting edge, a force-time recording such as in Fig. 11.3 would be obtained. A dynometer records time average cutting forces over 2Π radians, while the actual mean force is the average value during the period of contact, i.e. over θ radians.

Hence, the actual mean tangential force per cutting edge is,

$$\bar{F}_T = \frac{2\Pi}{\theta} T \text{ (having one cutting edge)}$$

or

$$= \frac{2\Pi}{\theta K} T \text{ (having K cutting edges)} \qquad (11.5)$$

The above mean force is an average of the instantaneous

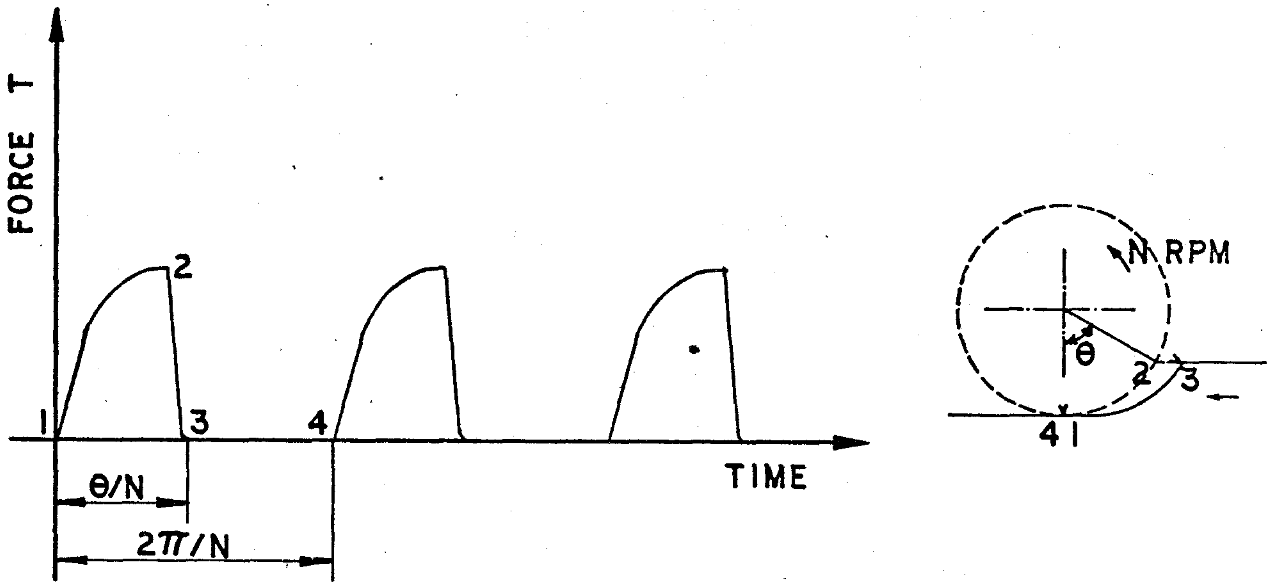

<u>FIG. 11.3</u> Cutting Force Cycle for a Saw Having One Cutting Edge.

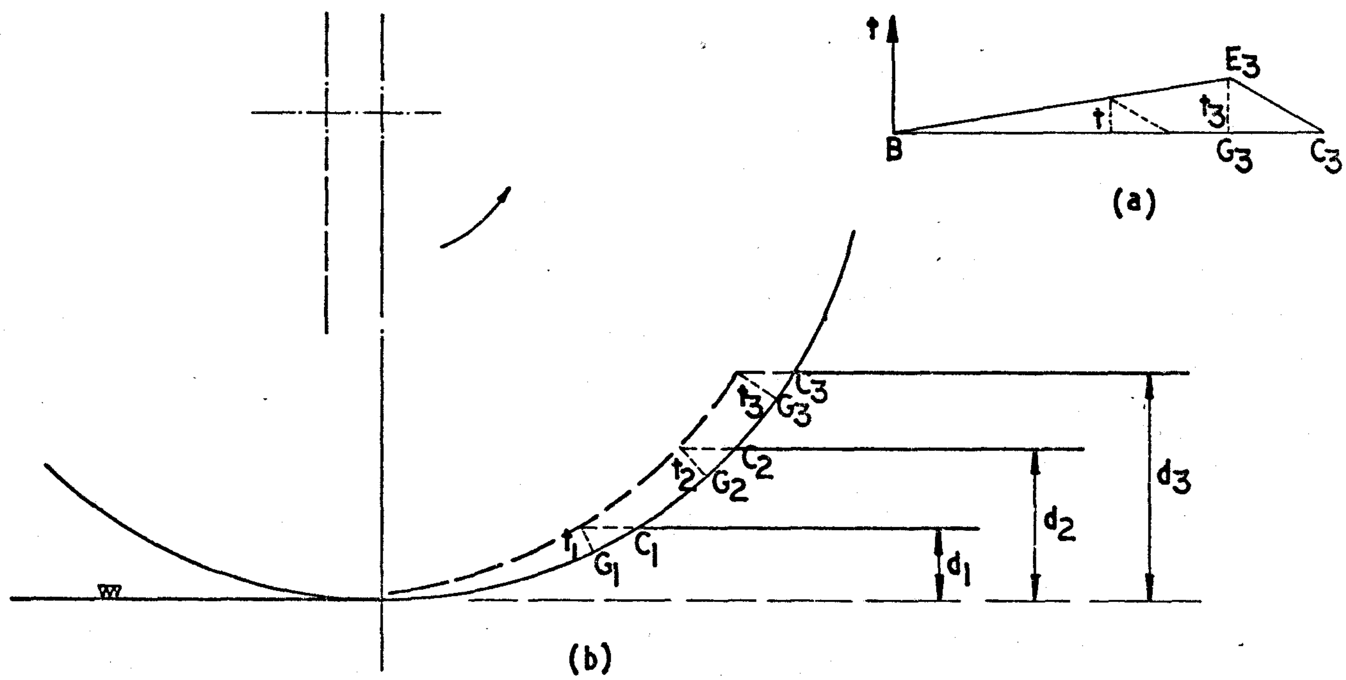

<u>FIG. 11.4(a) and (b)</u> Correlation of Maximum Chip Thickness with Thickness Along Chip Length.

value which varies from zero to a maximum where the chip has its greatest thickness, or

$$\bar{F}_T = \frac{\int_0^t F_T \, dt}{t} \tag{11.6}$$

where F_T is the instantaneous force and t is the maximum chip thickness*.

Multiplying both sides of equation (11.6) by t and differentiating with respect to t, the following is obtained,

$$t \frac{d\bar{F}_T}{dt} + \bar{F}_T = F_T \tag{11.7}$$

From equation (11.5)

$$\frac{d\bar{F}_T}{dt} = \frac{2\Pi}{K} \frac{d}{dt} (T/\theta) = \frac{2\Pi}{K\theta} \frac{dT}{dt} - \frac{2\Pi}{K\theta^2} T \frac{d\theta}{dt} \tag{11.8}$$

Substituting equations (11.8) and (11.5) in (11.7),

$$F_T = \frac{2\Pi t}{K\theta} \frac{dT}{dt} - \frac{2\Pi}{K} \frac{Tt}{\theta^2} \frac{d\theta}{dt} + \frac{2\Pi}{\theta K} T \tag{11.9}$$

Since θ and t are linearly dependent $d\theta/dt = \theta/t$. Therefore,

$$F_T = \frac{2\Pi t}{K\theta} \frac{dT}{dt} \tag{11.10}$$

By the chain rule

$$\frac{dT}{dt} = \frac{dT}{d(d)} \frac{d(d)}{dt}$$

---

* See note at end of the Chapter.

where d = depth of cut.

The differential on the right-hand side is obtained from equation (11.4) and the above equation becomes,

$$\frac{dT}{dt} = \frac{2\ N^2K^2D\ t}{24^2\ \ \nu^2}\ \frac{dT}{d(d)} \tag{11.11}$$

From equations (11.1b) and (11.4)

$$t = \frac{12\ \nu\ \theta}{K\ N} \tag{11.12}$$

After substitution of the above two equations into equation (11.10), the result is

$$F_T = \frac{\Pi D}{K}\ \frac{dT}{d(d)}\ \theta \tag{11.13}$$

Alden [27] hypothesized that grinding forces are linearly proportional to t (or θ, since t is linearly proportional to θ). Therefore, it seems reasonable to assume that dT/d(d) in equation (11.13) is constant, or that the dynamometer tangential force (T) versus depth of cut (d) curve is linear. Letting the differential equal C,

$$F_T = \frac{\Pi\ D\ C}{K}\ \theta \tag{11.14}$$

This equation gives the variation of instantaneous tangential cutting force with angle. A similar equation may be written for radial force distribution F_R.

Marshall and Shaw [25] observed that, for a series of tests, the ratio of tangential force T to the radial force R was very nearly constant. This ratio, designated $C_f = T/R$, is somewhat like the ordinary coefficient of friction and they term it the 'grinding coefficient'. Hence,

$$F_T = C_f\ F_R \tag{11.15}$$

The mean diameter, a, of a grit having a 45 mesh concentration is approximately 0.02 in, and if the grits are assumed to be packed alongside each other on a circumferential line, then

$$K = \Pi D/a$$

In equation (11.14)

$$F_T = a\ C\ \theta$$

$$F_R = F_T/C_f$$

or

$$\begin{aligned} F_R &= a\ C'\theta \\ F_T &= C_f\ F_R \end{aligned} \tag{11.16}$$

where C' is the slope of the R vs. d curve. Equation (11.16) represents cutting force distribution per cutting edge.

11.5. Cutting Force Data:

Some experimental curves of cutting forces versus feedrate for various depths of cut were obtained from the Boart Metal Industries of South Africa. Since a curve of cutting force versus depth of cut was required, this had to be graphically deduced from the available curves. However, the curves obtained did not seem reliable since there were not sufficient data points. The most reasonable curve obtained is shown in Fig. 11.5 which is dynamometer radial force versus depth of cut at 300 mm/sec feedrate. Within a depth of cut of 25 mm (1 in) it seems reasonable to assume that the curve is linear. Thus, in equation (11.16) for the feedrate and speed shown in Fig. 11.5,

$$F_R = a * 117.0 * \theta \qquad (\theta \text{ in radians})$$

force/cutting edge

If W is the width of the diamond tip, then the number of cutting edges along width is W/a

total force on line of grits along the width is (if W = 0.125)

$$F_R = \frac{1}{8}\ \frac{117.0\ \pi}{180}\ \theta = 0.260 \qquad (\theta \text{ in degrees}) \tag{11.17}$$

$$F_T = C_f\ F_R$$

From the ratio of some data values of T and R, C_f was found to be approximately 0.2

Note:

Chip BE_3C_3 is shown in Fig. 11.4(a) having a maximum thickness t_3. t is any thickness along the length of the chip. As can be seen from Fig. 11.4(b), t is in effect a maximum

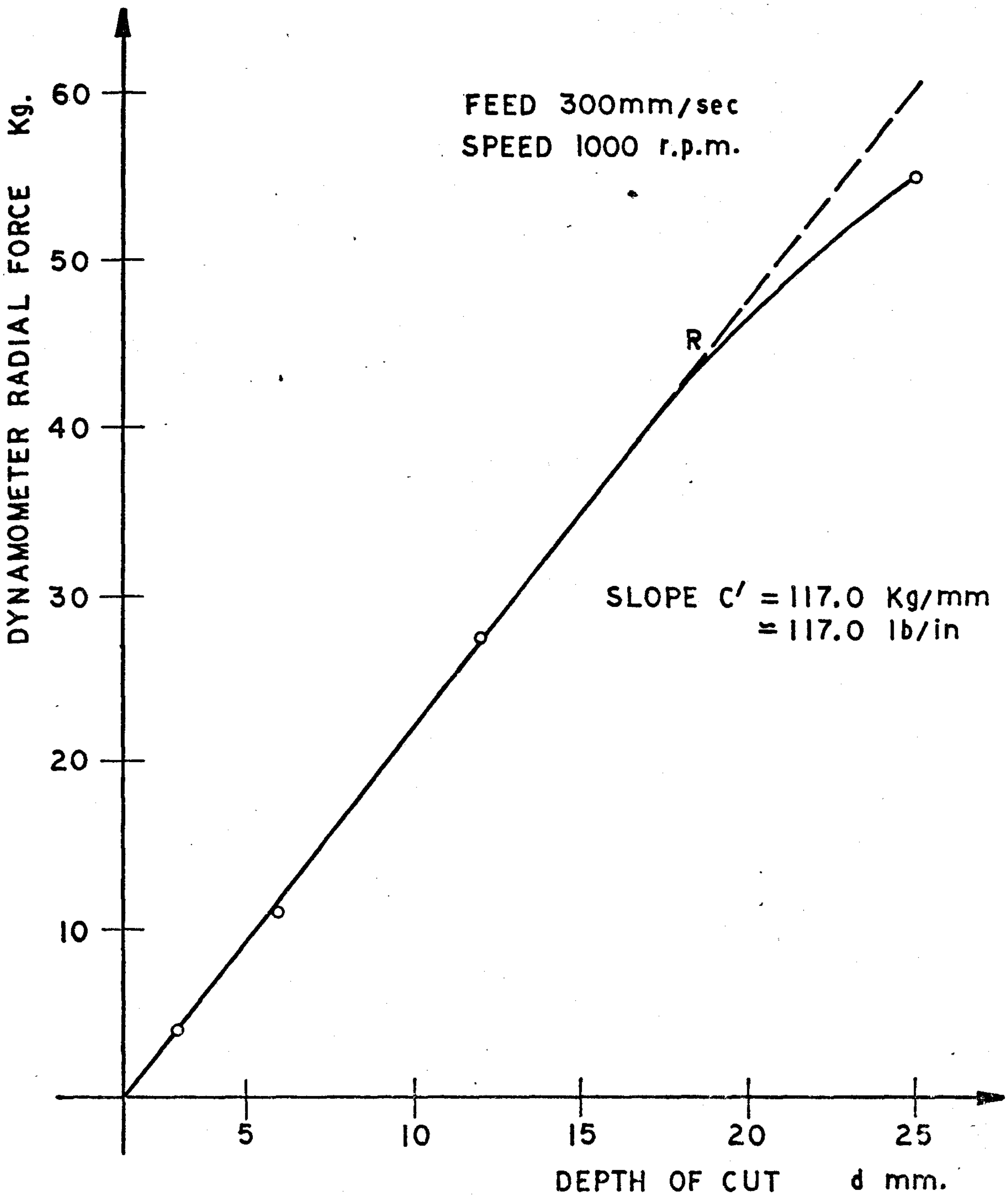

FIG. 11.5 Radial Cutting Force Versus Depth of Cut Curve at Fixed Feed and Speed for the Cutting of Stone with a Diamond Tipped Circular Saw.

thickness corresponding to some depth of cut d. For example. t_2 is a thickness t along the length of chip BE_3C_3, but is also the maximum chip thickness of chip BE_2C_2 corresponding to d_2.

Hence, the quantity t (chip thickness along chip length) and maximum chip thickness are synonymous, and is used as a variable in equation (11.6).

CHAPTER 12

STRESS ANALYSIS OF A SEGMENTED CIRCULAR SAW BLADE BY THE FINITE ELEMENT METHOD

12.1. Preliminary Analysis:

12.1.1. Origin of the problem of fatigue cracking.

A general description of the diamond circular saw and other topics related to it is presented in Appendix J. Some insight is thrown on the cutting mechanism of the saw blade in Chapter 11 and an analogy is drawn between this and the cutting mechanism of a grinding wheel.

In this analysis it is assumed that the saw blade is mounted on an orthogonal stone-cutting machine, i.e. on a rigid frame, with the work moving towards the blade. Also, an 'up-cutting' motion of the saw is assumed, hence the feed velocity is opposite to the blade velocity at the cutting position. The relative motion between saw and machine bed is indicated in Fig. 12.1.

Like a grinding wheel, a diamond circular saw is loaded externally by the cutting forces only. The region in which the cutting forces act is known as the 'cutting region'. The cutting forces consist of two components, one due to shearing action tangential to the blade surface and one normal to the blade surface. The two components equilibrate both the feed force and

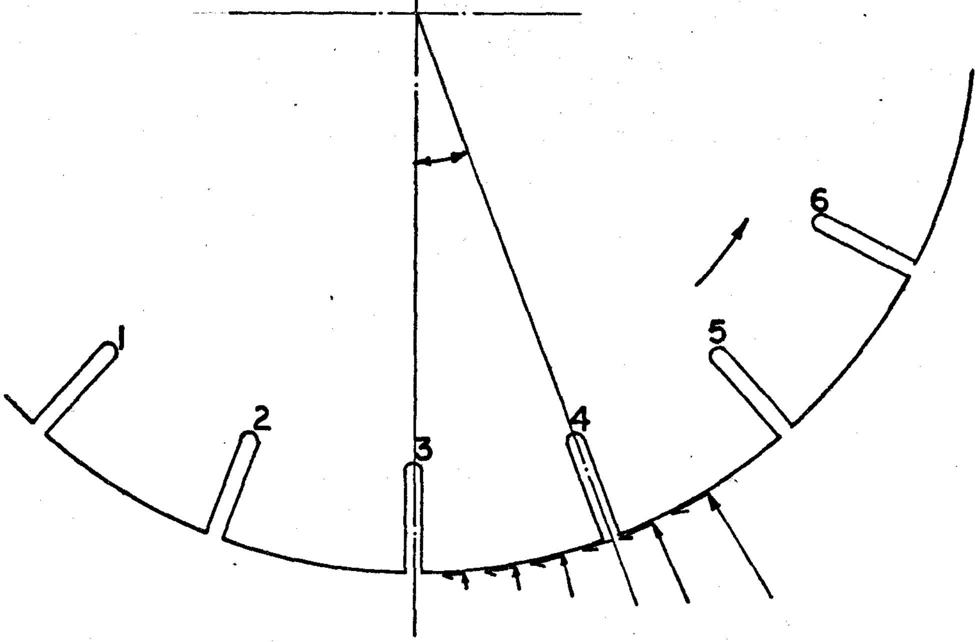

FIG. 12.1 Fictitious Force Distribution on Saw Blade to Represent Cutting Forces.

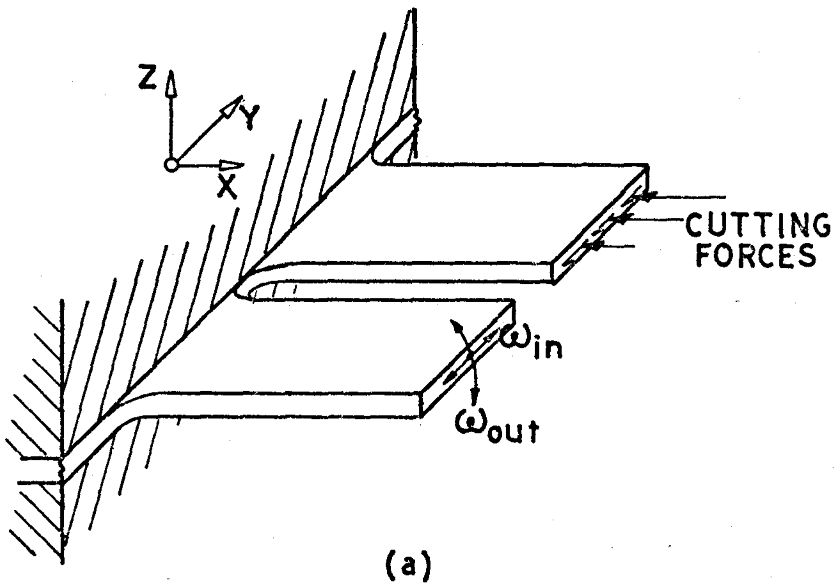

FIG. 12.2(a) Effect of Vibrations.

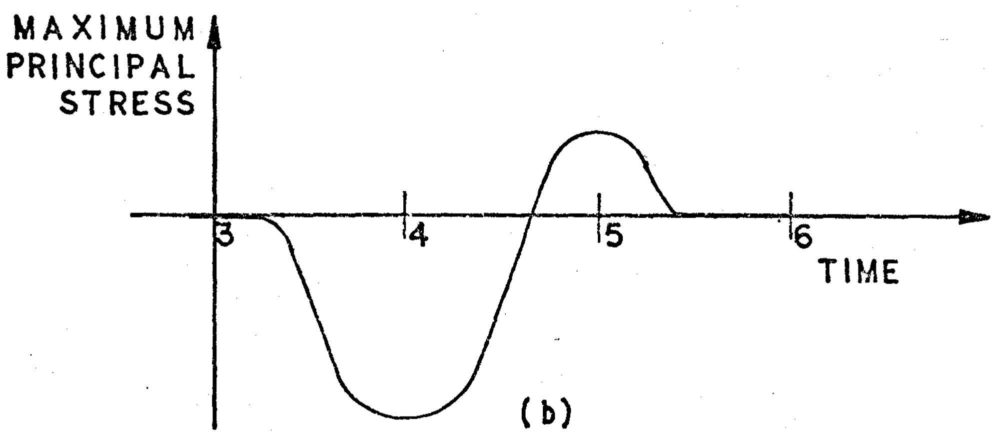

FIG. 12.2(b) Stress Spectrum.

the force required to abrade the work. It is assumed that side forces due to lateral contact of the blade with the work do not add significantly to the forces.

Because circular saw blades rotate at high speeds, the body of the blade is subjected to internal forces due to centrifugal action. These centrifugal forces are distributed over the entire blade body and stress the body beyond the normal static condition.

The normal and tangential cutting forces distribute themselves over the cutting region in some way, depending on the cutting conditions. Fig. 12.1 shows a representative distribution. A more detailed study of these forces is presented in Chapter 11. Fig. 12.1 represents an 'instantaneous' force distribution, and conditions are assumed to be the same from instant to instant. The number of slots included in the cutting region is usually more than one and depends on the depth of cut.

The combined effect of the cutting and centrifugal forces cause stress concentrations at the slot bases that are located in the vicinity of the cutting region.

If a slot moves from position 1 to position 6(Fig. 12.1) it passes through a cycle of stress. In position 1 and 2, the slot base is not very much affected by the cutting forces. In positions 3, 4 and 5 the slot base is most highly stressed, and finally the effect of the cutting forces diminishes on the slot in position 6. A cycle of stress that a slot base passes through is expected to be of the form shown in Fig. 12.2(b). Such a cycle of stress variation with time, known as a 'stress spectrum' is conducive to fatigue failure at the slot bases. Because cutting forces are assumed to be constant with time each slot base passes through the same cycle of stress.

If the saw blade is thin, then a state of plane stress may be assumed. Also, the fatigue problem is considered purely 2-dimensional because it is assumed that the flanges fitted on either side of the saw blade on assembly (see Fig. 12.3) prevent lateral motion of the saw blade. Ideal vibration-free conditions are assumed in order not to complicate the problem, even though vibration of the blade may add to the fatigue problem.

To throw some light on the vibration aspect, a segment or 'tooth' may be represented as a cantilever beam under the action of the cutting loads and also vibrating at frequencies ω_{in} and ω_{out} as shown in Fig. 12.2(a) where ω_{in} and ω_{out} are the frequencies of in plane and out of plane vibration, respectively. A representative principal stress spectrum at a point such as m due to alternating cutting forces is shown in Fig. 12.2(b). In plane vibrations of frequency ω_{in} cause slight viriations in stress and are shown as harmonics on the basic spectrum. If the slot base radius is small relative to the segment width, the effect of the in plane vibrations is negligible. The out of plane vibrations of frequency ω_{out} are not considered in the analysis.

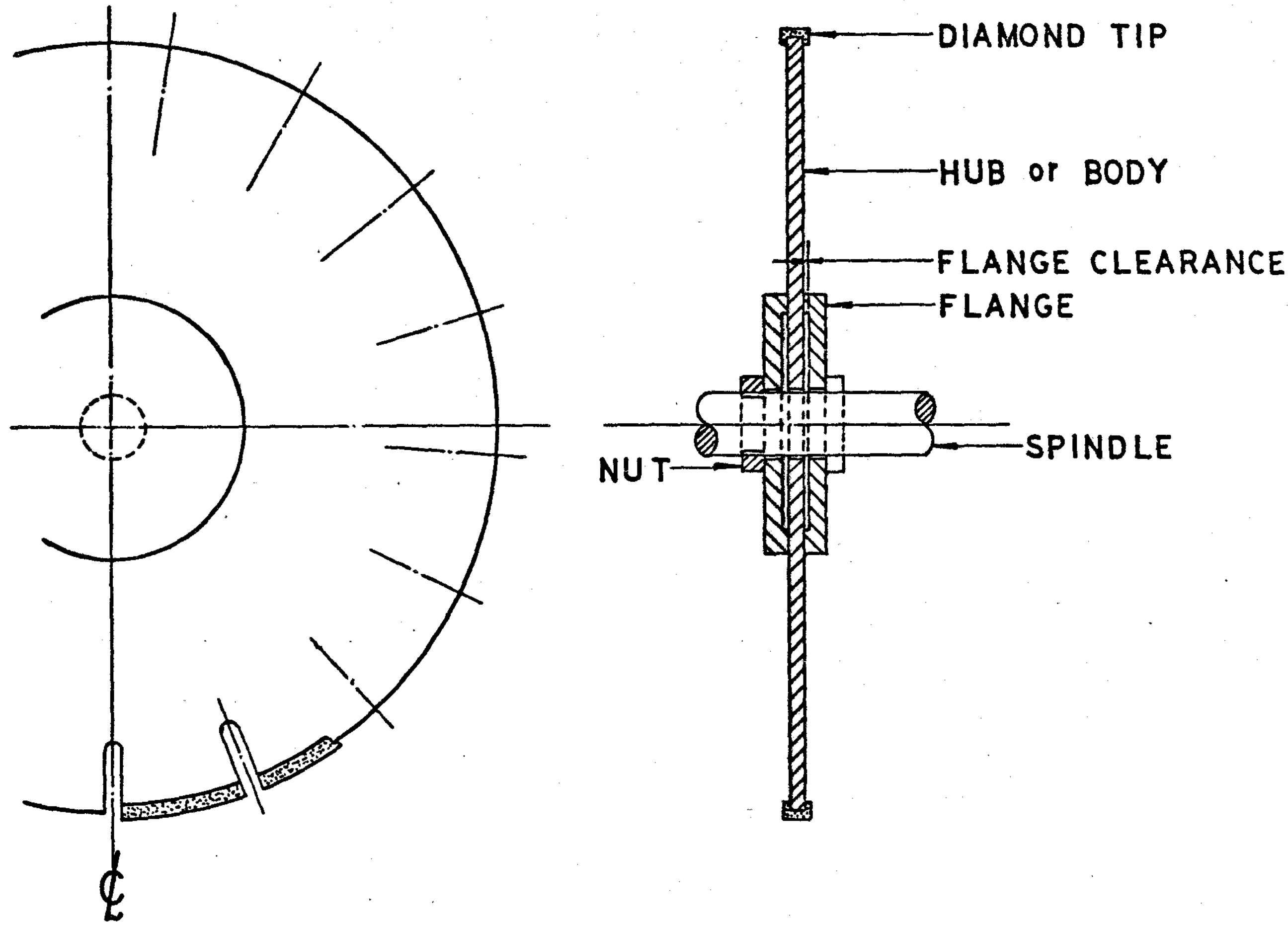

<u>FIG. 12.3</u> Plan and Cross-sectional Views of a Diamond Tipped Circular Saw.

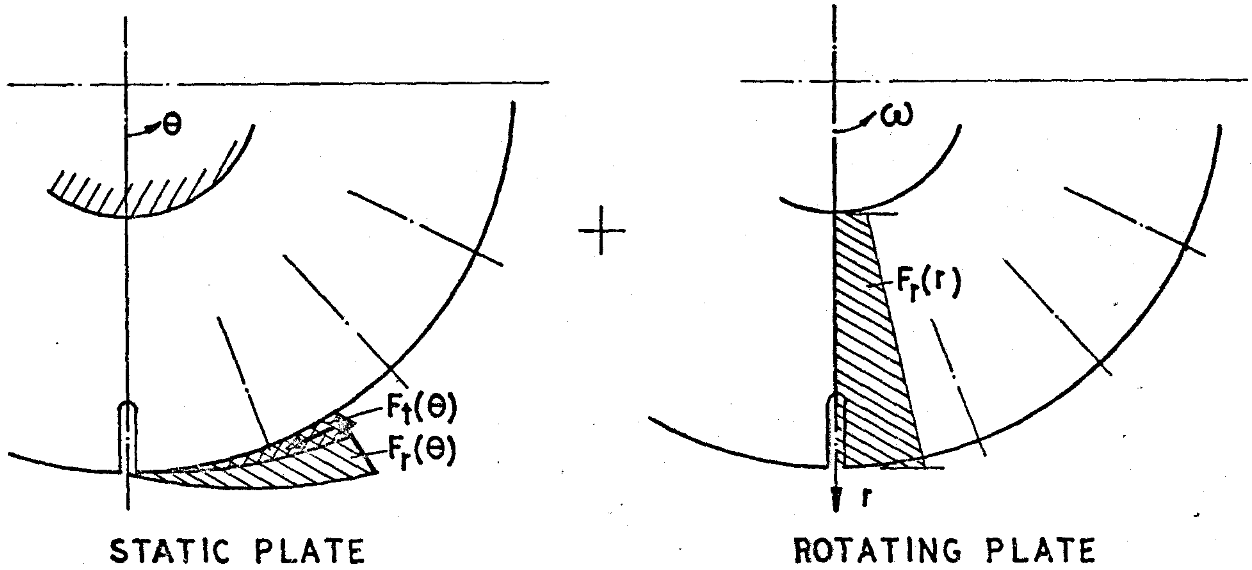

<u>FIG. 12.4</u> Resolution of Saw Blade Problem to Two Static Problems.

However, coupled with the basic stress spectrum, the out of plane vibration may have a substantial effect, and its consideration in the analysis is suggested as a point of future research. The vibration analysis may also be done by the finite element method. An invaluable reference regarding the vibration fatigue aspect is Lazan [15].

12.1.2. Fatigue considerations

It is well known that fatigue cracks are initiated in regions where the localized stress is highest. Usually these regions are around holes, notches and grooves, and are termed 'stress concentrations'.

There exists material [16,17] on artificial factors called 'stress concentration factors' which are used in predicting the strength reduction of bodies having stress concentrations. Factors for static as well as fatigue conditions have been found mostly by experimentation. The most well known of these are:

(i) The theoretical stress concentration factor for static conditions, K_t, defined as:

$$K_t = \frac{S_{max}}{S_{nom}}$$

where S_{max} is the maximum elastic stress caused by the stress concentration and S_{nom} is the nominal stress at the same point if there were no stress concentration.

(ii) The fatigue stress concentration factor, K_f, defined as:

$$K_f = \frac{\text{fatigue strength of unnotched specimen}}{\text{fatigue strength of notched specimen}}$$

K_t and K_f are related by the 'notch-sensitivity' of the material.

(iii) The notch-sensitivity, q, defined as:

$$q = \frac{K_f - 1}{K_t - 1}$$

Generally, K_f is less than K_t when $q < 1$. Notch-sensitivity was introduced by Peterson [18] who found it to be a material property.

In short, one designs as if no stress concentration exists and then reduces the strength of the material by a factor K_t or K_f, depending on the conditions existing. Conversely, the stress is magnified by the value of the concentration factor and is hoped to approximate the actual stress. Unfortunately, these stress concentration factors are useful only for simple members such as notched shafts, tension specimens and simple bending and torsion specimens.

In more complicated structures it is necessary to trace carefully the path which the stresses take within the structure to locate the regions of high alternating stress. It is apparent that the finite element method is most useful for this aspect of the problem.

The stress at the critical region is usually not a simple stress, but some conbination of alternating normal stress and alternating shear stress superimposed upon static stresses. However, the state of stress at a point within a body can be described completely by the principal stresses and their directions no matter how complicated the system is.

Waisman [19] and Miner [12] show how an actual stress spectrum may be replaced by an equivalent one of constant amplitude. If the principal stress is a simple sinusoidal one, it can be split into an alternating stress superimposed upon a static stress. The alternating component can be described by its amplitude.

A seemingly plausible theory concerning behaviour of metals under complex alternating stresses has been developed by G. Sines [21] and is discussed in the next section.

12.1.3. Fatigue Criterion

The assumptions are made that in the case of an isotropic material, the directions of the principal stresses are unimportant and only the magnitudes are significant. Also each principal stress varies at the same frequency.

From the examination of data on the effect of different combinations of purely alternating stress it appears that the alternation of shear stress causes the fatigue damage, and this fact lends support to the octahedral-shear stress theory.

Peterson [22], however, states that although fatigue failure may start on shear planes, most fatigue fractures follow the normal stress direction.

Tests on the effect of mean axial stress on the permissible amplitude of alternating axial stress show the following:

The amplitude of allowable alternating stress is decreases by tensile mean stress and is increased by compressive mean stress.

Based upon diverse experimental data available, Sines [21] has developed a criterion of fatigue failure which includes the effect of different combinations of alternating stress with static stresses. It is the simple statement that the permissible alternation of the octahedral-shear stress is a linear function of the sum of the orthogonal normal static stresses. Or mathematically:

$$\frac{1}{3}\{(P_1 - P_2)^2 + (P_2 - P_3)^2 + (P_1 - P_3)^2\}^{1/2} <$$

$$A - a(S_1 + S_2 + S_3 + R_1' + R_2' + R_3') \quad (12.1)$$

where P_1, P_2 and P_3 are the amplitudes of the alternating principal stresses and S_1, S_2, and S_3 are the orthogonal static (or mean) stresses. The orthogonal axes 1', 2', 3' for the residual stresses $R_{1;}$, etc., need not be in the same directions as those for the static normal stresses. The A is a constant for the material, proportional to the reversed fatigue strength, and the a gives the variation of the permissible range of stress with static stress. Both A and a are given for the desired cyclic lifetime. The expression on the left must not exceed the right-hand side or failure will occur before the desired lifetime.

It can be seen that inducing compressive residual stresses (which are negative in sign) will permit greater alternation of stress for the same cyclic life. Conversely, tensile residual stresses are to be avoided.

For a biaxial state of stress and in the absence of residual stresses equation (12.1) reduces to:

$$\frac{\sqrt{2}}{3}\{(P_1^2 + P_2^2) - P_1P_2\}^{1/2}$$

$$+ a\{S_1 + S_2\} < A \qquad (12.2)$$

From the above equation it can be seen that compressive (negative) mean stresses are beneficial. An increase in 'biaxiality' is also beneficial, i.e. when P_1 and P_2 approach each other in value. If $P_2 = P_1/2$, then $P_2^2 = P_1^2/4$ and $P_1P_2 = P_1^2/2$. Thus a larger quantity is substracted than the quantity added to the term under the square-root.

The graphical presentation of equation (12.2) appears as a series of "concentric" ellipses, the size of the ellipse depending on the sum of the static normal stresses.

12.1.4. Determination of Constants for Criterion

The values A and a which describe the fatigue properties of a material can be determined from two fatique curves in which the static stresses are appreciably different. Two curves which are convenient for their determination are the reversed axial test and the zero-tension fluctuating stress.

In the reversed axial test the criterion of equation (12.2) reduces to

$$\frac{\sqrt{2}}{3} P_1 = A$$

Thus $A = (\sqrt{2}/3)f_1$ where f_1 is the amplitude of the reversed axial stress which would cause failure at the desired cyclic lifetime.

For the zero-tension fluctuating stress cycle the criterion reduces to

$$\frac{\sqrt{2}}{3} P_1{}' = A - aP_1{}'$$

in which $S_1{}' = P_1{}'$. Solving the above equation,

$$a = \frac{A}{P_1{}'} - \frac{\sqrt{2}}{3} = \frac{\sqrt{2}}{3} \left(\frac{f_1}{f_1{}'} - 1\right)$$

where $f_1{}'$ is the amplitude of the fluctuating stress which would cause failure at the same lifetime as the reversed stress f_1.

12.1.5 Qualitative Nature of Problem

It will be deduced from Appendix J that there are a great many interdependent factors that determine the choice of blade for a particular stone-cutting operation. The factors directly or indirectly affecting the stresses in the saw blade are:

(1) Varying properties of stone, each within its class varying by geographic origin.

(2) Economics and production.

(3) Machine types, e.g. hand operated gantry or orthogonal machine, manual feed or automatic feed.

(4) Mode of cutting, up-cutting or down-cutting.

(5) Cutting parameters: speed of rotation, feedrate, depth of cut.

(6) Internal vibrations. Older machines obviate the use of thin blades.

(7) Method of cooling and flowrate of coolant.

(8) Material properties of blade body.

(9) Blade thickness.

(10) Blade diameter.

(11) Flange size and thickness.

(12) Segment tip properties: material of tip type of bond, grit size and concentration, width and thickness of segment.

(13) Number of slots.

(14) Slot shape.

Since the aim is to study the effect of slot shape on the blade stresses it seems reasonable to keep all but the last of the above factors constant and vary only the slot shape. A comparative study can then be made by studying the changes in stress due to changes in slot shapes.

All but the last of the above factors affect the cutting forces. After a choice of blade for an operation is made then cutting forces are dependent on the cutting variables, if all other external factors are ignored. By choosing the cutting variables, the cutting forces are fixed and, since cutting forces give rise to the stresses, the problem is reduced to one of a rotating irregularly shaped plate under the action of a system of cutting forces.

The fatigue criterion of equation (12.2) may be used as a basis for comparison of the effects of different slot shapes.

In the next section the blade chosen for the analysis is described.

12.1.6. Model Saw Blade

A used diamond tipped segmented circular saw blade which failed due to fatigue cracking was made available by the courtesy of the Boart Metal Industries of South Africa. This blade, which was of the conventional type, i.e. having a simple parallel sided slot with semi-circular root, was used as a model. The blade dimensions were as follows:

Diameter, 30 cm. ($\approx$ 12 in)

Central Hole Diameter, 1 in

Number of Slots, 17

Blade Thickness, 0.0625 in

Slot Width, 0.125 in

Slot Depth, 1 in to center of slot base circle

Slot Base Circle Radius, 0.0625 in.

The above nomenclature is clarified in Fig. 12.3. In order to calculate the cutting force distribution in Chapter 11, the following cutting parameters were used:

Blade speed, 1000 rpm

Feed rate, 300 mm/sec

Depth of cut, ~ 0.9 in.

The depth of cut was chosen for convenience to cover 1 1/2 segments. The hub or body material was made of a tool steel hardened to around 42-44 Rockwell C. The diamond impregnated tips were made of tungsten carbide.

12.2. Secondary Analysis:

12.2.1. Formulation for Stress Analysis

When considered as a free body, the problem of the saw blade is essentially one of a rotating irregularly shaped plate under the action of cutting forces over part of the periphery. Rotation of the blade causes internal stresses of the blade body by the centrifugal forces which act over the entire blade body. Although the diamond tips do the actual cutting, they do not significantly change the blade stiffness and were ignored.

As the blade was assumed to be elastic, it was possible to resolve the problem as the sum of two static problems*:

(i) The problem of stresses due to cutting forces,

(ii) The problem of stress due to free rotation, or centrifugal forces.

These two problems are shown diagrammatically in Fig. 12.4.

12.2.2. Subregions

The greatest concentration of stress exists at the slots in the immediate vicinity of the cutting forces and hence it was necessary to critically analyse this region.

Because the loading by the cutting forces is unsymmetric, it was not possible to section off and analyse a portion of the blade. This meant that the entire blade had to be analysed, and because the blade represented a multiply-connected system, the method of partitioning could not be used. It was decided that the best method of solving the problem would be by the method of subregions described in Chapter 9. Four successive approximations were made using this method, the initial approximation followed by three subregions. An outline of the relative portions of the blade isolated are shown in dotted lines in Fig. 12.5. The mesh of the first and second approximations

* Since it was a simple matter of adding force column vectors, these two problems were solved in one computer program.

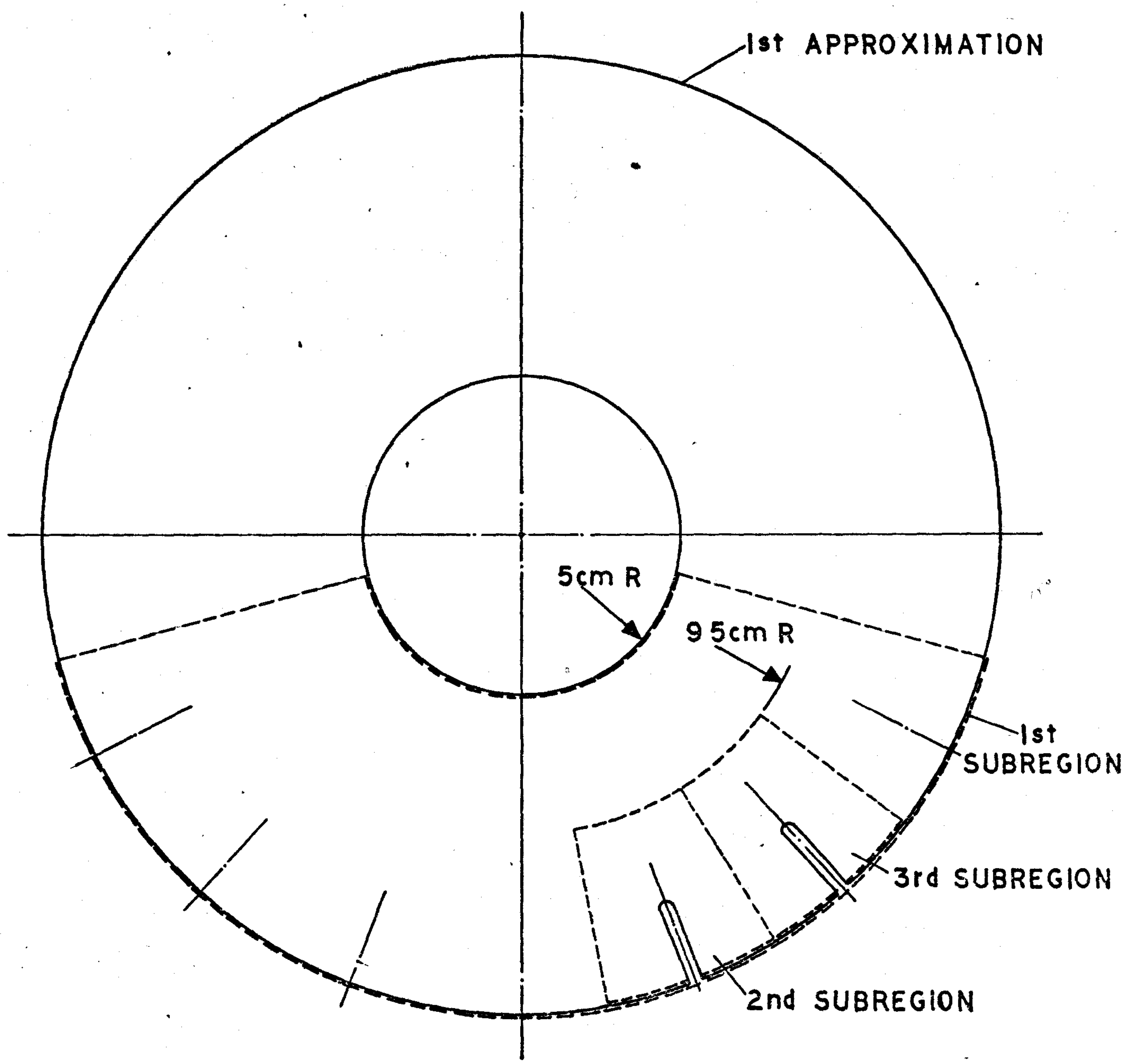

FIG. 12.5 Outlines of the Subregions Isolated for the Sequential Stress Analysis of Saw Blade.

were drawn up without much consideration to the slot shape. The third and fourth subregions were accurately drawn up in order to vary the shape of the slot. The subregions are discussed in the sections which follow.

12.3. First Approximation:

12.3.1. Mesh

It was decided to use the TRIM3 element for the first approximation because the physical approximation by this element would be better than by the TRIM6 element if restricted by number of nodes. The mesh drawn for this case is shown in Fig. 12.6, and consists of 410 elements and 279 nodes. The semi-circular slot bases were modestly approximated by two straight lines. The basic TRIM3 finite element program was used for the first approximation. The boundary conditions applied are discussed below.

12.3.2. Force Boundary Conditions

In Chapter 11 approximate cutting force distributions for radial and tangential forces were found to be linear with the angle measured from the vertical. These were:

$$F_r = 0.26\ \theta$$

$$F_t = 0.2\ F_r$$

In Chapter 4 these distributed boundary forces were discussed in an example and were discretized to concentrated

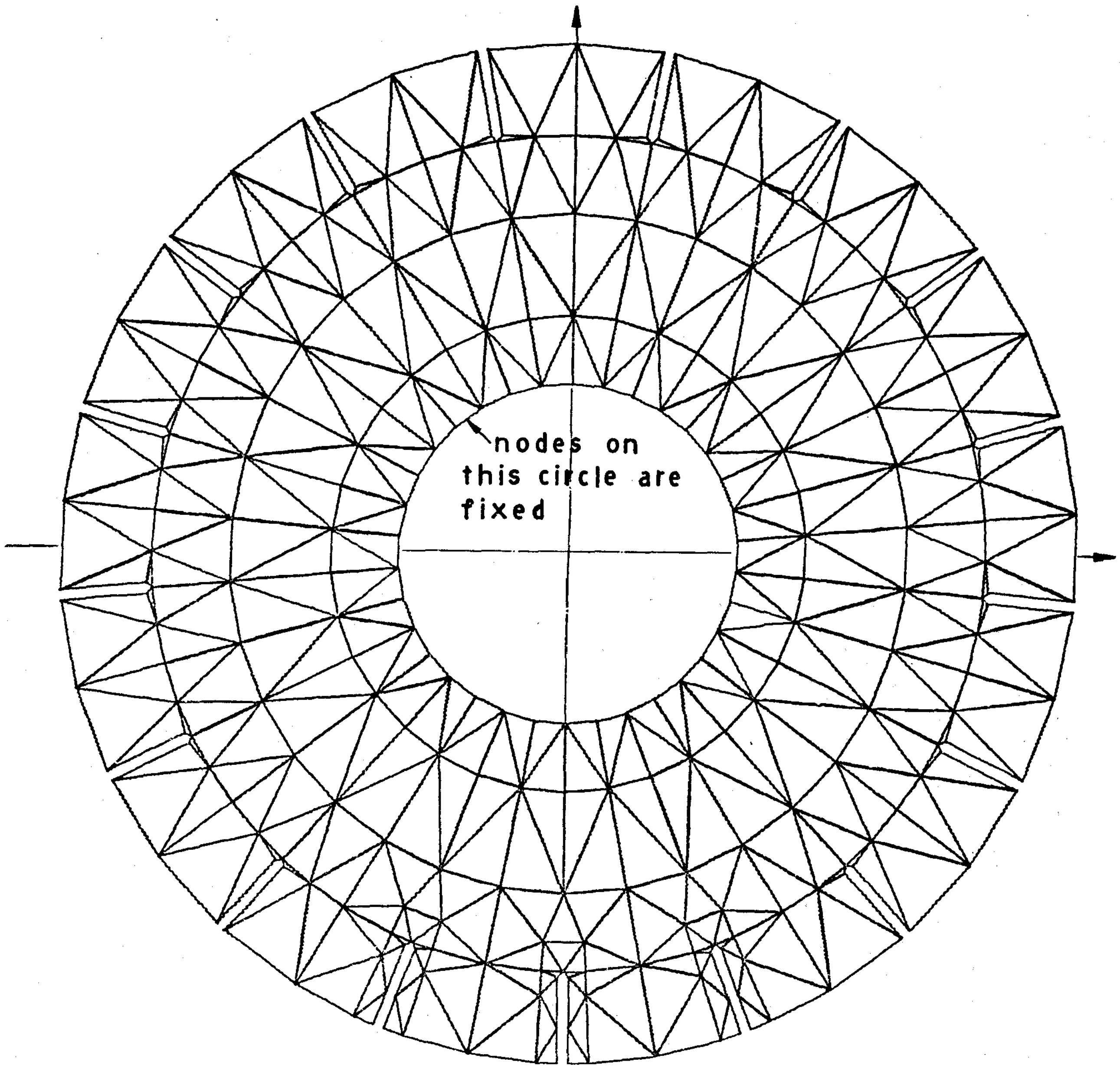

FIG. 12.6 Input Mesh of TRIM3 Elements for First Approximation of Saw Blade Stresses. Mesh Contains 460 Elements and 279 Nodes.

nodal forces by two methods, the results of which are given in Table 4.1. These results are shown graphically in Fig. 12.7 where the mesh of Fig. 12.6 is laid out on a horizontal axis. Because of the absence of cutting edges at a slot, the net force over this region was lumped on the node on the left edge of the slot. This has the effect of changing the force distribution in the manner shown in dotted lines in Fig. 12.7.

12.3.3. Displacement Boundary Conditions

The assembly components of the saw blade consist of: (i) inner flange (ii) saw blade, (iii) outer flange and, (iv) nut fastener. These components are shown in Fig. 12.3.

Converting the problem to a static one made it possible to fix the inner boundary of the saw blade because the blade is in equilibrium when acted upon by the cutting forces. A simple calculation performed by treating the flanges as simply supported circular plates showed that no slippage would occur between saw blade and flanges. By this deduction the flanges could be taken as integral parts of the blade. Physically, this meant increasing the thickness of the blade over the area of the flanges by two flange thicknesses.

However, by increasing the thickness of the blade over the area of the flanges, the stiffness of the portion of the blade is increased a great deal, and it was of the opinion that the stresses at the slots would not be affected if the blade were

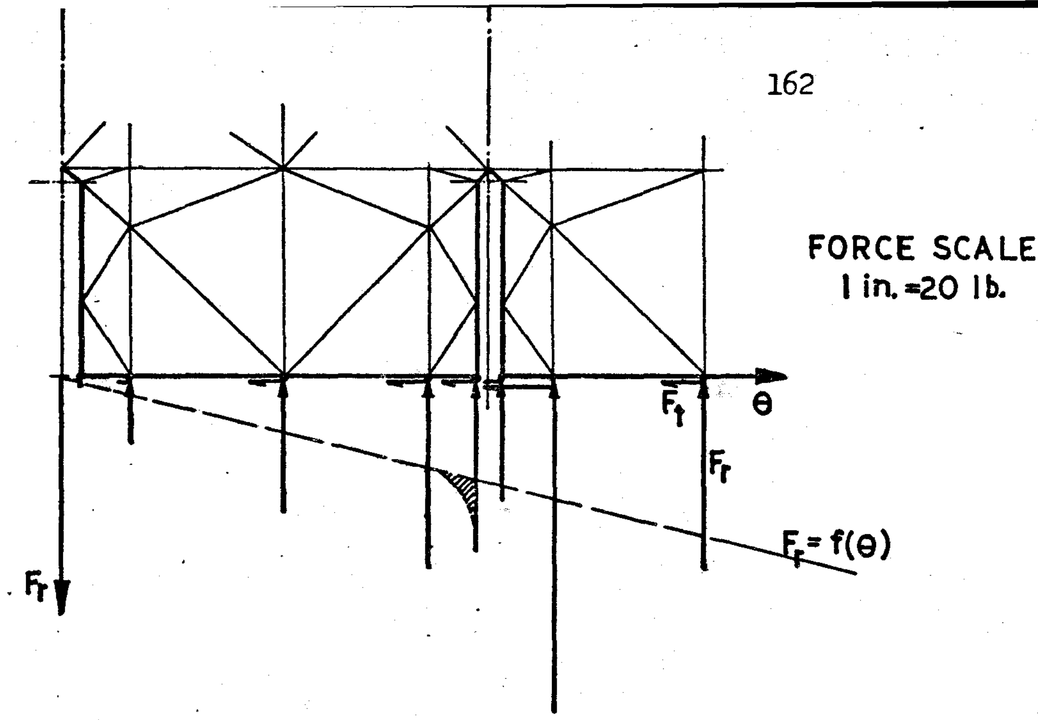

FIG. 12.7 Nodal Forces Applied Over Cutting Region on Mesh of 1^{st} Approximation (Polar System).

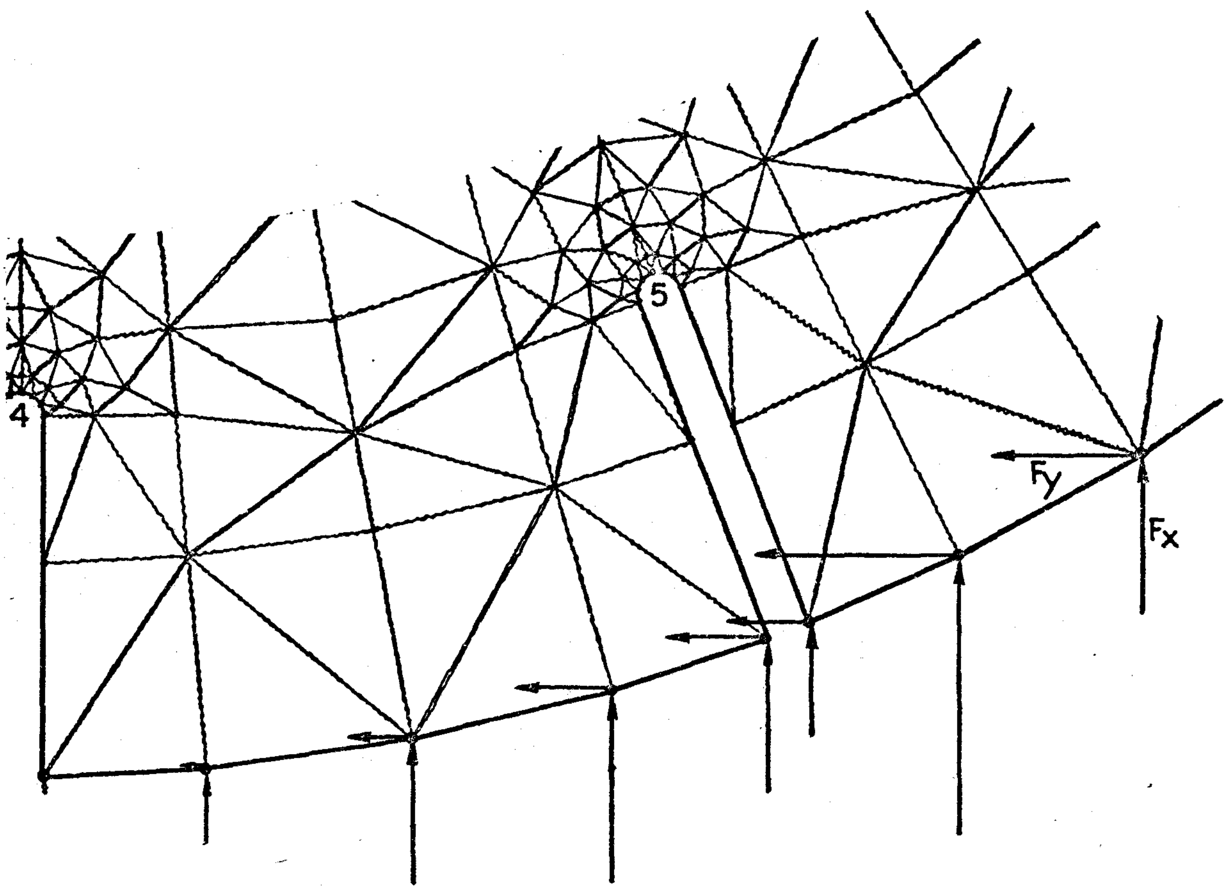

FIG. 12.10 Nodal Forces Applied Over Cutting Region on Mesh of 1^{st} Subregion.

rigidly fixed over the flange peripheries. To establish this, the problem was solved with the following two sets of boundary conditions:

(i) All nodes lying on the inner boundary of the blade were fixed in both the x and y directions, and the blade thickness was increased over the flange areas.

(ii) All nodes lying on the flange peripheries were fixed in the x and y directions.

These two cases are sketched in Figs.12.2(a) and (b). By comparison of the stresses obtained in the two cases it was found that they differed by an insignificant amount. Fig. 12.8(c) shows the distortion of some elements and a radial line lying on the y-axis as solved in the two cases. It is observed that the discrepancy between the displacements in the two cases is due to a rigid body rotation which does not affect the stresses. It was, thus, concluded that the blade could be fixed over the flange periphery, as was done in all subsequent cases.

12.3.4. Results of First Approximation

Principal stress contours for the area surrounding the region loaded by cutting forces are shown in Figs. 12.33(a) and (b). This region is the lower part of the main mesh of Fig. 12.6. These contours represent stresses due to the combined effect of cutting forces and centrifugal forces.

Although a detailed study of the behaviour of the

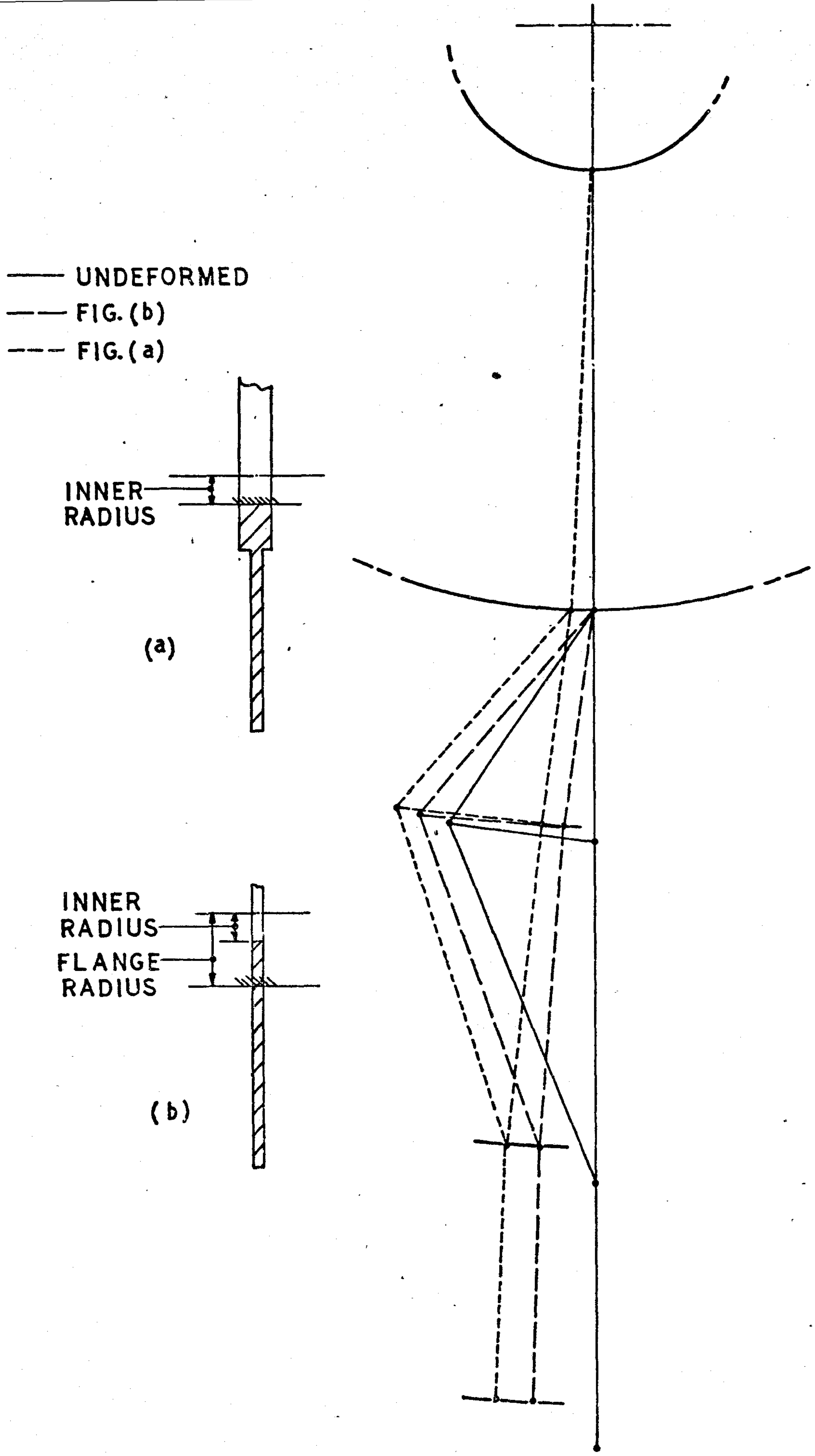

FIG. 12.8 Deformation of a Radial Line by Fixing the Nodes Lying on Two Different Circumferences Shown in (a) and (b).

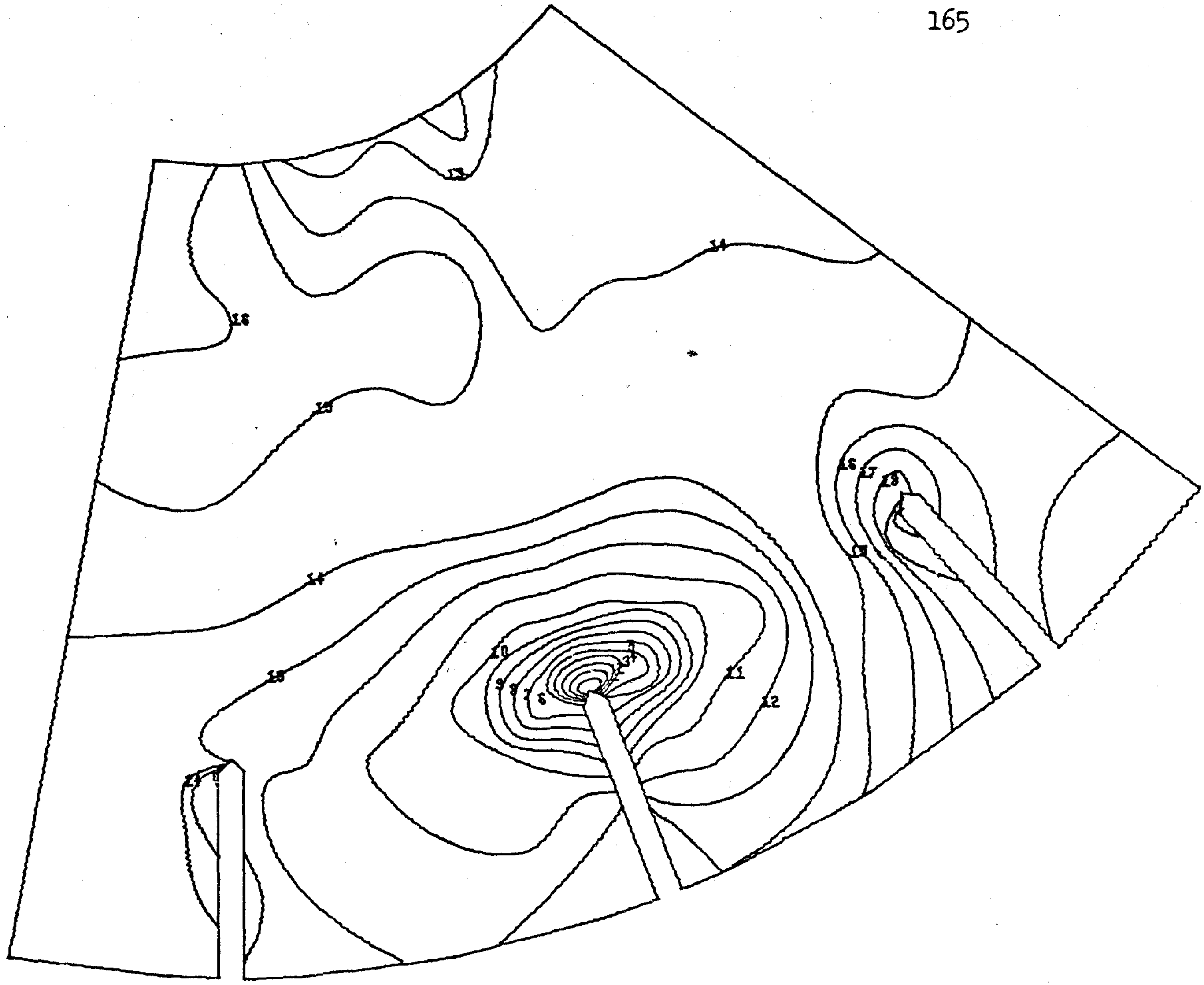

KEY TO CONTOURS-

CONTOUR	1	2	3	4	5	6	7	8	9	10
STRESS	-600	-550	-500	-450	-400	-350	-300	-250	-200	-150
CONTOUR	11	12	13	14	15	16	17	18	19	20
STRESS	-100	-50	0	50	100	150	200	250	300	350
CONTOUR	21	22	23							
STRESS	400	450	500							

FIG. 12.33(a) Maximum Principal Stress Contours of First Approximation.

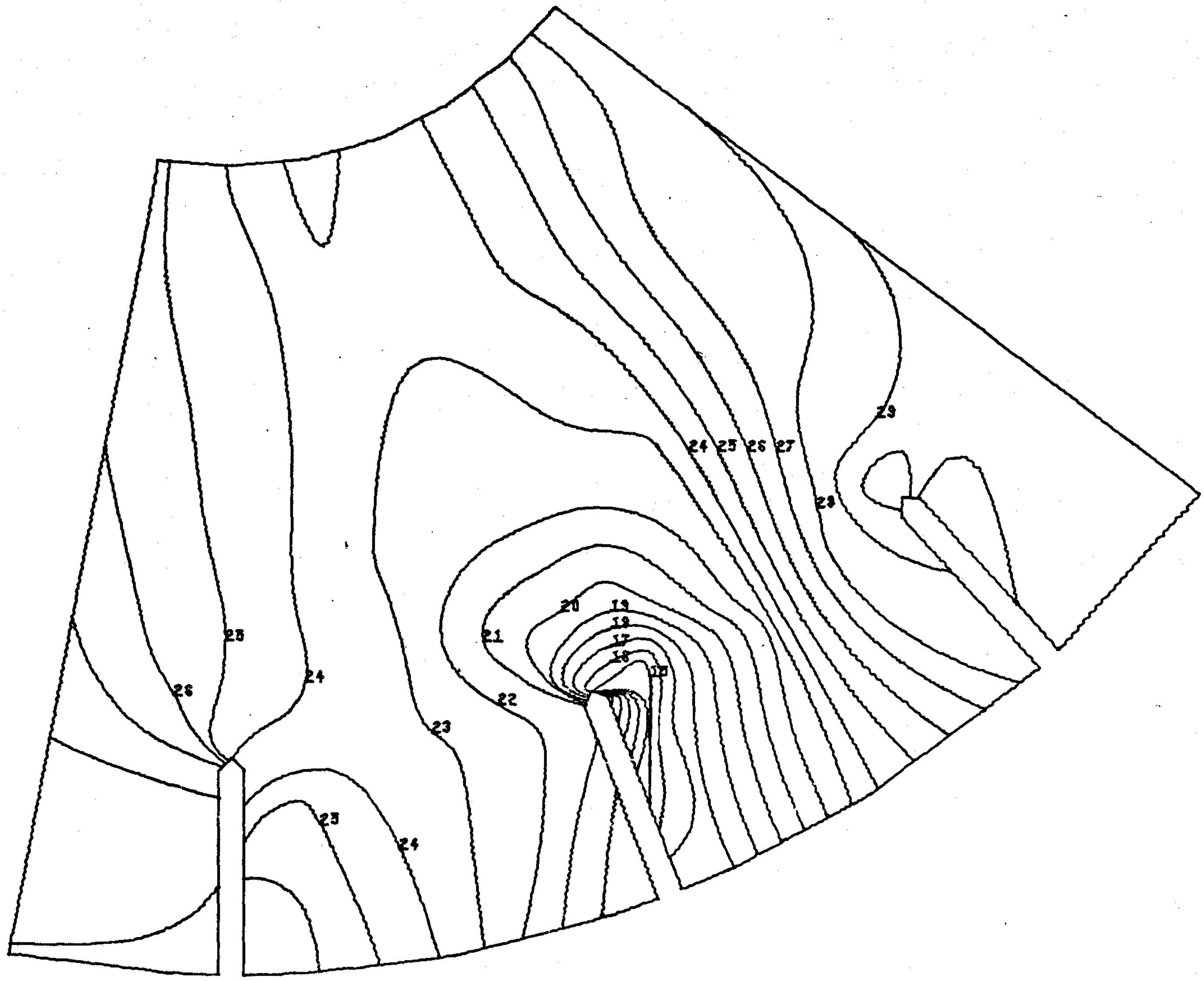

KEY TO CONTOURS-

CONTOUR	1	2	3	4	5	6	7	8	9	10
STRESS	-2800	-2700	-2600	-2500	-2400	-2300	-2200	-2100	-2000	-1900
CONTOUR	11	12	13	14	15	16	17	18	19	20
STRESS	-1800	-1700	-1600	-1500	-1400	-1300	-1200	-1100	-1000	-900
CONTOUR	21	22	23	24	25	26	27	28	29	30
STRESS	-800	-700	-600	-500	-400	-300	-200	-100	0	100

FIG. 12.33(b) Minimum Principal Stress Contours of First Approximation.

stresses cannot be made at this stage because of the coarseness of the mesh, the contour plots do establish the existence of the stress concentrations. The most highly stressed regions are seen to be those surrounding the second and third slots in Figs. 12.26. The first slot is not as highly stressed and, from the results of the entire mesh, the same can be said for slots beyond the third.

The region surrounding the second slot is in compression while the region surrounding the third slot is in tension. Looking at the loading system applied, this state of stress is expected because the loads tend to close the second slot and widen the third.

Table 12.5 shows the effect of centrifugal forces on two of the most highly stressed elements. Centrifugal forces increase the stress in a tensile element and reduce the stress in a compressive element.

Element	Cutting Forces Only		Combined Cutting and Centrifugal Forces	
	S_1 psi	S_2 psi	S_1 psi	S_2 psi
78	797.7	70.0	926.2	73.0
54	-728.7	-2951.2	-715.8	-2840.5

TABLE 12.5

The stresses obtained by the first approximation help in giving a general picture but the actual magnitudes are not accurate. The main objective of the first approximation was to determine the subregion to isolate, and thereafter, to obtain boundary displacements for the subregion.

12.4. Second Approximation or First Subregion:

12.4.1. Mesh for First Subregion

In Chapter 9 it was mentioned that the only way to determine the size and shape of a subregion is by trial and error. Hence, as a trial the first subregion was isolated from the main body of the blade to include seven slots of the lower half, as indicated in Fig. 12.5. A computer plot of the mesh drawn up for the subregion is shown in Fig. 12.9. This mesh was finer than the mesh of the first approximation. The regions surrounding the slots, especially, were subdivided in more detail.

For this subregion it was only necessary to define the mesh for one sector*. The rest of the mesh was generated simply by repeating the sector and adding a sector angle each time. The mesh consisted of 812 TRIM3 elememts and 478 nodes.

12.4.2. Finite Element Program for First Subregion

The mesh of Fig. 12.9 was beyond the scope of the basic finite element program. However, the subregion was now

---

* The region between two radial lines passing through successive slots. The sector angle is the angle defined as ϕ in Fig. 12.1.

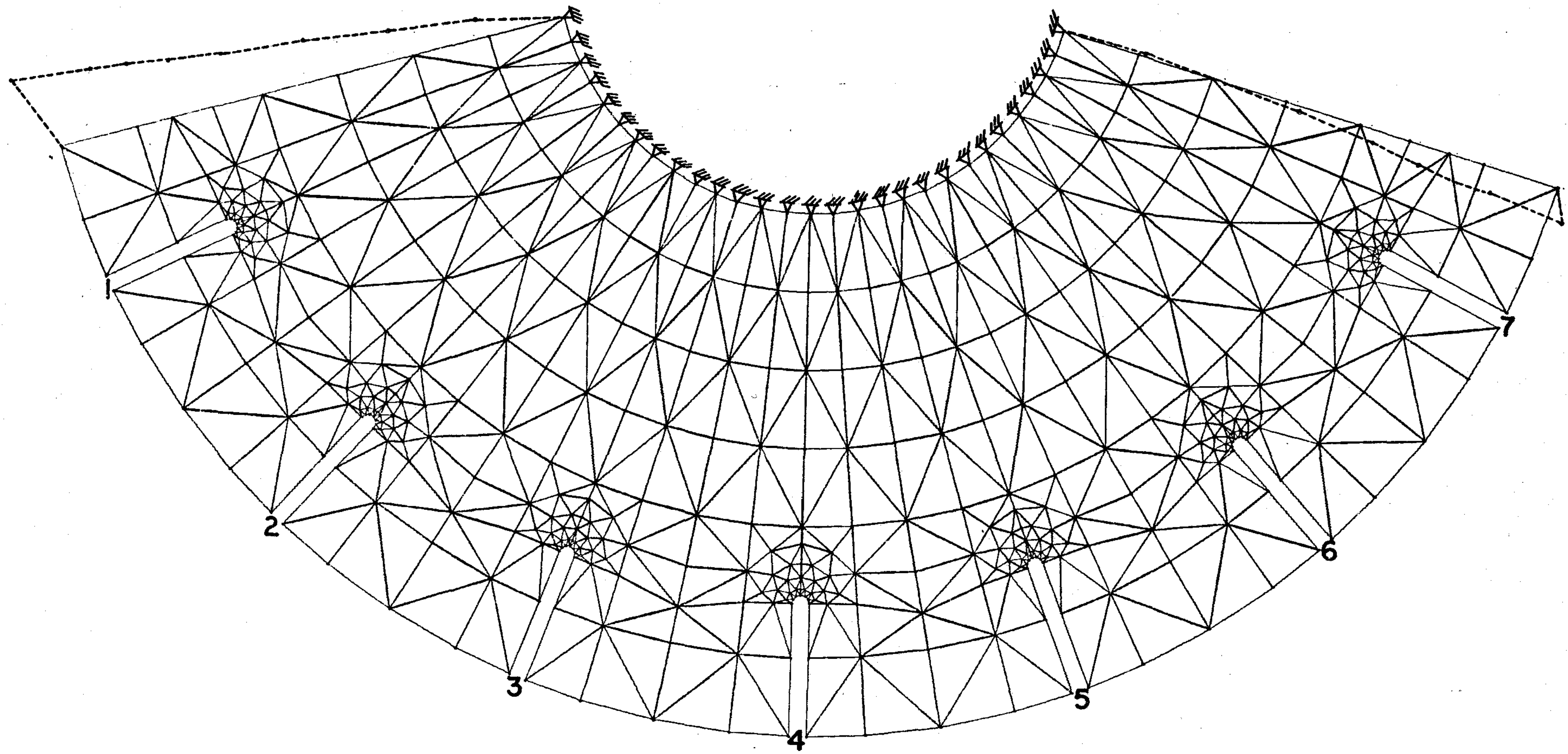

FIG. 12.9 Input Mesh of TRIM3 Elements for 1st Subregion (2nd Approximation).

simply connected and therefore, it was possible to use the method of partitions. The mesh was divided into 14 partitions, each partition covering one-half of a sector.

12.4.3. Force Boundary Conditions

The same force distribution used in the first approximation was again applied but, because the number of boundary nodes increased, the distribution had to be discretized for the new system of elements. In Fig. 12.10 the resulting concentrated nodal forces are represented as vectors.

12.4.4. Displacement Boundary Conditions

Nodes located on the inner boundary were again fixed in both the x and y directions. The displacements applied on the nodes at the left and right boundaries were obtained from the displacements found from the first approximation. The relative positions of the boundary nodes of the new mesh did not coincide with those of the old mesh, hence a linear interpolation was performed to find the boundary nodal displacements.

12.4.5. Results of Second Approximation

In Figs. 12.12(a) and (b) σ_x stresses are plotted against the radius for both the left and right sides of the subregion in order to compare the results of the first and second approximations at the boundaries at which the sections were made. The closeness of the comparison shows that the

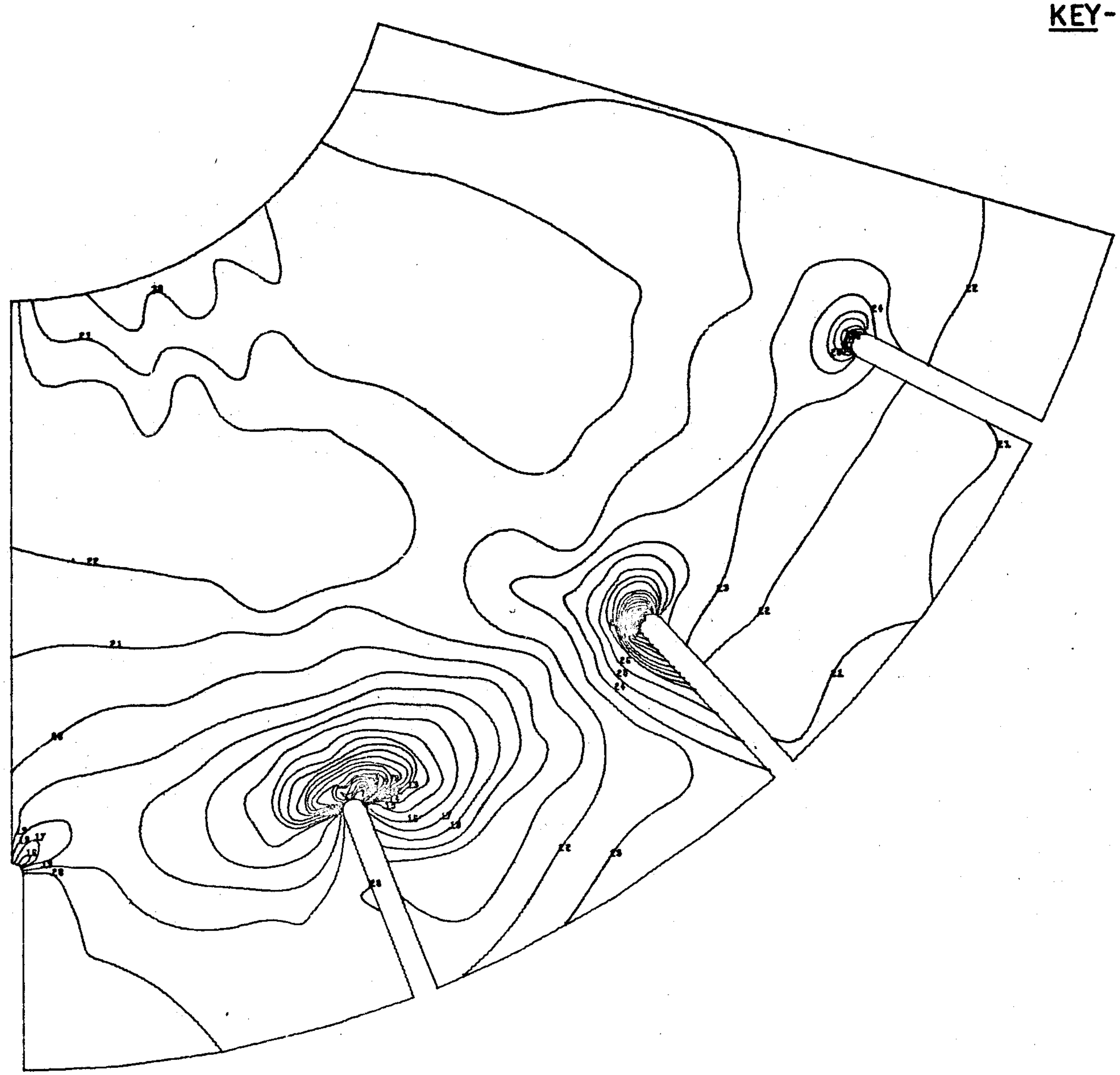

KEY-

1	-1000.000
2	-950.000
3	-900.000
4	-850.000
5	-800.000
6	-750.000
7	-700.000
8	-650.000
9	-600.000
10	-550.000
11	-500.000
12	-450.000
13	-400.000
14	-350.000
15	-300.000
16	-250.000
17	-200.000
18	-150.000
19	-100.000
20	-50.000
21	10.000
22	50.000
23	100.000
24	150.000
25	200.000
26	250.000
27	300.000
28	350.000
29	400.000
30	450.000
31	500.000
32	550.000
33	600.000
34	650.000
35	700.000
36	750.000
37	800.000
38	850.000
39	900.000
40	950.000
41	1000.000
42	1050.000
43	1100.000
44	1150.000
45	1200.000
46	1250.000
47	1300.000
48	1350.000
49	1400.000
50	1450.000
51	1500.000

FIG. 12.11(a) Maximum Principal Stress Contours of 2nd Approximation (1st Subregion)

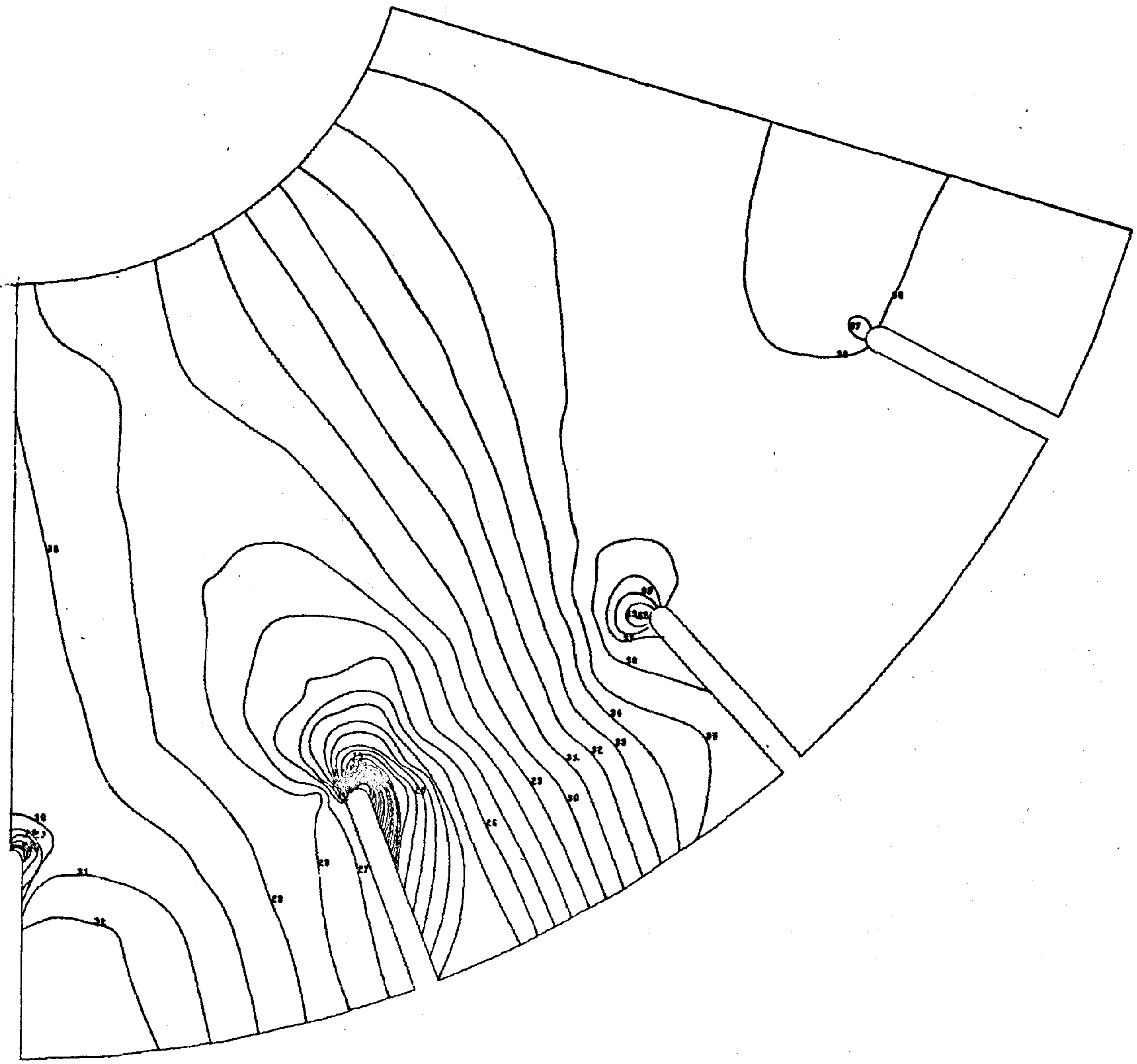

KEY-

1	-3500.000
2	-3400.000
3	-3300.000
4	-3200.000
5	-3100.000
6	-3000.000
7	-2900.000
8	-2800.000
9	-2700.000
10	-2600.000
11	-2500.000
12	-2400.000
13	-2300.000
14	-2200.000
15	-2100.000
16	-2000.000
17	-1900.000
18	-1800.000
19	-1700.000
20	-1600.000
21	-1500.000
22	-1400.000
23	-1300.000
24	-1200.000
25	-1100.000
26	-1000.000
27	-900.000
28	-800.000
29	-700.000
30	-600.000
31	-500.000
32	-400.000
33	-300.000
34	-200.000
35	-100.000
36	10.000
37	100.000
38	200.000
39	300.000
40	400.000
41	500.000

FIG. 12.11(b) Minimum Principal Stress Contours of 2nd Approximation (1st Subregion)

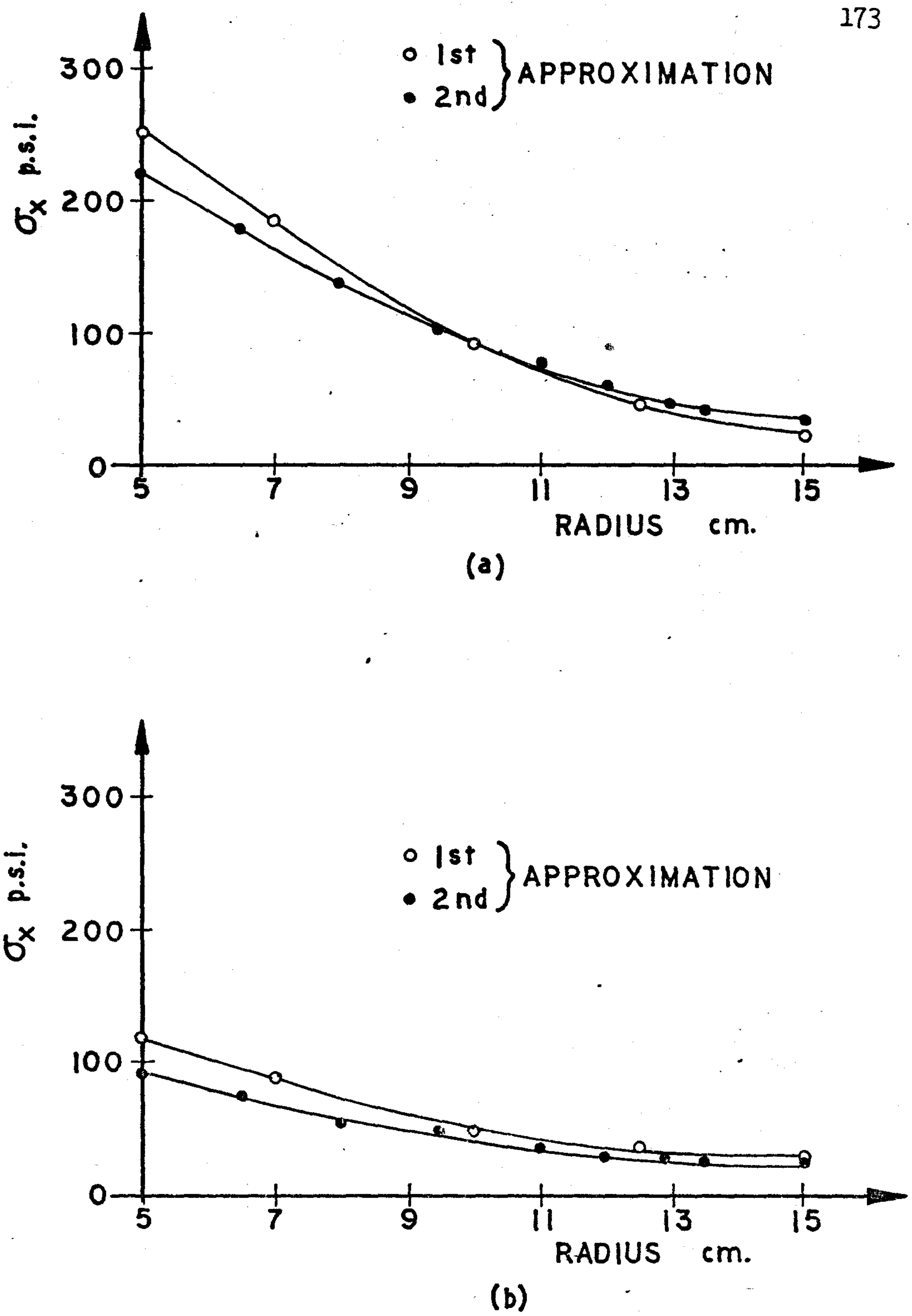

FIG. 12.12 Comparison of Stress Variation Along (a) Left Side and (b) Right Side of 1st Subregion as Solved by Two Approximations.

subregion size was large enough. The contour plots show that stresses are small in the area of the first three sectors and hence these sectors could have been omitted. Nevertheless, the extra sectors posed no problem as the method of partitions could solve many sectors with ease.

In Fig. 12.13 a comparison of x-displacements is made between the two approximations along a circle interior to the subregion. This figure shows that the magnitude of change in displacement is small a distance away from the slots. Because the subdivision was much finer at the slots in the new mesh, a comparison of displacements with the first approximation could not be made here.

The most highly stressed regions were those around slot positions 5 and 6 which are defined in Fig. 12.9. In Fig. 12.14 (a) and (b) the two principal stresses along the circumference of the slots at these two positions are plotted. Since the radii of curvature of the slot bases were constant, the angle is plotted on the abscissa instead of circumferential length. These two figures emphasize what the contour plots already established, that is, in passing from position 5 to position 6 the point of highest stress concentration on the slot base moves from point n to point m (see insets in Fig. 12.14). However, the stress at point m is tensile, while the stress at point n is highly compressive. Fatigue cracking can, therefore, be expected to

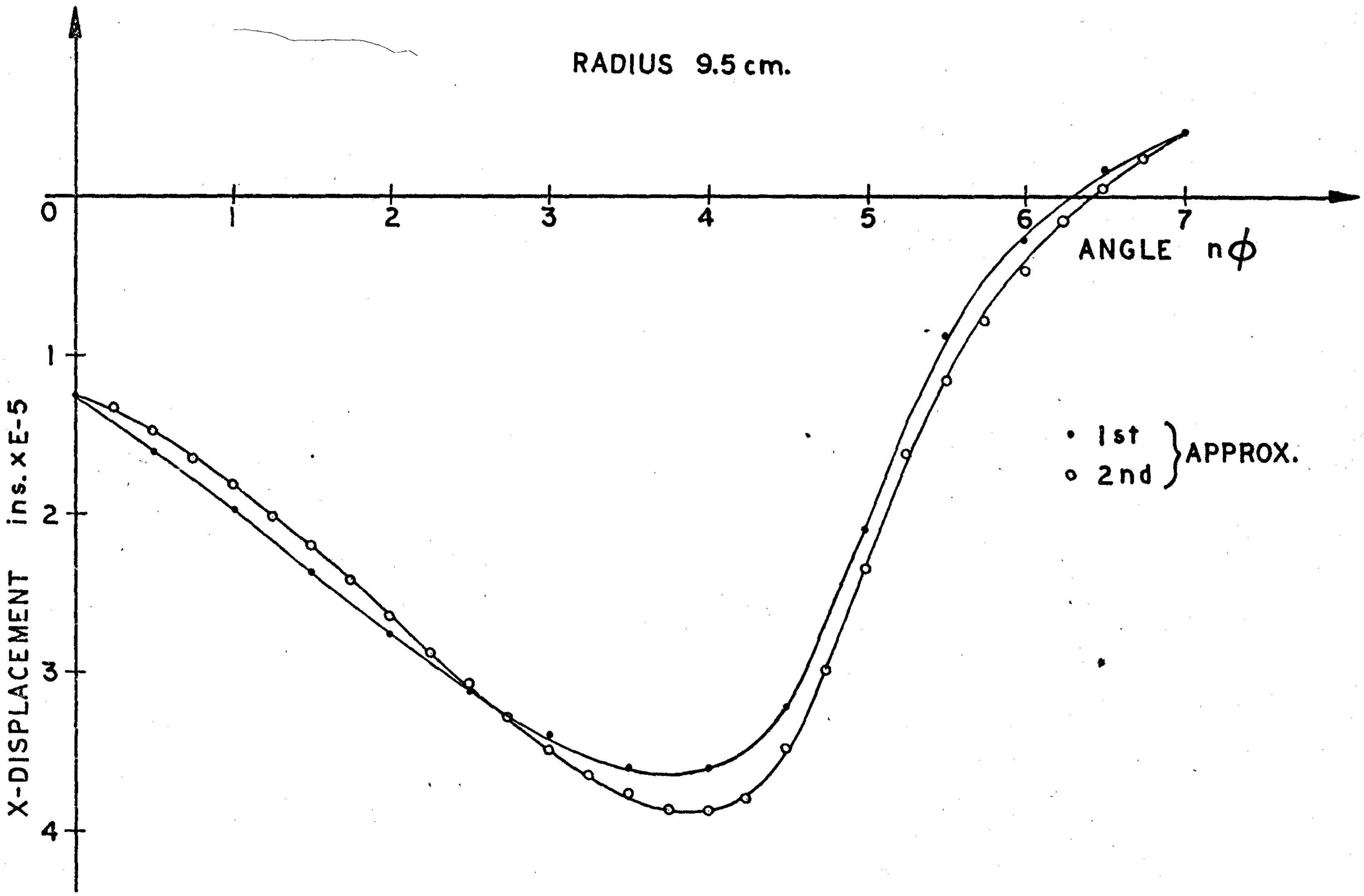

FIG. 12.13 Comparison of Displacement Results of 1st and 2nd Approximations Along an Arc. Angle ϕ is the Sector Angle.

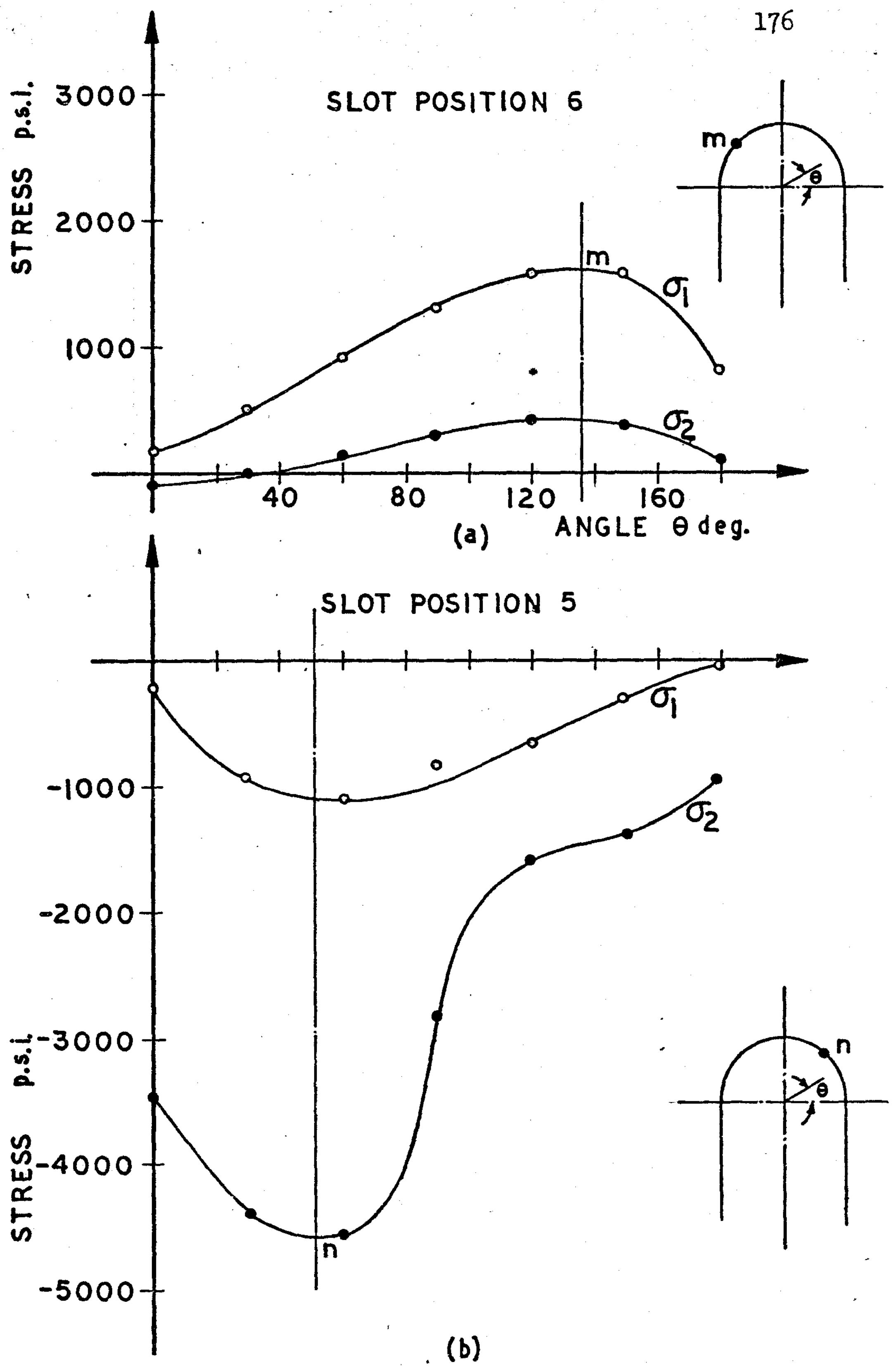

FIG. 12.14 Variation of Principal Stresses Along the Circumference of Slot Bases at Two Positions. Stresses σ_1 and σ_2 are Maximum and Minimum Principal Stresses Respectively.

start at either of these points. In section 12.5.6. the criterion of fatigue failure is used to establish that, of the two points, point n is the more critical.

12.4.6. Principal Stress Spectrum

In Fig. 12.15 the principal stresses σ_1 and σ_2 at the same angular position on the slot base circle as point n are plotted for slots 1 to 7. Stresses for slots beyond the 7th tend toward zero.

If the problem is considered to be a purely static one, then Fig. 12.15 simply represents the variation of principal stress with angle. However, since the blade is rotating and the force is fixed with respect to "ground", this curve can be interpreted as the variation of principal stresses with time. In other words, if t minutes is the time taken for a slot to rotate from position 4 to position 5, then slot position 5 is considered the 'new' position of 4 after t minutes. If T is the time period for one revolution of the saw, then T = 1/N minutes, where N is the blade speed in rpm. Having a total of n slots, then t = T/n. An interval on the abscissa axis of Fig. 12.15 in time co-ordinates would then be of magnitude t as shown for interval 1-2. In this way, the problem is converted from a static problem to a dynamic one, and Fig. 12.15 represents the principal stress spectra for the point of critical stress. From this figure, it can be seen that the two principal stresses σ_1 and σ_2 are in phase.

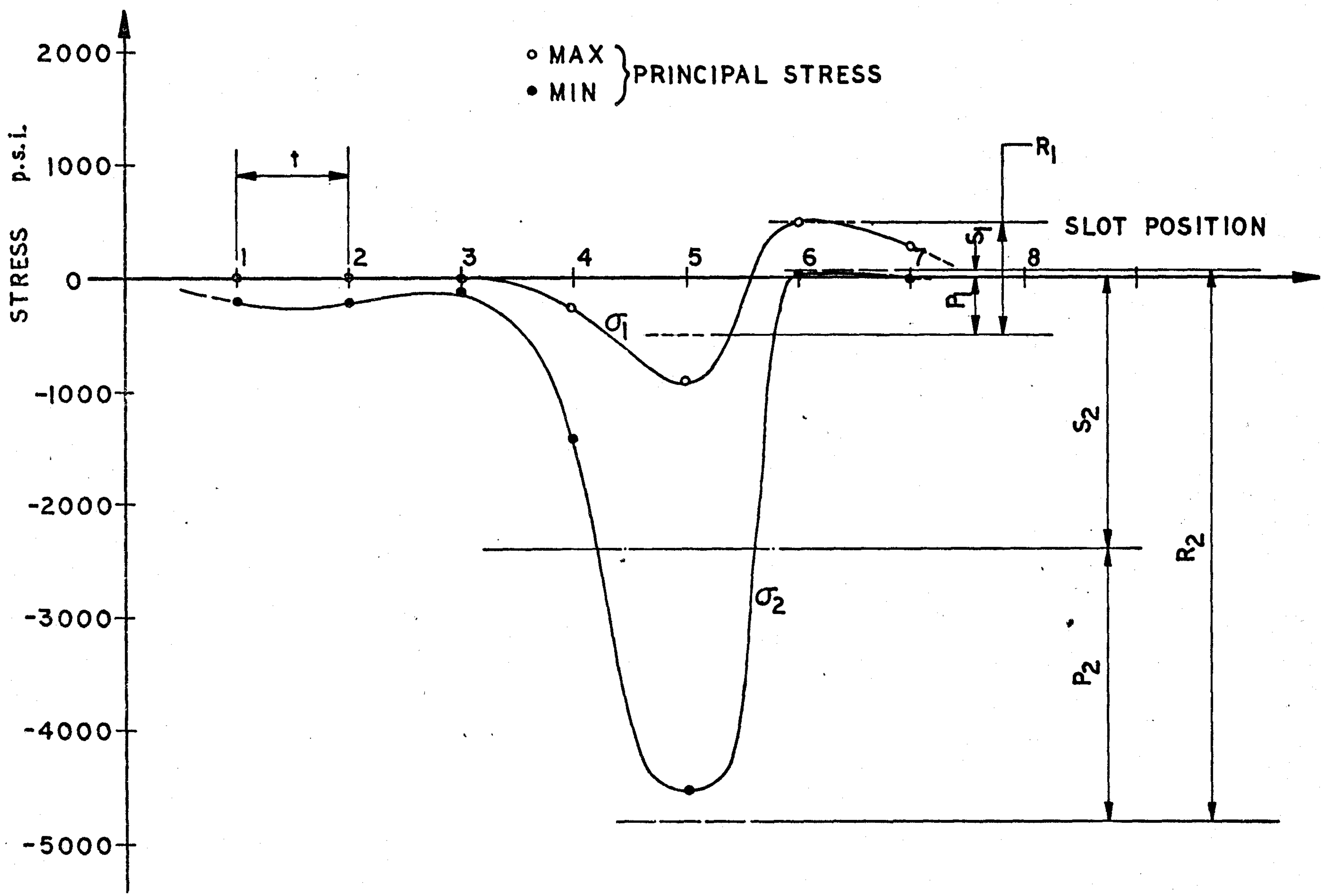

FIG. 12.15 Variation of Principal Stresses with Angular Position of Slot. R_1 and R_2 are Stress Ranges of σ_1 and σ_2 Respectively, Set by 3rd Approximation.

12.5. Third Approximation: Second and Third Subregions:

12.5.1. Isolation of Second and Third Subregions

In the previous section it was pointed out that the regions surrounding slots (labelled as 5 and 6 in Fig. 12.9) are the most critically stressed. The stresses in these regions were found to be, respectively, compressive and tensile in nature and the peaks of the stress spectra were found to fall in these two regions. For this reason, the second and third subregions were isolated in the manner shown in Fig. 12.15, in order to find more accurately the levels of the peak stresses. The inner boundaries of these subregions were chosen to be arcs of a circle of radius 9.5 cm as displacements were found to change insignificantly over this arc from the first to the second approximation (see Fig. 12.13).

The two subregions are identical in shape except that they are off-set by a sector angle. Having defined the mesh for one subregion, the mesh for the other could thus be easily deduced.

To obtain the peak stress levels, these two subregions were solved as separate finite element problems, and together they constituted the third approximation.

12.5.2. Mesh for Generalized Slot Shape

Since it was intended to study slot shapes in the third approximation a computer program was written to generate a finite element mesh for various slot shapes. To do this a 'generalized slot shape' was defined as in Fig. 12.16 so that new shapes could be generated simply by changing the following so-called 'slot variables',

r_H = radius of slot base circle

d = slot depth

γ = slope of slot sides

ψ = angle defining intersection point of slot side and slot base circle.

The computer program generated nodal co-ordinates and nodal numbers for a mesh of TRIM6 element. Referring to Fig. 12.15, this program divided lengths l_1 and l_2 respectively into n_1 and n_2 intervals of an arithmetic series. The right-angle subtended between l_2 and the centre-line was divided into n_3 equi-angular intervals. In short, the input quantities to this problem were:

slot variables: d, r_H, γ, ψ

mesh variables: n_1, n_2, n_3

The cases run to study the effect of slot shape on stresses were divided into three sets:

(i) r_H was varied and γ and ψ kept constant.

(ii) γ was varied and r_H and ψ kept constant.

(iii) ψ was varied and r_H and γ kept constant.

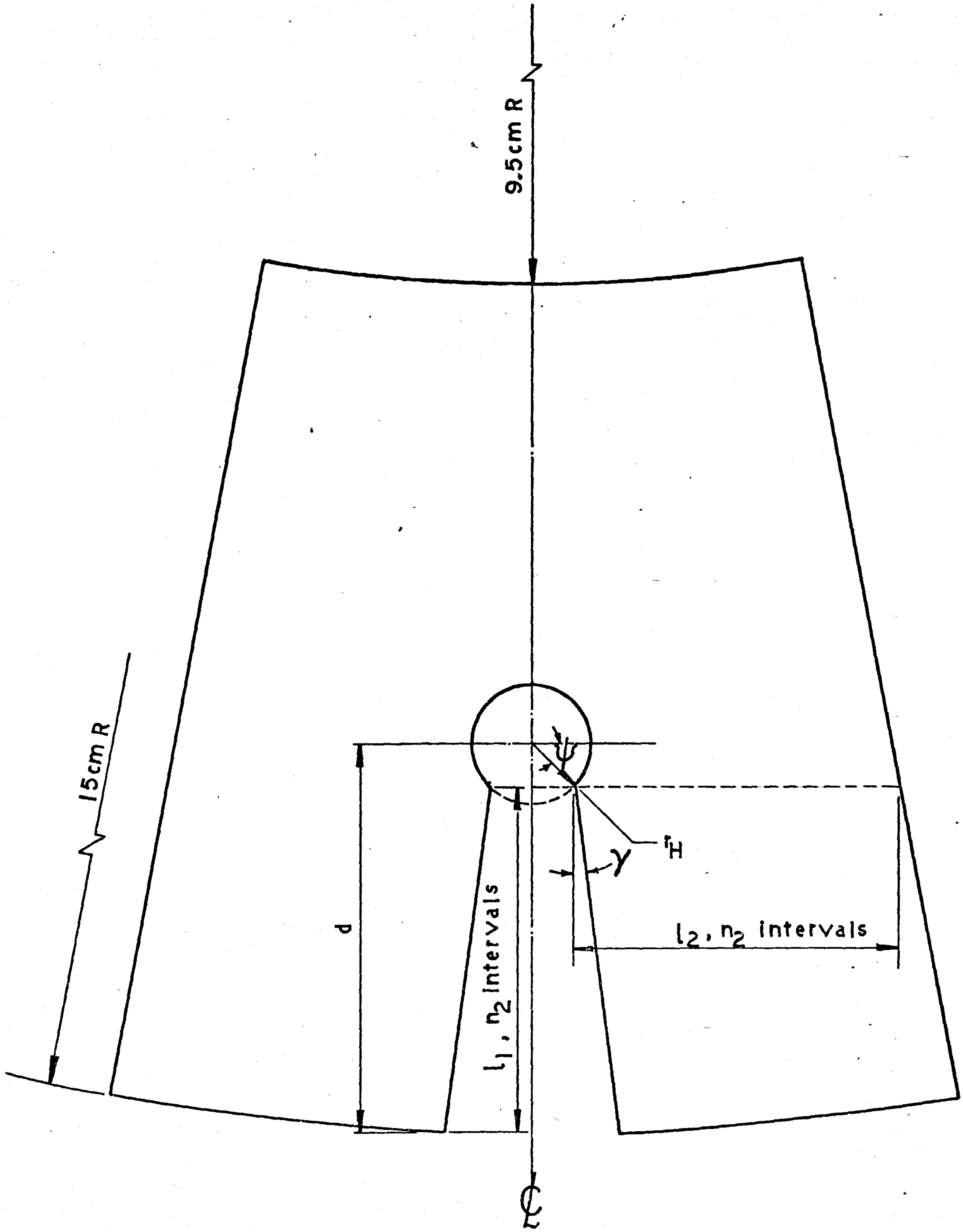

FIG. 12.16 Generalized Slot Shape.

The slot variables for case studied are listed in Table 12.1 in which each case is given as Shape Number. This table also includes some improved shapes which are discussed in section 12.5.6. The mesh of at least one case from each set is included in Figs. 12.17 to 12.23.

12.5.3. Finite Element Program

It is shown in Chapter 8 that the TRIM3 element gives poor results at boundaries and that the TRIM6 element is generally superior to the latter element. Since stresses were required accurately near the slot boundary it was decided to use TRIM6 elements for the third approximation. The finite element program chosen to solve the third approximation was the Method of Partitioning for TRIM6 elements.

12.5.4. Force Boundary Conditions

The portion of the distributed loading that covered the second subregion was discretized by the consistent approach for TRIM6 elements (Chapter 4).

As an example, the forces on the mesh for Shape No. 1 are drawn in on Fig. 12.17.

12.5.5. Displacement Boundary Conditions

Except for nodes lying on the blade periphery, the displacements of all boundary nodes were prescribed for both subregions. It was decided that to interpolate linearly from the displacements obtained from the second approximation would no

SHAPE No. I

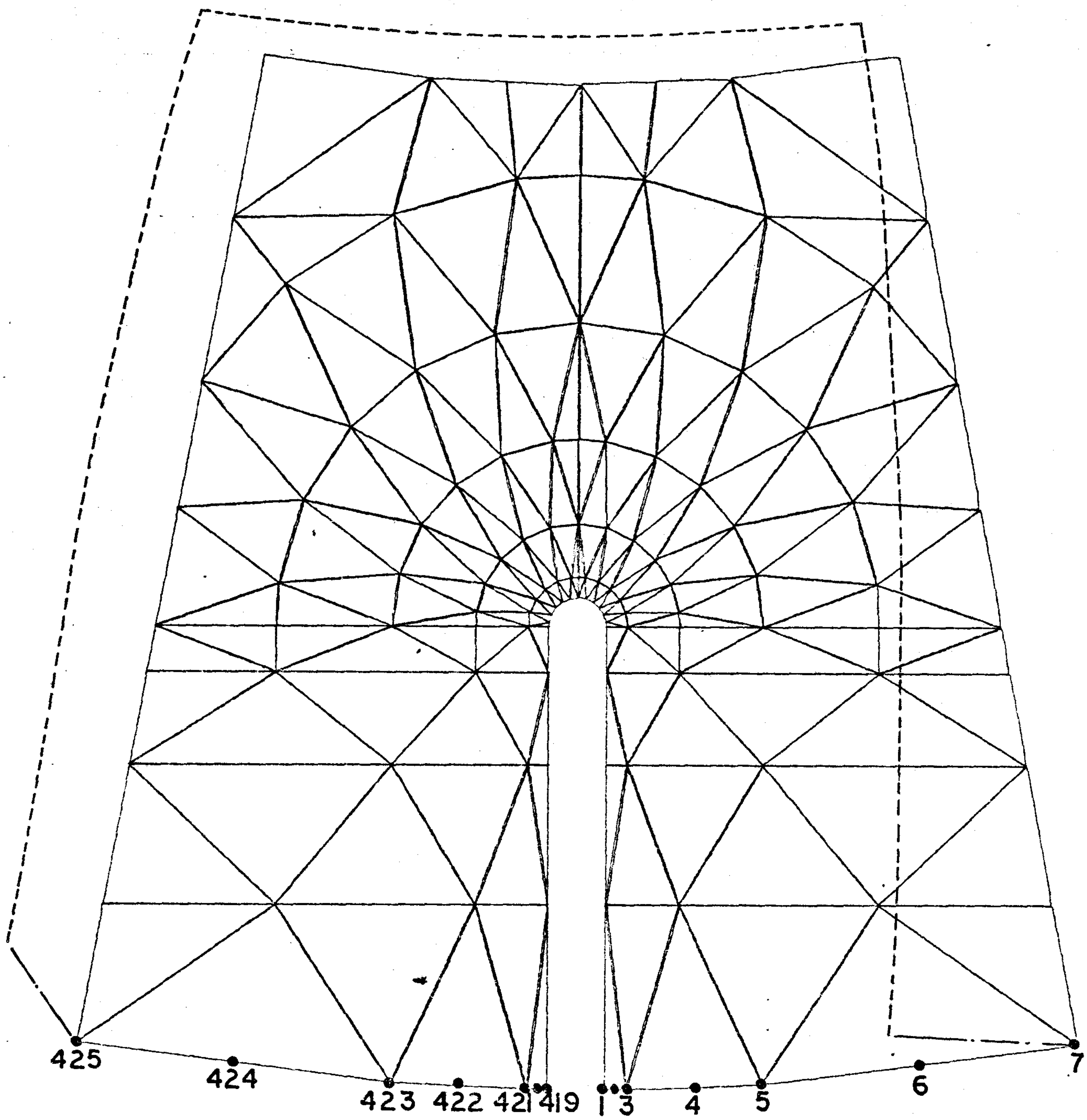

PRESCRIBED FORCES

NODE	X-FORCE	Y-FORCE
425	-1.1632284E+00	2.8938819E+00
424	-2.4300668E+00	4.4637615E+00
423	-8.0398129E+00	1.6762578E+01
422	-1.3335530E+00	2.1814379E+00
421	-4.9535282E+00	8.5596987E+00
420	-2.1210637E-01	3.4102826E-01
419	-4.4920934E+00	7.0963084E+00
1	-2.3220514E-01	3.5629990E-01
2	-2.3971080E-01	3.6168879E-01
3	-2.5033519E+00	3.7891872E+00
4	-1.8923210E+00	2.5658394E+00
5	-1.1279169E+01	1.5801699E+01
6	-6.3901559E+00	6.8347427E+00
7	-2.1417455E+01	2.5759201E+01

Fig. 12.17

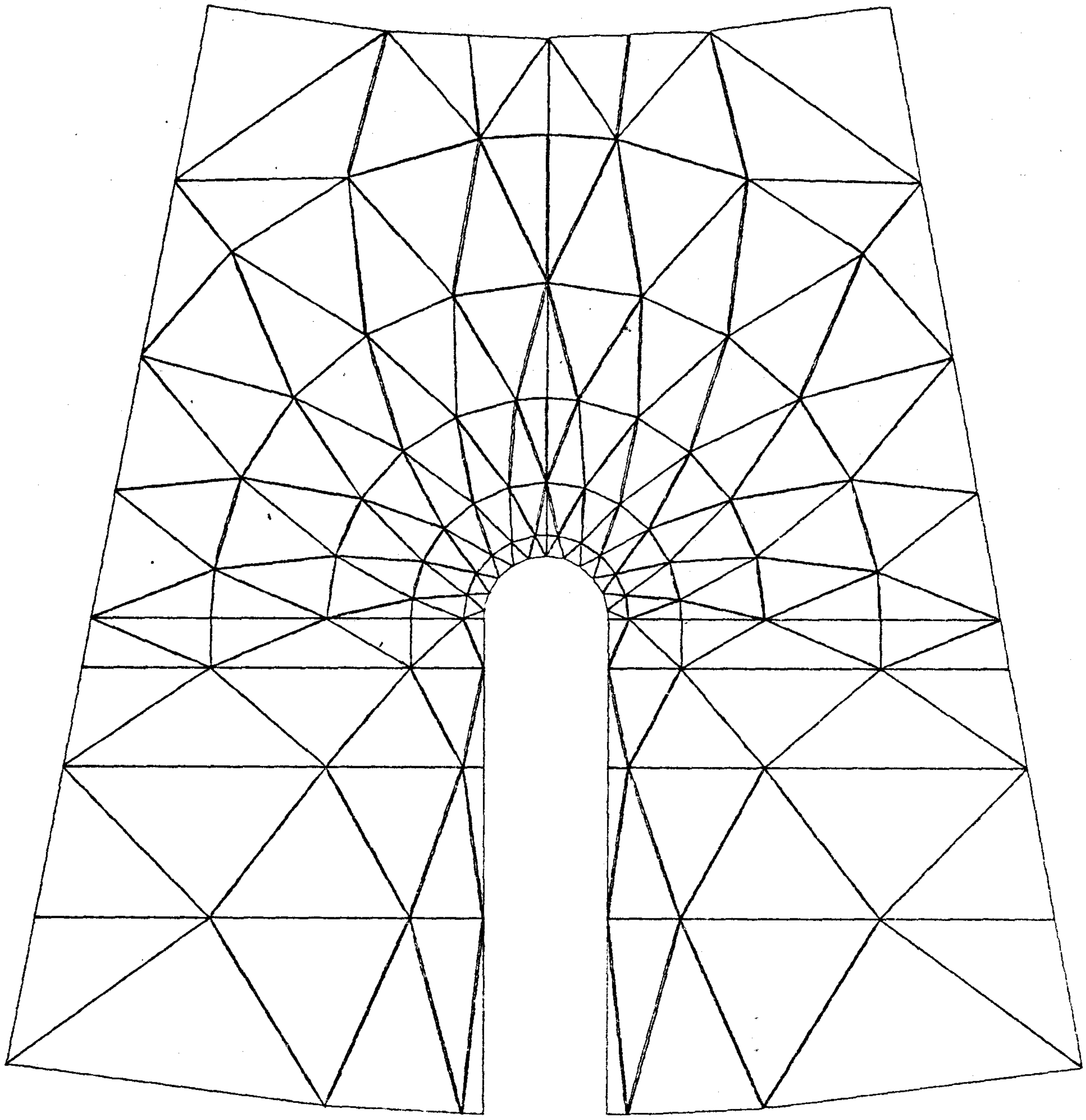

Fig. 12.18

SHAPE No. 7

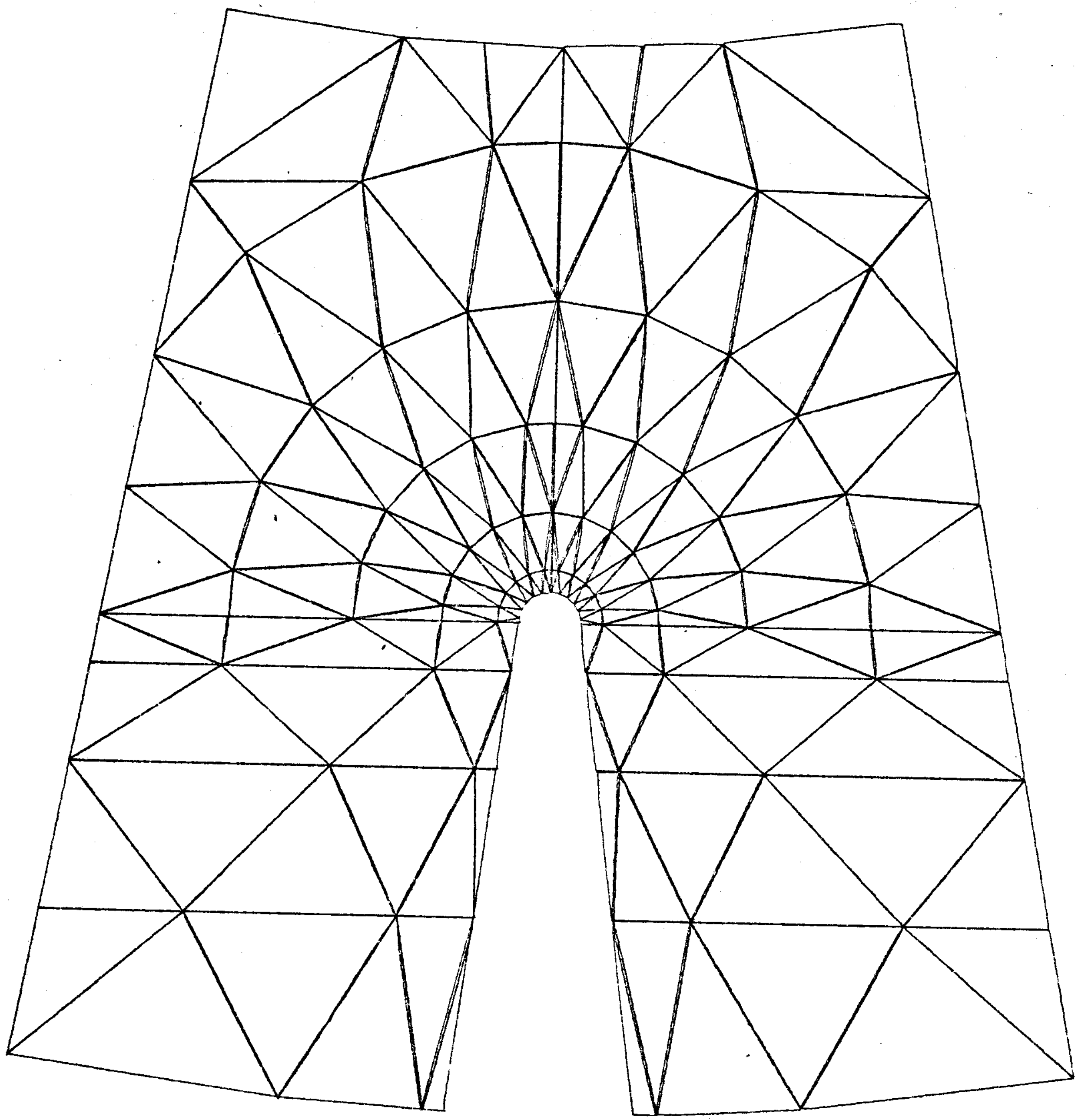

Fig. 12.19

SHAPE No. 8

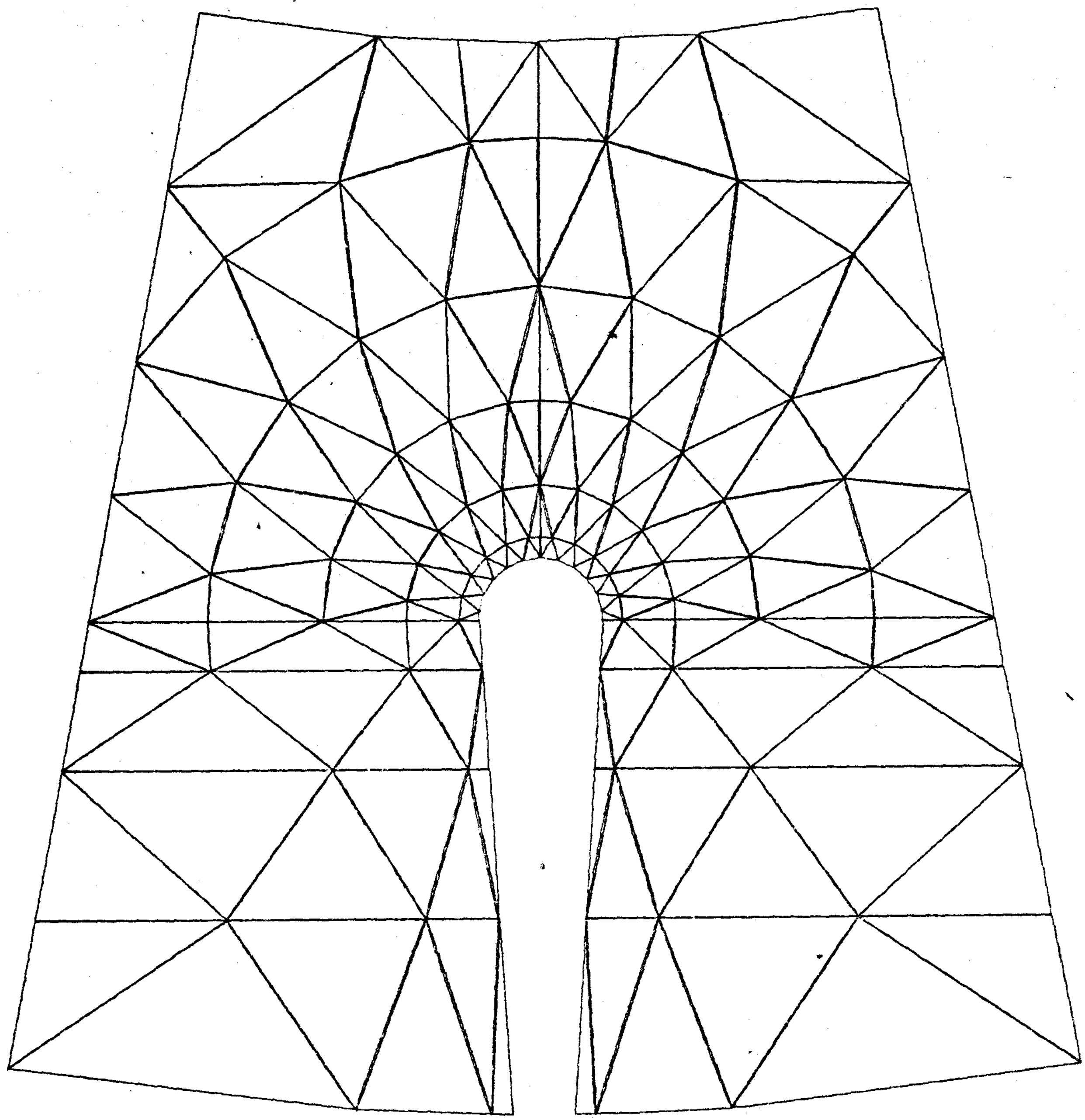

Fig. 12.20

SHAPE No. 9

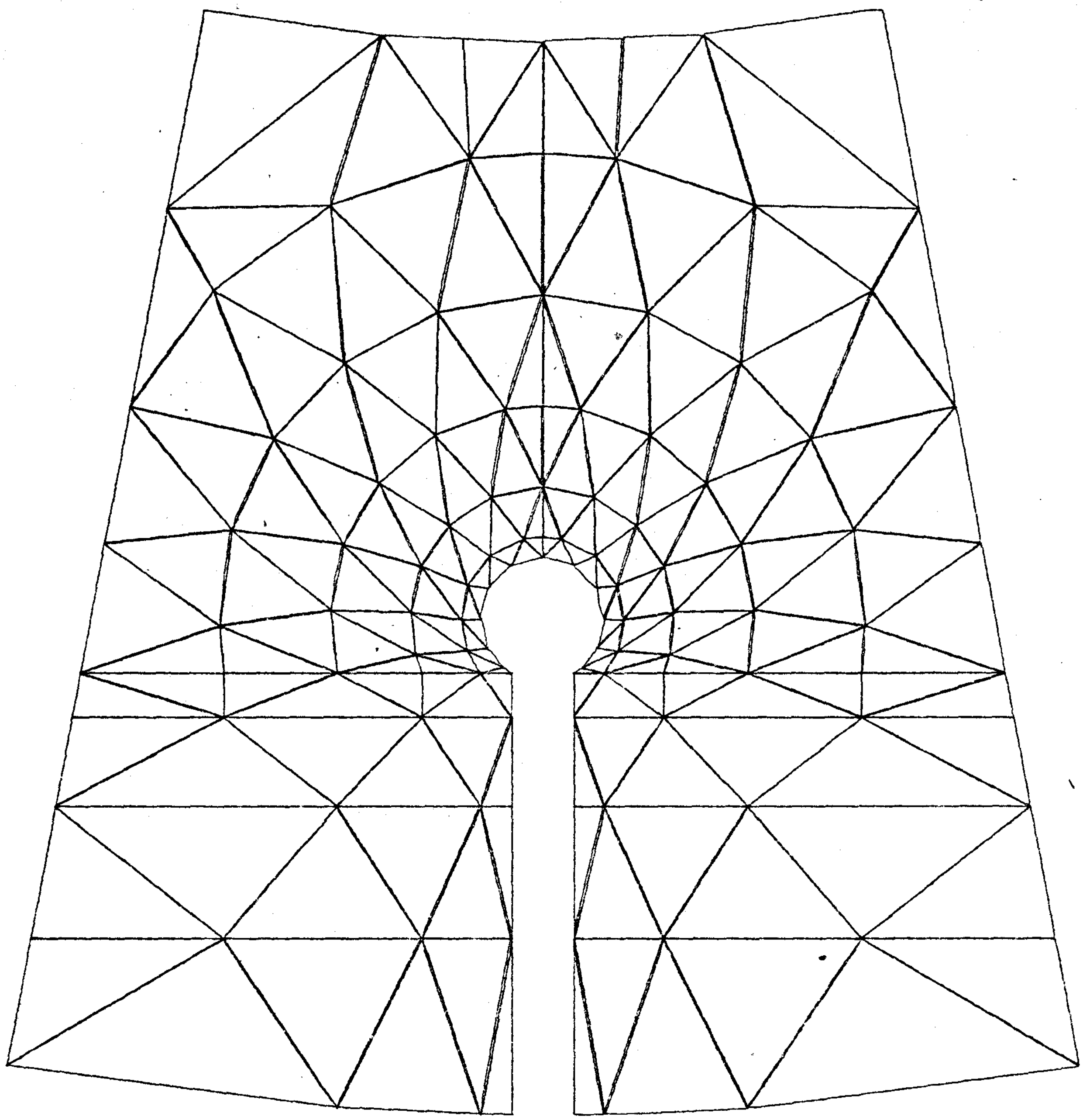

Fig. 12.21

SHAPE No. 12

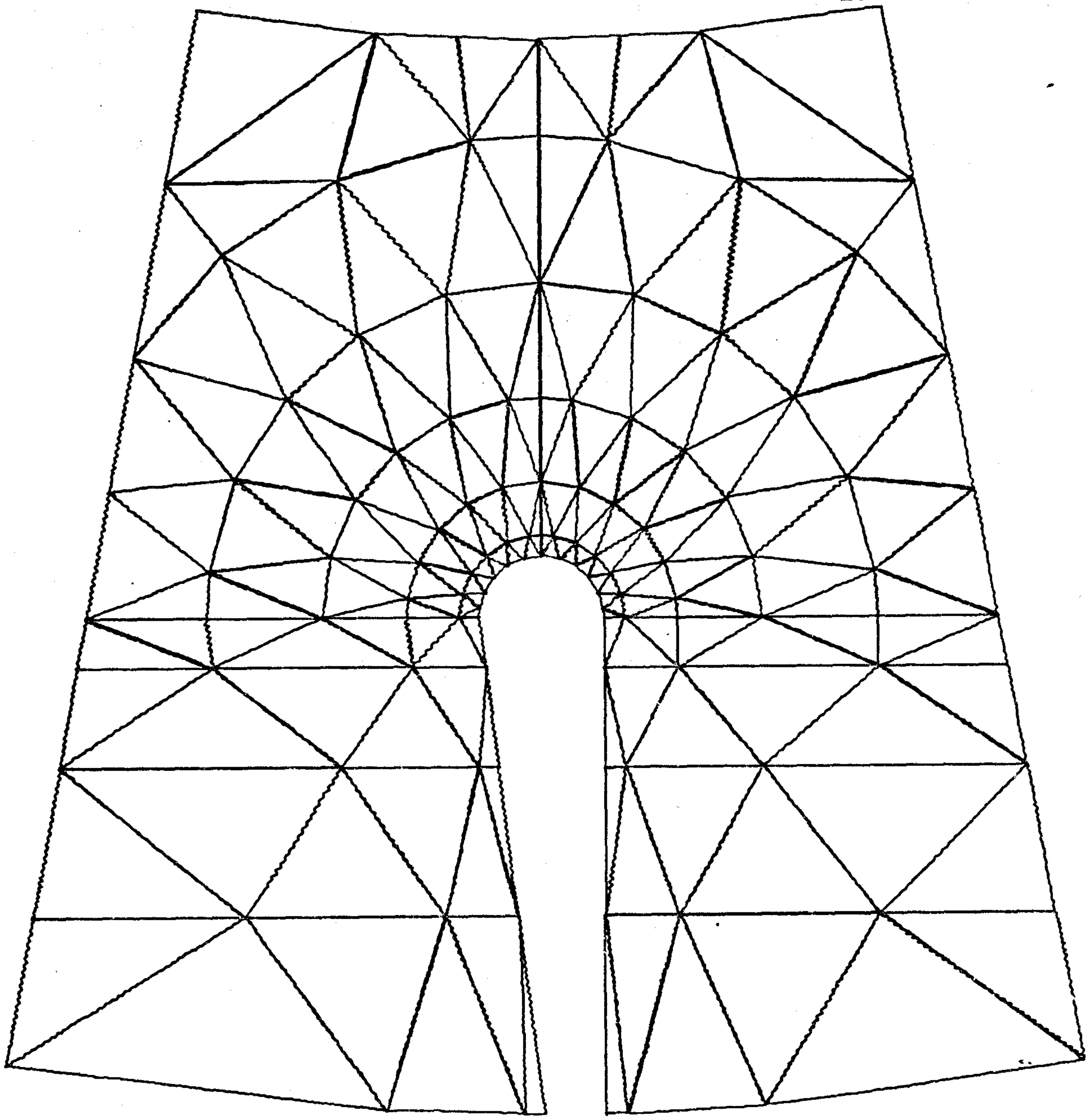

Fig. 12.2.2

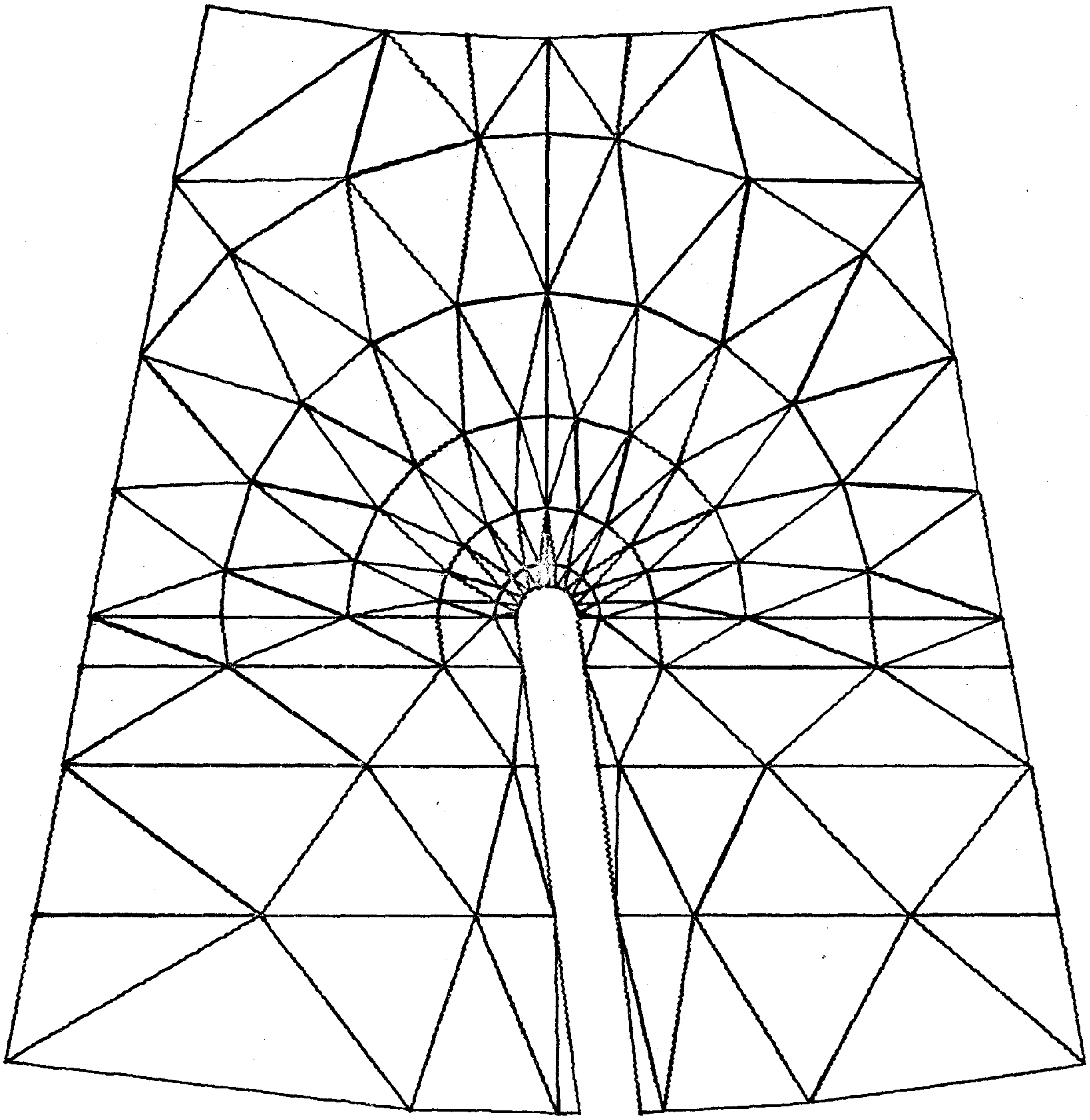

Fig. 12.23

longer suffice as it would mean constraining the sides of the TRIM6 boundary elements to straight lines. Hence, a spline interpolation was performed to obtain the boundary displacements more accruately.

As an example, the applied deformation of the boundaries of the second subregion for Shape No. 1 is shown in Fig. 12.17.

12.5.6. Results of Third Approximation

In Fig. 12.23 principal stresses along the circumference of the slot base circle for some slot shapes are plotted in a similar manner to that described in section 12.4.5. for Fig. 12.14. Since Shape No. 11 has a negative angle ψ (see second inset), the curves corresponding to this shape start to the left of the origin. In Fig. 12.24(b) σ_1 is plotted for Shape No. 1 only as the curve did not change significantly with shape. For the same reason only one curve for σ_2 is plotted in Fig. 12.24(a). It can be seen that the slot shapes used showed significant reduction in the peak stresses compared to the basic shape, which is Shape No. 1. Also, the peak stresses remain at the same angular points defined as points m and n.

The fatigue criterion discussed at the beginning of the chapter was used to decide which of the two points was the more critical, as follows:

In 2-dimensions the criterion is

$$\frac{\sqrt{2}}{3} \{P_1^{\,2} + P_2^{\,2} - P_1P_2\}^{1/2} + a\{S_1 + S_2\} < A$$

The expression on the left of the inequality is termed the 'fatigue stress' and is to be minimised to obtain an improved slot. The P's are the principal stress amplitudes and the S's are the static stresses. These are indicated in Fig. 12.15. The octahedral shear stress is defined as

$$\sigma_{oct} = \frac{\sqrt{2}}{3} \{P_1^{\,2} + P_2^{\,2} - P_1 P_2\}^{1/2}$$

For the basic slot shape the octahedral shear stress and the static stresses are tabulated in Table 12.2 to compare points m and n. The octahedral shear stress at point n is more than double that of point m. However, it still cannot be concluded as to which point is more critical because point n has a highly compressive net static stress, and compressive static stresses are known to reduce the fatigue stress. Because of the absence of fatigue data for the material of the saw blade, an average value for parameter "a" of 0.1 was arrived at by scanning fatigue data for various types of steels. Hence, the fatigue stress for the two points become:

point n, fatigue stress = 1044 - 241 = 803 psi

point m, fatigue stress = 455 - 3 = 452 psi.

Thus, point n is the more critical by a wide margin. The peak principal stresses for point n are filled-in in dotted lines on Fig. 12.15. From this figure it can be seen that the σ_1 cycle can be approximated by a reversed stress cycle and the σ_2 cycle by a zero-compression fluctuating cycle.

12.5.7. Principal Stress Contours

In the tables in the previous section, the stresses of, at the most, two critical points were discussed. Some curves were provided to indicate the variation of stress along the slot base circle for a few chosen slot shapes. This, however, gives information in a limited region only.

In order to get a 'picture' of the principal stress fields in the totally isolated regions, stress contour plots were drawn by computer using the subroutine discussed in Chapter 10. These controu plots are included in Figs. 12.26 to 12.32 which correspond to the slot shapes described in Figs. 12.17 to 12.23, respectively. A slot shape from each set in Table 12.1 is respresented.

Four contour plots labelled (a), (b), (c) and (d) in each figure describe the stress fields for each shape. These are:

(a) Maximum principal stress, σ_1, contours for the second subregion (slot number 5).

(b) Minimum principal stress, σ_2, contours for the above subregion.

(c) Maximum principal stress, σ_1, contours for the third subregion (slot number 6).

(d) Minimum principal stress, σ_2, contours for the above subregion.

Table 12.3 is a list of the critical principal stresses at the peaks of the principal stress spectra obtained respectively from the second and third subregions, for the various shapes studied. The corresponding fatigue stress calculations are tabulated in Table 12.4. The last column of this table contains the reduction in fatigue stresses as compared to the basic slot shape (No. 1). In Fig. 12.25 this reduction is used as a basis to compare the effect of changing one slot variable at a time. This figure represents the first three sets of Table 12.4. It can be seen that the greatest improvement is caused by increasing the slot base radius r_H. Improvement caused by increasing angle γ falls off atter 5° and improvement caused by increasing angle ψ (in the negative direction) falls off after -48°. By making slot angle γ negative a substantial decrease in fatigue stress results, as shown by the line below the abscissa.

It is important to note that by increasing either γ or r_H, while keeping the other variables constant, the slot is widened and the available cutting area of the saw is consequently reduced. Though the fatigue life may increase the cutting efficiency decreases. This fact was kept in mind when designing the hybrid shapes No. 12 and No. 13.

In order to speculate on an improved shape, two hybrid slot shapes were designed by a combination of variables r_H and γ. The vertical sectioning line drawn on Fig. 12.25 shows that the maximum decrease in stress was obtained by a large r_H and a negative γ. This fact was used in Shape No. 12 of Fig. 12.22 in which the right hand slot side has $\gamma = 0^o$, the left hand slot side had $\gamma = -7\ 1/2^0$ and the slot base circle radius $r_H = 1/8$ in. This shape is seen to be a cross between shapes No. 3 and No. 8. By making angle γ equal to zero for the right hand slot side it was possible to make the angle more negative for the left hand slot side and still maintain the same slot width as in the basic shape. The other shape is Shape No. 13 shown in Fig. 12.23 in which an attempt was made to take advantage of the improvement caused by making γ positive and negative for the respective slot sides. The sesult was a parallel sided slot which was similar to the basic slot but skewed to the center-line by $7\ 1/2^o$. The two hybrid shapes discussed above have the appearance of a lathe cutting tool with a positive rake angle.

From the last set in Table 12.4 it can be seen that the two hybrid shapes give the largest reduction in fatigue stress, and thus greatest improvement in fatigue life is expected from them. Comparing the results of Shapes 11 and 13 in Table 12.4, it can be seen that P_2 are almost equal for the two shapes but P_1 is much larger for Shape No. 13. Yet, the percentage reduction for Shape No. 13 is three times larger. This is the effect of increase in 'biaxiality', i.e. decrease in P_2 but increase in P_1.

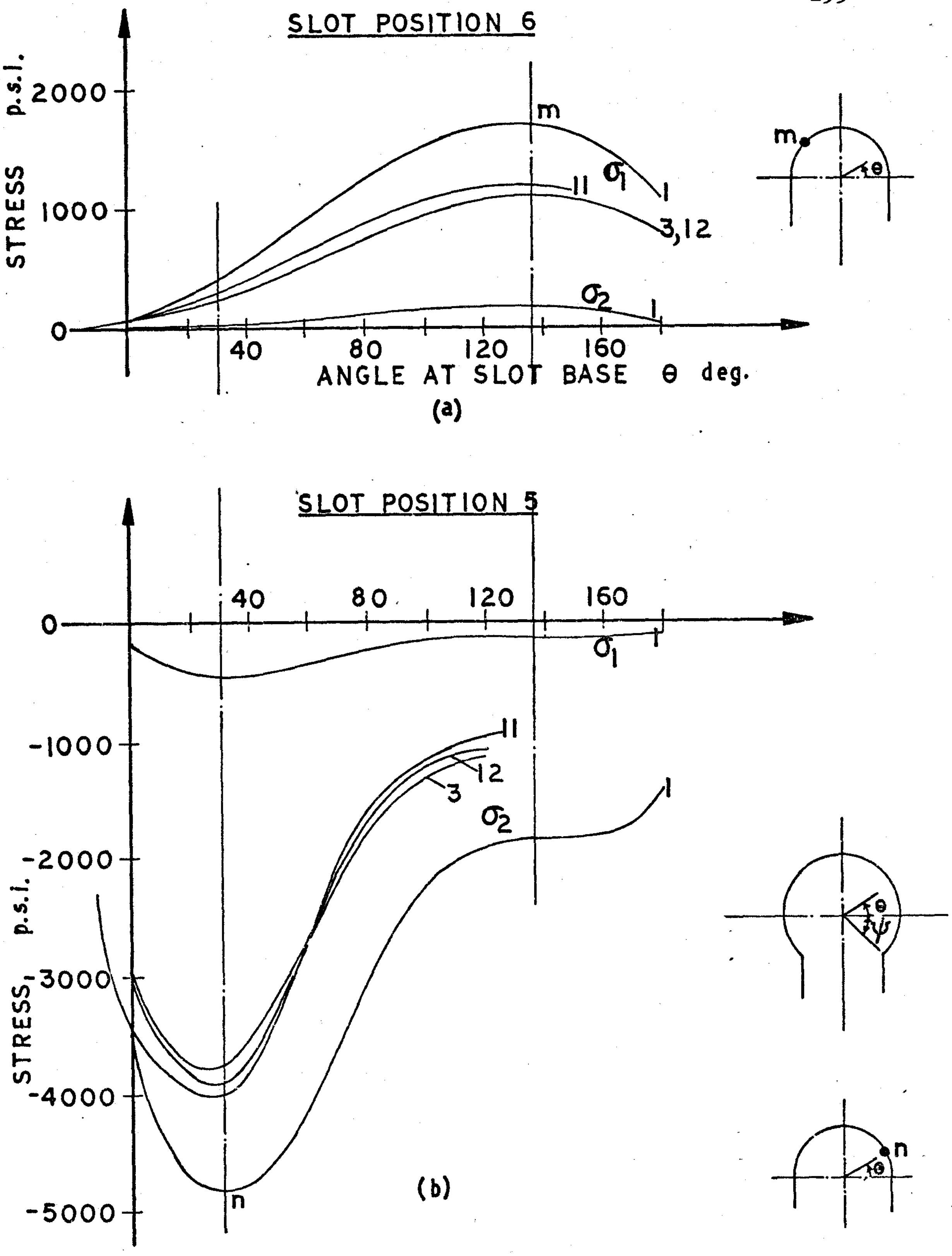

FIG. 12.24 Variation of Principal Stresses σ_1 and σ_2 Along Circumference of Slot Base Circles for Two Highly Stressed Slot Positions. Figure (a) Corresponds to 3rd Subregion and Figure (b) to the 2nd. Numbers Alongside Each Curve are Shape Numbers.

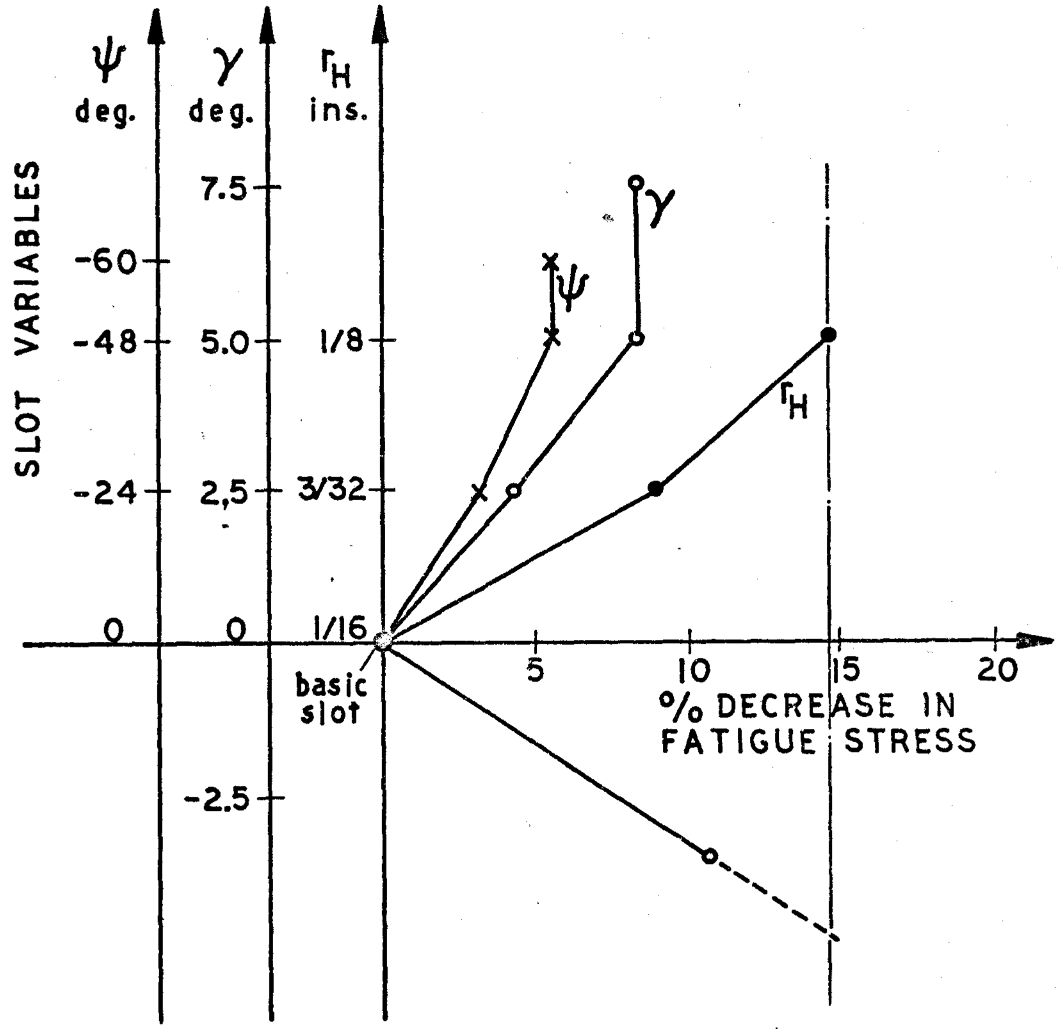

FIG. 12.25 Effect of Varying Slot Shape on Fatigue Stress.

The contours are labelled by number and the corresponding stress values are given in the Key below each plot. For purposes of comparison the same sets of contours were plotted for the various shapes.

At a glance it can be seen that there are definite localised changes in stress fields from shape to shape, but differences disappear at distances of 5 to 6 slot radii away from the slots. Peaks in the stress field appear as closed-loop contours, and high stress gradients appear as bunched contours.

The stress contours of the following figures are of interest:

(i) Fig. 12.26, are the contours for the basic slot shape, which are used to compare the other shapes.

(ii) Fig. 12.27. The bunching of the contours is definitely less near the slot, and many of the higher-valued contours disappear. Also, contours at the concentration are spread over a wider region, see Fig. 12.27(b).

(iii) Fig. 12.28. Since there is no significant change in slot shape, there is no significant change in the stress field.

(iv) Fig. 12.30. Although it would be expected that the larger base circle of this 'keyhole' shape would relieve the concentration to a large degree, this is not so. As can be seen, stress relief is hampered by the abrupt discontinuity in shape where the base circle meets the slot side.

SHAPE No I

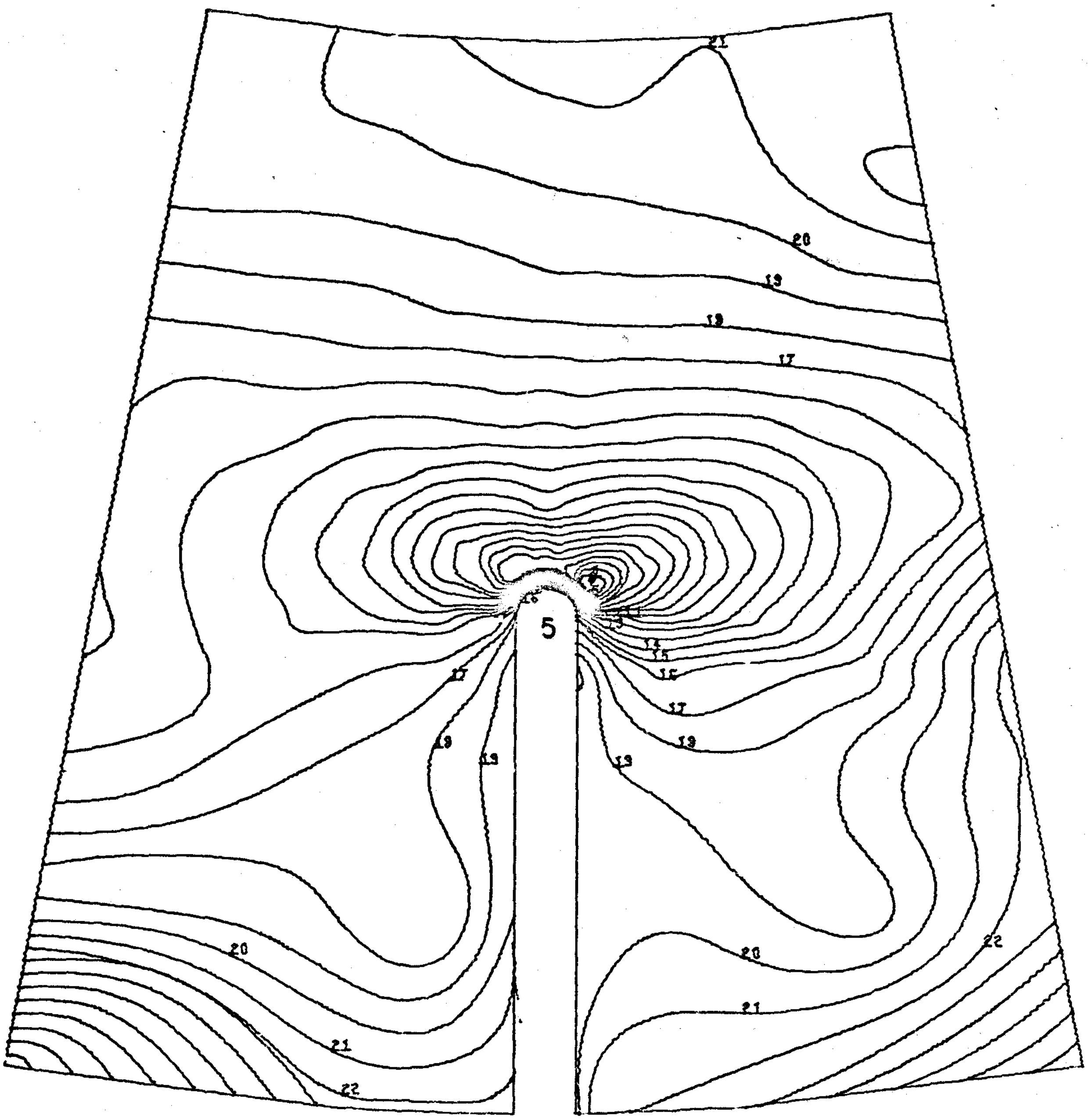

CONTOURS FOR MAXIMUM PRINCIPAL STRESSES

KEY TO CONTOURS-

CONTOUR	1	2	3	4	5	6	7	8	9	10
STRESS	-900	-850	-800	-750	-700	-650	-600	-550	-500	-450
CONTOUR	11	12	13	14	15	16	17	18	19	20
STRESS	-400	-350	-300	-250	-200	-150	-100	-50	0	50
CONTOUR	21	22	23	24	25	26	27	28	29	30
STRESS	100	150	200	250	300	350	400	450	500	550
CONTOUR	31									
STRESS	600									

Fig. 12.26 a

SHAPE No. 1

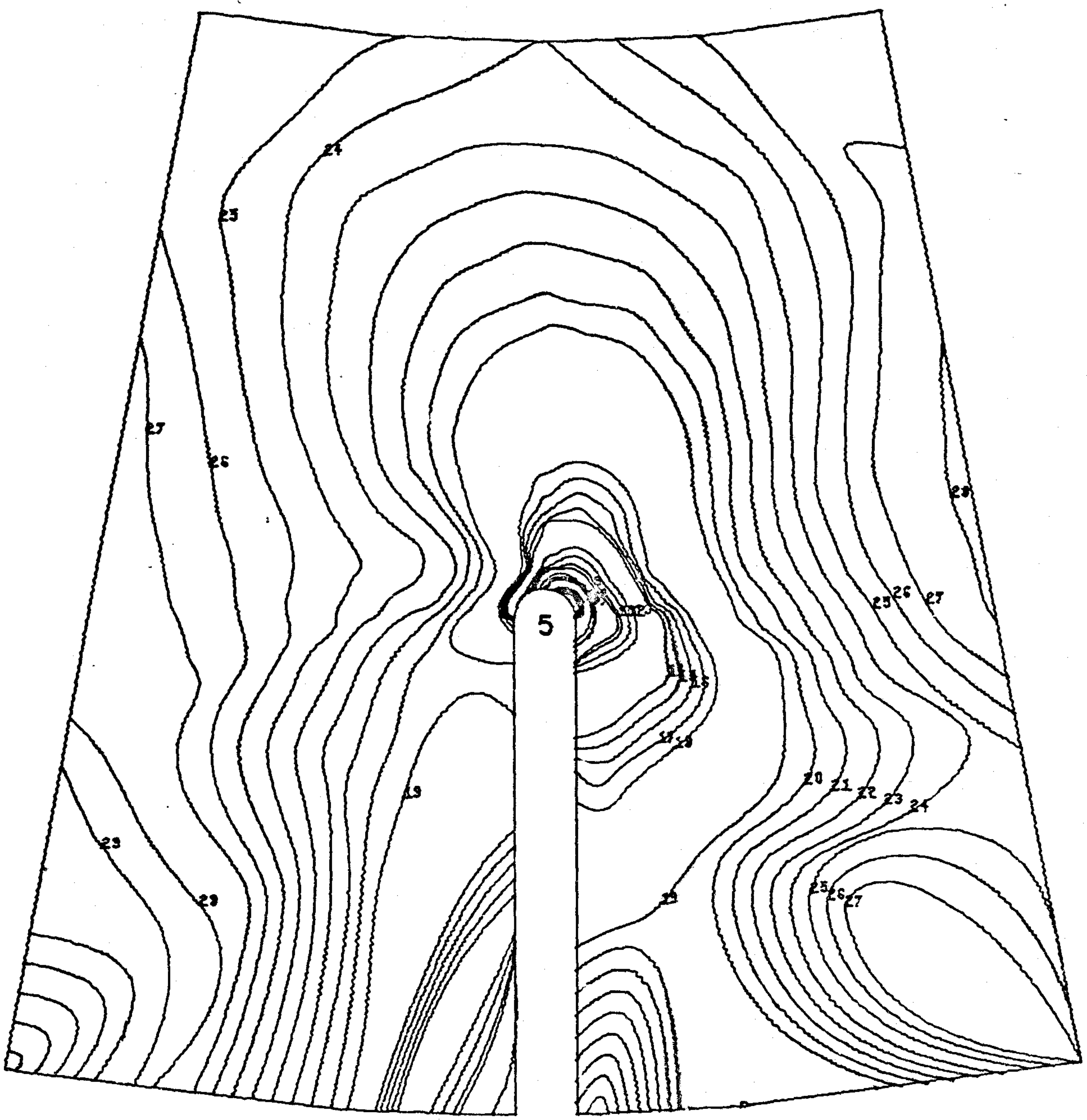

CONTOURS FOR MINIMUM PRINCIPAL STRESSES

KEY TO CONTOURS-

CONTOUR	1	2	3	4	5	6	7	8	9	10
STRESS	-4100	-4000	-3900	-3800	-3650	-3500	-2750	-2550	-2350	-2050
CONTOUR	11	12	13	14	15	16	17	18	19	20
STRESS	-2000	-1900	-1800	-1500	-1450	-1400	-1350	-1300	-1050	-1000
CONTOUR	21	22	23	24	25	26	27	28	29	30
STRESS	-950	-900	-850	-800	-750	-700	-650	-550	-500	-450
CONTOUR	31	32	33	34	35					
STRESS	-400	-350	-300	-250	-200					

Fig. 12.26 b

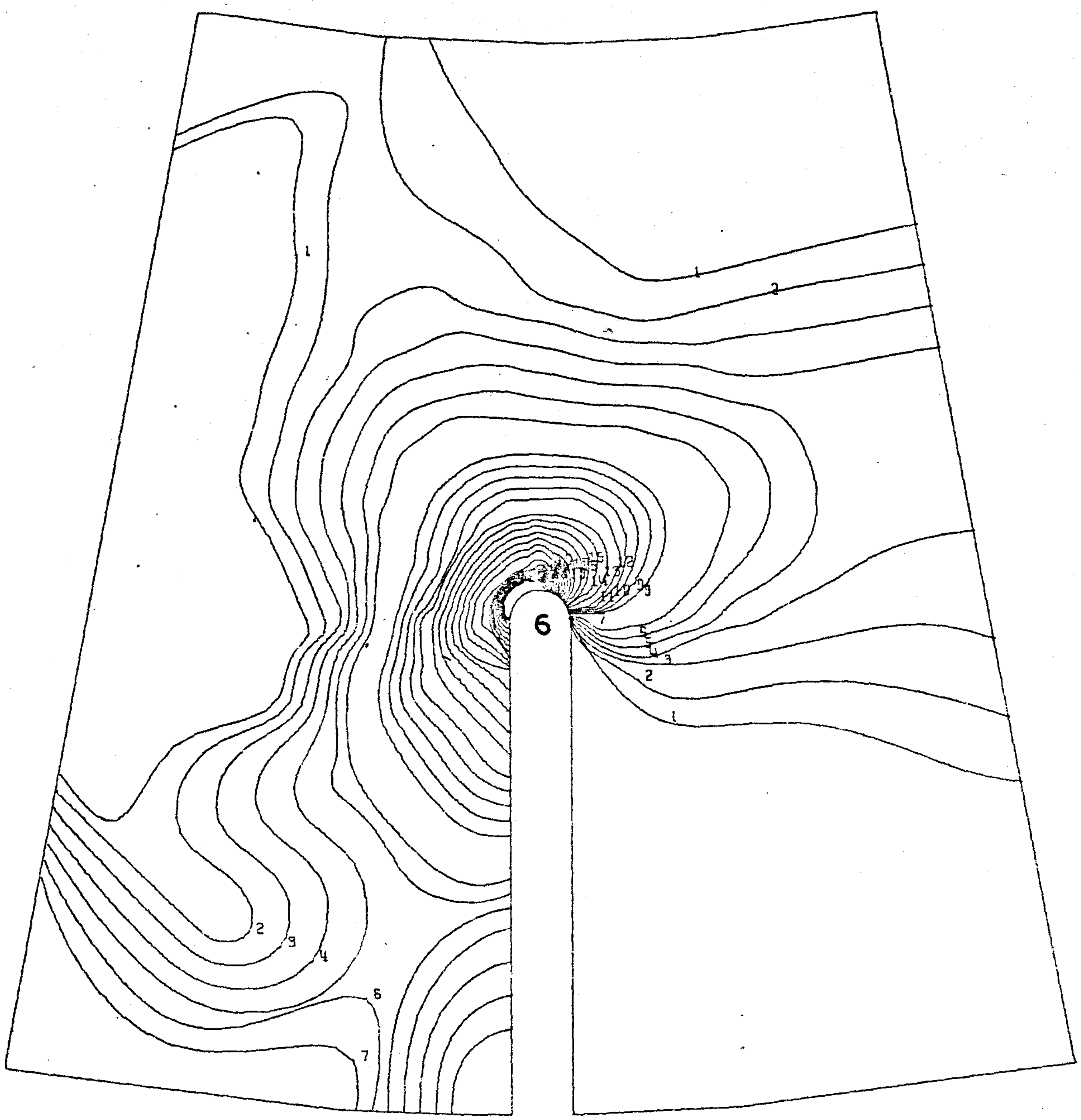

CONTOURS FOR MAXIMUM PRINCIPAL STRESSES

KEY TO CONTOURS-

CONTOUR	1	2	3	4	5	6	7	8	9	10
STRESS	70	90	110	130	150	170	230	250	270	290
CONTOUR	11	12	13	14	15	16	17	18	19	20
STRESS	310	350	390	430	470	510	550	590	650	710
CONTOUR	21	22	23	24	25	26	27	28		
STRESS	770	830	890	950	1010	1070	1130	1190		

Fig. 12.26 c

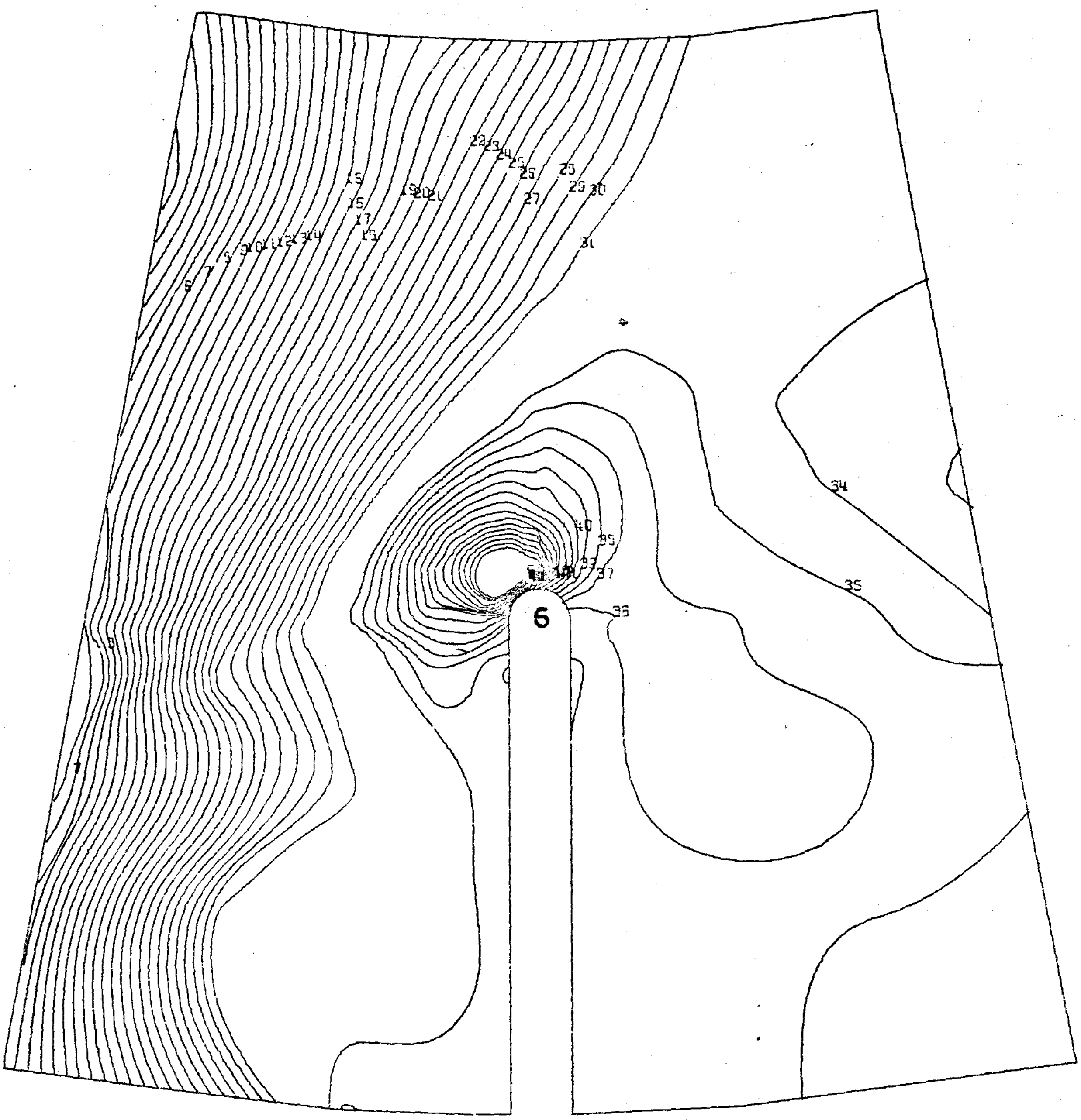

CONTOURS FOR MINIMUM PRINCIPAL STRESSES

KEY TO CONTOURS-

CONTOUR	1	2	3	4	5	6	7	8	9	10
STRESS	-700	-680	-660	-640	-620	-600	-580	-560	-540	-520
CONTOUR	11	12	13	14	15	16	17	18	19	20
STRESS	-500	-480	-460	-440	-420	-400	-380	-360	-340	-320
CONTOUR	21	22	23	24	25	26	27	28	29	30
STRESS	-300	-280	-260	-240	-220	-200	-180	-160	-140	-120
CONTOUR	31	32	33	34	35	36	37	38	39	40
STRESS	-100	-80	-60	-40	-20	0	20	40	60	80
CONTOUR	41	42	43	44	45	46	47	48	49	50
STRESS	100	120	140	160	180	200	220	240	260	280

Fig. 12.26 d

SHAPE No.3

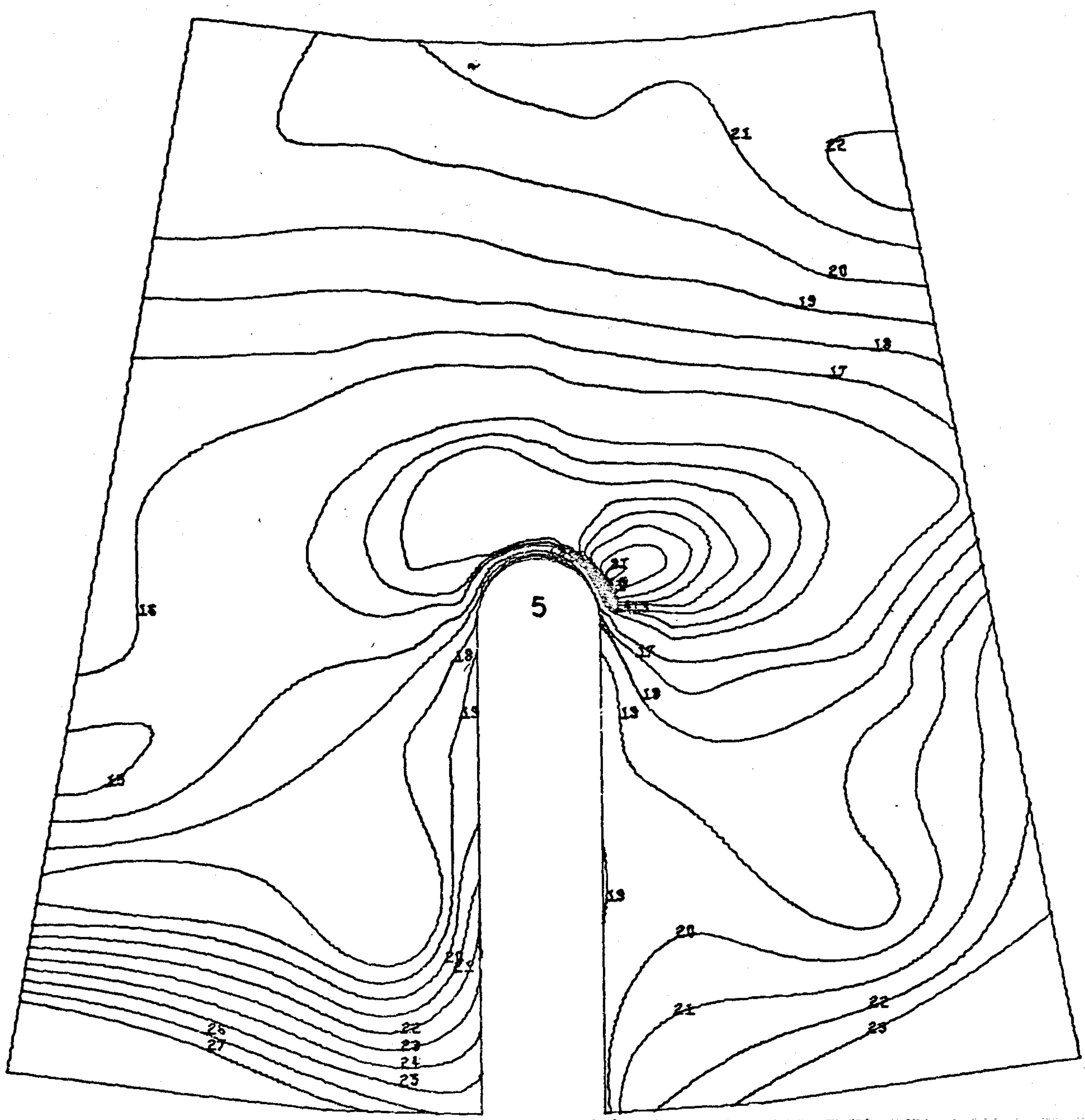

CONTOURS FOR MAXIMUM PRINCIPAL STRESSES

KEY TO CONTOURS-

CONTOUR	1	2	3	4	5	6	7	8	9	10
STRESS	-900	-850	-800	-750	-700	-650	-600	-550	-500	-450
CONTOUR	11	12	13	14	15	16	17	18	19	20
STRESS	-400	-350	-300	-250	-200	-150	-100	-50	0	50
CONTOUR	21	22	23	24	25	26	27	28	29	30
STRESS	100	150	200	250	300	350	400	450	500	550
CONTOUR	31									
STRESS	600									

Fig. 12.27 a

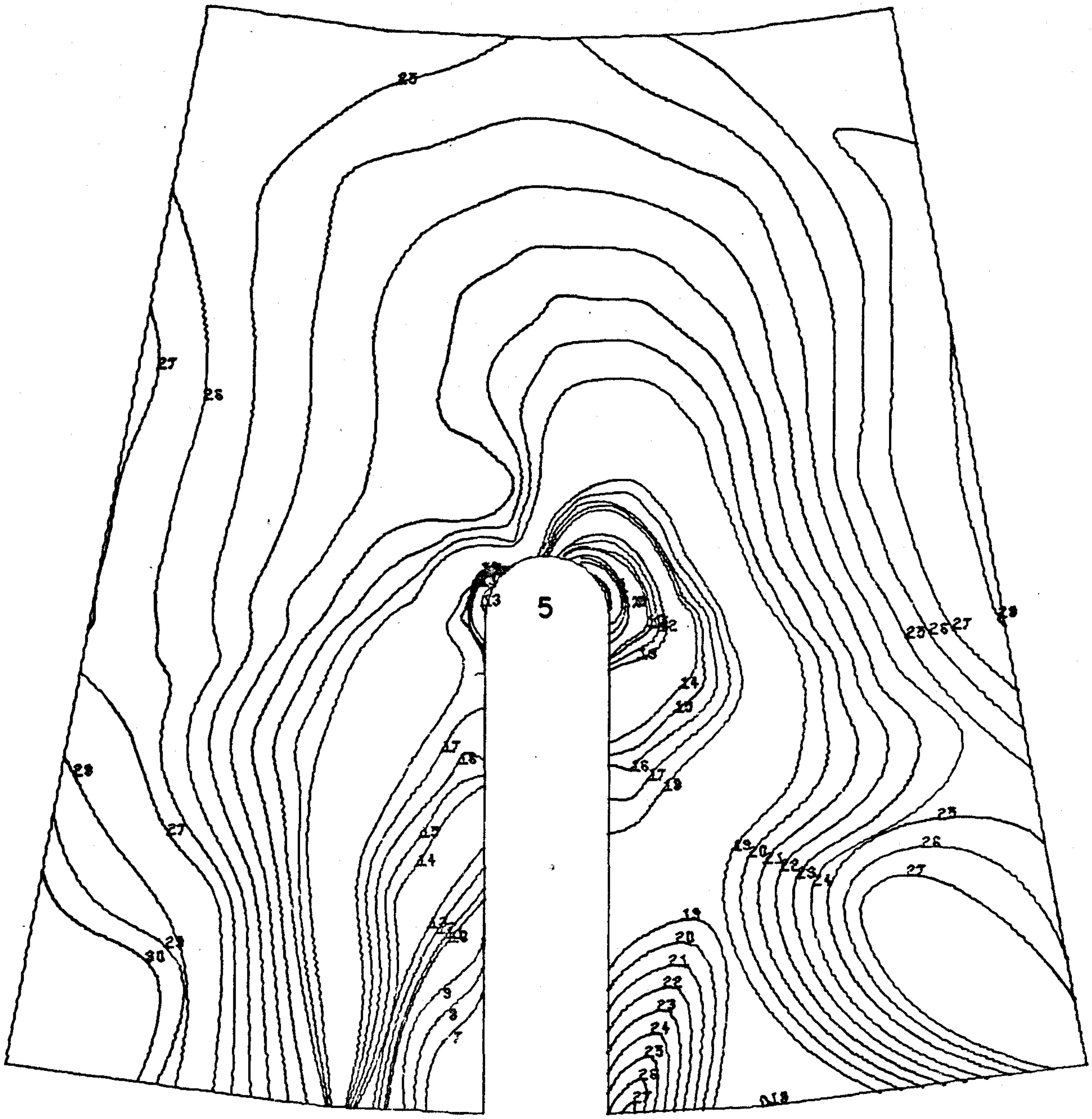

CONTOURS FOR MINIMUM PRINCIPAL STRESSES

KEY TO CONTOURS-

CONTOUR	1	2	3	4	5	6	7	8	9	10
STRESS	-4100	-4000	-3900	-3800	-3650	-3500	-2750	-2550	-2350	-2050
CONTOUR	11	12	13	14	15	16	17	18	19	20
STRESS	-2000	-1900	-1800	-1500	-1450	-1400	-1350	-1300	-1050	-1000
CONTOUR	21	22	23	24	25	26	27	28	29	30
STRESS	-950	-900	-850	-800	-750	-700	-650	-550	-500	-450
CONTOUR	31	32	33	34	35					
STRESS	-400	-350	-300	-250	-200					

Fig. 12.27 b

SHAPE No. 3

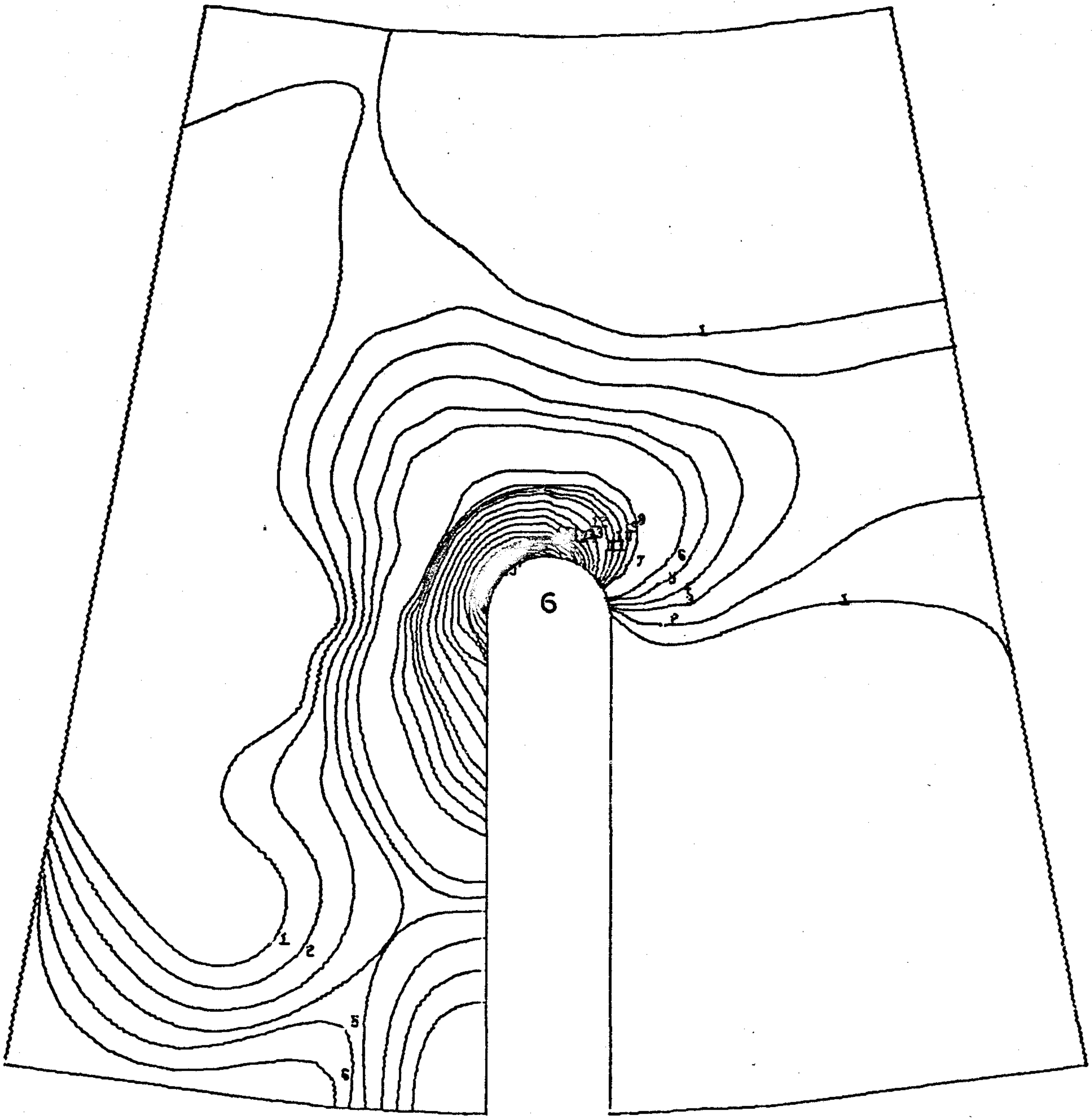

CONTOURS FOR MAXIMUM PRINCIPAL STRESSES

KEY TO CONTOURS-

CONTOUR	1	2	3	4	5	6	7	8	9	10
STRESS	70	90	110	130	150	170	230	250	270	290
CONTOUR	11	12	13	14	15	16	17	18	19	20
STRESS	310	350	390	430	470	510	550	590	650	710
CONTOUR	21	22	23	24	25	26	27	28		
STRESS	770	830	890	950	1010	1070	1130	1190		

Fig. 12.27 c

SHAPE No. 3

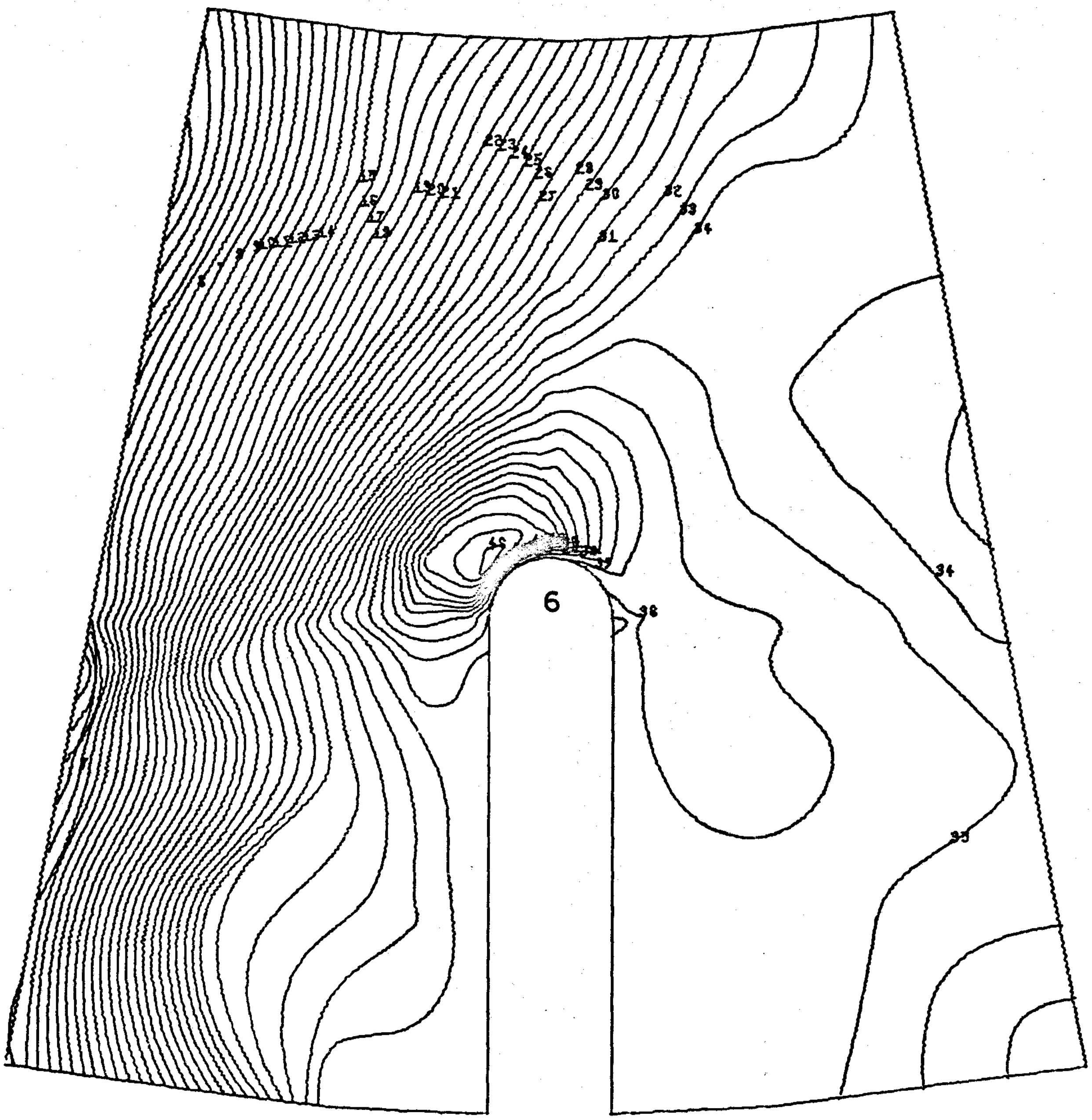

CONTOURS FOR MINIMUM PRINCIPAL STRESSES

KEY TO CONTOURS-

CONTOUR	1	2	3	4	5	6	7	8	9	10
STRESS	-700	-680	-660	-640	-620	-600	-580	-560	-540	-520
CONTOUR	11	12	13	14	15	16	17	18	19	20
STRESS	-500	-480	-460	-440	-420	-400	-380	-360	-340	-320
CONTOUR	21	22	23	24	25	26	27	28	29	30
STRESS	-300	-280	-260	-240	-220	-200	-180	-160	-140	-120
CONTOUR	31	32	33	34	35	36	37	38	39	40
STRESS	-100	-80	-60	-40	-20	0	20	40	60	80
CONTOUR	41	42	43	44	45	46	47	48	49	50
STRESS	100	120	140	160	180	200	220	240	260	280

Fig. 12.27 d

SHAPE No. 7

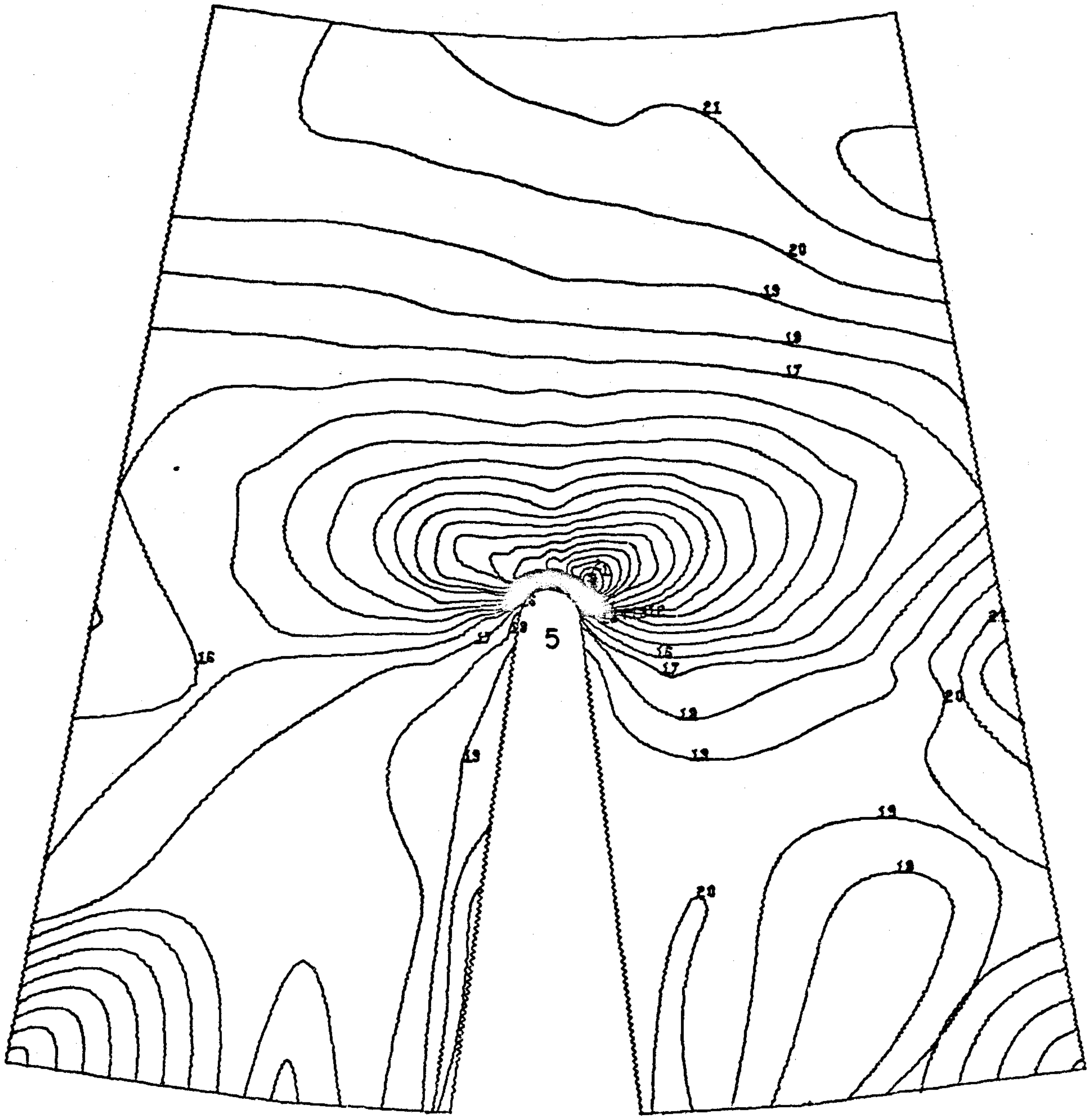

CONTOURS FOR MAXIMUM PRINCIPAL STRESSES

KEY TO CONTOURS-

CONTOUR	1	2	3	4	5	6	7	8	9	10
STRESS	-900	-850	-800	-750	-700	-650	-600	-550	-500	-450
CONTOUR	11	12	13	14	15	16	17	18	19	20
STRESS	-400	-350	-300	-250	-200	-150	-100	-50	0	50
CONTOUR	21	22	23	24	25	26	27	28	29	30
STRESS	100	150	200	250	300	350	400	450	500	550
CONTOUR	31									
STRESS	600									

Fig. 12.28 a

SHAPE No. 7

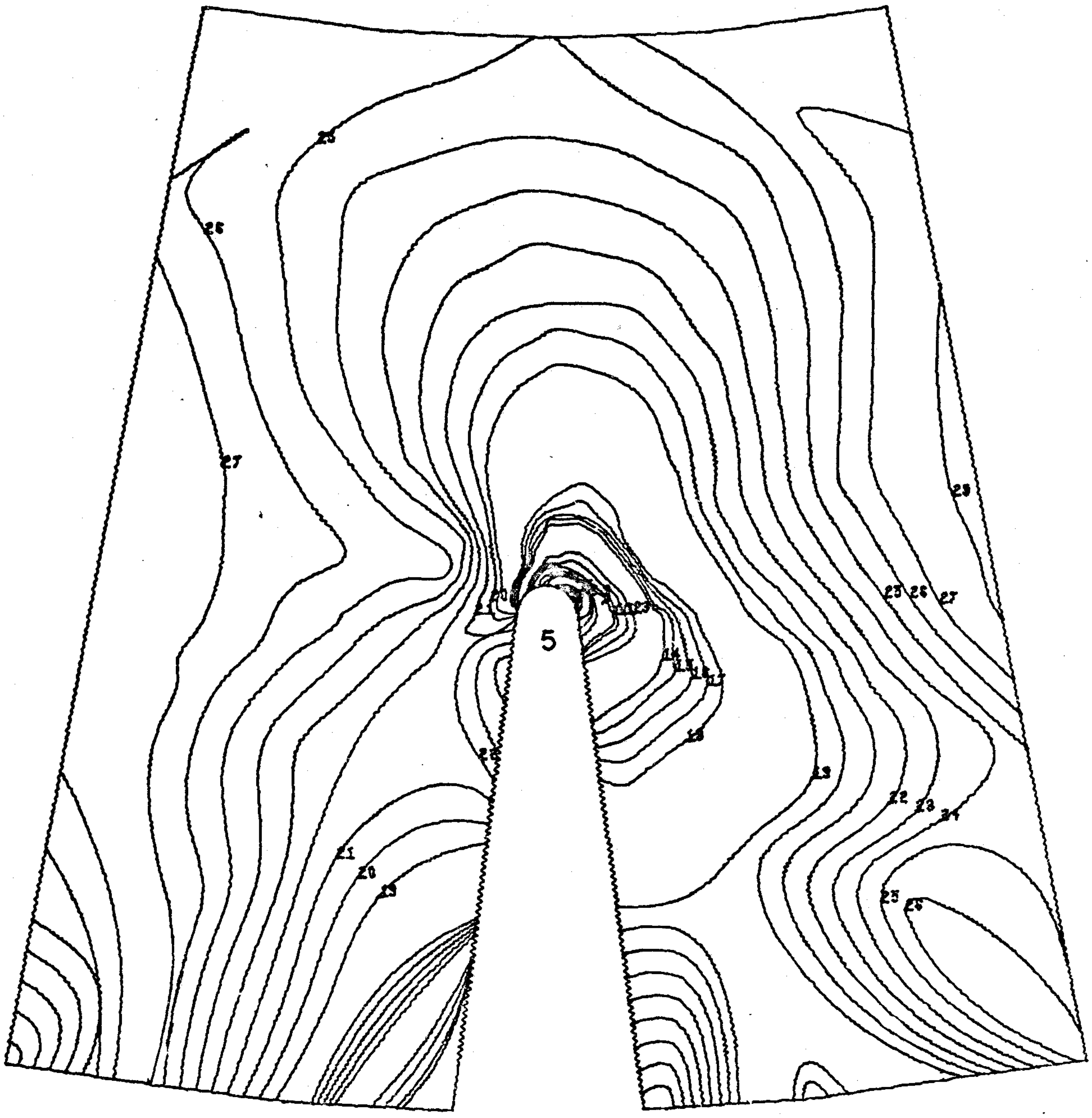

CONTOURS FOR MINIMUM PRINCIPAL STRESSES

KEY TO CONTOURS-

CONTOUR	1	2	3	4	5	6	7	8	9	10
STRESS	-4100	-4000	-3900	-3800	-3650	-3500	-2750	-2550	-2350	-2050
CONTOUR	11	12	13	14	15	16	17	18	19	20
STRESS	-2000	-1900	-1800	-1500	-1450	-1400	-1350	-1300	-1050	-1000
CONTOUR	21	22	23	24	25	26	27	28	29	30
STRESS	-950	-900	-850	-800	-750	-700	-650	-550	-500	-450
CONTOUR	31	32	33	34	35					
STRESS	-400	-350	-300	-250	-200					

Fig. 12.28 b

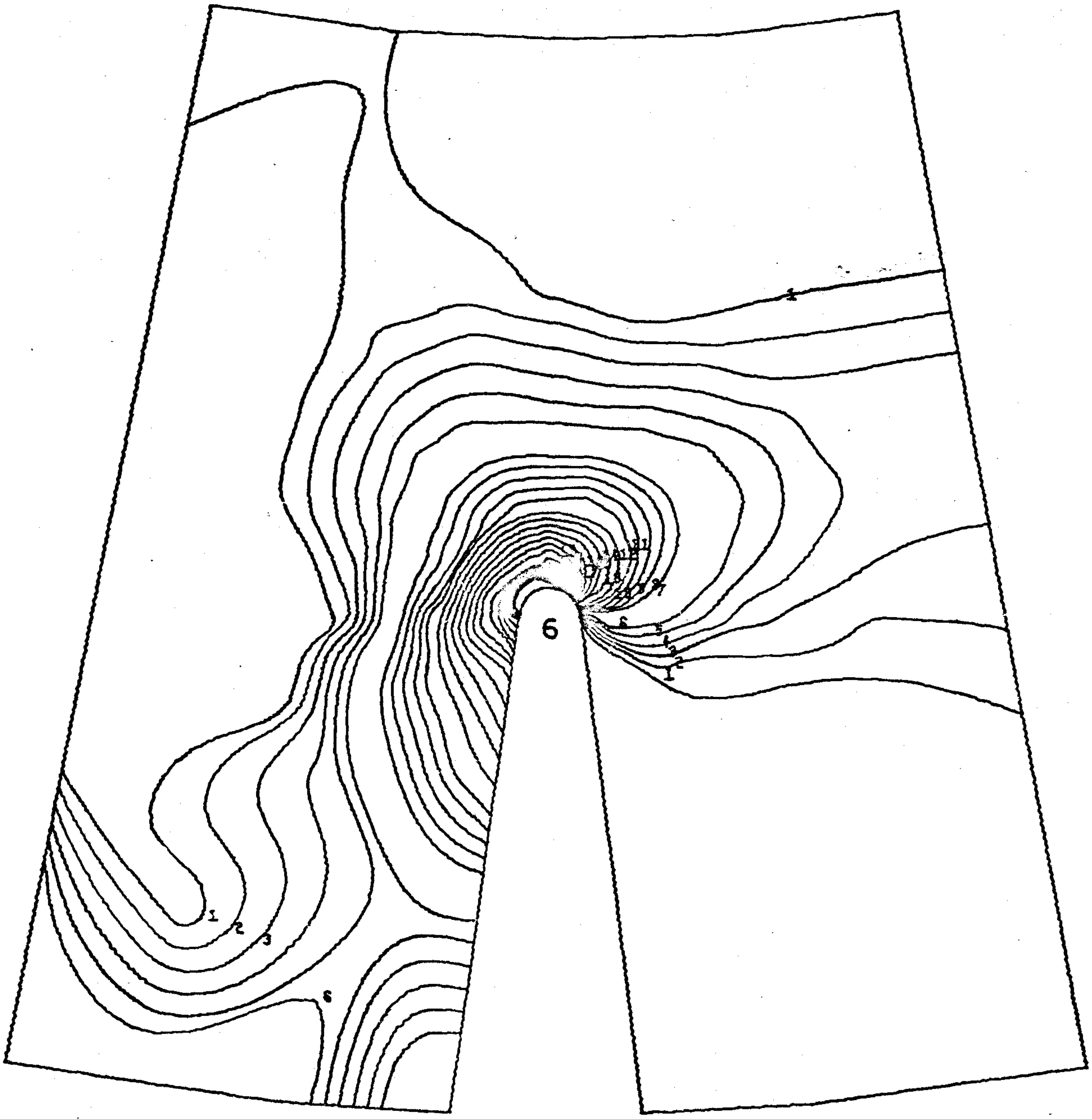

CONTOURS FOR MAXIMUM PRINCIPAL STRESSES

KEY TO CONTOURS-

CONTOUR	1	2	3	4	5	6	7	8	9	10
STRESS	70	90	110	130	150	170	230	250	270	290
CONTOUR	11	12	13	14	15	16	17	18	19	20
STRESS	310	350	390	430	470	510	550	590	650	710
CONTOUR	21	22	23	24	25	26	27	28		
STRESS	770	830	890	950	1010	1070	1130	1190		

Fig. 12.28 c

SHAPE No. 7

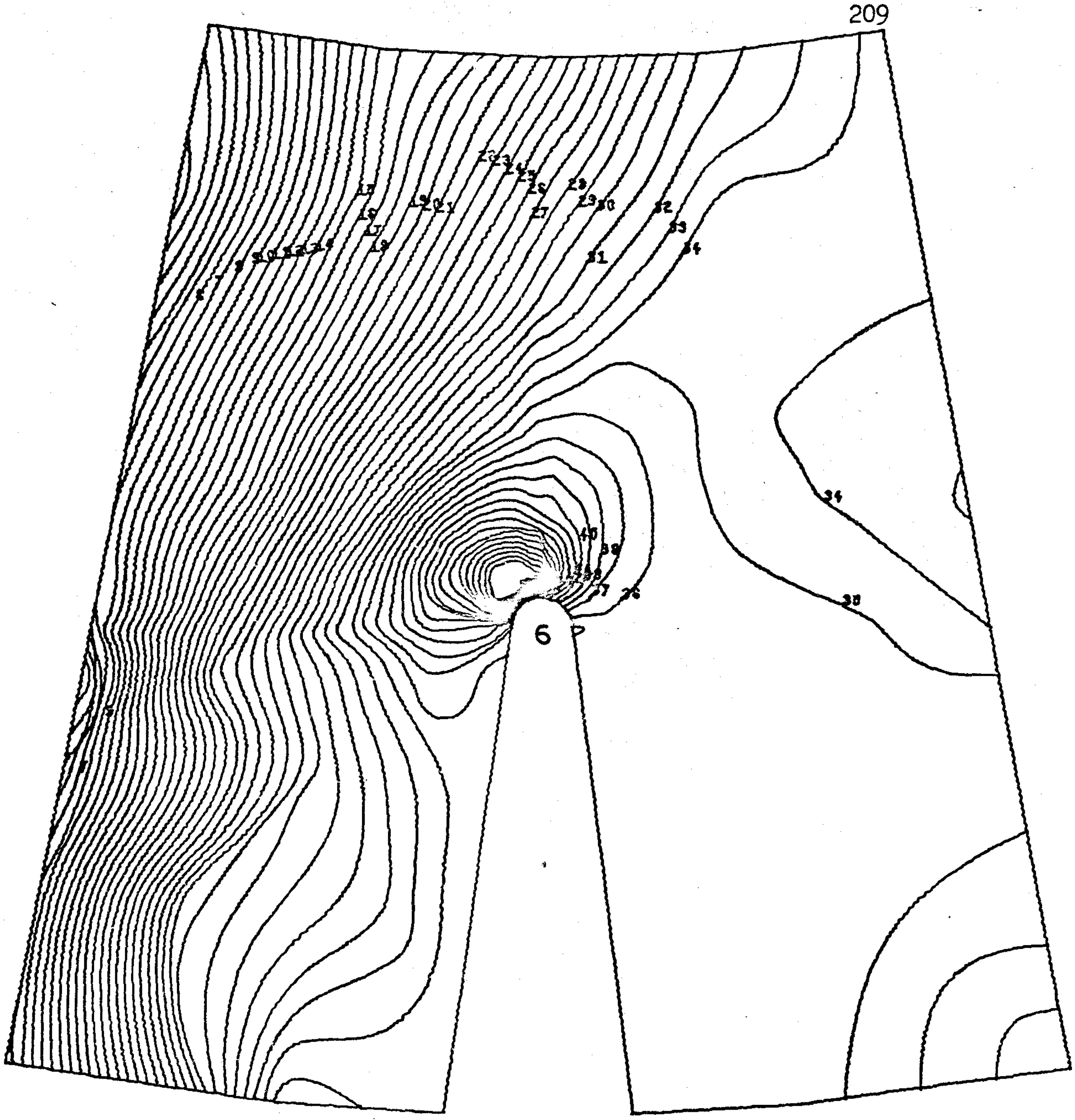

CONTOURS FOR MINIMUM PRINCIPAL STRESSES

KEY TO CONTOURS-

CONTOUR	1	2	3	4	5	6	7	8	9	10
STRESS	-700	-680	-660	-640	-620	-600	-580	-560	-540	-520
CONTOUR	11	12	13	14	15	16	17	18	19	20
STRESS	-500	-480	-460	-440	-420	-400	-380	-360	-340	-320
CONTOUR	21	22	23	24	25	26	27	28	29	30
STRESS	-300	-280	-260	-240	-220	-200	-180	-160	-140	-120
CONTOUR	31	32	33	34	35	36	37	38	39	40
STRESS	-100	-80	-60	-40	-20	0	20	40	60	80
CONTOUR	41	42	43	44	45	46	47	48	49	50
STRESS	100	120	140	160	180	200	220	240	260	280

Fig. 12.28 d

SHAPE No. 8

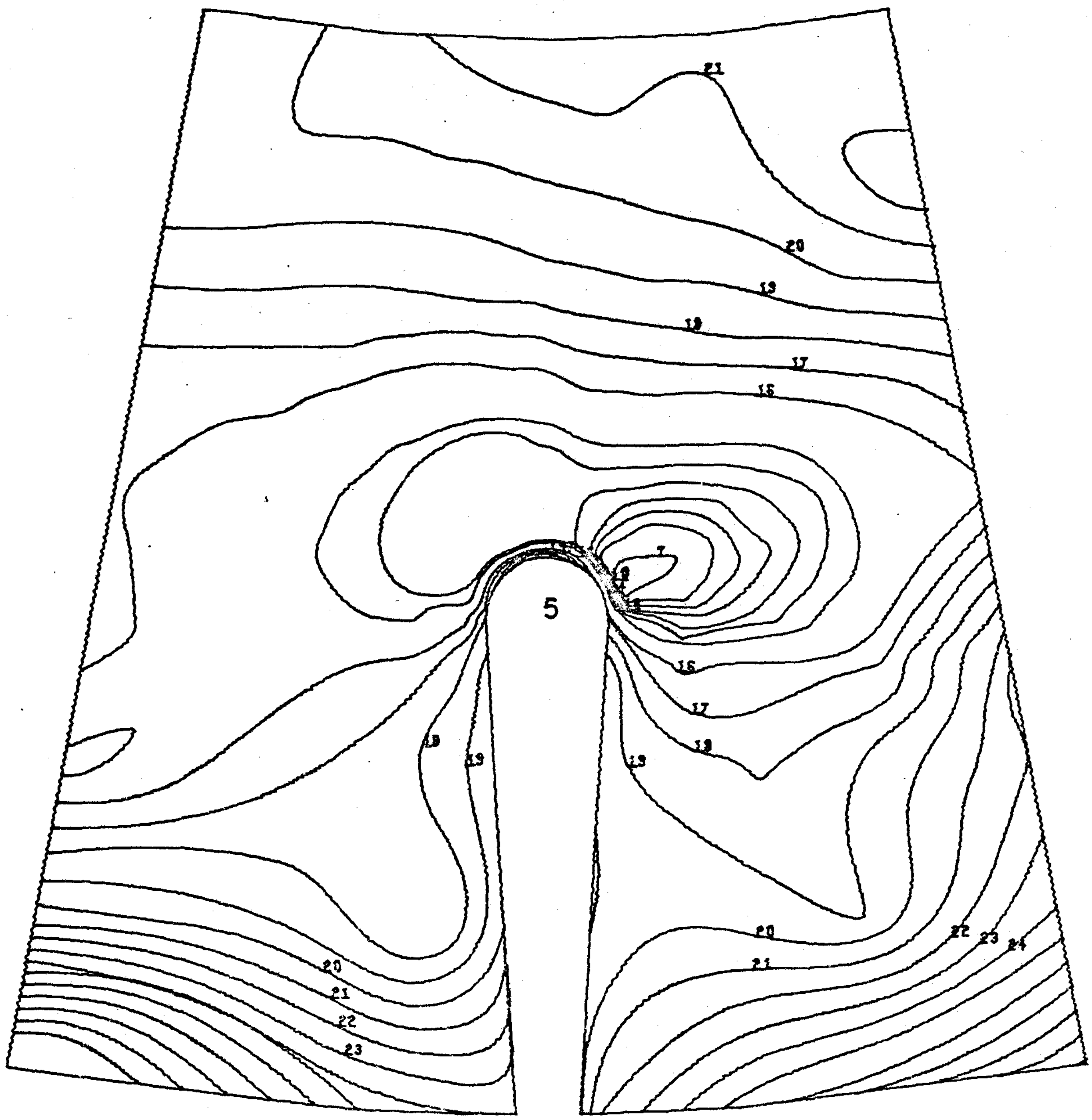

CONTOURS FOR MAXIMUM PRINCIPAL STRESSES

KEY TO CONTOURS-

CONTOUR	1	2	3	4	5	6	7	8	9	10
STRESS	-900	-850	-800	-750	-700	-650	-600	-550	-500	-450
CONTOUR	11	12	13	14	15	16	17	18	19	20
STRESS	-400	-350	-300	-250	-200	-150	-100	-50	0	50
CONTOUR	21	22	23	24	25	26	27	28	29	30
STRESS	100	150	200	250	300	350	400	450	500	550
CONTOUR	31									
STRESS	600									

Fig. 12.29 a

SHAPE No. 8

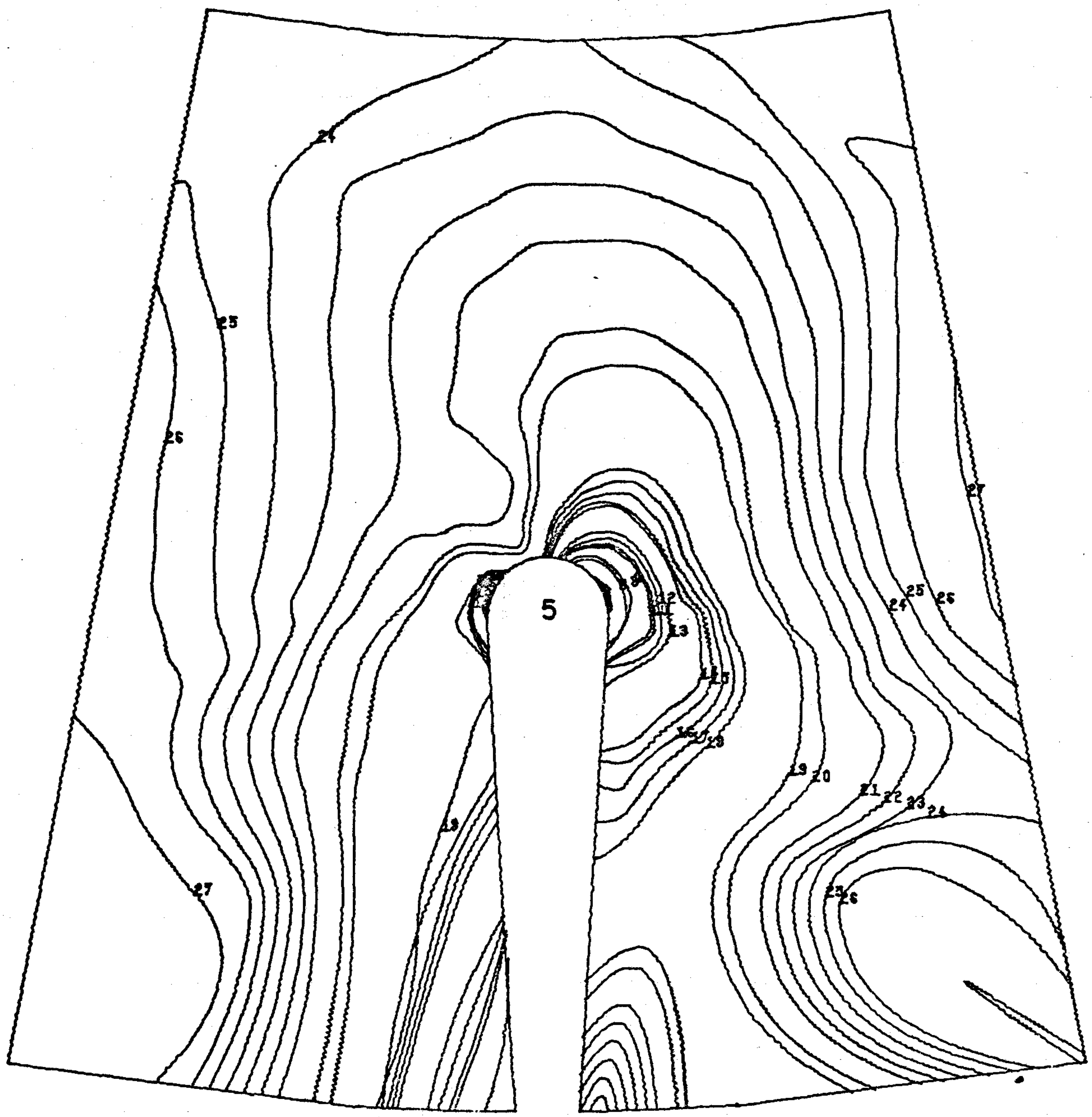

CONTOURS FOR MINIMUM PRINCIPAL STRESSES

KEY TO CONTOURS-

CONTOUR	1	2	3	4	5	6	7	8	9	10
STRESS	-4100	-4000	-3900	-3800	-3650	-3500	-2750	-2550	-2350	-2050
CONTOUR	11	12	13	14	15	16	17	18	19	20
STRESS	-2000	-1900	-1800	-1500	-1450	-1400	-1350	-1300	-1050	-1000
CONTOUR	21	22	23	24	25	26	27	28	29	30
STRESS	-950	-900	-850	-800	-750	-700	-650	-550	-500	-450
CONTOUR	31	32	33	34	35					
STRESS	-400	-350	-300	-250	-200					

Fig. 12.29 b

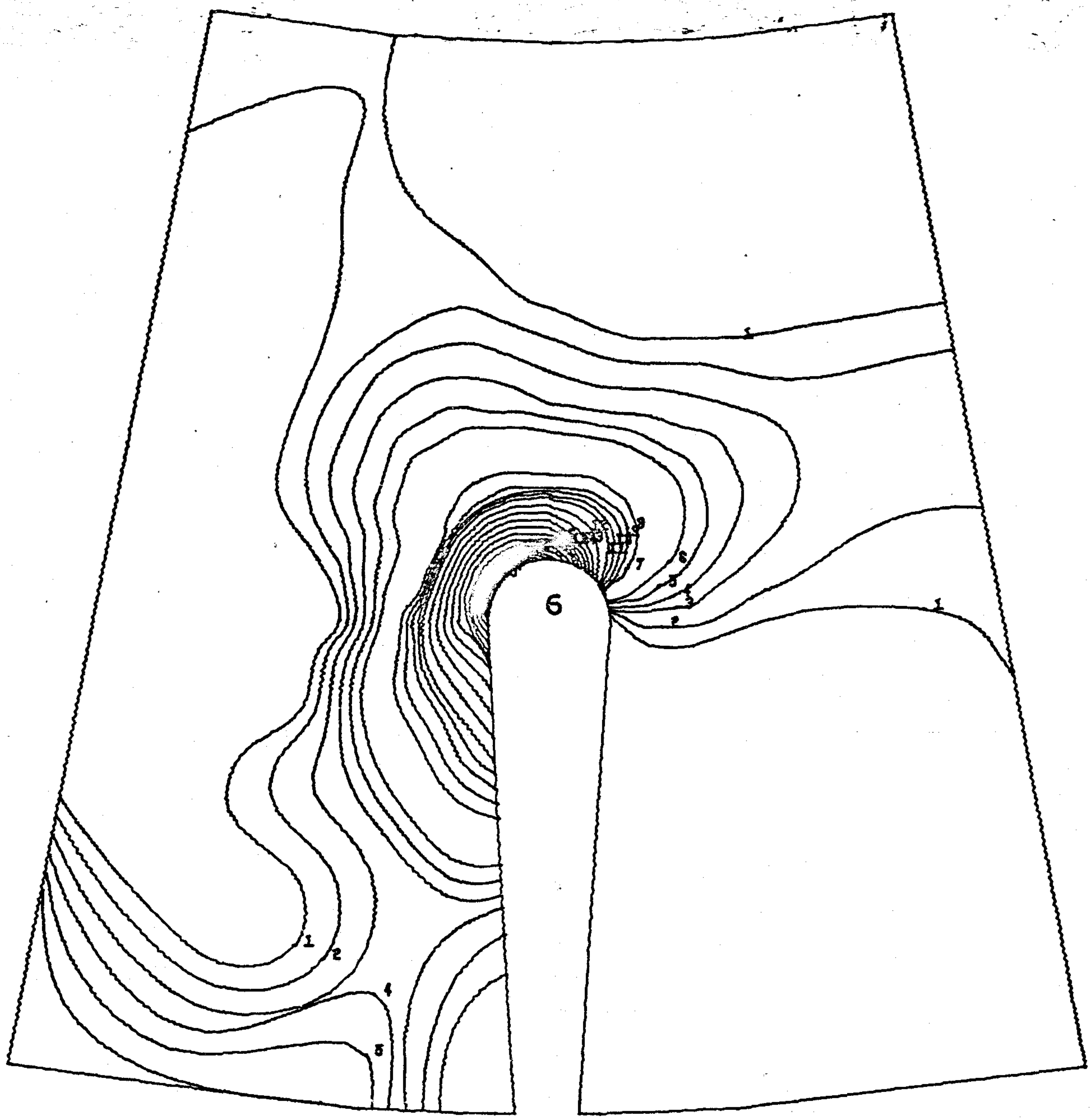

CONTOURS FOR MAXIMUM PRINCIPAL STRESSES
KEY TO CONTOURS-

CONTOUR	1	2	3	4	5	6	7	8	9	10
STRESS	70	90	110	130	150	170	230	250	270	290
CONTOUR	11	12	13	14	15	16	17	18	19	20
STRESS	310	350	390	430	470	510	550	590	650	710
CONTOUR	21	22	23	24	25	26	27	28		
STRESS	770	830	890	950	1010	1070	1130	1190		

Fig. 12.29 c

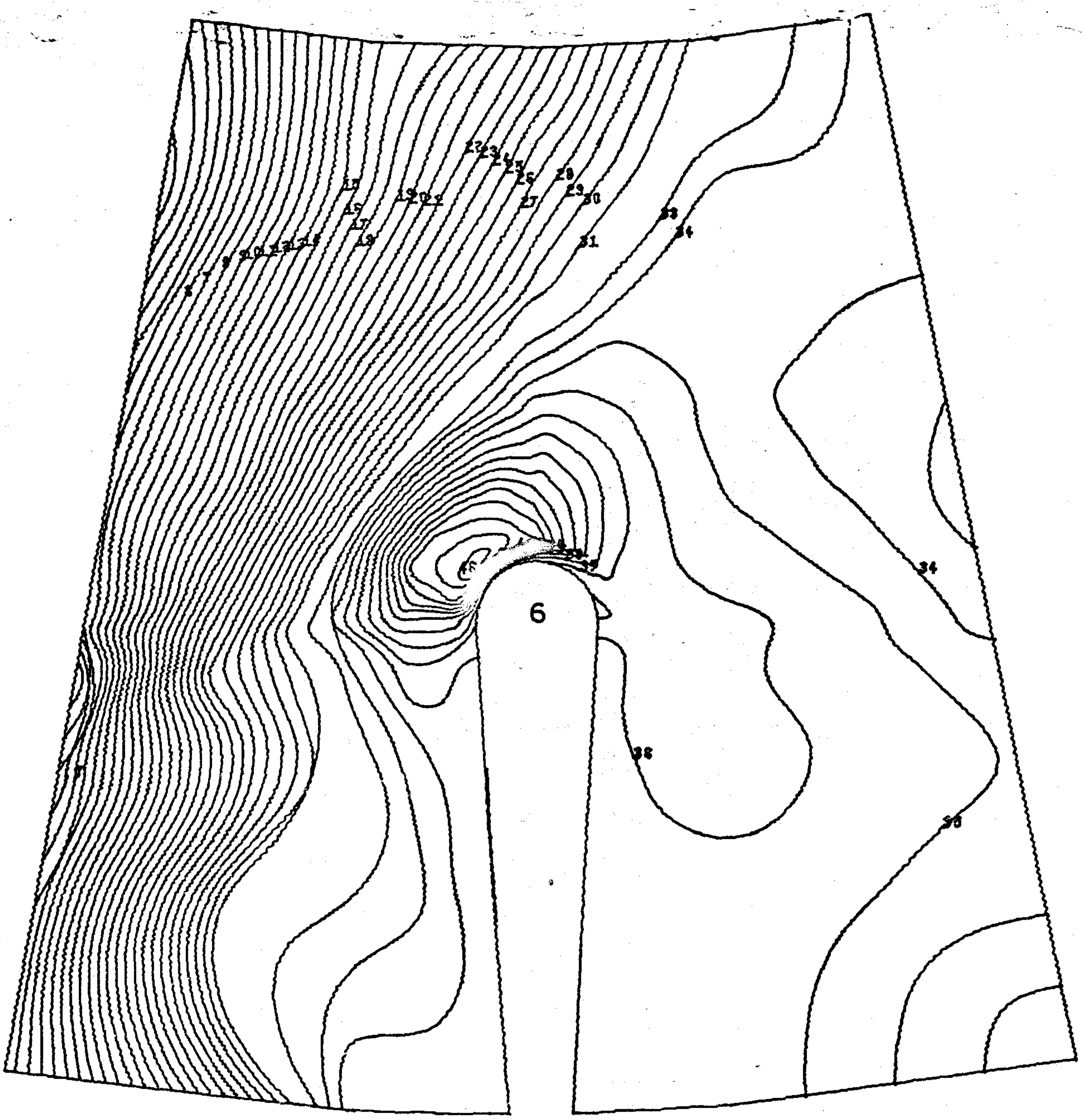

CONTOURS FOR MINIMUM PRINCIPAL STRESSES

KEY TO CONTOURS-

CONTOUR	1	2	3	4	5	6	7	8	9	10
STRESS	-700	-680	-660	-640	-620	-600	-580	-560	-540	-520
CONTOUR	11	12	13	14	15	16	17	18	19	20
STRESS	-500	-480	-460	-440	-420	-400	-380	-360	-340	-320
CONTOUR	21	22	23	24	25	26	27	28	29	30
STRESS	-300	-280	-260	-240	-220	-200	-180	-160	-140	-120
CONTOUR	31	32	33	34	35	36	37	38	39	40
STRESS	-100	-80	-60	-40	-20	0	20	40	60	80
CONTOUR	41	42	43	44	45	46	47	48	49	50
STRESS	100	120	140	160	180	200	220	240	260	280

Fig. 12.29 d

SHAPE No. 9

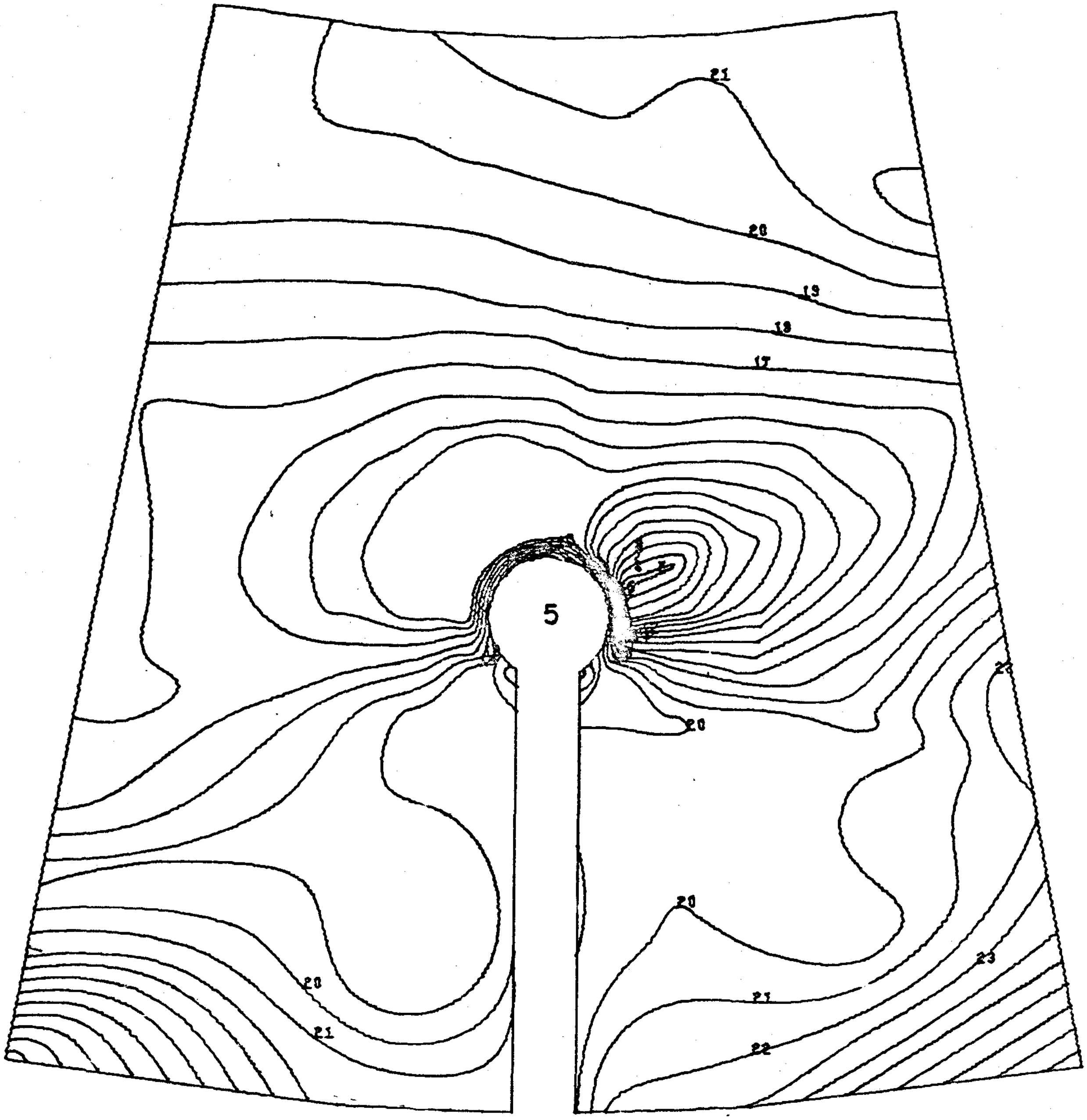

CONTOURS FOR MAXIMUM PRINCIPAL STRESSES

KEY TO CONTOURS-

CONTOUR	1	2	3	4	5	6	7	8	9	10
STRESS	-900	-850	-800	-750	-700	-650	-600	-550	-500	-450
CONTOUR	11	12	13	14	15	16	17	18	19	20
STRESS	-400	-350	-300	-250	-200	-150	-100	-50	0	50
CONTOUR	21	22	23	24	25	26	27	28	29	30
STRESS	100	150	200	250	300	350	400	450	500	550
CONTOUR	31									
STRESS	600									

Fig. 12.30 a

SHAPE No.9

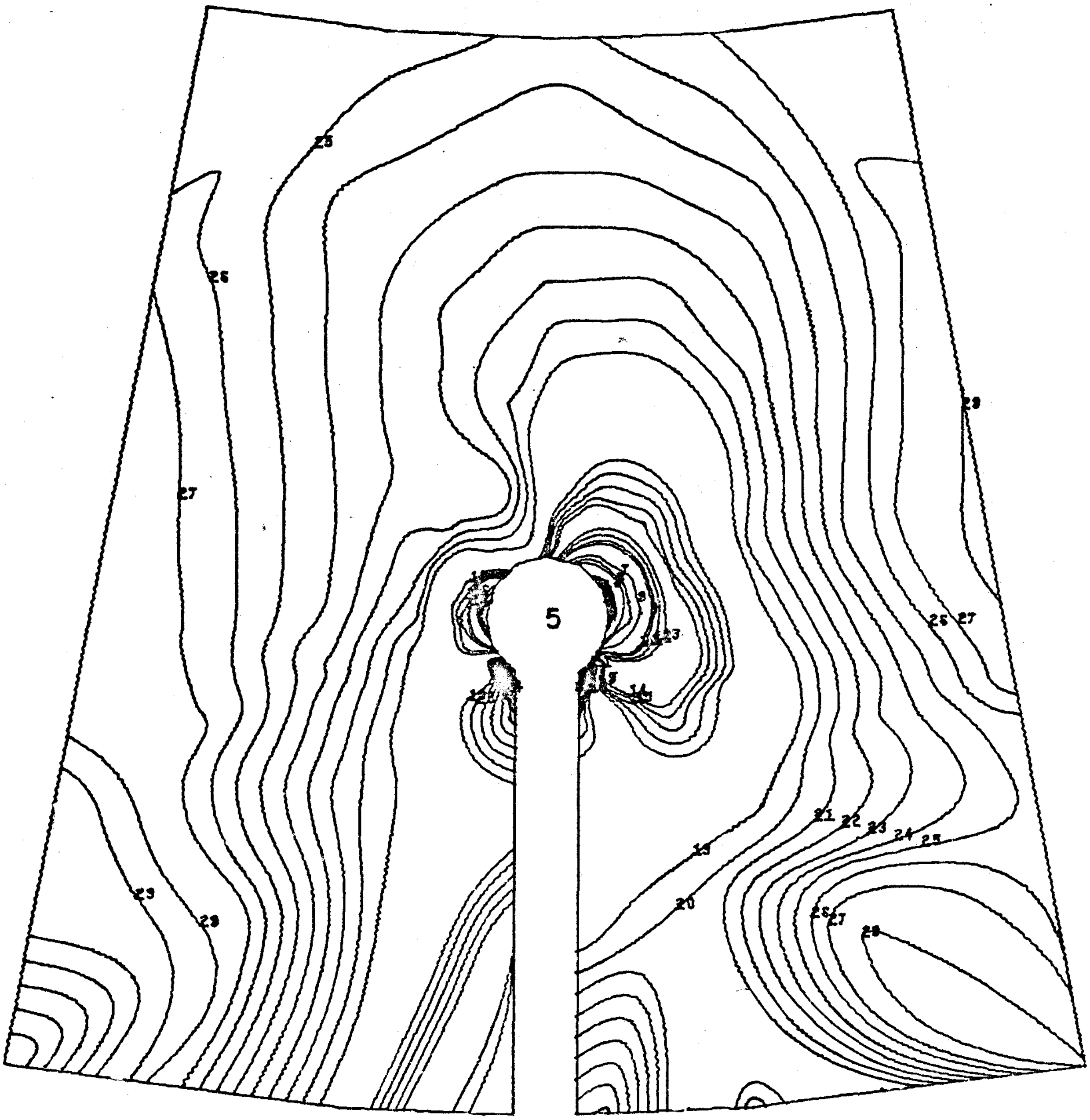

CONTOURS FOR MINIMUM PRINCIPAL STRESSES

KEY TO CONTOURS-

CONTOUR	1	2	3	4	5	6	7	8	9	10
STRESS	-4100	-4000	-3900	-3800	-3650	-3500	-2750	-2550	-2350	-2050
CONTOUR	11	12	13	14	15	16	17	18	19	20
STRESS	-2000	-1900	-1800	-1500	-1450	-1400	-1350	-1300	-1050	-1000
CONTOUR	21	22	23	24	25	26	27	28	29	30
STRESS	-950	-900	-850	-800	-750	-700	-650	-550	-500	-450
CONTOUR	31	32	33	34	35					
STRESS	-400	-350	-300	-250	-200					

Fig. 12.30 b

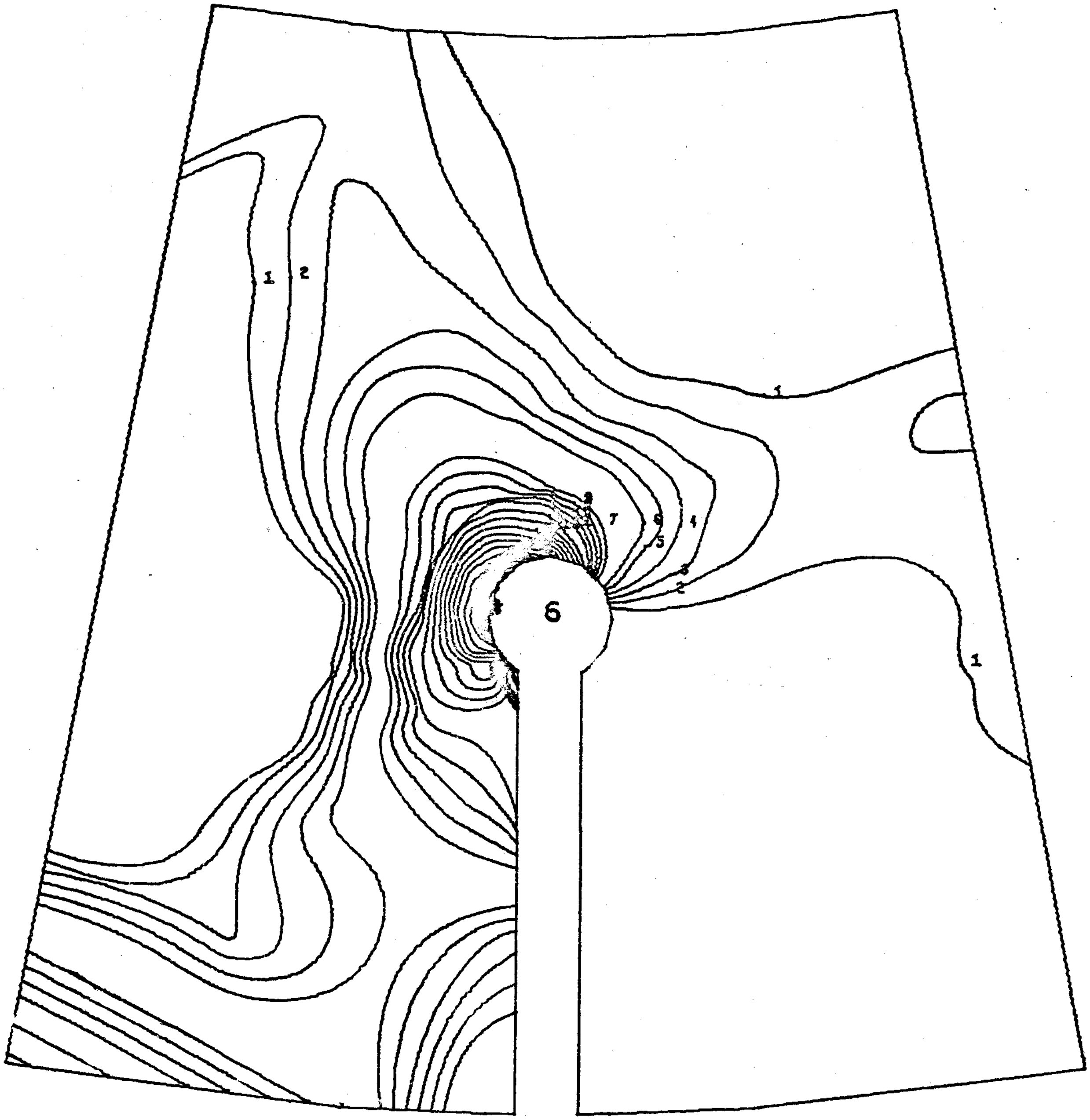

CONTOURS FOR MAXIMUM PRINCIPAL STRESSES

KEY TO CONTOURS-

CONTOUR	1	2	3	4	5	6	7	8	9	10
STRESS	70	90	110	130	150	170	230	250	270	290
CONTOUR	11	12	13	14	15	16	17	18	19	20
STRESS	310	350	390	430	470	510	550	590	650	710
CONTOUR	21	22	23	24	25	26	27	28		
STRESS	770	830	890	950	1010	1070	1130	1190		

Fig. 12.30 c

SHAPE No. 9

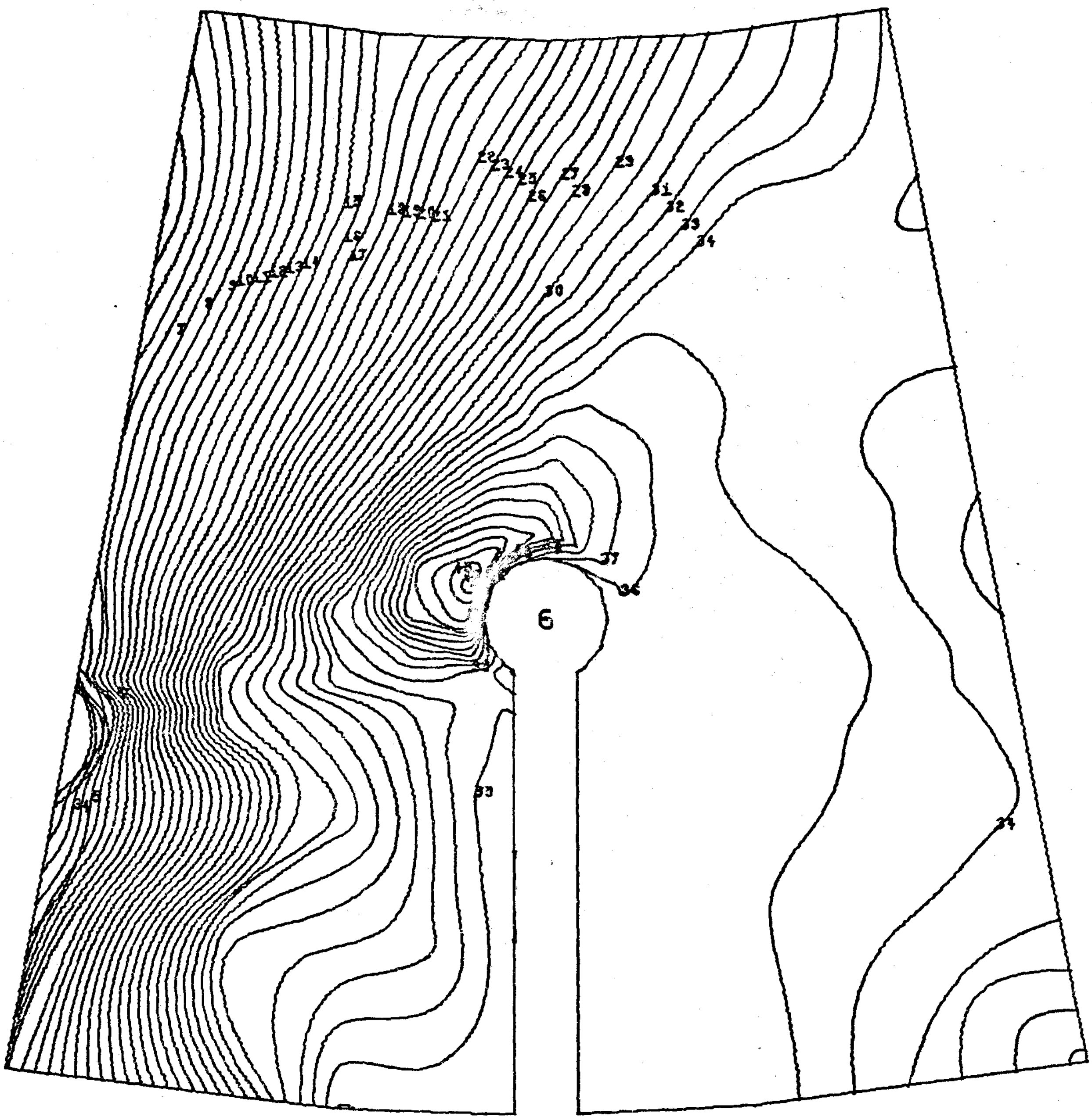

CONTOURS FOR MINIMUM PRINCIPAL STRESSES

KEY TO CONTOURS-

CONTOUR	1	2	3	4	5	6	7	8	9	10
STRESS	-700	-680	-660	-640	-620	-600	-580	-560	-540	-520
CONTOUR	11	12	13	14	15	16	17	18	19	20
STRESS	-500	-480	-460	-440	-420	-400	-380	-360	-340	-320
CONTOUR	21	22	23	24	25	26	27	28	29	30
STRESS	-300	-280	-260	-240	-220	-200	-180	-160	-140	-120
CONTOUR	31	32	33	34	35	36	37	38	39	40
STRESS	-100	-80	-60	-40	-20	0	20	40	60	80
CONTOUR	41	42	43	44	45	46	47	48	49	50
STRESS	100	120	140	160	180	200	220	240	260	280

Fig. 12.30 d

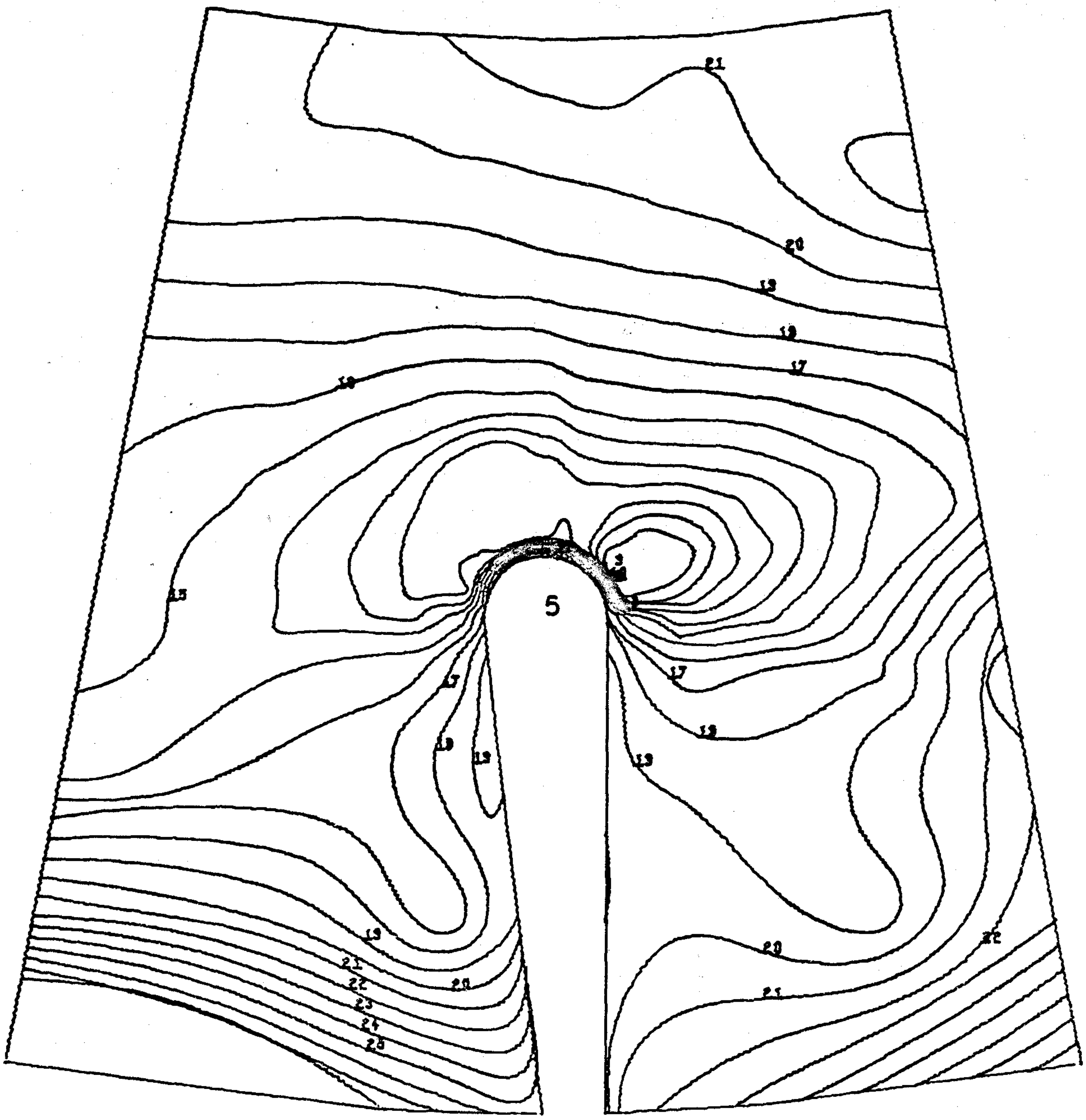

CONTOURS FOR MAXIMUM PRINCIPAL STRESSES

KEY TO CONTOURS-

CONTOUR	1	2	3	4	5	6	7	8	9	10
STRESS	-900	-850	-800	-750	-700	-650	-600	-550	-500	-450
CONTOUR	11	12	13	14	15	16	17	18	19	20
STRESS	-400	-350	-300	-250	-200	-150	-100	-50	0	50
CONTOUR	21	22	23	24	25	26	27	28	29	30
STRESS	100	150	200	250	300	350	400	450	500	550
CONTOUR	31									
STRESS	600									

Fig. 12.31 a

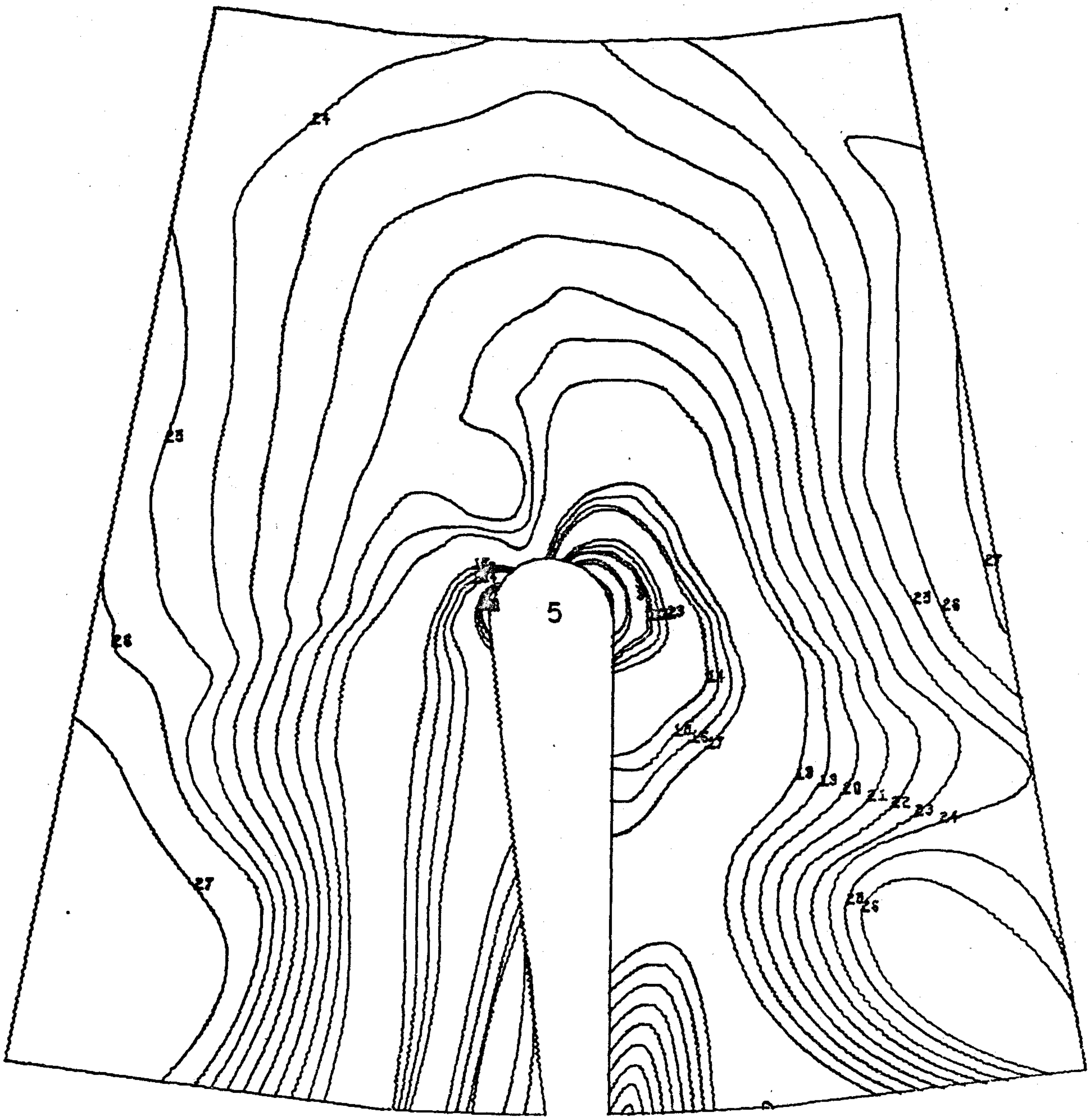

CONTOURS FOR MINIMUM PRINCIPAL STRESSES

KEY TO CONTOURS-

CONTOUR	1	2	3	4	5	6	7	8	9	10
STRESS	-4100	-4000	-3900	-3800	-3650	-3500	-2750	-2550	-2350	-2050
CONTOUR	11	12	13	14	15	16	17	18	19	20
STRESS	-2000	-1900	-1800	-1500	-1450	-1400	-1350	-1300	-1050	-1000
CONTOUR	21	22	23	24	25	26	27	28	29	30
STRESS	-950	-900	-850	-800	-750	-700	-650	-550	-500	-450
CONTOUR	31	32	33	34	35					
STRESS	-400	-350	-300	-250	-200					

Fig. 12.31 b

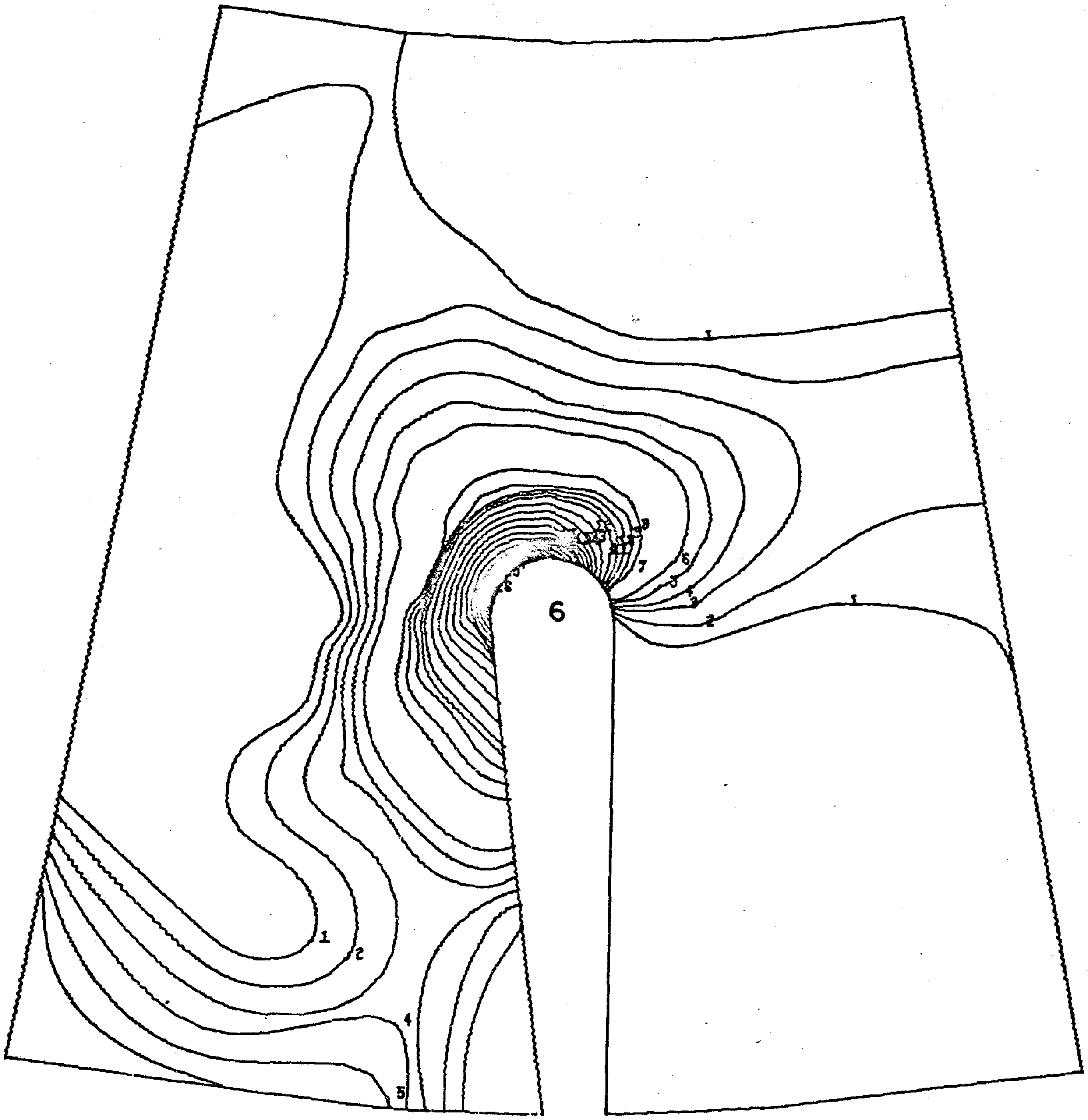

CONTOURS FOR MAXIMUM PRINCIPAL STRESSES

KEY TO CONTOURS-

CONTOUR	1	2	3	4	5	6	7	8	9	10
STRESS	70	90	110	130	150	170	230	250	270	290
CONTOUR	11	12	13	14	15	16	17	18	19	20
STRESS	310	350	390	430	470	510	550	590	650	710
CONTOUR	21	22	23	24	25	26	27	28		
STRESS	770	830	890	950	1010	1070	1130	1190		

Fig. 12.31 c

SHAPE No. 12

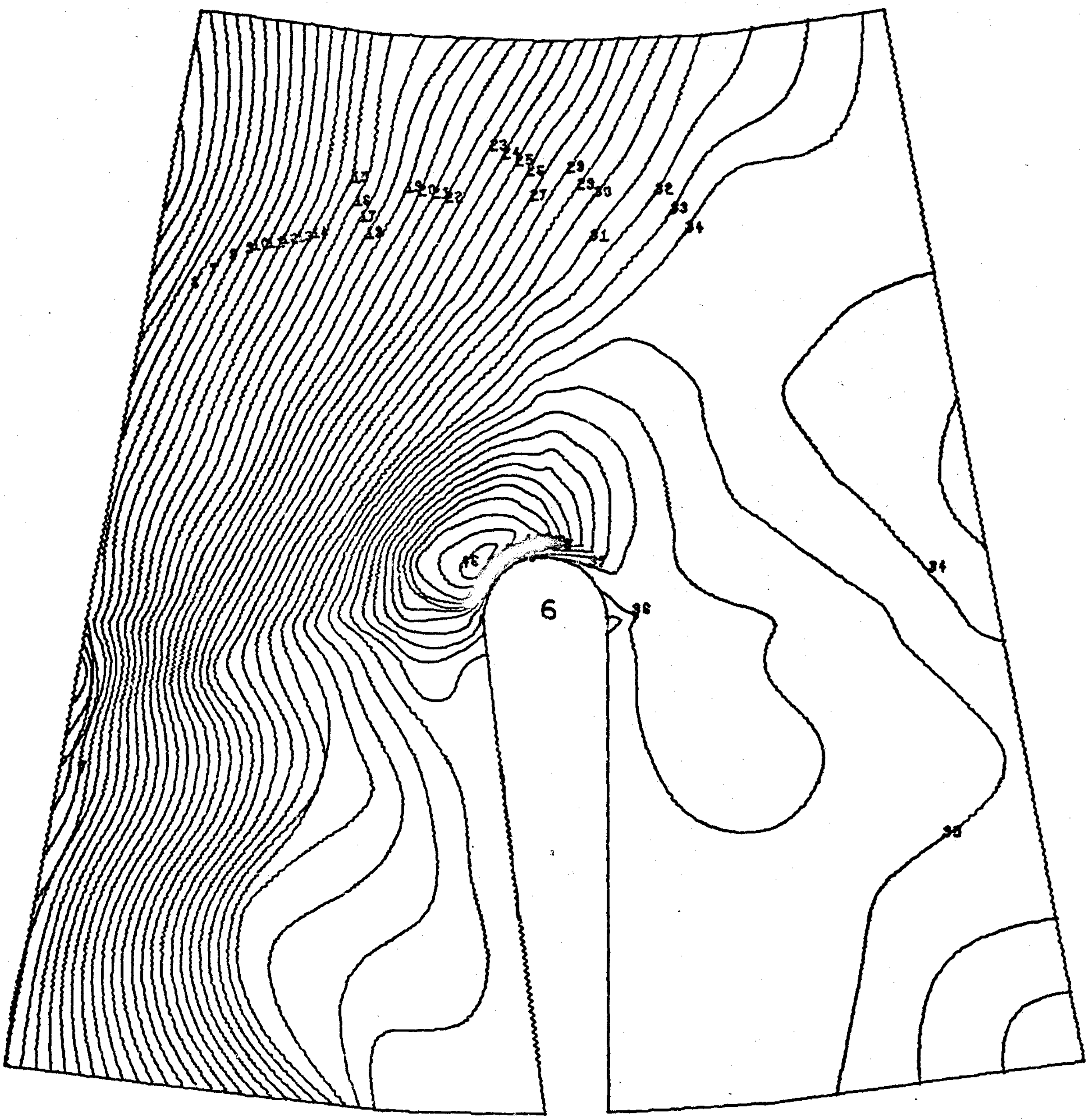

CONTOURS FOR MINIMUM PRINCIPAL STRESSES

KEY TO CONTOURS-

CONTOUR	1	2	3	4	5	6	7	8	9	10
STRESS	-700	-680	-660	-640	-620	-600	-580	-560	-540	-520
CONTOUR	11	12	13	14	15	16	17	18	19	20
STRESS	-500	-480	-460	-440	-420	-400	-380	-360	-340	-320
CONTOUR	21	22	23	24	25	26	27	28	29	30
STRESS	-300	-280	-260	-240	-220	-200	-180	-160	-140	-120
CONTOUR	31	32	33	34	35	36	37	38	39	40
STRESS	-100	-80	-60	-40	-20	0	20	40	60	80
CONTOUR	41	42	43	44	45	46	47	48	49	50
STRESS	100	120	140	160	180	200	220	240	260	280

Fig. 12.31d

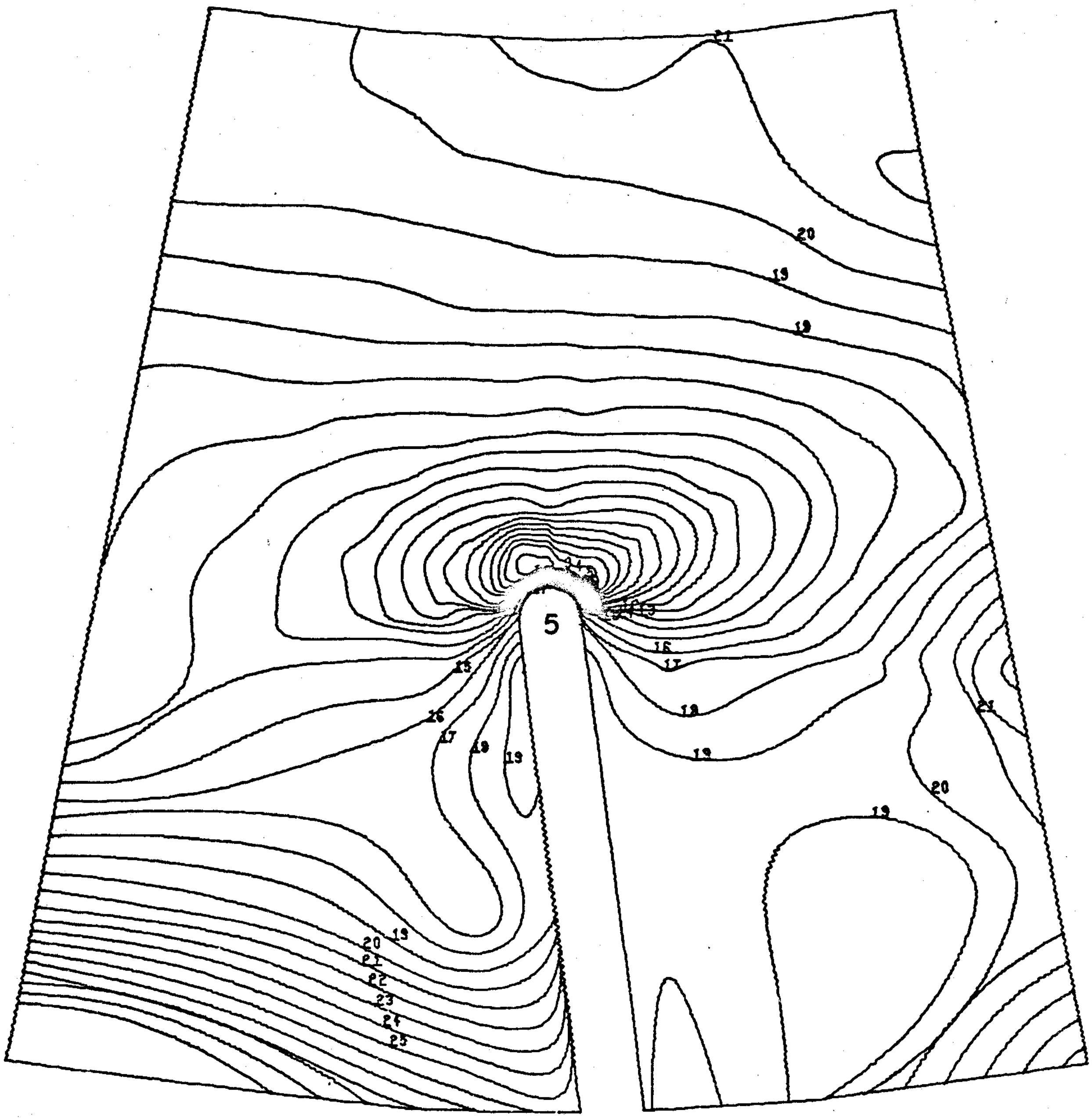

CONTOURS FOR MAXIMUM PRINCIPAL STRESSES

KEY TO CONTOURS-

CONTOUR	1	2	3	4	5	6	7	8	9	10
STRESS	-900	-850	-800	-750	-700	-650	-600	-550	-500	-450
CONTOUR	11	12	13	14	15	16	17	18	19	20
STRESS	-400	-350	-300	-250	-200	-150	-100	-50	0	50
CONTOUR	21	22	23	24	25	26	27	28	29	30
STRESS	100	150	200	250	300	350	400	450	500	550
CONTOUR	31									
STRESS	600									

Fig. 12.32 a

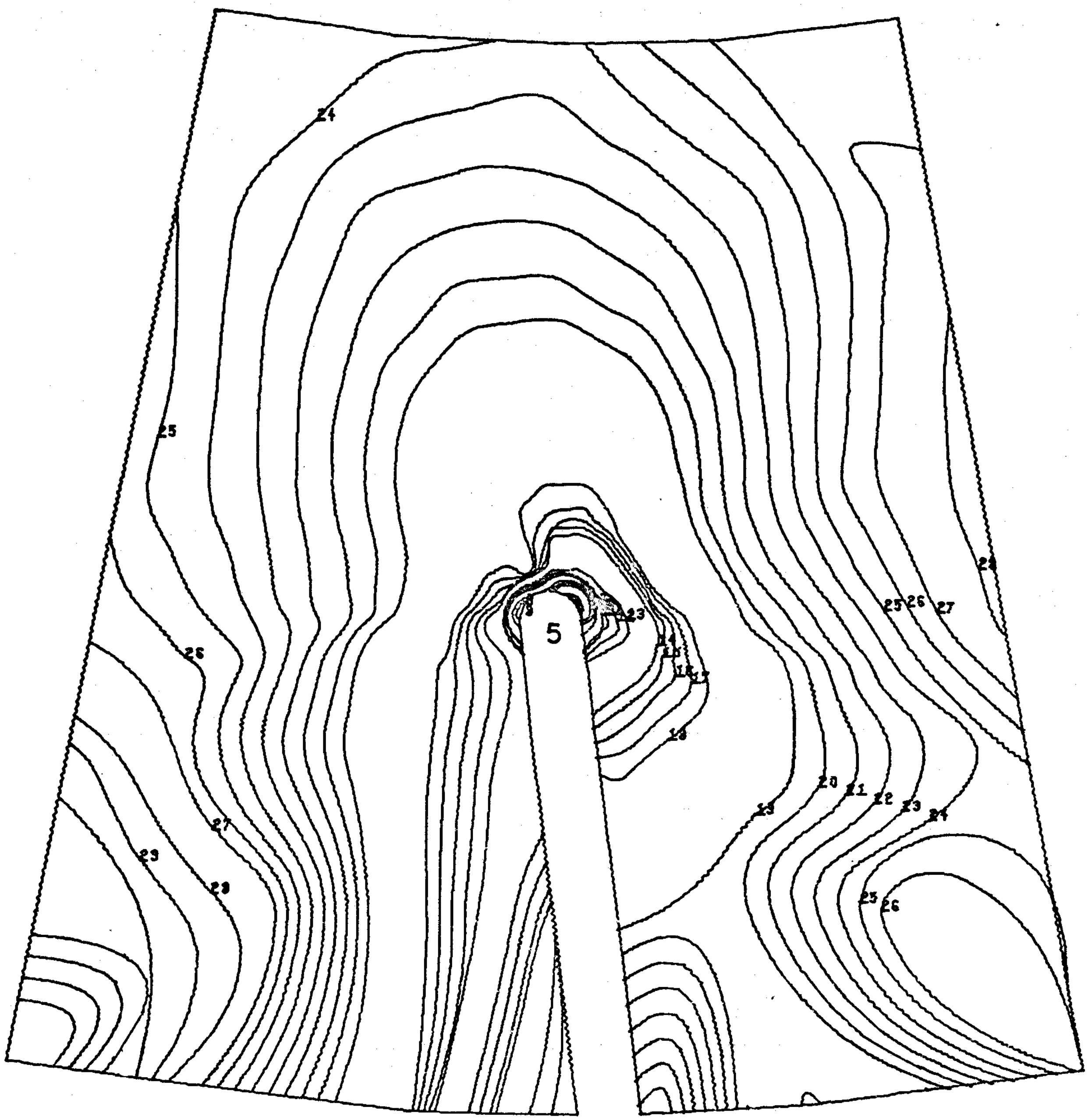

CONTOURS FOR MINIMUM PRINCIPAL STRESSES

KEY TO CONTOURS-

CONTOUR	1	2	3	4	5	6	7	8	9	10
STRESS	-4100	-4000	-3900	-3800	-3650	-3500	-2750	-2550	-2350	-2050
CONTOUR	11	12	13	14	15	16	17	18	19	20
STRESS	-2000	-1900	-1800	-1500	-1450	-1400	-1350	-1300	-1050	-1000
CONTOUR	21	22	23	24	25	26	27	28	29	30
STRESS	-950	-900	-850	-800	-750	-700	-650	-550	-500	-450
CONTOUR	31	32	33	34	35					
STRESS	-400	-350	-300	-250	-200					

Fig. 12.32 b

SHAPE No. 13

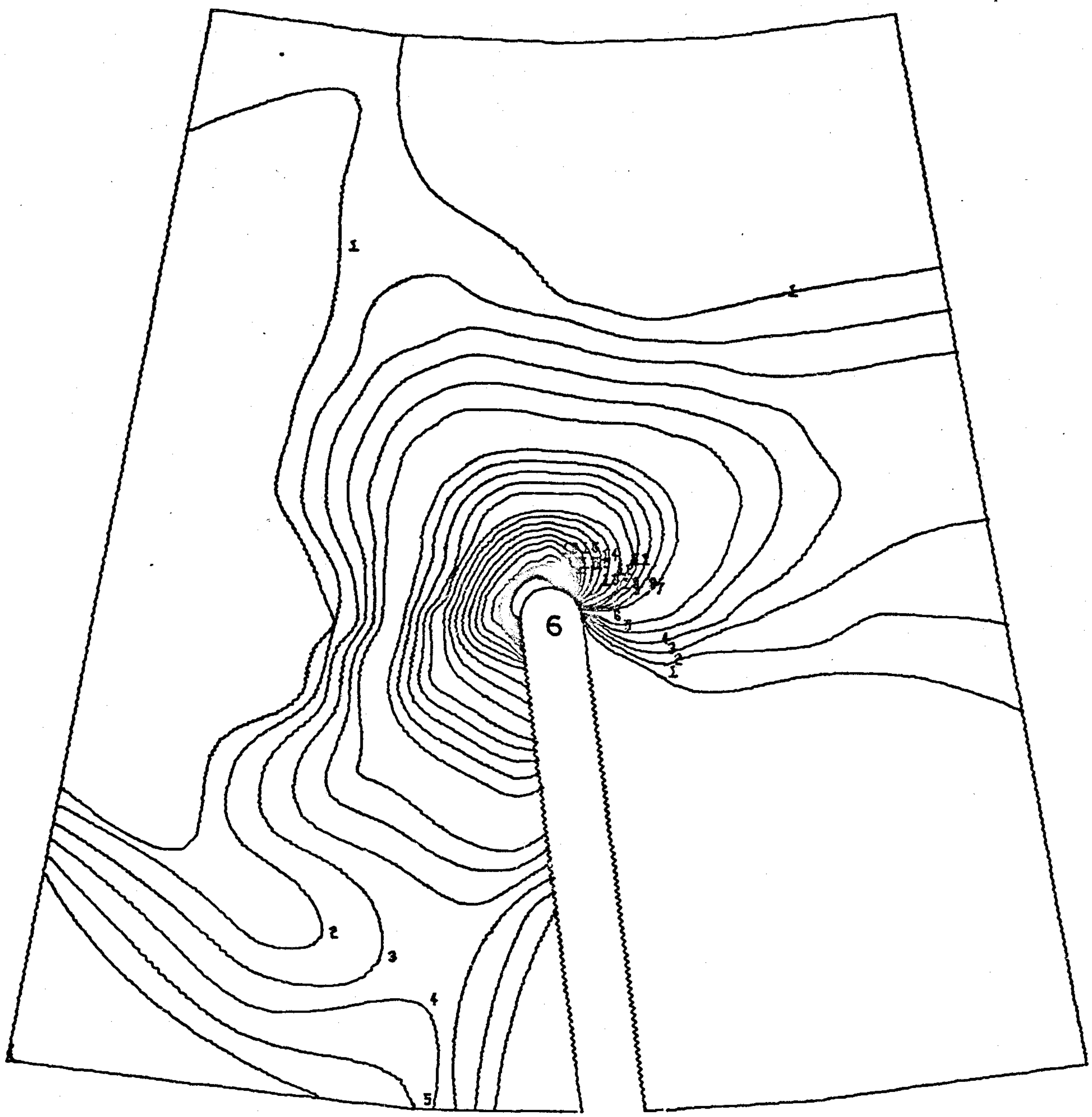

CONTOURS FOR MAXIMUM PRINCIPAL STRESSES

KEY TO CONTOURS-

CONTOUR	1	2	3	4	5	6	7	8	9	10
STRESS	70	90	110	130	150	170	230	250	270	290
CONTOUR	11	12	13	14	15	16	17	18	19	20
STRESS	310	350	390	430	470	510	550	590	650	710
CONTOUR	21	22	23	24	25	26	27	28		
STRESS	770	830	890	950	1010	1070	1130	1190		

Fig. 12.32 c

SHAPE No. 13

CONTOURS FOR MINIMUM PRINCIPAL STRESSES

KEY TO CONTOURS-

CONTOUR	1	2	3	4	5	6	7	8	9	10
STRESS	-700	-680	-660	-640	-620	-600	-580	-560	-540	-520
CONTOUR	11	12	13	14	15	16	17	18	19	20
STRESS	-500	-480	-460	-440	-420	-400	-380	-360	-340	-320
CONTOUR	21	22	23	24	25	26	27	28	29	30
STRESS	-300	-280	-260	-240	-220	-200	-180	-160	-140	-120
CONTOUR	31	32	33	34	35	36	37	38	39	40
STRESS	-100	-80	-60	-40	-20	0	20	40	60	80
CONTOUR	41	42	43	44	45	46	47	48	49	50
STRESS	100	120	140	160	180	200	220	240	260	280

Fig. 12.32 d

(v) Fig. 12.31. For this hybrid shape, the reduction in the bunching of the contours in both the compressive and tensile regions is very apparent. Many of the higher valued contours disappear.

(vi) Fig. 12.32. In this case, reduction in fatigue stress was obtained not because of the relief of stress but because of the proper combination of the peaks of the two principal stresses. The general behaviour of the stress fields is almost identical with the basic slot shape.

Another useful aspect of these contours is that one can obtain the variation of stress along any line simply by noting the values of the contours which intersect with the line.

12.6. Conclusions

(i) Of the shapes tried it was found that the hybrid slot shapes shown in Figs. 12.22 and 12.23 would theoretically behave the best under fatigue conditions. Other than reducing the fatigue stress, these two slot shapes have the following advantages:

(a) They do not reduce the cutting area of the blade, which is important economically.

(b) Because of the positive 'rake angle', they are expected to improve chip removal and coolant inflow. In fact, Shape No. 12 has a greater capacity for chip removal because it is recessed.

(ii) Increasing the slot base circle radius r_H reduces the fatigue stress.

(iii) The small decrease in fatigue stress due to changing slot angle γ in the positive direction did not warrant the large decrease in cutting surface. Making γ negative on the other hand decreases fatigue stress and does not reduce the cutting surface.

(iv) It was found that reducing d aggravated the fatigue stress. The results of two trials are given below:

SLOT DEPTH	FATIGUE STRESS	REDUCTION IN FATIGUE STRESS
d in	psi	%
3/4	932	-16.2
1/2	1041	-29.8

These results are consistent with those of the static case of a notched bar in bending [17], of which stress concentration curves are reproduced in Appendix I. In these curves the slot depth is (D - d)/2. Starting from the right of these curves it can be seen that, as the slot depth increases, the stress concentration increases up to a maximum after which an increase in slot depth produces a decrease in stress concentration. In view of these curves, the slot depth had to be reduced to a bare minimum, i.e. to the right of the peak. This would defeat the purpose of having the slots in the first place.

(v) An increase in the biaxiality of the principal stress amplitude was found to decrease the fatigue stress.

(vi) It was found that the critical principal stress spectra consists of,

(a) a reversed maximum principal stress cycle superposed upon,

(b) a zero-compression fluctuating minimum principal stress cycle.

(vii) The critical point on the slot base circle at which fatigue cracking was likely to cccur was found to be at 30° to the horizontal, and not at the slot root. Most of the cracks found on a used circular saw blade supported this fact.

(viii) In some stone cutting operations, diamond circular saw blades rotate at about 4000 cycles per minute. For an 8-hour day, this would mean that the saw has to endure about 2 million cycles of stress per day. Under these conditions, it can only be hoped to prolong the fatigue life of a saw and not to countermand fatigue failures completely.

(ix) The stresses in Table 12.3 can be seen to be generally low in magnitude. This is due to the fact that a small depth of cut and a small rotational speed were used in the model. In use, the saw speed is about 4000 surface feet per minute and the largest possible depths of cut are taken. Under such conditions the cutting forces become very large and their distributions became non-linear. The model chosen was only for comparative purposes.

(x) From the fatigue criterion (equation 12.1) it can be seen that compressive residual stresses improve fatigue life. Metallurgical methods such as shot peening may be used to introduce compressive residual stresses.

(xi) The propagation of fatigue cracks can be inhibited by removing the surface of the slot base from time to time - this could be done by drilling. This is a practical way of prolonging the life of a saw.

12.7. Suggestions for Further Work

(i) The cutting force distribution on diamond circular saws needs to be investigated by experiment, and the theory in Chapter 11 could be verified.

(ii) A photoelastic study of the saw blade can be made.

(iii) The finite element method can be used to include vibration and thermal effects for both in plane and out of plane problems.

(iv) The four finite element programs could be compiled to form a user-oriented finite element package. Also, a program can be derived from these to combine both TRIM3 and TRIM6 elements in one mesh.

(v) It was found that the most time consuming and error prone step when using the finite element method was the input of the mesh and the interpretation of the numerical results.

A facility used at some research centres is an oscilloscope on which the mesh is defined simply by control of a light pen. The results could be projected on the screen of such an oscilloscope in the form of stress contours described in Chapter 10. In this way a quick feedback can be obtained so that on-the-spot design changes can be made if necessary.

SET	SLOT SHAPE NO.	D IN	r_H IN	γ DEG	ψ DEG	FIG.
1	1	1.0	1/16	0.0	0.0	12.17
	2	1.0	3/32	0.0	0.0	
	3	1.0	1/8	0.0	0.0	12.18
	*4	1.0	3/32	0.0	-48.0	
2	5	1.0	1/16	2.5	0.0	
	6	1.0	1/16	5.0	0.0	
	7	1.0	1/16	7.5	0.0	12.19
	*8	1.0	1/8	-3.5	0.0	12.20
3	9	1.0	1/8	0.0	-60.0	12.21
	10	1.0	1/8	0.0	-48.0	
	11	1.0	1/8	0.0	-24.0	
4	†12	1.0	1/8	-7.0,0.0	0.0	12.22
	†13	1.0	1/16	-7.5,+7.5	0.0	12.23

TABLE 12.1 List of Slot Shapes Tried.

* These shapes do not fall completely in the classification as two variables were changed simultaneously.

† These were hybrid shapes that were not symmetric about the center-lines.

POINT	POSITION 6		POSITION 5		PRINCIPAL STRESS AMPLITUDES		STATIC STRESSES		OCTAHEDRAL SHEAR STRESSES	SUM OF STATIC STRESSES
	σ_1 psi	σ_2 psi	σ_1 psi	σ_2 psi	P_1 psi	P_2 psi	S_1 psi	S_2 psi	σ_{oct} psi	$S_1 + S_2$ psi
n	440	0	-460	-4810	450	2405	-10	-2405	1044	-2415
m	1730	166	-130	-1832	930	999	800	- 833	455	- 33

TABLE 12.2 Tabulation of Fatigue Stress Calculations for Two Points on Slot Shape No. 1.

SLOT SHAPE NUMBER	POSITION 6 (SUBREGION 3)		POSITION 5 (SUBREGION 2)	
	σ_1 psi	σ_2 psi	σ_1 psi	σ_2 psi
1	440	0	-460	-4810
2	380	0	-233	-4243
3	280	0	-147	-3880
4	264	0	-241	-4450
5	440	0	-400	-4570
6	440	0	-371	-4365
7	440	0	-363	-4352
8	270	0	-153	-4078
9	67	0	-200	-4367
10	102	0	-202	-4286
11	155	0	-151	-4025
12	270	0	-146	-3838
13	440	0	-367	-4036

TABLE 12.3 Tabulation of Peak Principal Stresses for Various Slot Shapes.

SLOT SHAPE NUMBER	PRINCIPAL STRESS AMPLITUDES		STATIC STRESSES		OCTAHEDRAL SHEAR STRESS	SUM OF STATIC STRESS	FATIGUE STRESS	REDUCTION
	P_1 psi	P_2 psi	S_1 psi	S_2 psi	σ_{oct} psi	$S_1+S_2=S$ psi	$\sigma_{oct}+$ a S	%
1	450	2405	-10	-2405	1044	-2415	802	0.0
2	307	2122	73	-2122	936	-2049	731	8.3
3	213	1940	67	-1940	870	-1873	683	14.8
4	253	2225	11	-2225	994	-2214	773	3.6
5	420	2285	20	-2285	993	-2265	766	4.4
6	405	2182	35	-2182	948	-2147	734	8.5
7	400	2176	40	-2176	946	-2136	733	8.5
8	212	2039	58	-2039	915	-1981	717	10.6
9	134	2184	-66	-2184	1000	-2250	775	3.4
10	152	2143	-50	-2143	976	-2193	757	5.6
11	153	2013	0	-2103	959	-2013	758	5.5
12	208	1919	62	-1919	859	-1857	673	16.0
13	404	2018	36	-2018	871	-1982	673	16.0

TABLE 12.4 Tabulation of Fatigue Stress Calculations and Improvements in Fatigue Stress for Various Slot Shapes.

REFERENCES

1. Deist, F.H. and Dimitriou, C., "The Finite Element Method", The South African Mechanical Engineer, Vol.19, No.5, Dec. 1969.
2. Holand, I. and Bell, C., "Finite Element Methods in Stress Analysis", Tapir, Trondheim, Norway, 1970.
3. Zienkiewicz, O.C., "The Finite Element Method in Structural and Continuum Mechanics", McGraw-Hill,1967.
4. Przemieniecki, J.S., "Theory of Matrix Structural Analysis", McGraw-Hill, 1968.
5. Petyt, M., "The Application of Finite Element Techniques to Plate and Shell Problems", Institute of Sound and Vibration Research, Report No.120, Feb. 1965.
6. Argyris, J.H., "Energy Theorems and Structural Analysis", Aircraft Engineering, Nov-Dec. 1954, Feb-May 1955.
7. Taig, I.C. and Kerr, R.I., "Some Problems in the Discrete Element Representation of Aircraft Structures", AGARDograph 72, p. 267.
8. Hessel, A., "Analysis of Plates and Shells by Matrix Methods", SAAB TN48.
9. Denke, P.H., "Digital Analysis of Non-linear Structures by the Force Method", AGARDograph 72, p.137.
10. Argyris, J.H., "Recent Advances in Matrix Methods of Structural Analysis", Pergamon Press, 1964.

11. Argyris, J.H., "Triangular Elements with Linearly Varying Strain for the Matrix Displacement Method", J. Royal Aeronautical Society Technical Note, Vol.69, pp.711-13, Oct. 1965.

12. Wilson, E.L., Ph.D. Thesis, University of California.

13. Wang, C., "Applied Elasticity", McGraw-Hill, 1953.

14. Ramstad, H., "Convergence and Numerical Accuracy with Special Reference to Plate Bending", Finite Element Methods, Edited by Holand, I. and Bell, K.

15. Lazan, B.J., "Fatigue Failure under Resonant Vibration Conditions", Fatigue, Edited by Dolan, T.J., American Society for Metals, Ohio, 1953.

16. Roar,, R.J., "Formulas for Stress and Strain", 4th Ed., McGraw-Hill, N.Y., 1965.

17. Peterson, R.E., "Stress Concentration Design Factors", Wiley, 1953.

18. Peterson, R.E., "Notch Sensitivity", Metal Fatigue, edited by Sines, G. and Waisman, J.L., McGraw-Hill, 1959.

19. Waisman, J.L., "Factors Affecting Fatigue Strength", Metal Fatigue, edited by Sines, G. and Waisman, J.L., McGraw-Hill, 1959.

20. Sines, G., "Behaviour of Metals under Complex Static and Alternating Stresses", Metal Fatigue, edited by Sines, G., and Waisman, J.L., McGraw-Hill, 1959.

21. Peterson, R.E,, "Fatigue Cracks and Fracture Surfaces - Mechanics of Development and Visual Appearance", Metal Fatigue, edited by Sines, G. and Waisman, J.L., McGraw-Hill, 1959.

22. Warnock, F.V. and Benham, P.P., "Mechanics of Solids and Strength of Materials", Pitman, 1965.

23. Backer, W.R., Marshall, E.R. and Shaw, M.C., "The Size Effect in Metal Cutting", Trans, ASME, Vol.74, Jan. 1952, pp.61-72.

24. Marshall, E.R. and Shaw, M.C., "Forces in Dry Surface Grinding", Trans. ASME, Vol.74, Jan. 1952, pp.51-59.

25. Reichenbach, G.S. and others, "The Role of Chip Thickness in Grinding", Trans. ASME, Vol.78, May 1956. pp.847-59.

26. Alden, G.I., "Operation of Grinding Wheels in Machine Grinding", Vol.26, 1914, p.451.

27. Guest, J.J., "The Theory of Grinding with Reference to the Selection of Speeds in Plain and Internal Work", Proc. Inst. of Mechanical Engineers, London, England, 1915, p.543.

28. Dall, A.H., "A Review of the Grinding Theories", Modern Machine Shop, Vol.12, No.6, Nov.1939, pp.92-113.

29. Cook, N.H., "Machine Tool Dynamometers", American Machinist, May 1954, pp.125-129.

30. Luce, E.C. and Newell, C.R., "An Abrasive Scale for Granite and Its Influence on Diamond Blade Evaluation", Industrial Diamond Revolution, Vol.28, June 1968, pp.268-70.

31. Hughes, F., "Grinding with Diamond Abrasives", Diamond Information No.L23, De Boers Industrial Diamond Division, Johannesburg.

32. Finnigan, G., "Machining Stone with Diamond Tools", Diamond Information No.L15, De Boers Industrial Diamond Division, Johannesburg.

33. Proceedings: The Industrial Diamond Revolution, A Technical Conference, Columbus, Ohio, U.S.A., Nov. 1967, Published by the Ind. Dia. Assoc. of Am. Inc., Chicago, Ill., 1968.

34. Pellizzari, E., "Stone Processing - An Italian Firm Examines the Contribution of Diamond", Seminar on Stone Processing Organized by De Boers Industrail Diamond Division at Vicenza Biannual Marble Fair, 1966.

APPENDIX A

AREA INTEGRALS BY NUMERICAL METHOD

This method is analogous to the finite element method. The integral is discretized as follows

$$E = \int_{Area} x^m y^n \, dx \, dy$$

$$\approx \sum_{i}^{j} (\bar{x}_i{}^m \cdot \bar{y}_i{}^n)(AREA_i) \qquad (A.1)$$

where j = number of sub-elements.

$\bar{x}_i$, $\bar{y}_i$ are the centroidal co-ordinates of the ith sub-elements.

$AREA_i$ is the area of the ith sub-element.

The triangular element is divided into an ensemble of little triangular sub-elements and 'dx dy' is approximated by the sub-element areas.

The degree of accuracy obtained by equation (A.1) is, of course, dependent on the fineness of sub-division. In the accompanying computer program an iterative approach is used in which the number of intervals on side 1-3 (Fig. A.1(a) is increased by one each cycle. Fig. A.1(a) represents the second cycle and Fig. A.1(b) the 12th cycle, which is a relatively fine sub-division. Convergence is assumed when the integral E at a certain cycle differs by less than a given percent from the integral of the previous cycle.

Table A.1 represents a comparison of the numerical

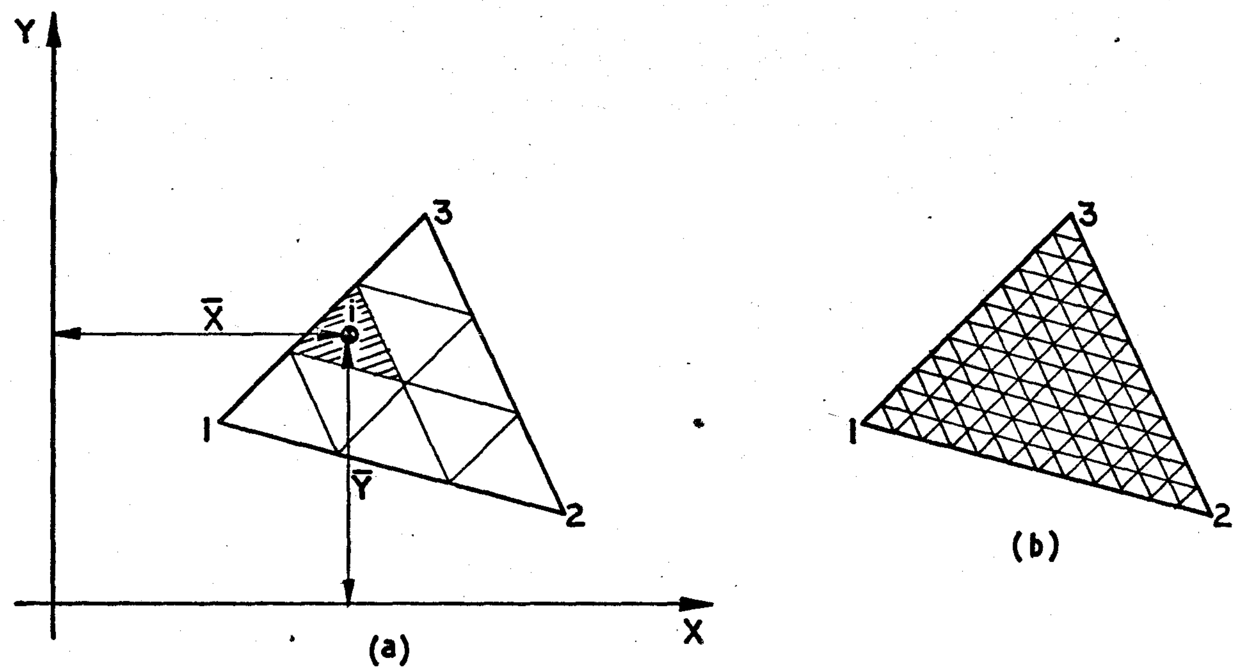

FIG. A.1(a) Course and (b)Fine Divisions for Numerical Area Integration.

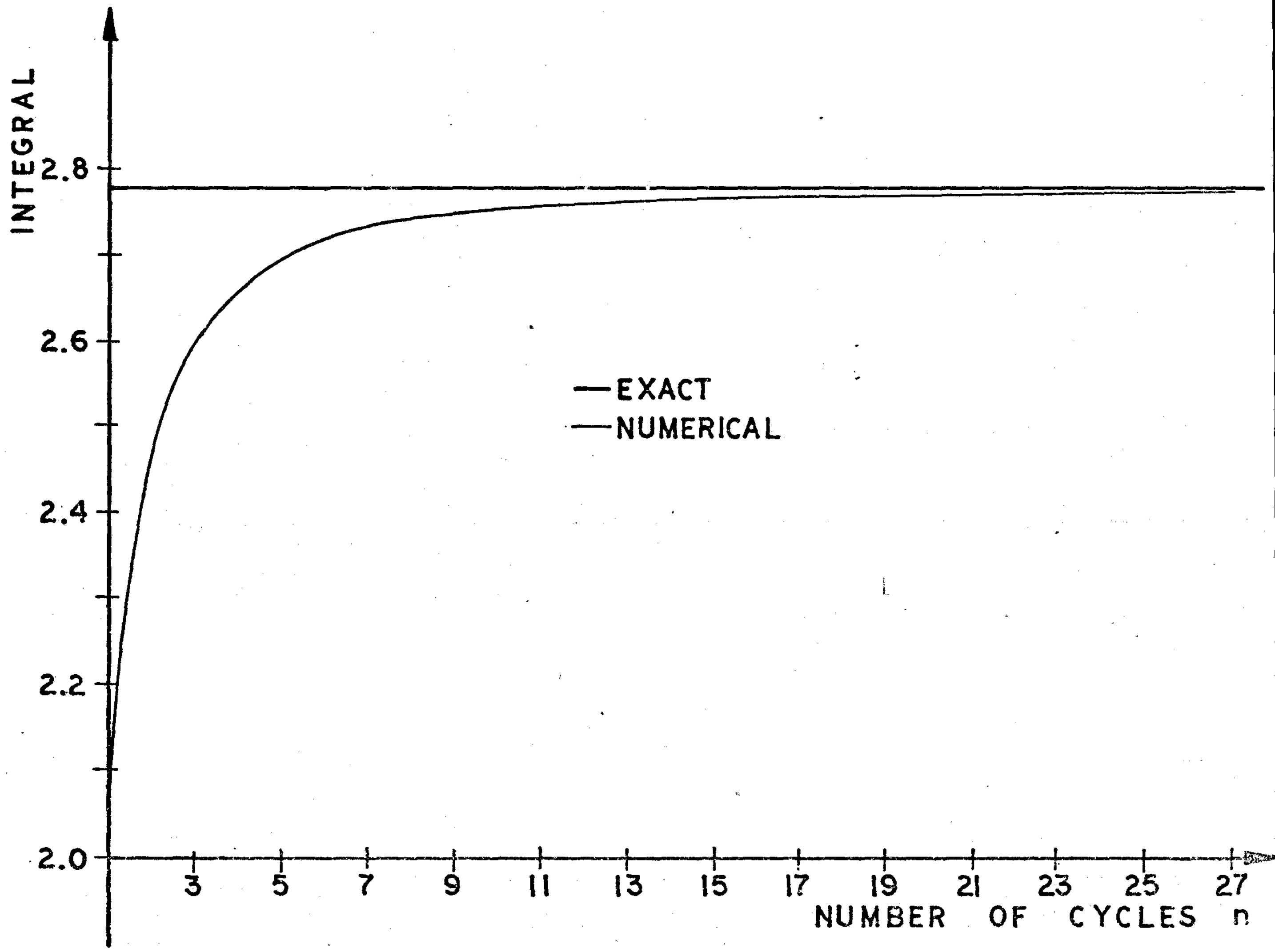

FIG. A.2 Rate of Convergence of Numerical Area Integration of y^2.

method with formal integration as developed in Appendix B. Convergnece to within .075 percent was the accepted in the numerical method.

INTEGRAL	NUMERICAL	FORMAL
x^3	85.73602	85.79785
x^2y	30.87772	30.89296
xy^2	11.37257	11.38229
y^3	4.28075	4.28750

TABLE A.1 Comparison of Results of Area Integrals by Two Methods. The Co-ordinates of the Triangle Used Were (2.00,2.00), (1.00,1.25), (2.50,0.75).

Fig. A.2 shows the rate of convergence of the numerical method. The execution time increases rapidly for fine sub-divisions, but in many cases convergence within .075 pc would be acceptable and the execution time for this accuracy is not excessive. For example, each of the integrals in Table A.1 take .0195 sec on the CDC 6400 computer. An any co-ordinate system could be used, the question of transformation of co-ordinates does not arise.

```
      SUBROUTINE INTEGRL(X,Y,M,N,NCYCLE,E)
      DIMENSION X(3),Y(3),AX(40),AY(40),BX(40),BY(40),XE(3),YE(3)
      ZERO= 0.075
      INTER= 1
      ITER= 0
      E= 0.0
15    INTER= INTER + 1
      EOLD= E
      DX31= (X(3) - X(1))/INTER
      DY31= (Y(3) - Y(1))/INTER
      DX32= (X(3) - X(2))/INTER
      DY32= (Y(3) - Y(2))/INTER
      AX(1)= X(3)
      AY(1)= Y(3)
      IELEM= -1
      E= 0.0
      LZ=0
      DO 1 II= 1,INTER
      IPOINT= II + 1
      IELEM= IELEM + 2
      BX(1)= AX(1) - DX31
      BY(1)= AY(1) - DY31
      BX(IPOINT)= AX(IPOINT - 1) - DX32
      BY(IPOINT)= AY(IPOINT - 1) - DY32
      IF(II .EQ. 1) GO TO 13
      DELX= (BX(IPOINT) - BX(1))/II
      DELY= (BY(IPOINT) - BY(1))/II
      DO 2 JJ=2,II
      BX(JJ)= BX(JJ-1) + DELX
2     BY(JJ)= BY(JJ-1) + DELY
13    CONTINUE
      IA= 0
      IB= 0
      DO 4 KK= 1,IELEM
      IF( (-1)**KK) 5,5,6
5     CONTINUE
      IB= IB + 1
      XE(1)= BX(IB)
      XE(2)= BX(IB+1)
      XE(3)= AX(IB)
      YE(1)= BY(IB)
      YE(2)= BY(IB+1)
      YE(3)= AY(IB)
      GO TO 7
6     CONTINUE
      IA= IA+1
      XE(1)= AX(IA)
      XE(2)= BX(IA+1)
      XE(3)= AX(IA+1)
      YE(1)= AY(IA)
      YE(2)= BY(IA+1)
```

```
      YE(3)= AY(IA+1)
7     CONTINUE
      AA= XE(2)*YE(3) - XE(3)*YE(2)
      BB= XE(1)*YE(3) - XE(3)*YE(1)
      CC= XE(1)*YE(2) - XE(2)*YE(1)
      AREA= (AA-BB+CC)/2.
      ORX= (XE(1)+XE(2)+XE(3))/3.
      ORY= (YE(1)+YE(2)+YE(3))/3.
      IF(M .EQ. 0)  GO TO 8
      XM= ORX**M
      GO TO 9
8     XM= 1.0
9     IF(N .EQ. 0) GO TO 10
      YN= ORY**N
      GO TO 11
10    YN= 1.0
11    E= E + XM*YN*AREA
4     CONTINUE
      DO 12 LL=1,IPOINT
      AX(LL)= BX(LL)
12    AY(LL)= BY(LL)
1     CONTINUE
      ITER= ITER + 1
      IF( ITER .EQ. NCYCLE )  GO TO 14
      IF( ITER .EQ. 1 )  GO TO 15
      IF( ABS(EOLD-E) .GE. 1.0E-10 ) GO TO 21
      DE= .0000001
      GO TO 22
21    DE= ABS( (EOLD-E)/E )
22    DE= DE*100.
      IF( DE.LE. ZERO)  RETURN
      GO TO  15
14    CONTINUE
      WRITE(6,150) M,N
      WRITE(6,151)  ITER, INTER, E
      WRITE(6,152) NCYCLE
      WRITE(6,154) E
      STOP
C
C
150   FORMAT( // 10X,*NUMERICAL DOUBLE INTEGRATION...ORDER OF X=*,I2,
     1*...ORDER OF Y=*,I2/10X,*CYCLE NUMBER*,4X,*NO. OF INTERVALS*,
     24X,*INTEGRAL*/)
151   FORMAT(2(15X,I3),13X,E11.4)
152   FORMAT(5X,*FAILED TO CONVERGE AFTER*,I3,* CYCLES*)
154   FORMAT(5X,*INTEGRAL AT LAST CYCLE=*,E11.4)
153   FORMAT(5X,*CONVERGED WITHIN*,F6.3,* PERCENT AFTER*,I3,* CYCLES*)
      END
```

APPENDIX B

AREA INTEGRALS BY FORMAL INTEGRATION

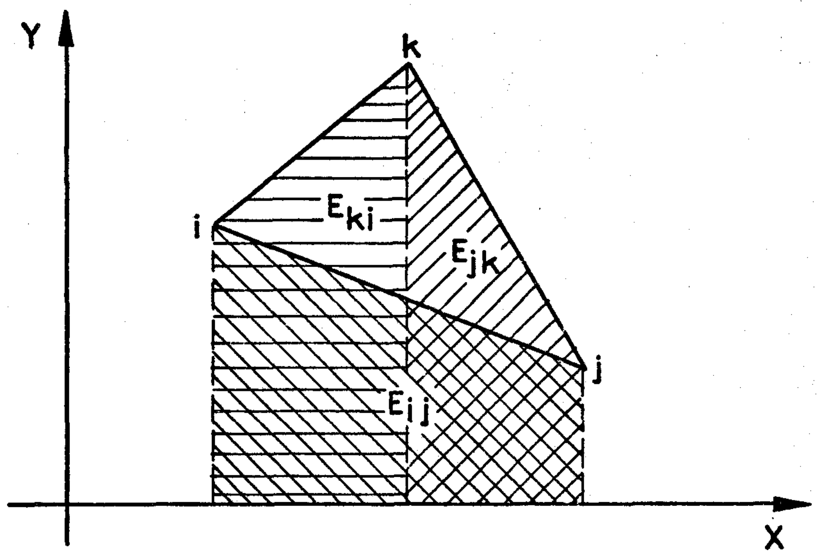

FIG. B.1

The formal integration is performed by dividing the integration into three parts as follows:

$$\int_{\substack{\text{triangle}\\ \text{area}}} x^m y^n \, dx \, dy = \int_{\substack{\text{area under}\\ i - j}} + \int_{\substack{\text{area under}\\ j - k}} + \int_{\substack{\text{area under}\\ k - i}}$$

or

$$E = E_{ij} + E_{jk} + E_{ki} \qquad \text{(B.1)}$$

Equation (B.1) is an algebraic sum and the contribution to the integral by the double-hatched area in Fig. B.1 vanishes.

Area integrals for x^3, x^2y, xy^2 and y^3 are given below. The functions given pertain to one side such as i-j only, and a summation has to be performed over all sides.

Also,

$$M_{ij} = \frac{y_j - y_i}{x_j - x_i}$$ is the shape of the line

$$C_{ij} = y_i - M_{xi}$$ is the constant for line i-j.

(i) Integral of x^3

$$E_{ij} = [M_{ij}x^5/5 + C_{ij}x^4/4]_{x_j}^{x_i}$$

(ii) Integral of x^2y

$$E_{ij} = [M_{ij}x^5/10 + M_{ij}C_{ij}x^4/8 + C_{ij}{}^2x^3/6]_{x_i}^{x_j}$$

(iii) Integral of xy^2

$$E_{ij} = [M_{ij}{}^3x^5/15 + M_{ij}{}^2C_{ij}x^4/4 + M_{ij}C_{ij}{}^2x^3/3$$

$$+ C_{ij}{}^3x^2/6]_{x_i}^{x_j}$$

(iv) Integral of y^3

$$E_{ij} = [M_{ij}{}^4x^5/20 + M_{ij}{}^3C_{ij}x^4/4 + M_{ij}C_{ij}{}^2x^3/2$$

$$+ M_{ij}C_{ij}{}^3x^2/2 + C_{ij}{}^4x/4]$$

APPENDIX C

NODAL POINT STRESSES*

Practical application of the method indicates that the computed nodal point displacements are realistic but, unless very fine mesh is used, considerable dffficulty may be encountered in plotting and evaluating element stresses. Furthermore, it is often desirable to obtain nodal point stresses, since maximum stresses normally are developed on the boundaries of a structure. Therefore, the purpose of this section is to introduce a method of determining nodal point stresses.

It has been shown that nodal point stresses, obtained by averaging the element stresses of all elements connected to the nodal point,produce good results for interior nodal points; however, this approach breaks down when applied to boundary nodal points (11).

Experience has indicated that the three components of element stresses do not represent the state of stress at any one point within the element. For example, consider the element shown in the figure below. Since stresses must be consistent with the nodal point displacements, σ_x approximate the horizontal stress of point A, σ_y approximates the vertical stress at point B, and τ_{xy} approximates the shearing stress at some interior point C. For this case, in determining stresses at nodal point 1, it is

* This is an excerpt from reference [12].

apparent that the horizontal stress at A must be weighted more heavily than the vertical stress at B. Therefore, a 'weighted average' method, which reflects this behaviour, is used to determine nodal point stresses.

The method involves the following calculations to determine the three components of stress at point 1.

$$\sigma_x = \frac{1}{S_x} \sum_n \frac{n^{(n)}}{a^{(n)} + b^{(n)}} \sigma_x(n)$$

$$\sigma_y = \frac{1}{S_y} \sum_n \frac{b^{(n)}}{a^{(n)} + b^{(n)}} \sigma_y(n)$$

$$\tau_{xy} = \frac{1}{N} \sum_n \tau_{xy}^{(n)}$$

where

$$a^{(n)} = |X_k^{(n)} + X_j^{(n)} - 2X_1|$$

$$b^{(n)} = |Y_k^{(n)} + Y_j^{(n)} - 2Y_1|$$

$$S_x = \sum \frac{a^{(n)}}{a^{(n)} + b^{(n)}}$$

$$S_y = \sum \frac{b^{(n)}}{a^{(n)} + b^{(n)}}$$

The summation is performed on all N elements connected at nodal point 1.

In general, the procedure yields results which agree very closely with the direct averaging method for interior nodal points but differ considerably for boundary nodal points.

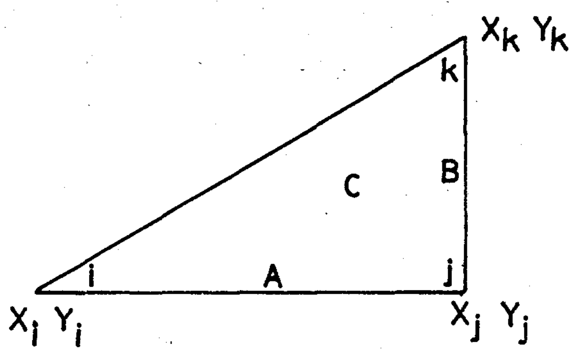

APPENDIX D

STRESSES IN POLAR CO-ORDINATE SYSTEM

By transformation from rectangular Cartesian co-ordinate system:

$$\sigma_r = (\sigma_x + \sigma_y)/2 + (\sigma_x - \sigma_y)/2 \cos 2\theta$$
$$+ \tau_{xy} \sin 2\theta$$

$$\sigma_\theta = (\sigma_x + \sigma_y)/2 - (\sigma_x - \sigma_y)/2 \cos 2\theta$$
$$- \tau_{xy} \sin 2\theta$$

$$\tau_{r\theta} = \tau_{xy} \cos 2\theta - (\sigma_x - \sigma_y)/2 \sin 2\theta$$

APPENDIX E

```
      PROGRAM TST(INPUT,OUTPUT,TAPE5=INPUT,TAPE6=OUTPUT,TAPE1,TAPE2,PU
     1H,TAPE7=PUNCH,TAPE3)
      DIMENSION X1(3), Y1(3), NF(50), NB(50,2), BV(50,2), T(5)
      DIMENSION A(30), ST(12000)
      COMMON /BLK2/ NPOIN,NELEM
      COMMON /BLK3/ D(3,3),DELTA,IAREA
      COMMON /BLK4/ DB(3,6),NODE(3)
      COMMON NOD(400,3),Z(200,2),F(400),U(400),SK(30,400),IT(400)
      EGUIVALENCE (ST(1),SK(1))
      EGUIVALENCE (A(1),U(1))
C
C     FINITE ELEMENT METHOD FOR PLANE STRESS/STRAIN
C     THREE NODAL (TRIM3) ELEMENTS USED
C     LIMITING PARAMETERS FOR THE DIMENSIONS GIVEN-
C     IBAN=30
C     NPOIN=200
C     NELEM=400
C
C     DATA INPUT
C
      READ (5,47) NPOIN,NELEM,NON,NBOUN,IWATE,NCENT,NCOLN,NTHICK,NPUNCH
      READ (5,46) E,P,DENS,RPM
      READ (5,46) (T(I),I=1,NTHICK)
C
      CALL COORD
C
C
C     FIND BANDWIDTH
C
      IBAN=0
      DO 2 I=1,NELEM
      DO 1 J=1,3
      N=NOD(I,J)
      DO 1 K=1,3
      M=NOD(I,K)
      IDIF=IABS(M-N)
      IF (IDIF.GT.IBAN) IBAN=IDIF
    1 CONTINUE
    2 CONTINUE
      IBAN=2*(IBAN+1)
      IF (IBAN.GT.30) GO TO 42
C     INITIALIZE MATRICES TO ZERO
C
      NFORCE=0
      NP=NPOIN*2
      DO 3 I=1,NP
      U(I)=0.0
    3 CONTINUE
      DO 4 I=1,IBAN
      DO 4 J=1,NP
      SK(I,J)=0.0
```

```
4       CONTINUE
C
C       PRINT INPUT DATA
C
        WRITE (6,59)
        WRITE (6,49)
C
        IF (NBOUN.EQ.0) GO TO 6
        DO 5 I=1,NBOUN
        READ (5,45) NF(I),NB(I,1),NB(I,2),BV(I,1),BV(I,2)
5       CONTINUE
6       CONTINUE
        WRITE (6,53) NPOIN
        WRITE (6,54) NELEM
        WRITE (6,55) NON
        WRITE (6,52) NBOUN
        WRITE (6,74) NCENT
        WRITE (6,75) NTHICK
        WRITE (6,78) NCCLN
        WRITE (6,79) IBAN
        WRITE (6,50) E
        WRITE (6,51) P
        WRITE (6,76) DENS
        WRITE (6,77) RPM
        DO 7 I=1,NTHICK
        WRITE (6,56) I,T(I)
7       CONTINUE
        IF (NBOUN.EQ.0) GO TO 13
        WRITE (6,71)
        DO 12 I=1,NBOUN
        IF (NB(I,1)) 11,8,11
8       IF (NB(I,2)) 11,9,10
9       WRITE (6,70) NF(I),BV(I,1),BV(I,2)
        GO TO 12
10      WRITE (6,70) NF(I),BV(I,1)
        GO TO 12
11      WRITE (6,72) NF(I),BV(I,2)
12      CONTINUE
13      CONTINUE
        CALL SECOND (T1)
        NFORCE=NFORCE+1
        DO 14 I=1,NP
        F(I)=0.
14      CONTINUE
        IF (NON.EQ.0) GO TO 16
        WRITE (6,69)
        DO 15 I=1,NON
        READ (5,48) K,F(2*K-1),F(2*K)
        WRITE (6,70) K,F(2*K-1),F(2*K)
15      CONTINUE
16      CONTINUE
```

```
      IF (NFORCE.GT.1) GO TO 25
      WRITE (6,59)
      WRITE (6,66)
      DO 17 I=1,NPOIN
      WRITE (6,65) I,Z(I,1),Z(I,2)
17    CONTINUE
      WRITE (6,59)
      WRITE (6,67)
      DO 19 I=1,NELEM
      ORX=0.
      ORY=0.
      DO 18 J=1,3
      JJ=NOD(I,J)
      ORX=ORX+Z(JJ,1)/3.
      ORY=ORY+Z(JJ,2)/3.
18    CONTINUE
      WRITE (6,68) I,(NOD(I,J),J=1,3),ORX,ORY
19    CONTINUE
C
C     DEFINE ELASTICITY MATRIX D FOR PLANE STRESS- ISOTROPIC MATERIAL
C
      E1=E/(1.-P**2)
      D(1,1)=E1
      D(1,2)=E1*P
      D(1,3)=0.0
      D(2,1)=D(1,2)
      D(2,2)=D(1,1)
      D(2,3)=0.0
      D(3,1)=0.0
      D(3,2)=0.0
      D(3,3)=E1*(1.-P)/2.
      WRITE (6,57)
      WRITE (6,58) ((D(I,J),J=1,3),I=1,3)
      WRITE (6,59)
      WRITE (6,61)
C
C     CALCULATION OF ELEMENT STIFFNESS MATRICES AND ASSEMBLY OF
C     OVERALL STIFFNESS MATRIX
C
      AREA=0.0
      IAREA=0
      REWIND 1
      REWIND 3
      DO 23 L=1,NELEM
      DO 20 I=1,3
      II=NOD(L,I)
      X1(I)=Z(II,1)
      Y1(I)=Z(II,2)
      NODE(I)=II
      IF (II.GT.NPOIN) NODE(I)=0
20    CONTINUE
```

```
      DO 21 K=1,NTHICK
      IF (IT(L).EQ.(K-1)) GO TO 22
21    CONTINUE
22    THICK=T(K)
      CALL FEM (X1,Y1,L,IBAN,THICK)
      AREA=AREA+DELTA
23    CONTINUE
C
      IF (IAREA.EQ.0) GO TO 24
      WRITE (6,73)
      STOP
24    CONTINUE
      REWIND 2
      WRITE (2) ((SK(K,I),I=1,NP),K=1,IBAN)
      WRITE (6,64) AREA
C
C     INTRODUCE PRESCRIBED DISPLACEMENTS
C
25    CONTINUE
      IF (NBOUN.EQ.0) GO TO 29
      DO 28 I=1,NBOUN
      M=NF(I)-1
      DO 27 J=1,2
      IF (NB(I,J)) 27,26,27
26    NPR=2*M+J
      SK(1,NPR)=SK(1,NPR)*1.0E+15
      F(NPR)=SK(1,NPR)*BV(I,J)
27    CONTINUE
28    CONTINUE
29    CONTINUE
C
C     CALCULATION AND SUPERPOSITION OF CENTRIFUGAL FORCES
C
      IF (NCENT.EQ.0) GO TO 30
      CALL CENT (DENS,RPM,NTHICK,T,NELEM)
30    CONTINUE
C
C     SOLUTION OF DISPLACEMENTS
C
      DO 31 I=1,IBAN
      A(I)=SK(I,2)
31    CONTINUE
      K=IBAN
      DO 34 J=2,NP
      DO 32 I=1,IBAN
      K=K+1
      ST(K)=A(I)
32    CONTINUE
      DO 33 I=1,IBAN
      A(I)=SK(I,J+1)
33    CONTINUE
```

```
34    CONTINUE
      IA=IBAN-1
      CALL BMATS (IA,NP,ST)
      CALL SOLBS (IA,NP,ST,F,U)
      WRITE (6,59)
C
      DO 35 I=1,NP,2
      I1=I+1
      J=(I+1)/2
      IF (NPUNCH.GT.0) WRITE (7,48) J,U(I),U(I1)
      WRITE (6,60) J,U(I),J,U(I1)
35    CONTINUE
C
C     REACTIVE FORCES
C
      IF (NBOUN.EQ.0) GO TO 41
      WRITE (6,62)
      REWIND 2
      READ (2) ((SK(K,I),I=1,NP),K=1,IBAN)
      DO 40 N=1,NBOUN
      M=NF(N)-1
      DO 39 JJ=1,2
      I=2*M+JJ
      F(I)=0.
      DO 38 J=1,NP
      IF (I.GT.J) GO TO 36
      K=J-I+1
      IF (K.GT.IBAN) GO TO 38
      STIFF=SK(K,I)
      GO TO 37
36    K=I-J+1
      IF (K.GT.IBAN) GO TO 38
      STIFF=SK(K,J)
37    F(I)=F(I)+STIFF*U(J)
38    CONTINUE
39    CONTINUE
      WRITE (6,63) NF(N),F(I-1),F(I)
40    CONTINUE
41    CONTINUE
C
      CALL STRESS (IWATE,NFORCE,NCOLN,NPOIN,NELEM,NPUNCH)
      CALL SECOND (T2)
      DT=T2-T1
      WRITE (6,44) DT
      IF (NFORCE.GE.NCOLN) GO TO 43
      REWIND 2
      READ (2) ((SK(K,I),I=1,NP),K=1,IBAN)
      READ (5,47) NON
      WRITE (6,59)
      GO TO 13
42    WRITE (6,80) IBAN
```

```
C
C
43    STOP
C
44    FORMAT (//10X,*TIME FOR RUN=*,E12.5)
45    FORMAT (3I3,2E14.7)
46    FORMAT (5E14.7)
47    FORMAT (9I3)
48    FORMAT (I3,2E14.7)
49    FORMAT (/40X,*INPUT     DATA*,/40X,14(*-*),//)
50    FORMAT (20X,*YOUNG S MODULUS                            =*,E12.5)
51    FORMAT (20X,*POISSON S RATIO                            =*,E12.5)
52    FORMAT (20X,*NUMBER OF PRESCRIBED DISPLACEMENTS  =*,I3)
53    FORMAT (20X,*NUMBER OF NODAL POINTS                    =*,I3)
54    FORMAT (20X,*NUMBER OF ELEMENTS                        =*,I3)
55    FORMAT (20X,*NUMEER OF PRESCRIBED FORCES               =*,I3)
56    FORMAT (20X,*THICKNESS T(*,I1,*)                          =*,E12.5)
57    FORMAT (1H1,/,30X,*ELASTICITY MATRIX*,/30X,17(*-*),///,25X,*D(I,J)
     1=*,//)
58    FORMAT (25X,3(E14.7,2X))
59    FORMAT (1H1)
60    FORMAT (10X,*U(*,I3,*)=*,E14.7,5X,*V(*,I3,*)=*,E14.7)
61    FORMAT (5X,*ELEMENT*,5X,*AREA*/)
62    FORMAT (1H1,10X,*REACTIVE FORCES-*/10X,16(*-*)//,10X,*NODE*,12X,*X
     1-FORCE*,16X,*Y-FORCE*)
63    FORMAT (10X,I3,7X,F15.5,8X,F15.5)
64    FORMAT (//5X,*TOTAL AREA=*,E15.8)
65    FORMAT (21X,I3,4X,E12.5,3X,E12.5)
66    FORMAT (20X,*NODE*,4X,*X-COORDINATE*,3X,*Y-COORDINATE*/)
67    FORMAT (20X,*ELEMENT  NODE1  NODE2  NODE3   X-CENTROID    Y-CENTRO
     1ID*/)
68    FORMAT (22X,I3,1X,3(4X,I3),3X,E12.5,2X,E12.5)
69    FORMAT (//20X,*PRESCRIBED FORCES*,/20X,17(*-*),/20X,*NODE*,12X,*X-
     1FORCE*,16X,*Y-FORCE*)
70    FORMAT (21X,I3,2(9X,E14.7))
71    FORMAT (//20X,*PRESCRIBED DISPLACEMENTS*,/20X,24(*-*),/20X,*NODE*,
     19X,*X-DISPLACEMENT*,9X,*Y-DISPLACEMENT*)
72    FORMAT (21X,I3,32X,E14.7)
73    FORMAT (///5X,*ERROR IN INPUT MESH. NEGATIVE AREAS*)
74    FORMAT (20X,*CENTRIFUGAL FORCE OPTION                  =*,I3)
75    FORMAT (20X,*NUMBER OF THICKNESS CHANGES               =*,I3)
76    FORMAT (20X,*DENSITY OF MATERIAL                       =*,E12.5)
77    FORMAT (20X,*SPEED REVS. PER MIN.                      =*,E12.5)
78    FORMAT (20X,*NUMBER OF FORCE COLUMNS                   =*,I3)
79    FORMAT (20X,*BANDWIDTH                                 =*,I3)
80    FORMAT (*  JOB ABORTED. BANDWIDTH EXCEEDS MAX ALLOWED, EQUALS*,I5)
      END
```

```
      SUBROUTINE COORD
      COMMON /BLK2/ NPOIN,NELEM
      COMMON NOD(400,3),Z(200,2),F(400),U(400),SK(30,400),IT(400)
C
C     INPUT OF NODAL NUMBERS AND NODAL COORDINATES
C
      DO 1 I=1,NELEM
      READ (5,3) K,(NOD(K,J),J=1,3),IT(K)
1     CONTINUE
      DO 2 I=1,NPOIN
      READ (5,4) K,Z(K,1),Z(K,2)
2     CONTINUE
C
      RETURN
C
3     FORMAT (5I3)
4     FORMAT (I3,3X,2(2X,E14.7))
      END


      SUBROUTINE PRINCE (SX,SY,SXY,PI,S1,S2,THETA)
C
C     TO FIND PRINCIPAL STRESSES AND PRINCIPLE ANGLE
C     PRINCIPAL ANGLE IS THE ANGLE BETWEEN S1 AND Y-AXIS
C
      Q1=(SX+SY)/2.
      Q2=(SX-SY)/2.
      Q3=SXY
      Q4=SQRT(Q2**2+Q3**2)
      S1=Q1+Q4
      S2=Q1-Q4
      IF (ABS(SXY).GT.1.0E-10) GO TO 1
      THETA=90.
      RETURN
1     THETA=ATAN((S1-SY)/SXY)
      THETA=THETA*180./PI
      RETURN
      END
```

```
      SUBROUTINE CENT (DENS,RPM,NTHICK,T,NELEM)
      DIMENSION NODE(3), X(3), Y(3), B(3), C(3), T(1)
      COMMON NOD(400,3),Z(200,2),F(400),U(400),SK(30,400),IT(400)
      REAL IX,IY,IXY
C
C     SUPERPOSITION OF CENTRIFUGAL FORCES
C
      REWIND 3
      PI=2.*ASIN(1.)
      OMEGA=2.*PI*RPM/60.
      GRAVITY=32.2*12.
      FACT=DENS*OMEGA**2/GRAVITY
      DO 5 I=1,NELEM
      DO 1 K=1,NTHICK
      IF (IT(I).EQ.(K-1)) GO TO 2
1     CONTINUE
2     THICK=T(K)
      FACTOR=FACT*THICK
      READ (3) ORX,ORY,DELTA,(NODE(J),J=1,3),(X(J),Y(J),J=1,3)
      DO 3 K=1,3
      X(K)=X(K)-ORX
      Y(K)=Y(K)-ORY
3     CONTINUE
      IX=(X(1)**2+X(2)**2+X(3)**2)/12.
      IY=(Y(1)**2+Y(2)**2+Y(3)**2)/12.
      IXY=(X(1)*Y(1)+X(2)*Y(2)+X(3)*Y(3))/12.
      B(1)=Y(2)-Y(3)
      B(2)=Y(3)-Y(1)
      B(3)=Y(1)-Y(2)
      C(1)=X(3)-X(2)
      C(2)=X(1)-X(3)
      C(3)=X(2)-X(1)
      FXA=-FACTOR*ORX*DELTA/3.
      FYA=-FACTOR*ORY*DELTA/3.
      DO 4 J=1,3
      FXB=-FACTOR/2.*(B(J)*IX+C(J)*IXY)
      FYB=-FACTOR/2.*(B(J)*IXY+C(J)*IY)
      FX=FXA+FXB
      FY=FYA+FYB
      JJ=2*NODE(J)-1
      F(JJ)=F(JJ)-FX
      F(JJ+1)=F(JJ+1)-FY
4     CONTINUE
5     CONTINUE
      RETURN
      END
```

```
      SUBROUTINE BMAT (X1,Y1,B,DELTA)
      DIMENSION X1(1), Y1(1), A(3,2), B(3,1)
C
C     TO FIND STRAIN-DISPLACEMENT MATRIX (B)
C
      K=0
      DO 6 ISUB=1,3
      IF (ISUB-2) 1,2,3
1     I1=2
      I2=3
      GO TO 4
2     I1=3
      I2=1
      GO TO 4
3     I1=1
      I2=2
4     CONTINUE
      A(1,1)=(Y1(I1)-Y1(I2))/2./DELTA
      A(1,2)=0.0
      A(2,1)=0.0
      A(2,2)=(X1(I2)-X1(I1))/2./DELTA
      A(3,1)=A(2,2)
      A(3,2)=A(1,1)
      DO 5 J=1,2
      K=K+1
      DO 5 I=1,3
5     B(I,K)=A(I,J)
6     CONTINUE
      RETURN
      END
```

```
      SUBROUTINE FEM (X1,Y1,LL,IBAN,THICK)
      DIMENSION X1(3), Y1(3)
      DIMENSION CK(6,6), B(3,6)
      COMMON /BLK3/ D(3,3),DELTA,IAREA
      COMMON /BLK4/ DB(3,6),NODE(3)
      COMMON NOD(400,3),Z(200,2),F(400),U(400),SK(30,400),IT(400)
C
C     1) TO FIND ELEMENT STIFFNESS MATRIX
C     2) ASSEMBLY OF OVERALL STIFFNESS MATRIX
C
C
C     AREA OF TRIANGULAR ELEMENT
C
      T=THICK
      AA=(X1(2)*Y1(3)-X1(3)*Y1(2))/2.
      BE=(X1(1)*Y1(3)-X1(3)*Y1(1))/2.
      CC=(X1(1)*Y1(2)-X1(2)*Y1(1))/2.
      DELTA=AA-BB+CC
      WRITE (6,10) LL,DELTA
      IF (DELTA.LE.0.0) IAREA=IAREA+1
      ORX=(X1(1)+X1(2)+X1(3))/3.
      ORY=(Y1(1)+Y1(2)+Y1(3))/3.
      WRITE (3) ORX,ORY,DELTA,(NODE(I),I=1,3),(X1(I),Y1(I),I=1,3)
C
C     FIND MATRIX B
C
      CALL BMAT (X1,Y1,B,DELTA)
C
C     FORM PRODUCT (D)*(B)=(DB)
C
      DO 1 IA=1,3
      DO 1 JA=1,6
      DB(IA,JA)=0.0
      DO 1 KA=1,3
      DB(IA,JA)=DB(IA,JA)+D(IA,KA)*B(KA,JA)
1     CONTINUE
      WRITE (1) LL,((DB(I,J),J=1,6),I=1,3),(NODE(I),I=1,3)
C
C     FORM ELEMENT STIFFNESS MATRIX
C
      DO 2 IA=1,6
      DO 2 JA=1,6
      CK(IA,JA)=0.0
      DO 2 KA=1,3
      CK(IA,JA)=CK(IA,JA)+B(KA,IA)*DB(KA,JA)*T*DELTA
2     CONTINUE
C
C     ASSEMBLY OF OVERALL STIFFNESS MATRIX (SK)
C     ONLY SUPER-DIAGONALS OF BANDED STIFFNESS MATRIX ARE STORED
C
      DO 8 I=1,3
```

```
      II=NODE(I)
      IF (II.EQ.0) GO TO 8
      DO 7 J=1,3
      JJ=NODE(J)
      IF (JJ.EQ.0) GO TO 7
      IF (JJ.LT.II) GO TO 7
      IK=2*II-1
      IC=2*I-1
      DO 6 IA=1,2
      JK=2*JJ-1
      JC=2*J-1
      DO 5 JA=1,2
      IF (I.NE.J) GO TO 3
      IF (JA.LT.IA) GO TO 4
3     JM=JK-IK+1
      IF (JM.GT.IBAN) GO TO 9
      SK(JM,IK)=SK(JM,IK)+CK(IC,JC)
4     JK=JK+1
      JC=JC+1
5     CONTINUE
      IK=IK+1
      IC=IC+1
6     CONTINUE
7     CONTINUE
8     CONTINUE
      RETURN
9     WRITE (6,11) LL
      STOP
C
10    FORMAT (5X,I5,5X,E14.7)
11    FORMAT (1H1,1X,*JOB ABORTED. BANDWIDTH ERROR FOR ELEMENT NO.*,I5)
      END
```

```
      SUBROUTINE BMATS (NP,NR,BAND)
      DIMENSION BAND(1)
C
C     BAND MATRIX DECOMPOSITION FOR SYMMETRIC MATRICES
C     ONLY THE BAND ELEMENTS OF THE UPPER TRIANGULAR HALF OF THE
C     MATRIX ARE STORED IN ARRAY BAND.
C     THE ELEMENTS ARE STORED ROW BY ROW SUCH THAT THE DIAGONAL
C     ELEMENTS FORM A COLUMN
C     THE BAND MATRIX A IS DECOMPOSED INTO LU (LOWER AND
C     UPPER TRIANGULAR FORMS)
C     ONLY THE ELEMENTS OF THE DECOMPOSED FACTOR U ARE STORED
C     IN ARRAY BAND
C     SUBROUTINE SOLBS USES THE DECOMPOSED FACTOR TO SOLVE FOR X,
C     GIVEN ANY COLUMN VECTOR B.
C
C     VARIABLE DICTIONARY FOR ARGUMENT LIST
C     NP = NO. OF SUPERDIAGONALS IN BAND MATRIX
C     NR = NO. OF ROWS IN BAND MATRIX
C     BAND(I) = ARRAY CONTAINING THE BAND ELEMENTS OF THE UPPER
C     TRIANGULAR HALF OF THE MATRIX
C
      NC=NP+1
      ID=1
      NEL=NC*NR
    1 CONTINUE
      IF (BAND(ID)) 3,2,3
    2 WRITE (6,8) ID
      GO TO 7
    3 CONTINUE
      DO 5 I=1,NP
      J=ID+I*NC-1
      IF (J.GE.NEL) GO TO 6
      K=ID+I-1
      NT=NP-I+1
      DO 4 II=1,NT
      J=J+1
      K=K+1
      BAND(J)=BAND(J)-BAND(ID+I)*BAND(K)/BAND(ID)
    4 CONTINUE
    5 CONTINUE
    6 CONTINUE
      ID=ID+NC
      IF (ID.LT.NEL) GO TO 1
    7 RETURN
C
    8 FORMAT (21H DIAGONAL ELEMENT NO.,I4,21H IS ZERO. RUN ABORTED)
      END
```

```
      SUBROUTINE SOLBS (NP,NR,BAND,B,X)
      DIMENSION BAND(1), B(1), X(1)
      DOUBLE PRECISION S,BD,DP
C
C     BAND MATRIX SOLUTION FOR SYMMETRIC MATRICES.
C     SOLVING THE DECOMPOSED BAND MATRIX, GIVEN A COLUMN VECTOR B.
C     THE DECOMPOSED FACTOR IS OBTAINED FROM SUBROUTINE BMATS
C     AND STORED IN ARRAY BAND
C     THAT IS, SOLVE  (LU)X = B FOR X, FOR A GIVEN B.
C
C     VARIABLE DICTIONARY FOR ARGUMENT LIST
C     NP = NO. OF SUPERDIAGONALS IN BAND MATRIX
C     NR = NO. OF ROWS IN BAND MATRIX
C     BAND(I) = ARRAY CONTAINING THE DECOMPOSED FACTOR.
C     B(I) = COLUMN VECTOR IN MATRIX EQUATION (BAND) X = B
C     X(I) = SOLUTION VECTOR FOR ABOVE MENTIONED MATRIX EQUATION.
C
      NC=NP+1
      NEL=NC*NR
C
C     SOLVING FOR X IN AX = B
C     BAND MATRIX A IS DECOMPOSED INTO  LU
C     THEREFORE    (L * U) X = B
C     CALL                 UX = Z,       THEN   LZ = B
C
C     NOTE-
C     DUE TO THE ANALYTICAL PROCEDURE, IT IS NOT NECESSARY TO MAINTAIN
C     SEPARATE STORAGE LOCATIONS FOR ARRAYS X AND Z.   FOR EACH EQUATION
C     IN WHICH X HAS BEEN SUBSTITUTED FOR Z, A COMMENT CARD PRECEDES
C     THE EQUATION AND CONTAINS THE ACTUAL ANALYTICAL EQUATION.
C
C     SOLVING LOWER TRIANGULAR FORM LZ = B  FOR GIVEN B.
C
C     Z(1)  = B(1)
      X(1)=B(1)
      ID=NC+1
      DO 3 K=2,NR
      S=0.0D0
      DO 1 I=1,NP
      IF ((K-I).LE.0) GO TO 2
      L=ID-I*(NC-1)
      BD=BAND(L)/BAND(L-I)
C     DP = Z(K-I)
      DP=X(K-I)
      S=S-BD*DP
      X(K)=S+B(K)
1     CONTINUE
2     ID=ID+NC
C     Z(K)  = S + B(K)
3     CONTINUE
C
```

```
C       SOLVING UPPER TRIANGULAR FORM  UX = Z  FOR THE ABOVE Z.
C
C       X(NR) = Z(NR) / BAND(NEL - NP)
        X(NR)=X(NR)/BAND(NEL-NP)
        KK=NR-1
        KR=KK
4       CONTINUE
        ID=KR*NC-NP
C       S = Z(KR)
        S=X(KR)
        DO 5 I=1,NP
        IF ((KR+I).GT.NR) GO TO 6
        BD=BAND(ID+I)
        DP=X(KR+I)
        S=S-BD*DP
5       CONTINUE
6       BD=BAND(ID)
        X(KR)=S/BD
        KR=KR-1
        IF (KR.GE.1) GO TO 4
        RETURN
        END
```

```
      SUBROUTINE STRESS (IWATE,NFORCE,NCOLN,NPOIN,NELEM,NPUNCH)
      DIMENSION S(300,3)
      DIMENSION NST(10)
      COMMON /BLK4/ DB(3,6),NODE(3)
      COMMON NOD(400,3),Z(200,2),F(400),U(400),SK(30,400),IT(400)
      EQUIVALENCE (S(1),SK(1))
C
C     CALCULATION OF STRESSES
C
C     ELEMENT STRESSES S(L,M)
C     L= ELEMENT NUMBER
C     M=1,2,3 FOR SX,SY,SXY RESP
C
      DO 1 I=1,NELEM
      DO 1 J=1,3
    1 S(I,J)=0.0
      PI=2.*ASIN(1.0)
      REWIND 1
      DO 5 L=1,NELEM
      READ (1) LL,((DB(I,J),J=1,6),I=1,3),(NODE(I),I=1,3)
      K=0
      DO 3 I=1,3
      KK=2*NODE(I)-1
      DO 3 J=1,2
      K=K+1
      IF (NODE(I).EQ.0) GO TO 2
      F(K)=U(KK)
      KK=KK+1
      GO TO 3
    2 F(K)=0.
    3 CONTINUE
      DO 4 I=1,3
      DO 4 J=1,6
    4 S(L,I)=S(L,I)+DB(I,J)*F(J)
    5 CONTINUE
      WRITE (6,19)
      DO 6 I=1,NELEM
      CALL PRINCE (S(I,1),S(I,2),S(I,3),PI,S1,S2,THETA)
      WRITE (6,20) I,(S(I,J),J=1,3),S1,S2,THETA
      IF (NPUNCH.GT.0) WRITE (7,24) I,(S(I,J),J=1,3),S1,S2,THETA
    6 CONTINUE
C
C     AVERAGE STRESSES AT NODAL POINTS
C
      REWIND 3
      WRITE (6,18)
      WRITE (6,21)
      WRITE (6,22)
      DO 15 I=1,NPOIN
      K=0
      DO 9 L=1,NELEM
```

```
      DC 8 J=1,3
      IF (NOD(L,J)-I) 8,7,8
 7    JK=J
      K=K+1
      NST(K)=L
 8    CONTINUE
 9    CONTINUE
      SX=0.
      SY=0.
      SXY=0.
      IF (K.LE.IWATE) GC TO 11
      DC 10 JJ=1,K
      KK=NST(JJ)
      SX=SX+S(KK,1)
      SY=SY+S(KK,2)
      SXY=SXY+S(KK,3)
10    CCNTINUE
      SX=SX/K
      SY=SY/K
      SXY=SXY/K
      GC TO 14
C
C     WEIGHTED AVERAGE NODAL STRESSES
C
11    SXX=0.
      SYY=0.
      DC 13 JJ=1,K
      KK=NST(JJ)
      A=0.
      B=0.
      DC 12 N=1,3
      NK=NOD(KK,N)
      IF (NK.EQ.I) GO TO 12
      A=A+Z(NK,1)
      B=B+Z(NK,2)
12    CONTINUE
      A=A-2.*Z(I,1)
      B=B-2.*Z(I,2)
      A=ABS(A)
      B=ABS(B)
      AB=A/(A+B)
      BA=B/(A+B)
      SXX=SXX+AB
      SYY=SYY+BA
      SX=SX+AB*S(KK,1)
      SY=SY+BA*S(KK,2)
      SXY=SXY+S(KK,3)
13    CONTINUE
      SX=SX/SXX
      SY=SY/SYY
      SXY=SXY/K
```

```
14    CALL PRINCE (SX,SY,SXY,PI,S1,S2,THETA)
      WRITE (6,20) I,SX,SY,SXY,S1,S2,THETA
      IF (NPUNCH.GT.0) WRITE (7,24) I,SX,SY,SXY,S1,S2,THETA
      WRITE (3) I,SX,SY,SXY
15    CONTINUE
C
C     RADIAL AND TANGENTIAL STRESSES
C
      REWIND 3
      DO 16 N=1,NPOIN
      READ (3) I,SX,SY,SXY
      ZI1=Z(I,1)
      ZI2=Z(I,2)
      R=SQRT(ZI1**2+ZI2**2)
      IF (R.LE.1.0E-50) R=1.
      SINQ=ZI2/R
      COSQ=ZI1/R
      COS2Q=1.-2.*SINQ*SINQ
      SIN2Q=2.*SINQ*COSQ
      Q1=(SX+SY)/2.
      Q2=(SX-SY)/2.
      Q3=SXY
      Q7=Q2*COS2Q
      Q8=Q3*SIN2Q
      S(I,1)=Q1+Q7+Q8
      S(I,2)=Q1-Q7-Q8
      S(I,3)=Q3*COS2Q-Q2*SIN2Q
16    CONTINUE
      WRITE (6,23)
      DO 17 I=1,NPOIN
      WRITE (6,20) I,(S(I,J),J=1,3)
      IF (NPUNCH.GT.0) WRITE (7,24) I,(S(I,J),J=1,3)
17    CONTINUE
C
C
      RETURN
C
18    FORMAT (1H1)
19    FORMAT (1H1,20X,*ELEMENT*,4X,*SX*,9X,*SY*,8X,*SXY*,9X,*S1*,9X,*S2*
     1,6X,*THETA*/)
20    FORMAT (23X,I3,5(2X,F9.2),2X,F7.3)
21    FORMAT (25X,*AVERAGE STRESSES AT NODAL POINTS*/)
22    FORMAT (21X,* NODE   *,4X,*SX*,9X,*SY*,8X,*SXY*,9X,*S1*,9X,*S2*,6X,
     1*THETA*/)
23    FORMAT (1H1,20X,* NODE  *,4X,*SR*,9X,*ST*,8X,*SRT*)
24    FORMAT (I3,5(2X,F9.2),2X,F7.3)
      END
```

```
      PROGRAM TST(INPUT,OUTPUT,TAPE5=INPUT,TAPE6=OUTPUT,TAPE1,TAPE2,TA
     13,PUNCH,TAPE7=PUNCH)
      DIMENSION X1(6), Y1(6), NODE(6), NF(40), NB(40,2), BV(40,2), T(5)
      DIMENSION A(46), ST(16100)
      COMMON /BLK1/ NPOIN,NELEM
      COMMON /BLK2/ D(3,3),DELTA,THICK
      COMMON NOD(300,6),Z(175,2),F(350),U(350),SK(46,350),IT(300)
      EQUIVALENCE (ST(1),SK(1))
      EQUIVALENCE (A(1),U(1))
C
C     FINITE ELEMENT PROGRAM FOR PLANE STRESS OR PLANE
C     STRAIN PROBLEMS.
C     IDEALIZATION BY SIX NODAL (TRIM6) ELEMENTS
C
C     LIMITING PARAMETERS FOR THE DIMENSIONS GIVEN-
C     IBAN=46
C     NPOIN=175
C     NELEM=300
C
C     DATA INPUT
C
      READ (5,40) NPOIN,NELEM,NON,NBOUN,NCENT,NTHICK,NPUNCH
      READ (5,39) E,P,DENS,RPM
      READ (5,39) (T(I),I=1,NTHICK)
C
      NP=NPOIN*2
      CALL COORD (NPOIN,NELEM)
C
C     FIND BANDWIDTH
C
      IBAN=0
      DO 2 I=1,NELEM
      DO 1 J=1,6
      N=NOD(I,J)
      DO 1 K=1,6
      M=NOD(I,K)
      IDIF=IABS(M-N)
      IF (IDIF.GT.IBAN) IBAN=IDIF
    1 CONTINUE
    2 CONTINUE
      IBAN=2*(IBAN+1)
C
C     PRINT INPUT DATA
C
      WRITE (6,52)
      WRITE (6,42)
C
      DO 3 I=1,NBOUN
      READ (5,38) NF(I),NB(I,1),NB(I,2),BV(I,1),BV(I,2)
    3 CONTINUE
      WRITE (6,46) NPOIN
```

```
      WRITE (6,47) NELEM
      WRITE (6,48) NON
      WRITE (6,45) NBOUN
      WRITE (6,66) NCENT
      WRITE (6,67) NTHICK
      WRITE (6,70) IBAN
      WRITE (6,43) E
      WRITE (6,44) P
      WRITE (6,68) DENS
      WRITE (6,69) RPM
      DO 4 I=1,NTHICK
      WRITE (6,49) I,T(I)
4     CONTINUE
      WRITE (6,59)
      DO 9 I=1,NBOUN
      IF (NB(I,1)) 8,5,8
5     IF (NB(I,2)) 8,6,7
6     WRITE (6,58) NF(I),BV(I,1),BV(I,2)
      GO TO 9
7     WRITE (6,58) NF(I),BV(I,1)
      GO TO 9
8     WRITE (6,60) NF(I),BV(I,2)
9     CONTINUE
C
      DO 10 I=1,NP
      U(I)=0.0
      F(I)=0.0
10    CONTINUE
      DO 11 I=1,IBAN
      DO 11 J=1,NP
11    SK(I,J)=0.0
C
      IF (NON.EQ.0) GO TO 13
      WRITE (6,57)
      DO 12 I=1,NON
      READ (5,41) K,F(2*K-1),F(2*K)
      WRITE (6,58) K,F(2*K-1),F(2*K)
12    CONTINUE
13    CONTINUE
      WRITE (6,52)
      WRITE (6,63)
      WRITE (6,64)
      DO 15 L=1,NELEM
      ORX=0.0
      ORY=0.0
      DO 14 I=1,3
      II=NOD(L,I)
      ORX=ORX+Z(II,1)/3.
      ORY=ORY+Z(II,2)/3.
14    CONTINUE
      WRITE (6,65) L,(NOD(L,J),J=1,6),ORX,ORY
```

```
15      CONTINUE
C
C       DEFINE ELASTICITY MATRIX D FOR PLANE STRESS- ISOTROPIC MATERIAL
C
        E1=E/(1.-P**2)
        D(1,1)=E1
        D(1,2)=E1*P
        D(1,3)=0.0
        D(2,1)=D(1,2)
        D(2,2)=D(1,1)
        D(2,3)=0.0
        D(3,1)=0.0
        D(3,2)=0.0
        D(3,3)=E1*(1.-P)/2.
        WRITE (6,50)
        WRITE (6,51) ((D(I,J),J=1,3),I=1,3)
        WRITE (6,52)
C
C       CALCULATION OF ELEMENT STIFFNESS MATRICES AND ASSEMBLY OF
C       OVERALL STIFFNESS MATRIX
C
        AREA=0.0
        REWIND 1
        REWIND 2
        WRITE (6,54)
        DO 21 L=1,NELEM
        DO 16 I=1,3
        K=NOD(L,I)
        X1(I)=Z(K,1)
        Y1(I)=Z(K,2)
16      CONTINUE
        DO 17 I=1,6
        NODE(I)=NOD(L,I)
17      CONTINUE
        DO 18 K=1,NTHICK
        IF (IT(L).EQ.(K-1)) GO TO 19
18      CONTINUE
19      THICK=T(K)
        CALL FEM (X1,Y1,NODE,L,IBAN)
        DO 20 I=4,6
        K=NOD(L,I)
        Z(K,1)=X1(I)
        Z(K,2)=Y1(I)
20      CONTINUE
        AREA=AREA+DELTA
21      CONTINUE
C
C       CALCULATION OF CENTRIFUGAL FORCES
C
        IF (NCENT.EQ.0) GO TO 22
        CALL CENT (NODE,X1,Y1,DENS,RPM,NTHICK,T,NELEM)
```

```
22    CONTINUE
      WRITE (6,61)
      DO 23 I=1,NPOIN
      WRITE (6,62) I,Z(I,1),Z(I,2)
23    CONTINUE
      WRITE (1) ((SK(K,I),I=1,NP),K=1,IBAN)
C
C     INTRODUCE PRESCRIBED DISPLACEMENTS
C
      IF (NBOUN.EQ.0) GO TO 27
      DO 26 I=1,NBOUN
      M=NF(I)-1
      DO 25 J=1,2
      IF (NB(I,J)) 25,24,25
24    NPR=2*M+J
      SK(1,NPR)=SK(1,NPR)*1.0E+15
      F(NPR)=SK(1,NPR)*BV(I,J)
25    CONTINUE
26    CONTINUE
C
C     SOLUTION OF DISPLACEMENTS
C
27    CONTINUE
      DO 28 I=1,IBAN
      A(I)=SK(I,2)
28    CONTINUE
      K=IBAN
      DO 31 J=2,NP
      DO 29 I=1,IBAN
      K=K+1
      ST(K)=A(I)
29    CONTINUE
      DO 30 I=1,IBAN
      A(I)=SK(I,J+1)
30    CONTINUE
31    CONTINUE
      IA=IBAN-1
      CALL BMATS (IA,NP,ST)
      CALL SOLBS (IA,NP,ST,F,U)
C
      WRITE (6,52)
      DO 32 I=1,NP,2
      I1=I+1
      J=(I+1)/2
      IF (NPUNCH.GT.0) WRITE (7,71) J,U(I),U(I1)
      WRITE (6,53) J,U(I),J,U(I1)
32    CONTINUE
C
C     REACTIVE FORCES
C
      WRITE (6,55)
```

```
      REWIND 1
      READ (1) ((SK(K,I),I=1,NP),K=1,IBAN)
      DO 37 N=1,NBOUN
      M=NF(N)-1
      DO 36 JJ=1,2
      I=2*M+JJ
      F(I)=0.
      DO 35 J=1,NP
      IF (I.GT.J) GO TO 33
      K=J-I+1
      IF (K.GT.IBAN) GO TO 35
      STIFF=SK(K,I)
      GO TO 34
33    K=I-J+1
      IF (K.GT.IBAN) GO TO 35
      STIFF=SK(K,J)
34    F(I)=F(I)+STIFF*U(J)
35    CONTINUE
36    CONTINUE
      WRITE (6,56) NF(N),F(I-1),F(I)
37    CONTINUE
C
C     CALCULATION OF ELEMENT AND NODAL STRESSES
C
      CALL STRESS (NPOIN,NP,NELEM,X1,Y1,NPUNCH)
C
C
      STOP
C
38    FORMAT (3I3,2E14.7)
39    FORMAT (5E14.7)
40    FORMAT (15I3)
41    FORMAT (I3,2E14.7)
42    FORMAT (/40X,*INPUT     DATA*,/40X,14(*-*),//)
43    FORMAT (20X,*YOUNG S MODULUS                         =*,E12.5)
44    FORMAT (20X,*POISSON S RATIO                         =*,E12.5)
45    FORMAT (20X,*NUMBER OF PRESCRIBED DISPLACEMENTS      =*,I3)
46    FORMAT (20X,*NUMBER OF NODAL POINTS                  =*,I3)
47    FORMAT (20X,*NUMBER OF ELEMENTS                      =*,I3)
48    FORMAT (20X,*NUMBER OF PRESCRIBED FORCES             =*,I3)
49    FORMAT (20X,*THICKNESS T(*,I1,*)                         =*,E12.5)
50    FORMAT (1H1,/,30X,*ELASTICITY MATRIX*,/30X,17(*-*),///,25X,*D(I,J)
     1=*,//)
51    FORMAT (25X,3(E14.7,2X))
52    FORMAT (1H1)
53    FORMAT (10X,*U(*,I3,*)=*,E14.7,5X,*V(*,I3,*)=*,E14.7)
54    FORMAT (5X,*ELEMENT*,5X,*AREA*/)
55    FORMAT (1H1,10X,*REACTIVE FORCES-*/10X,16(*-*)//,10X,*NODE*,12X,*X
     1-FORCE*,16X,*Y-FORCE*)
56    FORMAT (10X,I3,7X,F15.5,8X,F15.5)
57    FORMAT (//20X,*PRESCRIBED FORCES*,/20X,17(*-*),/20X,*NODE*,12X,*X-
```

E.22

```
     1FORCE*,16X,*Y-FORCE*)
58    FORMAT (21X,I3,2(9X,E14.7))
59    FORMAT (//20X,*PRESCRIBED DISPLACEMENTS*,/20X,24(*-*),/20X,*NODE*,
     19X,*X-DISPLACEMENT*,9X,*Y-DISPLACEMENT*)
60    FORMAT (21X,I3,32X,E14.7)
61    FORMAT (1H1,10X,*NODE*,8X,*X-COORDINATE*,9X,*Y-COORDINATE*/)
62    FORMAT (11X,I3,2(7X,E14.7))
63    FORMAT (20X,*NODAL NUMBERS*,/20X,13(*-*))
64    FORMAT (/10X,*ELEMENT  NODE1  NODE2  NODE3  NODE4  NODE5  NODE6
     1X-CENTROID    Y-CENTROID*)
65    FORMAT (12X,I3,1X,6(4X,I3),2(2X,E12.5))
66    FORMAT (20X,*CENTRIFUGAL FORCE OPTION                =*,I3)
67    FORMAT (20X,*NUMBER OF THICKNESS CHANGES             =*,I3)
68    FORMAT (20X,*DENSITY OF MATERIAL                     =*,E12.5)
69    FORMAT (20X,*SPEED REVS. PER MIN.                    =*,E12.5)
70    FORMAT (20X,*BANDWIDTH                               =*,I3)
71    FORMAT (I3,2E14.7)
      END
```

```
      SUBROUTINE COORD (NPOIN,NELEM)
      COMMON NOD(300,6),Z(175,2),F(350),U(350),SK(46,350),IT(300)
C
C     INPUT OF NODAL NUMBERS AND NNODAL COORDINATES FOR
C     SYSTEM OF TRIM6 ELEMENTS
      DO 1 K=1,NELEM
      READ (5,3) I,(NOD(I,J),J=1,6),IT(I)
1     CONTINUE
      NCOORD=NPOIN
      DO 2 I=1,NCOORD
      READ (5,4) K,Z(K,1),Z(K,2)
2     CONTINUE
      RETURN
C
3     FORMAT (9I3)
4     FORMAT (11X,I3,2(7X,E14.7))
      END

      SUBROUTINE PCMAT (P)
      DIMENSION P(1)
      COMMON /BLK3/ C(6,6),PC(12,2),M
C     TO FORM PRODUCT P*C WHERE ONLY THE LOWER TRIANGLE OF SYMMETRIC
C     MATRIX P IS KNOWN. MATRIX C TO BE DERIVED FROM COMPLETE
C     COEFFICIENT MATRIX CT BY MEANS OF FUNCTION CR
      DO 1 I=1,12
      DO 1 J=1,2
1     PC(I,J)=0.0
      DO 2 I=1,12
      DO 2 J=1,2
      DO 2 K=1,12
      IF (K.LE.I) IK=I*(I-1)/2+K
      IF (K.GT.I) IK=K*(K-1)/2+I
2     PC(I,J)=PC(I,J)+P(IK)*CR(K,J)
      RETURN
      END

      FUNCTION CR (K,J)
      COMMON /BLK3/ C(6,6),PC(12,2),M
C     THIS FUNCTION RETURNS THE ELEMENT CT(K,J)   ,WHERE CT
C     IS THE COMPLETE (12 BY 12) COEFFICIENT MATRIX, BY EXTRACTING
C     THE PROPER ELEMENT FROM MATRIX C
      CR=0.0
      IF (J-2) 1,2,2
1     IF (K.LE.6) CR=C(K,M)
      GO TO 3
2     IF (K.GT.6) CR=C(K-6,M)
3     RETURN
      END
```

```
      SUBROUTINE FEM (X1,Y1,NODE,LL,IBAN)
      DIMENSION X1(1), Y1(1), NODE(1)
      DIMENSION P(78), N1(6), CK(2,2)
      COMMON /BLK2/ D(3,3),DELTA,T
      COMMON /BLK3/ C(6,6),PC(12,2),M
      COMMON NOD(300,6),Z(175,2),F(350),U(350),SK(46,350),IT(300)
C
C
C     (1) CALCULATION OF ELEMENT STIFFNESS MATRICES FOR TRIM 6
C     ELEMENTS
C     (2) ASSEMBLY OF OVERALL STIFFNESS MATRIX
C
C      TRANSFER ORIGIN TO CENTROID OF TRIANGLE
C
      ORX=(X1(1)+X1(2)+X1(3))/3.
      ORY=(Y1(1)+Y1(2)+Y1(3))/3.
      DO 1 I=1,3
      X1(I)=X1(I)-ORX
      Y1(I)=Y1(I)-ORY
1     CONTINUE
      X1(4)=(X1(1)+X1(3))/2.
      X1(5)=(X1(1)+X1(2))/2.
      X1(6)=(X1(2)+X1(3))/2.
      Y1(4)=(Y1(1)+Y1(3))/2.
      Y1(5)=(Y1(1)+Y1(2))/2.
      Y1(6)=(Y1(2)+Y1(3))/2.
      DELTA=1.5*(X1(2)*Y1(3)-X1(3)*Y1(2))
      WRITE (6,16) LL,DELTA
C
C     DEFINE COEFFICIENT MATRIX C
C
      DO 2 I=1,6
      C(I,1)=1.
      C(I,2)=X1(I)
      C(I,3)=Y1(I)
      C(I,4)=X1(I)**2
      C(I,5)=X1(I)*Y1(I)
      C(I,6)=Y1(I)**2
2     CONTINUE
C
      CALL INVMAT (C,6,6,1.0E-12,IERR,N1)
      IF (IERR.NE.0) GO TO 14
C
C      DEFINE LOWER TRIANGLE OF SYMMETRIC MATRIX P
C     P=INTEGRAL OF (Q)(TRANSPOSE)*(D)*(Q) OVER VOLUME OF ELEMENT
C
      DO 3 I=1,78
      P(I)=0.0
3     CONTINUE
      X2=(X1(1)**2+X1(2)**2+X1(3)**2)/12.
      Y2=(Y1(1)**2+Y1(2)**2+Y1(3)**2)/12.
```

```
      XY=(X1(1)*Y1(1)+X1(2)*Y1(2)+X1(3)*Y1(3))/12.
      WRITE (2) ORX,ORY,((C(I,J),J=1,6),I=1,6),(X1(I),Y1(I),I=1,6),DELTA
     1,X2,Y2,XY,(NODE(J),J=1,6)
      P(3)=D(1,1)
      P(5)=D(3,1)
      P(6)=D(3,3)
      P(10)=4.*D(1,1)*X2
      P(14)=2.*D(1,1)*XY+2.*D(3,1)*X2
      P(15)=D(1,1)*Y2+2.*D(1,3)*XY+D(3,3)*X2
      P(19)=4.*D(3,1)*XY
      P(20)=2.*D(3,1)*Y2+2.*D(3,3)*XY
      P(21)=4.*D(3,3)*Y2
      P(30)=D(3,1)
      P(31)=D(3,3)
      P(36)=D(3,3)
      P(38)=D(2,1)
      P(39)=D(2,3)
      P(44)=D(2,3)
      P(45)=D(2,2)
      P(49)=4.*D(3,1)*X2
      P(50)=2.*D(3,1)*XY+2.*D(3,3)*X2
      P(51)=4.*D(3,3)*XY
      P(55)=4.*D(3,3)*X2
      P(59)=2.*D(2,1)*X2+2.*D(3,1)*XY
      P(60)=D(2,3)*X2+(D(3,3)+D(2,1))*XY+D(3,1)*Y2
      P(61)=2.*D(2,3)*XY+2.*D(3,3)*Y2
      P(65)=2.*D(2,3)*X2+2.*D(3,3)*XY
      P(66)=D(2,2)*X2+2.*D(2,3)*XY+D(3,3)*Y2
      P(70)=4.*D(2,1)*XY
      P(71)=2.*D(2,1)*Y2+2.*D(2,3)*XY
      P(72)=4.*D(2,3)*Y2
      P(76)=4.*D(2,3)*XY
      P(77)=2.*D(2,2)*XY+2.*D(2,3)*Y2
      P(78)=4.*D(2,2)*Y2
C
      DO 4 I=1,78
      P(I)=P(I)*DELTA*T
4     CONTINUE
C
C     FORM PRODUCT (P)*(CJ) WHERE CJ IS (12X 2) SUBMATRIX
C     OF COMPLETE COEFFICIENT MATRIX (CT)
C
      DO 11 J=1,6
      JJ=NODE(J)
      IF (JJ.EQ.0) GO TO 11
      M=J
      CALL PCMAT (P)
      DO 10 I=1,6
      II=NODE(I)
      IF (II.EQ.0) GO TO 10
C
```

```
C       FORM PRODUCT (CI)(TRANSPOSE)*(PC)=(CK)
C       WHICH IS (2X2) SUBMATRIX OF OVERALL STIFFNESS MATRIX
C
        M=I
        DO 5 IA=1,2
        DO 5 JA=1,2
        CK(IA,JA)=0.0
        DO 5 KA=1,12
5       CK(IA,JA)=CK(IA,JA)+CR(KA,IA)*PC(KA,JA)
        IF (II.GT.JJ) GO TO 10
C
C       CR(KA,IA) IS A FUNCTION SUBPROGRAM
C
C
C
C       STORE CK(2,2) INTO PROPER LOCATION OF OVERALL STIFFNESS MATRIX SK
C       SK CONTAINS ONLY THE UPPER BAND OF OVERALL STIFFNESS MATRIX
C       OF WHICH THE DIAGONALS ARE STORED AS ROWS IN SK
C
        IK=2*II-1
        DO 9 IA=1,2
        JK=2*JJ-1
        DO 8 JA=1,2
        IF (I.NE.J) GO TC 6
        IF (JA.LT.IA) GO TO 7
6       JM=JK-IK+1
        IF (JM.GT.IBAN) GO TO 13
        SK(JM,IK)=SK(JM,IK)+CK(IA,JA)
7       JK=JK+1
8       CONTINUE
        IK=IK+1
9       CONTINUE
10      CONTINUE
11      CONTINUE
        DO 12 I=4,6
        X1(I)=X1(I)+ORX
        Y1(I)=Y1(I)+ORY
12      CONTINUE
        GO TO 15
13      WRITE (6,18) LL
14      WRITE (6,17) IERR
15      CONTINUE
        RETURN
C
16      FORMAT (5X,I5,5X,E14.7)
17      FORMAT (1H1,10X,*IERR=*,I7)
18      FORMAT (1H1,1X,*JOB ABORTED. BANDWIDTH ERROR FOR ELEMENT NO.*,I5)
        END
```

```
      SUBROUTINE CENT (NODE,X1,Y1,DENS,RPM,NTHICK,T,NELEM)
      DIMENSION NODE(1), X1(1), Y1(1), A(12,2), CTA(12,2), FF(12), T(1)
      COMMON /BLK3/ C(6,6),PC(12,2),M
      COMMON NOD(300,6),Z(175,2),F(350),U(350),SK(46,350),IT(300)
C
C     SUPERPOSITION OF CENTRIFUGAL FORCES
C
      FN1(X)=SM*X**5/5.+B*X**4/4.
      FN2(X)=SM**2*X**5/10.+SM*B*X**4/4.+B**2*X**3/6.
      FN3(X)=SM**3*X**5/15.+SM**2*B*X**4/4.+SM*B**2*X**3/3.+B**3*X**2/6.
      FN4(X)=SM**4*X**5/20.+SM**3*B*X**4/4.+SM**2*B**2*X**3/2.+B**4*X/4.
     1+SM*B**3*X**2/2.
C
C
      REWIND 2
      ZERO=1.0E-10
      PI=2.*ASIN(1.)
      OMEGA=2.*PI*RPM/60.
      GRAVITY=32.2*12.
      FACT=DENS*OMEGA**2/GRAVITY
      DO 1 I=1,12
      DO 1 J=1,2
1     A(I,J)=0.
      DO 9 L=1,NELEM
      READ (2) ORX,ORY,((C(I,J),J=1,6),I=1,6),(X1(I),Y1(I),I=1,6),DELTA,
     1X2,Y2,XY,(NODE(J),J=1,6)
      X3=0.
      X2Y=0.
      XY2=0.
      Y3=0.
      DO 2 I=1,3
      J=I+1
      IF (I.EQ.3) J=1
      DY=Y1(J)-Y1(I)
      DX=X1(J)-X1(I)
      IF (ABS(DX).LE.ZERO) GO TO 2
      SM=DY/DX
      B=Y1(I)-SM*X1(I)
      X3=X3+FN1(X1(I))-FN1(X1(J))
      X2Y=X2Y+FN2(X1(I))-FN2(X1(J))
      XY2=XY2+FN3(X1(I))-FN3(X1(J))
      Y3=Y3+FN4(X1(I))-FN4(X1(J))
2     CONTINUE
      DO 3 K=1,NTHICK
      IF (IT(L).EQ.(K-1)) GO TO 4
3     CONTINUE
4     THICK=T(K)
      FACTOR=FACT*THICK
      A(1,1)=ORX
      A(4,1)=ORX*X2
      A(5,1)=ORX*XY
```

```
      A(6,1)=ORX*Y2
      A(7,1)=ORY
      A(10,1)=ORY*X2
      A(11,1)=ORY*XY
      A(12,1)=ORY*Y2
      DO 5 I=1,12
      A(I,1)=A(I,1)*DELTA
5     CONTINUE
      A(2,2)=X2*DELTA
      A(3,2)=XY*DELTA
      A(4,2)=X3
      A(5,2)=X2Y
      A(6,2)=XY2
      A(8,2)=XY*DELTA
      A(9,2)=Y2*DELTA
      A(10,2)=X2Y
      A(11,2)=XY2
      A(12,2)=Y3
      DO 6 J=1,2
      I=0
      DO 6 M=1,6
      DO 6 N=1,2
      I=I+1
      CTA(I,J)=0.
      DO 6 K=1,12
6     CTA(I,J)=CTA(I,J)+CR(K,N)*A(K,J)
      DO 7 I=1,12
      FF(I)=-(CTA(I,1)+CTA(I,2))*FACTOR
7     CONTINUE
      JJ=0
      DO 8 I=1,6
      II=2*NODE(I)-1
      DO 8 J=1,2
      JJ=JJ+1
      F(II)=F(II)-FF(JJ)
8     II=II+1
9     CONTINUE
      RETURN
C
      END
```

```
      SUBROUTINE STRESS (NPOIN,NP,NELEM,X1,Y1,NPUNCH)
      DIMENSION SIG(300,6,3), UU(12)
      DIMENSION X1(1), Y1(1), NST(10), NNO(10), NODE(6)
      COMMON /BLK3/ C(6,6),PC(12,2),M
      COMMON NOD(300,6),Z(175,2),F(350),U(350),SK(46,350),IT(300)
      EQUIVALENCE (SIG(1),SK(1))
C
C     CENTROIDAL STRESSES
C
      PI=2.*ASIN(1.)
      REWIND 2
      WRITE (6,17)
      WRITE (6,11)
      DO 2 L=1,NELEM
      READ (2) ORX,ORY,((C(I,J),J=1,6),I=1,6),(X1(I),Y1(I),I=1,6),DELTA,
     1X2,Y2,XY,(NODE(J),J=1,6)
      JJ=0
      DO 1 I=1,6
      KK=2*NODE(I)-1
      DO 1 J=1,2
      JJ=JJ+1
      UU(JJ)=U(KK)
      KK=KK+1
    1 CONTINUE
      CALL SIGMA (0.0,0.0,UU,SX,SY,SXY)
      CALL PRINCE (SX,SY,SXY,PI,S1,S2,THETA)
      WRITE (6,12) L,SX,SY,SXY,S1,S2,THETA
    2 CONTINUE
C
C     NODAL STRESSES
C
      WRITE (6,18)
      WRITE (6,20)
      REWIND 2
      DO 4 L=1,NELEM
      READ (2) ORX,ORY,((C(I,J),J=1,6),I=1,6),(X1(I),Y1(I),I=1,6),DELTA,
     1X2,Y2,XY,(NODE(J),J=1,6)
      JJ=0
      DO 3 I=1,6
      KK=2*NODE(I)-1
      DO 3 J=1,2
      JJ=JJ+1
      UU(JJ)=U(KK)
      KK=KK+1
    3 CONTINUE
      DO 4 LI=1,6
      II=NOD(L,LI)
      CALL SIGMA (X1(LI),Y1(LI),UU,SX,SY,SXY)
      WRITE (6,19) L,II,SX,SY,SXY
      SIG(L,LI,1)=SX
      SIG(L,LI,2)=SY
```

```
      SIG(L,LI,3)=SXY
4     CONTINUE
C
C     NODAL AVERAGES
C
      WRITE (6,14)
      WRITE (6,15)
      REWIND 2
      DO 9 I=1,NPOIN
      K=0
      DO 7 L=1,NELEM
      DO 6 J=1,6
      IF (NOD(L,J)-I) 6,5,6
5     K=K+1
      NST(K)=L
      NNO(K)=J
6     CONTINUE
7     CONTINUE
      SX=0.
      SY=0.
      SXY=0.
      DO 8 JJ=1,K
      KK=NST(JJ)
      NN=NNO(JJ)
      SX=SX+SIG(KK,NN,1)
      SY=SY+SIG(KK,NN,2)
      SXY=SXY+SIG(KK,NN,3)
8     CONTINUE
      SX=SX/K
      SY=SY/K
      SXY=SXY/K
      CALL PRINCE (SX,SY,SXY,PI,S1,S2,THETA)
      WRITE (6,12) I,SX,SY,SXY,S1,S2,THETA
      IF (NPUNCH.GT.0) WRITE (7,13) I,SX,SY,SXY,S1,S2,THETA
C
C     RADIAL AND TANGENTIAL STRESSES
C
      ZI1=Z(I,1)
      ZI2=Z(I,2)
      R=SQRT(ZI1**2+ZI2**2)
      IF (R.LE.1.0E-50) R=1.
      COSQ=ZI1/R
      SINQ=ZI2/R
      COS2Q=1.-2.*SINQ*SINQ
      SIN2Q=2.*SINQ*COSQ
      Q1=(SX+SY)/2.
      Q2=(SX-SY)/2.
      Q3=SXY
      Q7=Q2*COS2Q
      Q8=Q3*SIN2Q
      SR=Q1+Q7+Q8
```

```
      SQ=Q1-Q7-Q8
      SRQ=Q3*COS2Q-Q2*SIN2Q
      WRITE (2) I,SR,SQ,SRQ
9     CONTINUE
C
      WRITE (6,16)
      REWIND 2
      DO 10 I=1,NPOIN
      READ (2) J,SR,SQ,SRQ
      IF (NPUNCH.GT.0) WRITE (7,13) J,SR,SQ,SRQ
      WRITE (6,12) J,SR,SQ,SRQ
10    CONTINUE
C
      RETURN
C
11    FORMAT (21X,*ELEMENT*,4X,*SX*,9X,*SY*,8X,*SXY*,9X,*S1*,9X,*S2*,6X,
     1*THETA*/)
12    FORMAT (23X,I3,5(2X,F9.2),2X,F7.3)
13    FORMAT (I3,5(2X,F9.2),2X,F7.3)
14    FORMAT (1H1,40X,*AVERAGE STRESSES AT NODAL POINTS*/41X,32(*-*)/)
15    FORMAT (21X,* NODE  *,4X,*SX*,9X,*SY*,8X,*SXY*,9X,*S1*,9X,*S2*,6X,
     1*THETA*/)
16    FORMAT (1H1,20X,* NODE  *,4X,*SR*,9X,*ST*,8X,*SRT*)
17    FORMAT (1H1,40X,*CENTROIDAL STRESSES*,/41X,19(*-*)/)
18    FORMAT (1H1,25X,*NODAL STRESSES*,/26X,14(*-*)/)
19    FORMAT (22X,I3,4X,I3,3(3X,E12.5))
20    FORMAT (20X,*ELEMENT*,2X,*NODE*,9X,*SX*,14X,*SY*,13X,*SXY*)
      END
```

```
      SUBROUTINE QMAT (X,Y,Q)
      DIMENSION Q(3,12)
C
C     DEFINE AUXILIARY MATRIX Q TO STRESS MATRIX
C
      DO 1  I=1,3
      DO 1  J=1,12
1     Q(I,J)=0.0
      Q(1,2)=1.0
      Q(1,4)=2.*X
      Q(1,5)=Y
      Q(2,9)=1.0
      Q(2,11)=X
      Q(2,12)=2.*Y
      Q(3,3)=1.0
      Q(3,5)=X
      Q(3,6)=2.*Y
      Q(3,8)=1.0
      Q(3,10)=2.*X
      Q(3,11)=Y
      RETURN
      END


      SUBROUTINE QCMAT (Q,QC)
      DIMENSION Q(3,12), QC(3,12)
      COMMON /BLK3/ C(6,6),PC(12,2),M
C
C     DEFINE AUXILIARY MATRIX QC TO STRESS MATRIX
C
      DO 1  I=1,3
      JJ=0
      DO 1  M=1,6
      DO 1  J=1,2
      JJ=JJ+1
      QC(I,JJ)=0.0
      DO 1  K=1,12
      QC(I,JJ)=QC(I,JJ)+Q(I,K)*CR(K,J)
1     CONTINUE
      RETURN
      END
```

```
      SUBROUTINE SIGMA (X,Y,UU,SX,SY,SXY)
      DIMENSION UU(1)
      DIMENSION Q(3,12), QC(3,12), QCU(3)
      COMMON /BLK2/ D(3,3),DELTA,T
      COMMON /BLK3/ C(6,6),PC(12,2),M
C
C     THIS SUBROUTINE CALCULATES THE STRESS AT A POINT WITHIN
C     A TRIM6 ELEMENT, GIVEN THE COORDINATES OF THE POINT AND THE
C     NODAL DISPLACEMENTS OF THE ELEMENT NODES
C
      CALL QMAT (X,Y,Q)
      CALL QCMAT (Q,QC)
      DO 1 I=1,3
      QCU(I)=0.0
      JJ=0
      DO 1 K=1,6
      DO 1 J=1,2
      JJ=JJ+1
      QCU(I)=QCU(I)+QC(I,JJ)*UU(JJ)
1     CONTINUE
      SX=0.
      SY=0.
      SXY=0.
      DO 2 J=1,3
      SX=SX+D(1,J)*QCU(J)
      SY=SY+D(2,J)*QCU(J)
      SXY=SXY+D(3,J)*QCU(J)
2     CONTINUE
      RETURN
      END

      SUBROUTINE PRINCE (SX,SY,SXY,PI,S1,S2,THETA)
C
C     TO FIND PRINCIPAL STRESSES AND PRINCIPAL ANGLE
C     PRINCIPAL ANGLE IS THE ANGLE BETWEEN S1 AND Y-AXIS
C
      Q1=(SX+SY)/2.
      Q2=(SX-SY)/2.
      Q3=SXY
      Q4=SQRT(Q2**2+Q3**2)
      S1=Q1+Q4
      S2=Q1-Q4
      IF (ABS(SXY).GT.1.0E-05) GO TO 1
      THETA=90.
      RETURN
1     THETA=ATAN((S1-SY)/SXY)
      THETA=THETA*180./PI
      RETURN
      END
```

```
      PROGRAM TST(INPUT,OUTPUT,TAPE5=INPUT,TAPE6=OUTPUT,TAPE1,TAPE2,TA
     13,TAPE4,PUNCH,TAPE7=PUNCH)
      DIMENSION X(500,2), NOD(600,3)
      DIMENSION XE(3,2), NF(60), NB(60,2), BV(60,2), NSTART(15), NEND(15
     1), NFIRST(15), NLAST(15), D(3,3)
      COMMON C(6,6),DBA(3,6),DB(3,6),A(6,6),B(3,6)
      COMMON ST(5050),U(700,2),BM(30,30)
C
C     FINITE ELEMENT PROGRAM USING THE METHOD OF PARTITIONS FOR
C     PLANE STRESS OR PLANE STRAIN PROBLEMS
C     IDEALIZATION BY THREE NODAL (TRIM3) TRIANGULAR ELEMENTS
C
C      LIMITING PARAMETERS FOR GIVEN DIMENSIONS
C     NPOIN= 500 (CAN BE INCREASED)
C     NELEM= 600 (CAN BE INCREASED)
C     NPART= 15 (CAN BE INCREASED)
C     MAXIMUM NUMBER OF NODES CONNECTING PARTITIONS = 15
C
C     READING AND PRINTING OF DATA
      READ (5,44) NPART,NPOIN,NELEM,NBOUN,NCOLN,NCONC,NCENT,NPUNCH
      READ (5,45) THICK,DENS,RPM,ANG
      DO 1 I=1,NPART
      READ (5,44) NSTART(I),NEND(I),NFIRST(I),NLAST(I)
    1 CONTINUE
      CALL COORD (NPOIN,NELEM,NOD,X)
      DO 2 I=1,NBOUN
      READ (5,46) NF(I),NB(I,1),NB(I,2),BV(I,1),BV(I,2)
    2 CONTINUE
      WRITE (6,49)
      WRITE (6,50) NPART
      WRITE (6,51) NPOIN
      WRITE (6,52) NELEM
      WRITE (6,53) NBOUN
      WRITE (6,54) NCOLN
      WRITE (6,55) NCONC
      WRITE (6,56) THICK
      WRITE (6,63)
      WRITE (6,65)
      DO 3 I=1,NPART
      WRITE (6,64) I,NSTART(I),NEND(I),NFIRST(I),NLAST(I)
    3 CONTINUE
      WRITE (6,59)
      DO 8 I=1,NBOUN
      IF (NB(I,1)) 7,4,7
    4 IF (NB(I,2)) 7,5,6
    5 WRITE (6,58) NF(I),BV(I,1),BV(I,2)
      GO TO 8
    6 WRITE (6,58) NF(I),BV(I,1)
      GO TO 8
    7 WRITE (6,60) NF(I),BV(I,2)
    8 CONTINUE
```

```
      WRITE (6,57)
      NPOIN2=NPOIN*2
      DO 9 I=1,NPOIN2
      U(I,1)=0.
9     CONTINUE
      DO 14 J=1,NCOLN
      IF (NCONC) 10,14,12
10    DO 11 I=1,NPOIN
      READ (5,45) U(2*I-1,J),U(2*I,J)
      WRITE (6,45) U(2*I-1,J),U(2*I,J)
11    CONTINUE
      GO TO 14
12    CONTINUE
      DO 13 I=1,NCONC
      READ (5,47) K,U(2*K-1,1),U(2*K,1)
      WRITE (6,58) K,U(2*K-1,1),U(2*K,1)
13    CONTINUE
      NCONC=-1
14    CONTINUE
      WRITE (6,61)
      DO 15 I=1,NPOIN
      WRITE (6,62) I,X(I,1),X(I,2)
15    CONTINUE
C
C     SUPERPOSITION OF CENTRIFUGAL FORCES
C
      IF (NCENT.EQ.0) GO TO 16
      CALL CENT (DENS,RPM,THICK,NELEM,NPOIN,NCOLN,X,NOD)
16    CONTINUE
C
C     YOUNG S MODULUS AND POISSON S RATIO FOR STEEL
C
      E=3.0E+07
      P=0.3
C
C     ELASTICITY MATRIX (D) FOR PLAIN STRESS CASE- ISOTROPIC MATERIAL
C
      DO 17 I=1,3
      DO 17 J=1,3
17    D(I,J)=0.0
      E1=E/(1.-P*P)
      D(1,1)=E1
      D(1,2)=E1*P
      D(2,1)=D(1,2)
      D(2,2)=D(1,1)
      D(3,3)=E/2./(1.+P)
C
C     FORMATION OF OVERALL STIFFNESS MATRIX IN TRIDIAGONALIZED
C     PARTITIONS
C
      NFREE=2
```

```
      INTER=0
      REWIND 1
      REWIND 4
      WRITE (6,48)
      DO 42 II=1,NPART
      DO 18 I=1,5050
      ST(I)=0.
18    CONTINUE
      DO 19 I=1,30
      DO 19 J=1,30
19    BM(I,J)=0.0
      NSTRT=NSTART(II)
      NEN=NEND(II)
      K=NFIRST(II)
      L=NLAST(II)
      NK=2*(L-K+1)
      MINUS=K-1
C
C     SEARCH FOR SIZE OF MATRIX BM
C
      I=NEN
      MINOD=NOD(I,1)
      MIN=MINOD
      NCN=MINOD
      IF (II.LT.NPART) GO TO 20
      NCN=0
      GO TO 23
20    KK=0
      DO 22 J=1,3
      IF (NOD(I,J).GT.NCN) NCN=NOD(I,J)
      IF (NOD(I,J).LE.L) GO TO 21
      KK=KK+1
21    IF (NOD(I,J).LT.MIN) MIN=NOD(I,J)
22    CONTINUE
      IF (KK.EQ.0) GO TO 23
      MINOD=MIN
      I=I-1
      GO TO 20
23    CONTINUE
      NCNN=2*(MINOD-K)
      NCN=NCN-L
      NCN=2*NCN
      IF (NCN.LE.0) NCN=1
      NCK=NK-NCNN
      IF (NCN.GT.30) GO TO 24
      IF (NCK.LE.30) GO TO 25
24    WRITE (6,43) NCK,NCN
      STOP
25    CONTINUE
      DO 32 LK=NSTRT,NEN
      MM=LK-INTER
```

```
      DO 26 I=1,3
      JJ=NOD(LK,I)
      XE(I,1)=X(JJ,1)
      XE(I,2)=X(JJ,2)
26    CONTINUE
C
C     CALCULATION OF ELEMENT STIFFNESS AND STRESS MATRICES
C
      CALL FEM (XE,D,ANG,THICK,MM)
      DO 32 LL=1,3
      DO 32 KK=1,3
      IF (NOD(LK,KK)-K) 32,27,27
27    IF (NOD(LK,KK)-L) 28,28,32
28    M=NFREE*(NOD(LK,KK)-K)
      N=NFREE*(NOD(LK,LL)-K)
      I=NFREE*(KK-1)
      J=NFREE*(LL-1)
      IF (N) 32,29,29
29    DO 31 NJ=1,NFREE
      DO 31 MI=1,NFREE
      MMI=M+MI
      NNJ=N+NJ
      IMI=I+MI
      JNJ=J+NJ
      IF (NNJ.GT.NK) GO TO 30
      IF (MMI.LT.NNJ) GO TO 31
      IJ=MMI*(MMI-1)/2+NNJ
      ST(IJ)=ST(IJ)+C(IMI,JNJ)
      GO TO 31
30    NNJ=NNJ-NK
      MMI=MMI-NCNN
      BM(MMI,NNJ)=BM(MMI,NNJ)+C(IMI,JNJ)
31    CONTINUE
32    CONTINUE
C
C     INTRODUCTION OF PRESCRIBED DISPLACEMENTS
C
      DO 38 I=1,NBOUN
      M=NF(I)-K
      MM=NF(I)-1
      IF (M) 38,33,33
33    IF (NF(I)-L) 34,34,38
34    DO 37 J=1,NFREE
      IF (NB(I,J)) 37,35,37
35    NMI=NFREE*M+J
      IJ=NMI*(NMI-1)/2+NMI
      ST(IJ)=ST(IJ)*1.0E+15
      DO 36 JJ=1,NCOLN
      JNJ=NFREE*MM+J
      U(JNJ,JJ)=ST(IJ)*BV(I,J)
36    CONTINUE
```

```
37    CONTINUE
38    CONTINUE
      INTER=NEN
      MI=NFREE*MINUS+1
      NJ=NFREE*L
      M=NJ-MI+1
      IF (II-NPART) 39,40,39
39    NA=NFREE*(NLAST(II+1)-MINUS)
      GO TO 41
40    NA=M+1
41    N=NA-M
      MM=M+1
      NST=M*(M+1)/2
      NCK=M-NCNN
      WRITE (4) M,N,NST,NCN,NCNN,NCK,(ST(I),I=1,NST),((BM(I,J),I=1,NCK),
     1J=1,NCN),((U(I,J),I=MI,NJ),J=1,NCOLN)
42    CONTINUE
      REWIND 1
      REWIND 2
      REWIND 3
      REWIND 4
C
C     SOLUTION OF TRIDIAGONAL SYSTEM OF SUBMATRIX EQUATIONS
C
      CALL SOLVE (NPART,NCOLN)
      REWIND 3
C
C     CALCULATION OF STRESSES
C
      CALL STRESS (NPART,NFIRST,NLAST,NCOLN,NELEM,NOD,NFREE,NPOIN,NPUNCH
     1)
C
C
      STOP
C
43    FORMAT (1H1,*SPACE FOR BM TOO SMALL , VARIABLES ARE*,2I5)
44    FORMAT (9I3)
45    FORMAT (4E14.7)
46    FORMAT (3I3,2E14.7)
47    FORMAT (I3,2E14.7)
48    FORMAT (1H1)
49    FORMAT (/21X,*INPUT DATA*,/21X,10(*-*)//)
50    FORMAT (10X,*TOTAL NUMBER OF PARTITIONS- NPART=*,8X,I3)
51    FORMAT (10X,*TOTAL NUMBER OF NODAL POINTS- NPOIN=*,6X,I3)
52    FORMAT (10X,*TOTAL NUMBER OF ELEMENTS- NELEM=*,10X,I3)
53    FORMAT (10X,*TOTAL NUMBER OF NODAL POINTS WITH *,/15X,*PRESCRIBED
     1DISPLACEMENTS- NBOUN=*,5X,I3)
54    FORMAT (10X,*TOTAL NUMBER OF LOAD VECTORS- NCOLN=*,6X,I3)
55    FORMAT (10X,*NUMBER OF POINTS WITH CONCENTRATED LOADS=*,1X,I3)
56    FORMAT (10X,*PLANE THICKNESS- THICK=*,19X,E14.7)
57    FORMAT (//10X,*PRESCRIBED FORCES*,/10X,17(*-*),/10X,*NODE*,12X,*X-
```

```
     1FORCE*,16X,*Y-FORCE*)
58    FORMAT (11X,I3,2(9X,E14.7))
59    FORMAT (//10X,*PRESCRIBED DISPLACEMENTS*,/10X,24(*-*),/10X,*NODE*,
     19X,*X-DISPLACEMENT*,9X,*Y-DISPLACEMENT*)
60    FORMAT (11X,I3,32X,E14.7)
61    FORMAT (1H1,10X,*NODE*,8X,*X-COORDINATE*,9X,*Y-COORDINATE*/)
62    FORMAT (11X,I3,2(7X,E14.7))
63    FORMAT (//10X,*PARTITION  1ST ELEMENT  LAST ELEMENT  1ST NODE  LAS
     1T NODE*)
64    FORMAT (12X,I3,12X,I3,11X,I3,7X,I3,8X,I3)
65    FORMAT (10X,*---------  ----------  -----------  --------  -----
     1----*)
      END
```

```
      SUBROUTINE COORD (NPOIN,NELEM,NOD,X)
      DIMENSION X(500,2), NOD(600,3)
C
C     INPUT OF NODAL NUMBERS AND NODAL COORDINATES
C      FOR SYSTEM OF TRIM3 ELEMENTS
C
      DO 1 I=1,NELEM
      READ (5,3) K,(NOD(K,J),J=1,3)
1     CONTINUE
      DO 2 J=1,NPOIN
      READ (5,4) X(J,1),X(J,2)
2     CONTINUE
C
      RETURN
C
3     FORMAT (4(2X,I3))
4     FORMAT (3X,2E14.7)
      END


      SUBROUTINE PRIN (D,C,N)
C * * * * * * * * * * * * * * * * * * * * * *
C     SUBROUTINE  FOR CALCULATION OF PRINCIPAL STRESSES OF ELEMENTS
C     PRINCIPAL ANGLE IS THE ANGLE BETWEEN Y AXIS AND STRESS-1
C * * * * * * * * * * * * * * * * * * * * * *
      DIMENSION D(3,6), C(6,6)
      DO 1 J=1,N
      C(1,J)=(D(1,J)+D(2,J))*.5+SQRT((D(1,J)-D(2,J))**2/4.+D(3,J)**2)
      C(2,J)=(D(1,J)+D(2,J))*.5-SQRT((D(1,J)-D(2,J))**2/4.+D(3,J)**2)
      C(3,J)=57.3*ATAN((C(1,J)-D(2,J))/D(3,J))
1     CONTINUE
      RETURN
      END
```

```
      SUBROUTINE CENT (DENS,RPM,THICK,NELEM,NPOIN,NCOLN,Z,NOD)
      DIMENSION NODE(3), X(3), Y(3), B(3), C(3), Z(NPOIN,2), NOD(NELEM,3
     1)
      COMMON E(6,6),DBA(3,6),DB(3,6),A(6,6),G(3,6)
      COMMON ST(5050),U(700,2),BM(30,30)
      REAL IX,IY,IXY
C
C     SUPERPOSITION OF CENTRIFUGAL FORCES
C
      PI=2.*ASIN(1.)
      OMEGA=2.*PI*RPM/60.
      GRAVITY=32.2*12.
      FACTOR=DENS*THICK*OMEGA**2/GRAVITY
      DO 4 I=1,NELEM
      DO 1 J=1,3
      K=NOD(I,J)
      NODE(J)=K
      X(J)=Z(K,1)
      Y(J)=Z(K,2)
1     CONTINUE
      ORX=(X(1)+X(2)+X(3))/3.
      ORY=(Y(1)+Y(2)+Y(3))/3.
      DO 2 K=1,3
      X(K)=X(K)-ORX
      Y(K)=Y(K)-ORY
2     CONTINUE
      DELTA=1.5*(X(2)*Y(3)-X(3)*Y(2))
      IX=(X(1)**2+X(2)**2+X(3)**2)/12.
      IY=(Y(1)**2+Y(2)**2+Y(3)**2)/12.
      IXY=(X(1)*Y(1)+X(2)*Y(2)+X(3)*Y(3))/12.
      B(1)=Y(2)-Y(3)
      B(2)=Y(3)-Y(1)
      B(3)=Y(1)-Y(2)
      C(1)=X(3)-X(2)
      C(2)=X(1)-X(3)
      C(3)=X(2)-X(1)
      FXA=-FACTOR*ORX*DELTA/3.
      FYA=-FACTOR*ORY*DELTA/3.
      DO 3 J=1,3
      FXB=-FACTOR/2.*(B(J)*IX+C(J)*IXY)
      FYB=-FACTOR/2.*(B(J)*IXY+C(J)*IY)
      FX=FXA+FXB
      FY=FYA+FYB
      JJ=2*NODE(J)-1
      DO 3 K=1,NCOLN
      U(JJ,K)=U(JJ,K)-FX
3     U(JJ+1,K)=U(JJ+1,K)-FY
4     CONTINUE
      RETURN
      END
```

```
      SUBROUTINE FEM (XE,D,ANG,TH,MM)
      DIMENSION D(3,3), BTDBA(6,6), XE(3,2), R(3,3), ZX(3), ZY(3), R1(3,
     13)
      COMMON C(6,6),DBA(3,6),DB(3,6),A(6,6),B(3,6)
      COMMON ST(5050),U(700,2),BM(30,30)
C
C     CALCULATION OF ELEMENT STIFFNESS AND STRESS MATRICES
C
      DO 2 J=1,6
      DO 1 I=1,3
      B(I,J)=0.
      DB(I,J)=0.
      DBA(I,J)=0.
1     CONTINUE
      DO 2 I=1,6
      A(I,J)=0.
      BTDBA(I,J)=0.
2     C(I,J)=0.
      DO 3 J=1,3
      DO 3 I=1,3
3     R(I,J)=0.
      ORX=(XE(1,1)+XE(2,1)+XE(3,1))*.333333
      ORY=(XE(1,2)+XE(2,2)+XE(3,2))*.333333
      DO 4 I=1,3
      XE(I,1)=XE(I,1)-ORX
      XE(I,2)=XE(I,2)-ORY
4     CONTINUE
      ZX(1)=XE(2,2)-XE(3,2)
      ZX(2)=XE(3,2)-XE(1,2)
      ZX(3)=XE(1,2)-XE(2,2)
      ZY(1)=XE(3,1)-XE(2,1)
      ZY(2)=XE(1,1)-XE(3,1)
      ZY(3)=XE(2,1)-XE(1,1)
      ZK=XE(2,1)*XE(3,2)-XE(3,1)*XE(2,2)
      Z=3.*ZK
      A(1,1)=ZK/Z
      A(2,1)=ZX(1)/Z
      A(3,1)=ZY(1)/Z
      A(4,2)=A(1,1)
      A(5,2)=A(2,1)
      A(6,2)=A(3,1)
      A(1,3)=ZK/Z
      A(2,3)=ZX(2)/Z
      A(3,3)=ZY(2)/Z
      A(4,4)=A(1,3)
      A(5,4)=A(2,3)
      A(6,4)=A(3,3)
      A(1,5)=ZK/Z
      A(2,5)=ZX(3)/Z
      A(3,5)=ZY(3)/Z
      A(4,6)=A(1,5)
```

```
      A(5,6)=A(2,5)
      A(6,6)=A(3,5)
      B(1,2)=1.
      B(3,3)=1.
      B(3,5)=1.
      B(2,6)=1.
      IF (ANG) 5,8,5
5     CS=COS(ANG*.017453)
      SS=SIN(ANG*.017453)
      R(1,1)=CS**2
      R(2,1)=SS**2
      R(3,1)=SS*CS
      R(1,2)=R(2,1)
      R(2,2)=R(1,1)
      R(3,2)=-R(3,1)
      R(1,3)=2.*R(3,2)
      R(2,3)=2.*R(3,1)
      R(3,3)=R(1,1)-R(2,1)
      DO 6 J=1,3
      DO 6 I=1,3
      R1(I,J)=0.
      DO 6 K=1,3
6     R1(I,J)=R1(I,J)+D(I,K)*R(J,K)
      DO 7 J=1,3
      DO 7 I=1,3
      D(I,J)=0.
      DO 7 K=1,3
7     D(I,J)=D(I,J)+R(I,K)*R1(K,J)
8     DO 9 J=1,6
      DO 9 I=1,3
      DO 9 K=1,3
9     DB(I,J)=DB(I,J)+D(I,K)*B(K,J)
      DO 10 J=1,6
      DO 10 I=1,3
      DO 10 K=1,6
10    DBA(I,J)=DBA(I,J)+DB(I,K)*A(K,J)
C
C     STRESS MATRIX IS FORMED
C
      IF (MM) 12,12,11
11    WRITE (1) ((DBA(I,J),I=1,3),J=1,6),ORX,ORY
12    CONTINUE
      VOL=.5*TH*Z
      DO 13 J=1,6
      DO 13 I=1,6
      DO 13 K=1,3
13    BTDBA(I,J)=BTDBA(I,J)+B(K,I)*DBA(K,J)*VOL
      DO 14 J=1,6
      DO 14 I=1,6
      DO 14 K=1,6
14    C(I,J)=C(I,J)+A(K,I)*BTDBA(K,J)
```

```
C
C     STIFFNESS MATRIX C IS FORMED
C
      RETURN
      END


      SUBROUTINE STRESS (NPART,NFIRST,NLAST,NCOLN,NELEM,NOD,NFREE,NPOIN,
     1NPUNCH)
      DIMENSION NOD(600,3), NFIRST(15), NLAST(15)
      COMMON C(6,6),DBA(3,6),DB(3,6),A(6,6),B(3,6)
      COMMON ST(5050),U(700,2),BM(30,30)
C
C     SUBROUTINE FOR CALCULATION OF STRESSES
C
      DO 1 II=1,NPART
      JJ=NPART+1-II
      M=NFREE*(NFIRST(JJ)-1)+1
      N=NFREE*NLAST(JJ)
      READ (3) ((U(I,J),I=M,N),J=1,NCOLN)
1     CONTINUE
      WRITE (6,9)
      WRITE (6,11)
      WRITE (6,10) ((I,U(2*I-1,J),U(2*I,J),I=1,NPOIN),J=1,NCOLN)
      IF (NPUNCH.GT.0) WRITE (7,7) ((I,U(2*I-1,J),U(2*I,J),I=1,NPOIN),J=
     11,NCOLN)
      WRITE (6,9)
      WRITE (6,12)
      DO 4 LL=1,NELEM
      READ (1) (((DBA(I,J),I=1,3),J=1,6),ORX,ORY)
      DO 2 J=1,NCOLN
      DO 2 I=1,3
      JJ=NOD(LL,I)
      C(2*I-1,J)=U(2*JJ-1,J)
2     C(2*I,J)=U(2*JJ,J)
      DO 3 J=1,NCOLN
      DO 3 I=1,3
      DB(I,J)=0.
      DO 3 K=1,6
3     DB(I,J)=DB(I,J)+DBA(I,K)*C(K,J)
      CALL PRIN (DB,A,NCOLN)
      WRITE (6,6) LL,((DB(I,J),I=1,3),(A(I,J),I=1,3),J=1,NCOLN)
      IF (NPUNCH.GT.0) WRITE (7,8) LL,((DB(I,J),I=1,3),(A(I,J),I=1,3),J=
     11,NCOLN)
      IF (NCOL.GT.1) GO TO 4
C
C     RADIAL AND TANGENTIAL STRESSES
C
      SX=DB(1,1)
      SY=DB(2,1)
```

```
      SXY=DB(3,1)
      ZI1=ORX
      ZI2=ORY
      R=SQRT(ZI1**2+ZI2**2)
      IF (R.LE.1.0E-50) R=1.
      SINQ=ZI2/R
      COSQ=ZI1/R
      COS2Q=1.-2.*SINQ*SINQ
      SIN2Q=2.*SINQ*COSQ
      Q1=(SX+SY)/2.
      Q2=(SX-SY)/2.
      Q3=SXY
      Q7=Q2*COS2Q
      Q8=Q3*SIN2Q
      SR=Q1+Q7+Q8
      SQ=Q1-Q7-Q8
      SRT=Q3*COS2Q-Q2*SIN2Q
      ST(LL)=SR
      ST(LL+NELEM)=SQ
      ST(LL+2*NELEM)=SRT
4     CONTINUE
      WRITE (6,9)
      WRITE (6,13)
      LL=NELEM
      DO 5 I=1,NELEM
      WRITE (6,6) I,ST(I),ST(I+LL),ST(I+2*LL)
      IF (NPUNCH.GT.0) WRITE (7,7) I,ST(I),ST(I+LL),ST(I+2*LL)
5     CONTINUE
C
C
      RETURN
C
6     FORMAT (23X,I3,5(2X,F9.2),2X,F7.3)
7     FORMAT (I3,2E14.7)
8     FORMAT (I3,5(2X,F9.2),2X,F7.3)
9     FORMAT (1H1)
10    FORMAT (40X,I4,2(3X,E16.8))
11    FORMAT (39X,* NODE*,3X,* X-DISPLACEMENT *,2X,* Y-DISPLACEMENT*)
12    FORMAT (21X,*ELEMENT*,4X,*SX*,9X,*SY*,8X,*SXY*,9X,*S1*,9X,*S2*,6X,
     1*THETA*/)
13    FORMAT (21X,*ELEMENT*,4X,*SR*,9X,*ST*,8X,*SRT*/)
      END
```

```
      SUBROUTINE SOLVE (NPART,NCOLN)
      DIMENSION AM(5050), YM(465), TF(100,2), F(100,2), DIS(100,2)
      DIMENSION PYM(100,30)
      COMMON C(6,6),DBA(3,6),DB(3,6),A(6,6),B(3,6)
      COMMON ST(5050),U(700,2),BM(30,30)
      EQUIVALENCE (AM(1),ST(1))
      EQUIVALENCE (TF(1),U(1))
      EQUIVALENCE (DIS(1),U(201))
      EQUIVALENCE (YM(1),U(401))
      EQUIVALENCE (F(1),PYM(1))
C
C     SUBROUTINE FOR SOLUTION OF EQUATIONS.
C
      DO 1 I=1,100
      DO 1 J=1,NCOLN
1     TF(I,J)=0.
      NYM=30*(30+1)/2
      DO 2 I=1,NYM
      YM(I)=0.
2     CONTINUE
      DO 11 LL=1,NPART
      READ (4) M,N,NST,NCN,NCNN,NCK,(AM(I),I=1,NST),((BM(I,J),I=1,NCK),J
     1=1,NCN),((F(I,J),I=1,M),J=1,NCOLN)
      DO 4 I=1,M
      DO 3 J=1,NCOLN
      F(I,J)=F(I,J)-TF(I,J)
3     CONTINUE
4     CONTINUE
      DO 5 I=1,NYM
      AM(I)=AM(I)-YM(I)
5     CONTINUE
      CALL INVSYM (AM,M,IERR)
      IF (IERR.NE.0) STOP
      WRITE (2) M,N,NST,NCN,NCNN,NCK,(AM(I),I=1,NST),((BM(I,J),I=1,NCK),
     1J=1,NCN),((F(I,J),I=1,M),J=1,NCOLN)
      IF (NPART-LL) 12,12,6
6     CALL MATM (AM,F,DIS,M,NCOLN)
      CALL MATTM (BM,DIS,TF,N,M,NCOLN,NCN,NCNN)
      DO 7 J=1,NCN
      DO 7 I=1,M
      PYM(I,J)=0.
      DO 7 K=1,M
      IF (K.LE.I) IK=I*(I-1)/2+K
      IF (K.GT.I) IK=K*(K-1)/2+I
      BMATT=BMAT(K,J,BM,NCN,M,NCNN)
7     PYM(I,J)=PYM(I,J)+AM(IK)*BMATT
      DO 10 I=1,NCN
      DO 9 J=1,NCN
      IF (I.LT.J) GO TO 9
      IJ=I*(I-1)/2+J
      YM(IJ)=0.
```

```
      DO 8 K=1,M
      BMATT=BMAT(K,I,BM,NCN,M,NCNN)
      YM(IJ)=YM(IJ)+BMATT*PYM(K,J)
8     CONTINUE
9     CONTINUE
10    CONTINUE
      NYM=NCN*(NCN+1)/2
11    CONTINUE
12    REWIND 4
      CALL MATM (AM,F,DIS,M,NCOLN)
      WRITE (3) ((DIS(I,J),I=1,M),J=1,NCOLN)
      IF (NPART-1) 17,17,13
13    NA=NPART-1
      DO 16 LL=1,NA
      BACKSPACE 2
      BACKSPACE 2
      READ (2) M,N,NST,NCN,NCNN,NCK,(AM(I),I=1,NST),((BM(I,J),I=1,NCK),J
     1=1,NCN),((F(I,J),I=1,M),J=1,NCOLN)
      DO 14 J=1,NCOLN
      DO 14 I=1,M
      TF(I,J)=0.
      DO 14 K=1,N
      BMATT=BMAT(I,K,BM,NCN,M,NCNN)
14    TF(I,J)=TF(I,J)+BMATT*DIS(K,J)
      DO 15 J=1,NCOLN
      DO 15 I=1,M
15    F(I,J)=F(I,J)-TF(I,J)
      CALL MATM (AM,F,DIS,M,NCOLN)
      WRITE (3) ((DIS(I,J),I=1,M),J=1,NCOLN)
16    CONTINUE
17    CONTINUE
      RETURN
      END
```

```
      FUNCTION BMAT (I,J,BM,NCN,M,NCNN)
      DIMENSION BM(30,30)
      BMAT=0.
      IF (I.LE.NCNN) RETURN
      IF (J.GT.NCN) RETURN
      II=I-NCNN
      BMAT=BM(II,J)
      RETURN
      END


      SUBROUTINE MATM (D,B,DB,M,NCOLN)
      DIMENSION D(1), B(100,2), DB(100,2)
      DO 1 J=1,NCOLN
      DO 1 I=1,M
      DB(I,J)=0.
      DO 1 K=1,M
      IF (K.LE.I) IK=I*(I-1)/2+K
      IF (K.GT.I) IK=K*(K-1)/2+I
    1 DB(I,J)=DB(I,J)+D(IK)*B(K,J)
      RETURN
      END


      SUBROUTINE MATTM (BM,DIS,TF,N,M,NCOLN,NCN,NCNN)
      DIMENSION BM(30,30), DIS(100,2), TF(100,2)
      DO 1 J=1,NCOLN
      DO 1 I=1,N
      TF(I,J)=0.
      DO 1 K=1,M
      BMATT=BMAT(K,I,BM,NCN,M,NCNN)
    1 TF(I,J)=TF(I,J)+BMATT*DIS(K,J)
      RETURN
      END
```

```
      PROGRAM TST(INPUT,OUTPUT,TAPE5=INPUT,TAPE6=OUTPUT,TAPE1,TAPE2,TA
     13,TAPE4,PUNCH,TAPE7=PUNCH)
      DIMENSION X(500,2), NOD(300,6)
      DIMENSION NODE(6), X1(6), Y1(6), C(12,12)
      DIMENSION NF(60), NB(60,2), BV(60,2)
      DIMENSION NSTART(25), NEND(25), NFIRST(25), NLAST(25)
      COMMON ST(5050),PYM(100,60),U(700,2),BM(40,60)
      COMMON /BLK2/ D(3,3),DELTA
      COMMON /BLK5/ NPUNCH
      DATA IBM,JBM/40,60/
C
C     FINITE ELEMENT PROGRAM USING THE METHOD OF PARTITIONS
C     FOR PLANE STRESS OR PLANE STRAIN PROBLEMS,
C     IDEALIZATION BY SIX NODAL (TRIM6) ELEMENTS.
C
C     LIMITING PARAMETERS FOR DIMENSIONS PROVIDED-
C     NPOIN = 500 (CAN BE INCREASED)
C     NELEM= 300 (CAN BE INCREASED)
C     NUMBER OF NODES PER PARTITION = 50 (MAXIMUM)
C     NUMBER OF NODES CONNECTING PARTITIONS = 20 (MAXIMUM)
C
C     READING AND PRINTING OF DATA
C
      READ (5,49) NPART,NPOIN,NELEM,NBOUN,NCOLN,NCONC,NCENT,NPUNCH
      READ (5,50) THICK,DENS,RPM
      DO 1 I=1,NPART
      READ (5,49) NSTART(I),NEND(I),NFIRST(I),NLAST(I)
1     CONTINUE
      CALL COORD (NPOIN,NELEM,NOD,X)
      DO 2 I=1,NBOUN
      READ (5,51) NF(I),NB(I,1),NB(I,2),BV(I,1),BV(I,2)
2     CONTINUE
C
C     YOUNG S MODULUS AND POISSON S RATIO FOR STEEL
C
      E=3.0E+07
      P=0.3
C
      WRITE (6,54)
      WRITE (6,55) NPART
      WRITE (6,56) NPOIN
      WRITE (6,57) NELEM
      WRITE (6,58) NBOUN
      WRITE (6,59) NCOLN
      WRITE (6,60) NCONC
      WRITE (6,61) THICK
      WRITE (6,77) NCENT
      WRITE (6,78) E
      WRITE (6,79) P
      WRITE (6,80) DENS
      WRITE (6,81) RPM
```

```
      WRITE (6,68)
      WRITE (6,70)
      DO 3 I=1,NPART
      WRITE (6,69) I,NSTART(I),NEND(I),NFIRST(I),NLAST(I)
3     CONTINUE
      WRITE (6,64)
      DO 8 I=1,NBOUN
      IF (NB(I,1)) 7,4,7
4     IF (NB(I,2)) 7,5,6
5     WRITE (6,63) NF(I),BV(I,1),BV(I,2)
      GO TO 8
6     WRITE (6,63) NF(I),BV(I,1)
      GO TO 8
7     WRITE (6,65) NF(I),BV(I,2)
8     CONTINUE
      WRITE (6,62)
      NPOIN2=NPOIN*2
      DO 9 I=1,NPOIN2
      U(I,1)=0.
9     CONTINUE
      DO 14 J=1,NCOLN
      IF (NCONC) 10,14,12
10    DO 11 I=1,NPOIN
      READ (5,50) U(2*I-1,J),U(2*I,J)
      WRITE (6,50) U(2*I-1,J),U(2*I,J)
11    CONTINUE
      GO TO 14
12    CONTINUE
      DO 13 I=1,NCONC
      READ (5,52) K,U(2*K-1,1),U(2*K,1)
      WRITE (6,63) K,U(2*K-1,1),U(2*K,1)
13    CONTINUE
      NCONC=-1
14    CONTINUE
      WRITE (6,73)
      WRITE (6,74)
      WRITE (6,75)
      DO 16 L=1,NELEM
      ORX=0.0
      ORY=0.0
      DO 15 I=1,3
      II=NOD(L,I)
      ORX=ORX+X(II,1)/3.
      ORY=ORY+X(II,2)/3.
15    CONTINUE
      WRITE (6,76) L,(NOD(L,J),J=1,6),ORX,ORY
16    CONTINUE
C
C     ELASTICITY MATRIX (D) FOR PLAIN STRESS CASE- ISOTROPIC MATERIAL
C
      DO 17 I=1,3
```

```
      DC 17 J=1,3
17    D(I,J)=0.0
      E1=E/(1.-P*P)
      D(1,1)=E1
      D(1,2)=E1*P
      D(2,1)=D(1,2)
      D(2,2)=D(1,1)
      D(3,3)=E/2./(1.+P)
C
C     FORMATION OF SUEMATRICES OF OVERALL STIFFNESS MATRIX
C     AND FORCE MATRIX
C
      NFREE=2
      INTER=0
      REWIND 1
      REWIND 4
      WRITE (6,53)
      DC 45 II=1,NPART
      DC 18 I=1,5050
      ST(I)=0.
18    CCNTINUE
      DC 19 I=1,IBM
      DC 19 J=1,JBM
19    BM(I,J)=0.0
      NSTRT=NSTART(II)
      NEN=NEND(II)
      K=NFIRST(II)
      L=NLAST(II)
      NK=2*(L-K+1)
      MINUS=K-1
C
C     SEARCH FOR SIZE CF MATRIX BM
C
      I=NEN
      MINOD=NOD(I,1)
      MIN=MINOD
      NCN=MINOD
      IF (II.LT.NPART) GO TO 20
      NCN=0
      GC TO 23
20    KK=0
      DC 22 J=1,6
      IF (NOD(I,J).GT.NCN) NCN=NOD(I,J)
      IF (NOD(I,J).LE.L) GO TO 21
      KK=KK+1
21    IF (NOD(I,J).LT.MIN) MIN=NOD(I,J)
22    CCNTINUE
      IF (KK.EQ.0) GC TO 23
      MINOD=MIN
      I=I-1
      GO TO 20
```

```
23    CONTINUE
      NCNN=2*(MINOD-K)
      NCN=NCN-L
      NCN=2*NCN
      IF (NCN.LE.0) NCN=1
      NCK=NK-NCNN
      IF (NCN.GT.JBM) GO TO 24
      IF (NCK.LE.IBM) GO TO 25
24    WRITE (6,48) NCK,NCN
      STOP
25    CONTINUE
      DO 35 LK=NSTRT,NEN
      MM=LK-INTER
      DO 26 I=1,3
      JJ=NOD(LK,I)
      NODE(I)=JJ
      X1(I)=X(JJ,1)
      Y1(I)=X(JJ,2)
26    CONTINUE
      DO 27 I=4,6
      JJ=NOD(LK,I)
      NODE(I)=JJ
27    CONTINUE
C
C     CALCULATION OF ELEMENT STIFFNESS AND STRESS MATRICES
C
      CALL FEM (X1,Y1,THICK,MM,NODE,C)
C
C     SUPERPOSITION OF CENTRIFUGAL FORCES
C
      IF (MM.LE.0) GO TO 29
      DO 28 I=4,6
      J=NODE(I)
      X(J,1)=X1(I)
      X(J,2)=Y1(I)
28    CONTINUE
      IF (NCENT.EQ.0) GO TO 29
      CALL CENT (DENS,RPM,THICK,NELEM,NPOIN,NCOLN,NODE,X1,Y1)
29    CONTINUE
      DO 35 LL=1,6
      DO 35 KK=1,6
      IF (NOD(LK,KK)-K) 35,30,30
30    IF (NOD(LK,KK)-L) 31,31,35
31    M=NFREE*(NOD(LK,KK)-K)
      N=NFREE*(NOD(LK,LL)-K)
      I=NFREE*(KK-1)
      J=NFREE*(LL-1)
      IF (N) 35,32,32
32    DO 34 NJ=1,NFREE
      DO 34 MI=1,NFREE
      MMI=M+MI
```

```
      NNJ=N+NJ
      IMI=I+MI
      JNJ=J+NJ
      IF (NNJ.GT.NK) GC TO 33
      IF (MMI.LT.NNJ) GC TO 34
      IJ=MMI*(MMI-1)/2+NNJ
      ST(IJ)=ST(IJ)+C(IMI,JNJ)
      GC TO 34
33    NNJ=NNJ-NK
      MMI=MMI-NCNN
      BM(MMI,NNJ)=BM(MMI,NNJ)+C(IMI,JNJ)
34    CCNTINUE
35    CCNTINUE
C
C     INTRODUCTION OF PRESCRIBED DISPLACEMENTS
C
      DC 41 I=1,NBOUN
      M=NF(I)-K
      MM=NF(I)-1
      IF (M) 41,36,36
36    IF (NF(I)-L) 37,37,41
37    DC 40 J=1,NFREE
      IF (NB(I,J)) 40,38,40
38    NMI=NFREE*M+J
      IJ=NMI*(NMI-1)/2+NMI
      ST(IJ)=ST(IJ)*1.0E+15
      DC 39 JJ=1,NCOLN
      JNJ=NFREE*MM+J
      U(JNJ,JJ)=ST(IJ)*BV(I,J)
39    CONTINUE
40    CONTINUE
41    CCNTINUE
      INTER=NEN
      MI=NFREE*MINUS+1
      NJ=NFREE*L
      M=NJ-MI+1
      IF (II-NPART) 42,43,42
42    NA=NFREE*(NLAST(II+1)-MINUS)
      GC TO 44
43    NA=M+1
44    N=NA-M
      MM=M+1
      NST=M*(M+1)/2
      NCK=M-NCNN
      WRITE (4) M,N,NST,NCN,NCNN,NCK,(ST(I),I=1,NST),((BM(I,J),I=1,NCK),
     1J=1,NCN),((U(I,J),I=MI,NJ),J=1,NCOLN)
45    CONTINUE
      WRITE (6,66)
      DO 46 I=1,NPOIN
      WRITE (6,67) I,X(I,1),X(I,2)
46    CCNTINUE
```

```
      REWIND 1
      REWIND 2
      REWIND 3
      REWIND 4
C
C     SOLUTION OF TRIDIAGONAL SYSTEM OF SUBMATRIX EQUATIONS
C
      CALL SOLVE (NPART,NCOLN,IBM,JBM)
      REWIND 3
      DO 47 II=1,NPART
      JJ=NPART+1-II
      M=NFREE*(NFIRST(JJ)-1)+1
      N=NFREE*NLAST(JJ)
      READ (3) ((U(I,J),I=M,N),J=1,NCOLN)
47    CONTINUE
      WRITE (6,53)
      WRITE (6,72)
      WRITE (6,71) ((I,U(2*I-1,J),U(2*I,J),I=1,NPOIN),J=1,NCOLN)
C
C     CALCULATION OF STRESSES
C
      CALL STRESS (NPOIN,NELEM,X1,Y1,NODE,NCOLN,NOD,X)
C
C
      STOP
C
48    FORMAT (1H1,*SPACE FOR BM TOO SMALL , VARIABLES ARE*,2I5)
49    FORMAT (9I3)
50    FORMAT (4E14.7)
51    FORMAT (3I3,2E14.7)
52    FORMAT (I3,2E14.7)
53    FORMAT (1H1)
54    FORMAT (/21X,*INPUT DATA*,/21X,10(*-*)//)
55    FORMAT (10X,*TOTAL NUMBER OF PARTITIONS- NPART=*,8X,I3)
56    FORMAT (10X,*TOTAL NUMBER OF NODAL POINTS- NPOIN=*,6X,I3)
57    FORMAT (10X,*TOTAL NUMBER OF ELEMENTS- NELEM=*,10X,I3)
58    FORMAT (10X,*TOTAL NUMBER OF NODAL POINTS WITH *,/15X,*PRESCRIBED
     1DISPLACEMENTS- NBOUN=*,5X,I3)
59    FORMAT (10X,*TOTAL NUMBER OF LOAD VECTORS- NCOLN=*,6X,I3)
60    FORMAT (10X,*NUMBER OF POINTS WITH CONCENTRATED LOADS=*,1X,I3)
61    FORMAT (10X,*PLANE THICKNESS- THICK=*,19X,E14.7)
62    FORMAT (//10X,*PRESCRIBED FORCES*,/10X,17(*-*),/10X,*NODE*,12X,*X-
     1FORCE*,16X,*Y-FORCE*)
63    FORMAT (11X,I3,2(9X,E14.7))
64    FORMAT (//10X,*PRESCRIBED DISPLACEMENTS*,/10X,24(*-*),/10X,*NODE*,
     19X,*X-DISPLACEMENT*,9X,*Y-DISPLACEMENT*)
65    FORMAT (11X,I3,32X,E14.7)
66    FORMAT (1H1,10X,*NODE*,8X,*X-COORDINATE*,9X,*Y-COORDINATE*/)
67    FORMAT (11X,I3,2(7X,E14.7))
68    FORMAT (//10X,*PARTITION  1ST ELEMENT  LAST ELEMENT  1ST NODE  LAS
     1T NODE*)
```

```
69      FORMAT (12X,I3,12X,I3,11X,I3,7X,I3,8X,I3)
70      FORMAT (10X,*---------  -----------  ------------  --------  -----
       1----*)
71      FORMAT (40X,I4,2(3X,E16.8))
72      FORMAT (39X,* NODE*,3X,* X-DISPLACEMENT *,2X,* Y-DISPLACEMENT*)
73      FORMAT (1H1)
74      FORMAT (20X,*NODAL NUMBERS*,/20X,13(*-*))
75      FORMAT (/10X,*ELEMENT  NODE1  NODE2  NODE3  NODE4  NODE5  NODE6
       1X-CENTROID     Y-CENTROID*)
76      FORMAT (12X,I3,1X,6(4X,I3),2(2X,E12.5))
77      FORMAT (20X,*CENTRIFUGAL FORCE OPTION                =*,I3)
78      FORMAT (20X,*YOUNG S MODULUS                         =*,E12.5)
79      FORMAT (20X,*POISSON S RATIO                         =*,E12.5)
80      FORMAT (20X,*DENSITY OF MATERIAL                     =*,E12.5)
81      FORMAT (20X,*SPEED REVS. PER MIN.                    =*,E12.5)
        END

        SUBROUTINE COORD (NPOIN,NELEM,NOD,X)
        DIMENSION X(500,2), NOD(300,6)
C
C       INPUT OF NODAL NUMBERS AND NODAL COORDINATES
C       FOR SYSTEM OF TRIM6 ELEMENTS
C       (THIS IS AN EXAMPLE)
C
        DO 1 I=1,NELEM
        READ (5,4) K,(NOD(K,J),J=1,6)
1       CONTINUE
        READ (5,4) NCOORD
        PI=2.*ASIN(1.)
        FI=2.*PI/17.
        DO 2 I=1,NCOORD
        READ (5,3) K,X(K,1),X(K,2)
        R=SQRT(X(K,1)**2+X(K,2)**2)
        ANG=ASIN(X(K,1)/R)+FI
        X(K,1)=R*SIN(ANG)
        X(K,2)=-R*COS(ANG)
2       CONTINUE
C
        RETURN
C
3       FORMAT (2X,I3,2(2X,E12.5))
4       FORMAT (7(2X,I3))
        END
```

```
      SUBROUTINE PCMAT (P)
      DIMENSION P(1)
      COMMON /BLK3/ C(6,6),PC(12,2),M
C
C     TO FORM PRODUCT P*C WHERE ONLY THE LOWER TRIANGLE OF SYMMETRIC
C     MATRIX P IS KNOWN. MATRIX C TO BE DERIVED FROM COMPLETE
C     COEFFICIENT MATRIX CT BY MEANS OF FUNCTION CR
C
      DO 1 I=1,12
      DO 1 J=1,2
1     PC(I,J)=0.0
      DO 2 I=1,12
      DO 2 J=1,2
      DO 2 K=1,12
      IF (K.LE.I) IK=I*(I-1)/2+K
      IF (K.GT.I) IK=K*(K-1)/2+I
2     PC(I,J)=PC(I,J)+P(IK)*CR(K,J)
      RETURN
      END

      FUNCTION CR (K,J)
      COMMON /BLK3/ C(6,6),PC(12,2),M
C
C     THIS FUNCTION RETURNS THE ELEMENT CT(K,J)   ,WHERE CT
C     IS THE COMPLETE (12 BY 12) COEFFICIENT MATRIX, BY EXTRACTING
C     THE PROPER ELEMENT FROM MATRIX C
C
      CR=0.0
      IF (J-2) 1,2,2
1     IF (K.LE.6) CR=C(K,M)
      GO TO 3
2     IF (K.GT.6) CR=C(K-6,M)
3     RETURN
      END
```

```
      SUBROUTINE FEM (X1,Y1,THICK,MM,NODE,CC)
      DIMENSION X1(1), Y1(1), NODE(1), CC(12,12)
      DIMENSION P(78), N1(6), CK(2,2)
      COMMON /BLK2/ D(3,3),DELTA
      COMMON /BLK3/ C(6,6),PC(12,2),M
C
C
C     CALCULATION OF ELEMNT STIFFNESS MATRIX FOR TRIM6 ELEMENT
C
C      TRANSFER ORIGIN TO CENTROID OF TRIANGLE
C
      ORX=(X1(1)+X1(2)+X1(3))/3.
      ORY=(Y1(1)+Y1(2)+Y1(3))/3.
      DO 1 I=1,3
      X1(I)=X1(I)-ORX
      Y1(I)=Y1(I)-ORY
1     CONTINUE
      X1(4)=(X1(1)+X1(3))/2.
      X1(5)=(X1(1)+X1(2))/2.
      X1(6)=(X1(2)+X1(3))/2.
      Y1(4)=(Y1(1)+Y1(3))/2.
      Y1(5)=(Y1(1)+Y1(2))/2.
      Y1(6)=(Y1(2)+Y1(3))/2.
      DELTA=1.5*(X1(2)*Y1(3)-X1(3)*Y1(2))
C
C     DEFINE COEFFICIENT MATRIX C
C
      DO 2 I=1,6
      C(I,1)=1.
      C(I,2)=X1(I)
      C(I,3)=Y1(I)
      C(I,4)=X1(I)**2
      C(I,5)=X1(I)*Y1(I)
      C(I,6)=Y1(I)**2
2     CONTINUE
C
      CALL INVMAT (C,6,6,1.0E-12,IERR,N1)
      IF (IERR.NE.0) GO TO 12
C
C      DEFINE LOWER TRIANGLE OF SYMMETRIC MATRIX P
C     P=INTEGRAL OF (Q)(TRANSPOSE)*(D)*(Q) OVER VOLUME OF ELEMENT
C
      DO 3 I=1,78
      P(I)=0.0
3     CONTINUE
      X2=(X1(1)**2+X1(2)**2+X1(3)**2)/12.
      Y2=(Y1(1)**2+Y1(2)**2+Y1(3)**2)/12.
      XY=(X1(1)*Y1(1)+X1(2)*Y1(2)+X1(3)*Y1(3))/12.
      IF (MM.LE.0) GO TO 4
      WRITE (1) ORX,ORY,((C(I,J),J=1,6),I=1,6),(X1(I),Y1(I),I=1,6),DELTA
     1,X2,Y2,XY,(NODE(J),J=1,6)
```

E.58

```
4     CONTINUE
      P(3)=D(1,1)
      P(5)=D(3,1)
      P(6)=D(3,3)
      P(10)=4.*D(1,1)*X2
      P(14)=2.*D(1,1)*XY+2.*D(3,1)*X2
      P(15)=D(1,1)*Y2+2.*D(1,3)*XY+D(3,3)*X2
      P(19)=4.*D(3,1)*XY
      P(20)=2.*D(3,1)*Y2+2.*D(3,3)*XY
      P(21)=4.*D(3,3)*Y2
      P(30)=D(3,1)
      P(31)=D(3,3)
      P(36)=D(3,3)
      P(38)=D(2,1)
      P(39)=D(2,3)
      P(44)=D(2,3)
      P(45)=D(2,2)
      P(49)=4.*D(3,1)*X2
      P(50)=2.*D(3,1)*XY+2.*D(3,3)*X2
      P(51)=4.*D(3,3)*XY
      P(55)=4.*D(3,3)*X2
      P(59)=2.*D(2,1)*X2+2.*D(3,1)*XY
      P(60)=D(2,3)*X2+(D(3,3)+D(2,1))*XY+D(3,1)*Y2
      P(61)=2.*D(2,3)*XY+2.*D(3,3)*Y2
      P(65)=2.*D(2,3)*X2+2.*D(3,3)*XY
      P(66)=D(2,2)*X2+2.*D(2,3)*XY+D(3,3)*Y2
      P(70)=4.*D(2,1)*XY
      P(71)=2.*D(2,1)*Y2+2.*D(2,3)*XY
      P(72)=4.*D(2,3)*Y2
      P(76)=4.*D(2,3)*XY
      P(77)=2.*D(2,2)*XY+2.*D(2,3)*Y2
      P(78)=4.*D(2,2)*Y2
C
      DO 5 I=1,78
      P(I)=F(I)*CELTA*THICK
5     CONTINUE
C
C     FORM PRODUCT (P)*(CJ) WHERE CJ IS (12X 2) SUBMATRIX
C     OF COMPLETE COEFFICIENT MATRIX (CT)
C
      DC 10 J=1,6
      JJ=NODE(J)
      IF (JJ.EQ.0) GO TO 10
      M=J
      CALL PCMAT (P)
      DC 9 I=1,6
      II=NODE(I)
      IF (II.EQ.0) GO TO 9
C
C     FORM PRODUCT (CI)(TRANSPOSE)*(PC)=(CK)
C     WHICH IS (2X2) SUBMATRIX OF ELEMENT STIFFNESS MATRIX
```

```
C
      M=I
      DC 6 IA=1,2
      DC 6 JA=1,2
      CK(IA,JA)=0.0
      DC 6 KA=1,12
6     CK(IA,JA)=CK(IA,JA)+CR(KA,IA)*PC(KA,JA)
C
C     CR(KA,IA) IS A FUNCTION SUBPROGRAM
C
      IK=2*I-1
      DC 8 IA=1,2
      JK=2*J-1
      DC 7 JA=1,2
      CC(IK,JK)=CK(IA,JA)
      JK=JK+1
7     CCNTINUE
      IK=IK+1
8     CCNTINUE
C
9     CCNTINUE
10    CCNTINUE
      DC 11 I=4,6
      X1(I)=X1(I)+ORX
      Y1(I)=Y1(I)+ORY
11    CONTINUE
      RETURN
      WRITE (6,13) LL
12    WRITE (6,14) IERR
      STCP
C
13    FORMAT (2X,I5)
14    FORMAT (1H1,10X,*IERR=*,I7)
      END
```

```
      SUBROUTINE CENT (DENS,RPM,THICK,NELEM,NPOIN,NCOLN,NODE,X1,Y1)
      DIMENSION NODE(1), X1(1), Y1(1), A(12,2), CTA(12,2), FF(12)
      COMMON ST(5050),FYM(100,60),U(700,2),BM(40,60)
      COMMON /BLK3/ C(6,6),PC(12,2),M
C
C     SUPERPOSITION OF CENTRIFUGAL FORCES
C
      FN1(X)=SM*X**5/5.+B*X**4/4.
      FN2(X)=SM**2*X**5/10.+SM*B*X**4/4.+B**2*X**3/6.
      FN3(X)=SM**3*X**5/15.+SM**2*B*X**4/4.+SM*B**2*X**3/3.+B**3*X**2/6.
      FN4(X)=SM**4*X**5/20.+SM**3*B*X**4/4.+SM**2*B**2*X**3/2.+B**4*X/4.
     1+SM*B**3*X**2/2.
C
C
      BACKSPACE 1
      NP=NPOIN*2
      ZERO=1.0E-10
      PI=2.*ASIN(1.)
      OMEGA=2.*PI*RPM/60.
      GRAVITY=32.2*12.
      FACT=DENS*OMEGA**2/GRAVITY
      DO 1 I=1,12
      DO 1 J=1,2
1     A(I,J)=0.
      READ (1) ORX,ORY,((C(I,J),J=1,6),I=1,6),(X1(I),Y1(I),I=1,6),DELTA,
     1X2,Y2,XY,(NODE(J),J=1,6)
      X3=0.
      X2Y=0.
      XY2=0.
      Y3=0.
      DO 2 I=1,3
      J=I+1
      IF (I.EQ.3) J=1
      DY=Y1(J)-Y1(I)
      DX=X1(J)-X1(I)
      IF (ABS(DX).LE.ZERO) GO TO 2
      SM=DY/DX
      B=Y1(I)-SM*X1(I)
      X3=X3+FN1(X1(I))-FN1(X1(J))
      X2Y=X2Y+FN2(X1(I))-FN2(X1(J))
      XY2=XY2+FN3(X1(I))-FN3(X1(J))
      Y3=Y3+FN4(X1(I))-FN4(X1(J))
2     CONTINUE
      FACTOR=FACT*THICK
      A(1,1)=ORX
      A(4,1)=ORX*X2
      A(5,1)=ORX*XY
      A(6,1)=ORX*Y2
      A(7,1)=ORY
      A(10,1)=ORY*X2
      A(11,1)=ORY*XY
```

```
      A(12,1)=ORY*Y2
      DC 3 I=1,12
      A(I,1)=A(I,1)*DELTA
3     CCNTINUE
      A(2,2)=X2*DELTA
      A(3,2)=XY*DELTA
      A(4,2)=X3
      A(5,2)=X2Y
      A(6,2)=XY2
      A(8,2)=XY*DELTA
      A(9,2)=Y2*DELTA
      A(10,2)=X2Y
      A(11,2)=XY2
      A(12,2)=Y3
      DC 4 J=1,2
      I=0
      DC 4 M=1,6
      DO 4 N=1,2
      I=I+1
      CTA(I,J)=0.
      DC 4 K=1,12
4     CTA(I,J)=CTA(I,J)+CR(K,N)*A(K,J)
      DC 5 I=1,12
      FF(I)=-(CTA(I,1)+CTA(I,2))*FACTOR
5     CCNTINUE
      JJ=0
      DC 7 I=1,6
      II=2*NODE(I)-1
      DC 7 J=1,2
      JJ=JJ+1
      DC 6 K=1,NCOLN
      U(II,K)=U(II,K)-FF(JJ)
6     CCNTINUE
7     II=II+1
      RETURN
C
      END
```

```
      SUBROUTINE SOLVE (NPART,NCOLN,IBM,JBM)
      DIMENSION YYM(100), YM(60,60)
      DIMENSION AM(5050), TF(100,2), F(100,2), DIS(100,2)
      COMMON ST(5050),PYM(100,60),U(700,2),BM(40,60)
      EGUIVALENCE (AM(1),ST(1))
      EGUIVALENCE (TF(1),U(1))
      EQUIVALENCE (DIS(1),U(201))
      EGUIVALENCE (YM(1),PYM(1))
      EGUIVALENCE (F(1),U(401))
      EGUIVALENCE (YYM(1),U(601))
C
C     SCLUTION OF TRIDIAGONAL SYSTEM OF SUBMATRIX EQUATIONS
C
      CALL SECOND (TI)
      DC 1 I=1,100
      DC 1 J=1,NCOLN
    1 TF(I,J)=0.
      JE=JBM
      DC 2 I=1,JBM
      DC 2 J=1,JBM
      YM(I,J)=0.
    2 CCNTINUE
C
C     ELIMINATION
C
      DO 13 LL=1,NPART
      CALL SECOND (T1)
      READ (4) M,N,NST,NCN,NCNN,NCK,(AM(I),I=1,NST),((BM(I,J),I=1,NCK),J
     1=1,NCN),((F(I,J),I=1,M),J=1,NCOLN)
      DC 4 I=1,M
      DC 3 J=1,NCOLN
      F(I,J)=F(I,J)-TF(I,J)
    3 CONTINUE
    4 CONTINUE
      DC 6 I=1,JB
      DC 5 J=1,JB
      IF (I.LT.J) GO TC 5
      IJ=I*(I-1)/2+J
      AM(IJ)=AM(IJ)-YM(I,J)
    5 CONTINUE
    6 CCNTINUE
      CALL INVSYM (AM,M,IERR)
      IF (IERR.NE.0) STOP
      WRITE (2) M,N,NST,NCN,NCNN,NCK,(AM(I),I=1,NST),((BM(I,J),I=1,NCK),
     1J=1,NCN),((F(I,J),I=1,M),J=1,NCOLN)
      IF (NPART-LL) 14,14,7
    7 CALL MATM (AM,F,DIS,M,NCCLN)
      CALL MATTM (BM,DIS,TF,N,M,NCOLN,NCN,NCNN)
      DC 8 J=1,NCN
      DC 8 I=1,M
      PYM(I,J)=0.
```

```
      DO 8 K=1,M
      IF (K.LE.I) IK=I*(I-1)/2+K
      IF (K.GT.I) IK=K*(K-1)/2+I
      BMATT=BMAT(K,J,BM,NCN,M,NCNN)
 8    PYM(I,J)=PYM(I,J)+AM(IK)*BMATT
      DO 12 J=1,NCN
      DO 10 I=1,NCN
      YYM(I)=0.
      IY=I
      DO 9 K=1,M
      BMATT=BMAT(K,I,BM,NCN,M,NCNN)
      YYM(IY)=YYM(IY)+BMATT*PYM(K,J)
 9    CONTINUE
 10   CONTINUE
      DO 11 I=1,NCN
      YM(I,J)=YYM(I)
 11   CONTINUE
 12   CONTINUE
      JB=NCN
      CALL SECOND (T2)
      DT=T2-T1
      WRITE (6,20) LL,DT
 13   CONTINUE
 14   REWIND 4
      CALL MATM (AM,F,DIS,M,NCOLN)
      WRITE (3) ((DIS(I,J),I=1,M),J=1,NCOLN)
      IF (NPART-1) 19,19,15
 15   NA=NPART-1
C
C     BACKWARD SUBSTITUTION
C
      DO 18 LL=1,NA
      BACKSPACE 2
      BACKSPACE 2
      READ (2) M,N,NST,NCN,NCNN,NCK,(AM(I),I=1,NST),((BM(I,J),I=1,NCK),J
     1=1,NCN),((F(I,J),I=1,M),J=1,NCOLN)
      DO 16 J=1,NCOLN
      DO 16 I=1,M
      TF(I,J)=0.
      DO 16 K=1,N
      BMATT=BMAT(I,K,BM,NCN,M,NCNN)
 16   TF(I,J)=TF(I,J)+BMATT*DIS(K,J)
      DO 17 J=1,NCOLN
      DO 17 I=1,M
 17   F(I,J)=F(I,J)-TF(I,J)
      CALL MATM (AM,F,DIS,M,NCOLN)
      WRITE (3) ((DIS(I,J),I=1,M),J=1,NCOLN)
 18   CONTINUE
 19   CONTINUE
      CALL SECOND (TJ)
      DT=TJ-TI
```

```
      WRITE (6,21) DT
      RETURN
C
20    FORMAT (*   TIME FOR PARTITION *,I5,* =*,E14.7)
21    FORMAT (*   TIME FOR SOLUTION=*,E14.7)
      END
```

```
      FUNCTION BMAT (I,J,BM,NCN,M,NCNN)
      DIMENSION BM(40,60)
C
C     RETURNS PROPER ELEMENT OF CONNECTIVITY MATRIX BY EXTRACTION
C     FROM MATRIX BM
C
      BMAT=0.
      IF (I.LE.NCNN) RETURN
      IF (J.GT.NCN) RETURN
      II=I-NCNN
      BMAT=BM(II,J)
      RETURN
      END
      SUBROUTINE MATM (D,B,DB,M,NCOLN)
      DIMENSION D(1), B(100,2), DB(100,2)
C
C     MATRIX MULTIPLICATION (D)*(B)
C
      DO 1 J=1,NCOLN
      DO 1 I=1,M
      DB(I,J)=0.
      DO 1 K=1,M
      IF (K.LE.I) IK=I*(I-1)/2+K
      IF (K.GT.I) IK=K*(K-1)/2+I
    1 DB(I,J)=DB(I,J)+D(IK)*B(K,J)
      RETURN
      END


      SUBROUTINE MATTM (BM,DIS,TF,N,M,NCOLN,NCN,NCNN)
      DIMENSION BM(40,60), DIS(100,2), TF(100,2)
C
C     MATRIX MULTIPLICATION (D)(TRANSPOSE)*(B)
C
      DO 1 J=1,NCOLN
      DO 1 I=1,N
      TF(I,J)=0.
      DO 1 K=1,M
      BMATT=BMAT(K,I,BM,NCN,M,NCNN)
    1 TF(I,J)=TF(I,J)+BMATT*DIS(K,J)
      RETURN
      END
```

```
      SUBROUTINE QMAT (X,Y,Q)
      DIMENSION Q(3,12)
      DO 1 I=1,3
      DO 1 J=1,12
    1 Q(I,J)=0.0
      Q(1,2)=1.0
      Q(1,4)=2.*X
      Q(1,5)=Y
      Q(2,9)=1.0
      Q(2,11)=X
      Q(2,12)=2.*Y
      Q(3,3)=1.0
      Q(3,5)=X
      Q(3,6)=2.*Y
      Q(3,8)=1.0
      Q(3,10)=2.*X
      Q(3,11)=Y
      RETURN
      END

      SUBROUTINE QCMAT (Q,QC)
      DIMENSION Q(3,12), QC(3,12)
      COMMON /BLK3/ C(6,6),PC(12,2),M
      DO 1 I=1,3
      JJ=0
      DO 1 M=1,6
      DO 1 J=1,2
      JJ=JJ+1
      QC(I,JJ)=0.0
      DO 1 K=1,12
      QC(I,JJ)=QC(I,JJ)+Q(I,K)*CR(K,J)
    1 CONTINUE
      RETURN
      END
```

```
      SUBROUTINE STRESS (NPOIN,NELEM,X1,Y1,NODE,NCOLN,NOD,X)
      DIMENSION SIG(300,6,3), UU(12)
      DIMENSION X(500,2), NOD(300,6)
      DIMENSION X1(1), Y1(1), NST(10), NNO(10), NODE(6)
      COMMON /BLK3/ C(6,6),PC(12,2),M
      COMMON /BLK5/ NPUNCH
      COMMON ST(5050),FYM(100,60),U(700,2),BM(40,60)
      EQUIVALENCE (SIG(1),ST(1))
C
C     CENTROIDAL STRESSES
C
      PI=2.*ASIN(1.)
      REWIND 1
      WRITE (6,17)
      WRITE (6,11)
      DO 2 L=1,NELEM
      READ (1) ORX,ORY,((C(I,J),J=1,6),I=1,6),(X1(I),Y1(I),I=1,6),DELTA,
     1X2,Y2,XY,(NODE(J),J=1,6)
      JJ=0
      DO 1 I=1,6
      KK=2*NODE(I)-1
      DO 1 J=1,2
      JJ=JJ+1
      UU(JJ)=U(KK,1)
      KK=KK+1
1     CONTINUE
      CALL SIGMA (0.0,0.0,UU,SX,SY,SXY)
      CALL PRINCE (SX,SY,SXY,PI,S1,S2,THETA)
      WRITE (6,12) L,SX,SY,SXY,S1,S2,THETA
2     CONTINUE
C
C     NODAL STRESSES
C
      WRITE (6,18)
      WRITE (6,20)
      REWIND 1
      DO 4 L=1,NELEM
      READ (1) ORX,ORY,((C(I,J),J=1,6),I=1,6),(X1(I),Y1(I),I=1,6),DELTA,
     1X2,Y2,XY,(NODE(J),J=1,6)
      JJ=0
      DO 3 I=1,6
      KK=2*NODE(I)-1
      DO 3 J=1,2
      JJ=JJ+1
      UU(JJ)=U(KK,1)
      KK=KK+1
3     CONTINUE
      DO 4 LI=1,6
      II=NOD(L,LI)
      CALL SIGMA (X1(LI),Y1(LI),UU,SX,SY,SXY)
      WRITE (6,19) L,II,SX,SY,SXY
```

```
      SIG(L,LI,1)=SX
      SIG(L,LI,2)=SY
      SIG(L,LI,3)=SXY
    4 CONTINUE
C
C     NCDAL AVERAGES
C
      WRITE (6,14)
      WRITE (6,15)
      REWIND 1
      DC 9 I=1,NPOIN
      K=0
      DC 7 L=1,NELEM
      DC 6 J=1,6
      IF (NOD(L,J)-I) 6,5,6
    5 K=K+1
      NST(K)=L
      NNC(K)=J
    6 CCNTINUE
    7 CONTINUE
      SX=0.
      SY=0.
      SXY=0.
      DC 8 JJ=1,K
      KK=NST(JJ)
      NN=NNO(JJ)
      SX=SX+SIG(KK,NN,1)
      SY=SY+SIG(KK,NN,2)
      SXY=SXY+SIG(KK,NN,3)
    8 CONTINUE
      SX=SX/K
      SY=SY/K
      SXY=SXY/K
      CALL PRINCE (SX,SY,SXY,PI,S1,S2,THETA)
      WRITE (6,12) I,SX,SY,SXY,S1,S2,THETA
      IF (NPUNCH.GT.0) WRITE (7,13) I,SX,SY,SXY,S1,S2,THETA
C
C     RACIAL AND TANGENTIAL STRESSES
C
      ZI1=X(I,1)
      ZI2=X(I,2)
      R=SQRT(ZI1**2+ZI2**2)
      IF (R.LE.1.0E-50) R=1.
      SINQ=ZI2/R
      COSQ=ZI1/R
      COS2Q=1.-2.*SINQ*SINQ
      SIN2Q=2.*SINQ*COSQ
      Q1=(SX+SY)/2.
      Q2=(SX-SY)/2.
      Q3=SXY
      Q7=Q2*COS2Q
```

```
      Q8=Q3*SIN2Q
      SR=Q1+Q7+Q8
      SQ=Q1-Q7-Q8
      SRQ=Q3*COS2Q-Q2*SIN2Q
      WRITE (1) I,SR,SQ,SRQ
9     CONTINUE
C
      WRITE (6,16)
      REWIND 1
      DO 10 I=1,NPOIN
      READ (1) J,SR,SQ,SRQ
      WRITE (6,12) J,SR,SQ,SRQ
10    CONTINUE
C
      RETURN
C
11    FORMAT (21X,*ELEMENT*,4X,*SX*,9X,*SY*,8X,*SXY*,9X,*S1*,9X,*S2*,6X,
     1*THETA*/)
12    FORMAT (23X,I3,5(2X,F9.2),2X,F7.3)
13    FORMAT (I3,5(2X,F9.2),2X,F7.3)
14    FORMAT (1H1,40X,*AVERAGE STRESSES AT NODAL POINTS*/41X,32(*-*)/)
15    FORMAT (21X,* NODE   *,4X,*SX*,9X,*SY*,8X,*SXY*,9X,*S1*,9X,*S2*,6X,
     1*THETA*/)
16    FORMAT (1H1,20X,* NODE   *,4X,*SR*,9X,*ST*,8X,*SRT*)
17    FORMAT (1H1,40X,*CENTROIDAL STRESSES*,/41X,19(*-*)/)
18    FORMAT (1H1,25X,*NODAL STRESSES*,/26X,14(*-*)/)
19    FORMAT (22X,I3,4X,I3,3(3X,E12.5))
20    FORMAT (20X,*ELEMENT*,2X,*NODE*,9X,*SX*,14X,*SY*,13X,*SXY*)
      END
```

```
      SUBROUTINE SIGMA (X,Y,UU,SX,SY,SXY)
      DIMENSION UU(1)
      DIMENSION Q(3,12), QC(3,12), QCU(3)
      CCMMON /BLK2/ D(3,3),DELTA
      COMMON /BLK3/ C(6,6),PC(12,2),M
C
C     THIS SUBROUTINE CALCULATES THE STRESS AT A POINT WITHIN
C     A TRIM6 ELEMENT, GIVEN THE COORDINATES OF THE POINT AND THE
C     NCDAL DISPLACEMENTS OF THE ELEMENT NCDES
C
      CALL QMAT (X,Y,Q)
      CALL QCMAT (Q,QC)
      DC 1 I=1,3
      QCU(I)=0.0
      JJ=0
      DC 1 K=1,6
      DC 1 J=1,2
      JJ=JJ+1
      QCU(I)=QCU(I)+QC(I,JJ)*UU(JJ)
1     CCNTINUE
      SX=0.
      SY=0.
      SXY=0.
      DC 2 J=1,3
      SX=SX+D(1,J)*QCU(J)
      SY=SY+D(2,J)*QCU(J)
      SXY=SXY+D(3,J)*QCU(J)
2     CCNTINUE
      RETURN
      END

      SUBROUTINE PRINCE (SX,SY,SXY,PI,S1,S2,THETA)
C
C     TC FIND PRINCIPAL STRESSES AND PRINCIPAL ANGLE
C     PRINCIPAL ANGLE IS THE ANGLE BETWEEN S1 AND Y-AXIS
C
      Q1=(SX+SY)/2.
      Q2=(SX-SY)/2.
      Q3=SXY
      Q4=SQRT(Q2**2+Q3**2)
      S1=Q1+Q4
      S2=Q1-Q4
      THETA=ATAN((S1-SY)/SXY)
      THETA=THETA*180./PI
      RETURN
      END
```

APPENDIX F

```
      SUBROUTINE FORCE(Q,A,COEFFT,FF)
      DIMENSION C(4,4),Q(2),N1(4),FF(4),F(4)
C
C     DISCRETIZATION OF LINEAR FORCE DISTRIBUTION ON A
C     TRIM3 ELEMENT SITUATED ON THE CIRCUMFERANCE OF A
C     CIRCULAR BOUNDARY BY CONSISTENT APPROACH
C
      PI= 2.*ASIN(1.)
      DO 1 I=1,4
      DO 1 J=1,4
    1 C(I,J)= 0.
      C(1,1)= 1.
      C(1,2)= Q(1)
      C(2,3)= 1.
      C(2,4)= Q(1)
      C(3,1)= 1.
      C(3,2)= Q(2)
      C(4,3)= 1.
      C(4,4)= Q(2)
      CALL INVMAT(C,4,4,1.0E-08,IERR,N1)
      IF(IERR .NE. 0)  STOP
      FF(1)= (Q(2)**2-Q(1)**2)/2.
      FF(2)= (Q(2)**3-Q(1)**3)/3.
      FF(3)= COEFFT*FF(1)
      FF(4)= COEFFT*FF(2)
      DO 3 I=1,4
      F(I)= 0.
      DO 4 J=1,4
    4 F(I)= F(I) + C(J,I)*FF(J)
    3 F(I)= A*F(I)
      J= 0
      DO 5 I=1,4,2
      J= J+1
      QQJJ= Q(J)*PI/180.
      FF(I)= -(F(I+1)*COS(QQJJ) + F(I)*SIN(QQJJ))
    5 FF(I+1)= -(F(I+1)*SIN(QQJJ) - F(I)*COS(QQJJ))
C
      RETURN
      END
```

```
      PROGRAM TST (INPUT,OUTPUT,TAPE5=INPUT,TAPE6=OUTPUT,
     1 PUNCH,TAPE7=PUNCH)
      DIMENSION C(6,6),Y(3),N1(6),FF(6),FX(6)
      DIMENSION  UX(20),UY(20),NUM(20)
      DIMENSION XC(500),YC(500)
      REAL K1,K2
      DATA (NUM(I),I=1,14)/425,424,423,422,421,420,419,1,2,3,4,5,6,7/
C
C     DISCRETIZATION OF LINEAR FORCE DISTRIBUTION ON
C     TRIM6 ELEMENTS SITUATED ON THE CIRCUMFERANCE OF A
C     CIRCULAR BOUNDARY BY CONSISTENT APPROACH
C
      NPROB=1
      NCOORD=119
      K1= 0.26
      K2= 0.2*K1
      R=15./2.54
      PI=2.*ASIN(1.)
      FI=2.*PI/17.
      NEL=7
C
      DO 11 NP=1,NPROB
      READ(5,105) TITLE
      WRITE(6,208) TITLE
      WRITE(7,208) TITLE
      SUMX=0.
      SUMY=0.
      DO 12 I=1,20
      UX(I)=0.
12    UY(I)=0.
      KI=0
      DO 15 I=1,NCOORD
15    READ(5,100) K,XC(K),YC(K)
      II=1
      KK=NUM(II)
      XX=XC(KK)
      YY=YC(KK)
      DO 10 K=1,NEL
      Y(1)=(ASIN(XX/R)+FI)*180./PI
      II=II+2
      IF(K.EQ.4) II=II-1
      KK=NUM(II)
      XX=XC(KK)
      YY=YC(KK)
      Y(2)=(ASIN(XX/R)+FI)*180./PI
      Y(3)=(Y(1)+Y(2))/2.
      DO 1 I=1,6
      DO 1 J=1,6
1     C(I,J)=0.
      C(1,1)=1.
      C(1,2)=Y(1)
```

F.2

```
      C(1,3)=Y(1)**2
      C(2,4)=1.
      C(2,5)=Y(1)
      C(2,6)=C(1,3)
      C(3,1)=1.
      C(3,2)=Y(2)
      C(3,3)=Y(2)**2
      C(4,4)=1.
      C(4,5)=Y(2)
      C(4,6)=C(3,3)
      C(5,1)=1.
      C(5,2)=Y(3)
      C(5,3)=Y(3)**2
      C(6,4)=1.
      C(6,5)=Y(3)
      C(6,6)=C(5,3)
      CALL INVMAT(C,6,6,1.0E-08,IERR,N1)
      IF(IERR .NE. 0)  STOP
      FF(1)=K1*(Y(2)**2-Y(1)**2)/2.
      FF(2)=K1*(Y(2)**3-Y(1)**3)/3.
      FF(3)=K1*(Y(2)**4-Y(1)**4)/4.
      FF(4)=K2*(Y(2)**2-Y(1)**2)/2.
      FF(5)=K2*(Y(2)**3-Y(1)**3)/3.
      FF(6)=K2*(Y(2)**4-Y(1)**4)/4.
      DO 3 I=1,6
      FX(I)=0.
      DO 4 J=1,6
4     FX(I)=FX(I)+C(J,I)*FF(J)
3     CONTINUE
      J=0
      DO 5 I=1,6,2
      J=J+1
      Q=Y(J)*PI/180.
      FF(I)=-(FX(I+1)*COS(Q)+FX(I)*SIN(Q))
      FF(I+1)=-(FX(I+1)*SIN(G)-FX(I)*COS(Q))
      IF( K .EQ.4) GO TO 13
      KI=KI+1
      UX(KI)=UX(KI)+FF(I)
      UY(KI)=UY(KI)+FF(I+1)
      GO TO 5
13    UX(NI)=  UX(NI)+FF(I)
      UY(NI)=UY(NI)+FF(I+1)
5     WRITE(6,205) J,FF(I),FF(I+1)
      NI=KI
      KI=KI-1
      IF(K.EQ.4) KI=NI+1
10    CONTINUE
      DO 14 I=1,NI
      WRITE(6,205) NUM(I),UX(I),UY(I)
      WRITE(7,206) NUM(I),UX(I),UY(I)
      SUMX=SUMX+UX(I)
```

```
      SUMY=SUMY+UY(I)
14    CONTINUE
      WRITE(6,212) SUMX,SUMY
      WRITE(6,211)
11    CONTINUE
C
      STOP
100   FORMAT(2X,I3,2(2X,E12.5))
208   FORMAT(*  FORCES FOR MESH NO.*,A5)
105   FORMAT(A5)
205   FORMAT(2X,I3,2(2X,E14.7))
206   FORMAT(I3,2E14.7)
211   FORMAT(1H1)
212   FORMAT(*  SUM X-FORCES*,E12.5,    *  SUM Y-FORCES*,E14.5)
      END
```

APPENDIX G

```
      PROGRAM TST(INPUT,OUTPUT,TAPE5=INPUT,TAPE6=OUTPUT,TAPE10)
      DIMENSION FI1(80), FI2(80), NUM(50)
      DIMENSION NOD(300,6), X(500), Y(500), SIG1(500), SIG2(500)
C
C     MAIN PROGRAM FOR CONTOUR PLOTTING OF MAXIMUM AND
C     MINIMUM PRINCIPAL STRESSES
C
      DATA TIT1/4HMESH/
      DATA (NUM(I),I=1,31)/24,28,18,7,5,1,2,4,14,23,35,50,48,47,65,102,1
     101,80,79,77,76,98,100,99,73,59,43,29,19,8,24/
C
C
      CALL PLOT (0.0,0.0,3)
      CALL DATE (D1)
      CALL LETTER (8,0.3,270.0,1.0,10.0,8HMOOSA    )
      CALL LETTER (10,0.3,270.0,1.0,7.6,D1)
C
      READ (5,9) NPLOT
      INUM=31
      NPOIN=279
      NCOORD=279
      NELEM=90
      ALEN=7.0
      KCG=2
      LAB=1
      ISC=1
      ITER=0
C
      FI1(1)=-600.
      SM1=500.
      STEP=50.
      I=1
    1 I=I+1
      FI1(I)=FI1(I-1)+STEP
      NCON1=I
      IF (FI1(I).LT.SM1) GO TO 1
      FI2(1)=-2800.
      SM2=50.
      STEP=100.
      I=1
    2 I=I+1
      FI2(I)=FI2(I-1)+STEP
      NCON2=I
      IF (FI2(I).LT.SM2) GO TO 2
      DO 6 NN=1,NPLOT
      READ (5,11) TIT2
      WRITE (6,10) TIT2
      CALL LETTER (4,0.2,90.0,1.0,0.2,TIT1)
      CALL LETTER (4,0.2,90.0,1.0,1.5,TIT2)
      ITER=ITER+1
      ISM=0
```

```
      DO 3 I=1,NELEM
      READ (5,7) K,(NOD(K,J),J=1,6)
3     CONTINUE
      DO 4 I=1,NCOORD
      READ (5,8) K,X(K),Y(K)
4     CONTINUE
      DO 5 I=1,NPOIN
      READ (5,9) K,SIG1(K),SIG2(K)
5     CONTINUE
      CALL CONPLOT (FI1,NCON1,NUM,INUM,NELEM,NPOIN,NOD,X,Y,SIG1,ALEN,NCO
     1ORD,ISC,LAB,KQQ,ISM,ITER)
      ISM=ISM+1
      ITER=ITER+1
      CALL CONPLOT (FI2,NCON2,NUM,INUM,NELEM,NPOIN,NOD,X,Y,SIG2,ALEN,NCO
     1ORD,ISC,LAB,KQQ,ISM,ITER)
6     CONTINUE
      CALL PLOT (5.,0.,999)
C
      STOP
C
7     FORMAT (7I3)
8     FORMAT (2X,I3,2(2X,E14.7))
9     FORMAT (I3,33X,2(2X,F9.2))
10    FORMAT (10X,12HMESH NUMBER ,A4)
11    FORMAT (A4)
      END
```

G.2

```
      SUBROUTINE CONPLOT (PHI,NCON,NUM,INUM,NELEM,NPOIN,NOD,X,Y,SIG,ALEN
     1,NCOORD,ISC,LAB,KQQ,ISM,ITER)
      DIMENSION PHI(1), NUM(1), XX(7), YY(7), INIT(99), NAC(99)
      DIMENSION X1(250), Y1(250), X2(250), Y2(250), XC(500), YC(500)
      DIMENSION NOD(300,6), X(500), Y(500), SIG(500)
      COMMON /BLK1/ A(3,500)
      COMMON /BLK2/ XMI,XMA,YMI,YMA,NI
C
C     SUPPLY IN ARRAY NUM NODAL NUMBERS ON BOUNDARY IN SEQUENCE
C     CLOCKWISE OR COUNTER-CLOCKWISE, ALSO REPEAT THE FIRST NODAL
C     NUMBER AGAIN AT THE END OF ARRAY NUM IF BOUNDARY IS CLOSED
C     LOOP. INUM SHOULD INCLUDE ALL ENTRIES IN NUM.
C
C     ALEN= LENGTH OF SQUARE .LE. 10 IN. IN WHICH PLOT DESIRED
C     PHI= ARRAY CONTAINING CONTOURS DESIRED
C     NCON= NUMBER OF CONTOURS
C     NELEM= NUMBER OF FINITE ELEMENTS
C     NPOIN= NUMBER OF NODES
C     NOD= ARRAY OF NODAL NUMBERS
C     NCOORD= NUMBER OF NODES WHOSE COORDS ARE DEFINED
C     IF NPOIN.GT.NCOORD, TRIM6 ELEMENT ASSUMED
C     IF NPOIN.EQ.NCOORD, TRIM3 ELEMENT ASSUMED
C     SIG= STRESSES AT NODES
C     ITER= PLOT NUMBER
C     ISM= OPTION TO USE SAME COORDINATES AND NODAL NUMBERS OF
C     PREVIOUS PLOT IF ISM.GT.0
C     ISC= SCALING OPTION
C        =1 PLOT DONE IN AREA ALEN*ALEN
C        =2 Y-LENGTH .EQ. 10 IN, PLOT DONE USING Y-SCALE
C     LAB= LABELLING OPTION OF CONTOURS
C     =1 CONTOURS LABELLED BY NUMBER
C     =0 NO LABELLING
C     KQQ=1 FOR SINGLE-VALUED CONTOURS
C        =2 FOR MULTI- VALUED CONTOURS
C
      XCOUT=0.010
      ZERO=1.0E-04
C
      IF (ISM.GT.0) GO TO 10
      IF (NPOIN.EQ.NCOORD) GO TO 3
C
C     DEFINE MID-SIDE NODE COORDINATES FOR 6 NODAL ELEMENT
C
      DO 2 I=1,NELEM
      DO 1 J=1,3
      K=NOD(I,J)
      XX(J)=X(K)
      YY(J)=Y(K)
    1 CONTINUE
      K=NOD(I,5)
      X(K)=(XX(1)+XX(2))/2.
```

```
      Y(K)=(YY(1)+YY(2))/2.
      K=NOD(I,6)
      X(K)=(XX(2)+XX(3))/2.
      Y(K)=(YY(2)+YY(3))/2.
      K=NOD(I,4)
      X(K)=(XX(3)+XX(1))/2.
      Y(K)=(YY(3)+YY(1))/2.
2     CONTINUE
3     CONTINUE
C
C     FIND LIMITS
C
      J=1
      XMA=X(J)
      XMI=X(J)
      YMA=Y(J)
      YMI=Y(J)
      DO 4 I=J,NPOIN
      IF (X(I).GT.XMA) XMA=X(I)
      IF (X(I).LT.XMI) XMI=X(I)
      IF (Y(I).GT.YMA) YMA=Y(I)
      IF (Y(I).LT.YMI) YMI=Y(I)
4     CONTINUE
      XDIF=XMA-XMI
      YDIF=YMA-YMI
      GO TO (5,7), ISC
5     IF (YDIF.GT.XDIF) GO TO 6
      YW=YDIF*ALEN/XDIF
      XI=10.
      YI=10.
      XJ=XI-ALEN
      YJ=YI-YW
      SCALE=XDIF/ALEN
      GO TO 8
6     XW=XDIF*ALEN/YDIF
      XI=10.
      YI=10.
      XJ=XI-XW
      YJ=YI-ALEN
      SCALE=YDIF/ALEN
      GO TO 8
7     SCALE=YDIF/10.0
      XI=XDIF/SCALE
      YI=10.0
      XJ=0.
      YJ=0.
8     CONTINUE
C
C     SCALE AND CONSTRAIN ALL DATA TO FIRST PLOTTER QUADRANT
C
      DO 9 I=1,NPOIN
```

```
      X(I)=(X(I)-XMI)/SCALE
      Y(I)=(Y(I)-YMI)/SCALE
9     CONTINUE
      XMI=0.
      YMI=0.
      XMA=XDIF/SCALE
      YMA=YDIF/SCALE
C
C     PLOT BOUNDARY
C
10    CONTINUE
      XSKIP=1.0+XJ
      YSKIP=YJ+0.2
      IF (ITER.GT.1) YSKIP=0.0
      CALL PLOT (XSKIP,YSKIP,-3)
      IN=INUM-1
      DO 12 J=1,IN
      I1=NUM(J)
      IF (J.EQ.1) GO TO 11
      IF (I1.EQ.NUM(1)) GO TO 12
11    I2=NUM(J+1)
      CALL PLOT (X(I1),Y(I1),3)
      CALL PLOT (X(I2),Y(I2),2)
12    CONTINUE
C
C     SEARCH FOR CONTOURS
C
      DO 56 NI=1,NCON
      CON=PHI(NI)
C
      WRITE (6,59) NI,CON
C
      KSS=0
      KL=0
      KNN=3
      DO 17 L=1,NELEM
      KK=0
      DO 15 J=1,3
      I1=NOD(L,J)
      K=J+1
      IF (J.EQ.3) K=1
      I2=NOD(L,K)
      IF (SIG(I1).GT.SIG(I2)) GO TO 13
      S1=SIG(I2)
      S2=SIG(I1)
      GO TO 14
13    S1=SIG(I1)
      S2=SIG(I2)
14    CONTINUE
      IF (CON.GT.S1) GO TO 15
      IF (CON.LT.S2) GO TO 15
```

```
      KK=KK+1
      KSS=KSS+1
      DS1=SIG(I1)-SIG(I2)
      DS2=CON-SIG(I2)
      IF (ABS(DS1).LE.1.0E-5) GO TO 56
      DX=X(I1)-X(I2)
      DY=Y(I1)-Y(I2)
      XX(KK)=X(I2)+DS2/DS1*DX
      YY(KK)=Y(I2)+DS2/DS1*DY
15    CONTINUE
      IF (KK.LT.2) GO TO 17
      KL=KL+1
      IF (KL.LE.245) GO TO 16
      WRITE (6,60)
      GO TO 56
16    CONTINUE
      X1(KL)=XX(1)
      Y1(KL)=YY(1)
      X2(KL)=XX(2)
      Y2(KL)=YY(2)
17    CONTINUE
      IF (KL.GT.1) GO TO 18
      WRITE (6,61)
      GO TO 56
18    CONTINUE
C
C     FIND STARTING OR END POINTS OF CONTOURS
C
      IN=0
      DO 21 J=1,KL
      XA=X1(J)
      YA=Y1(J)
      KOUNT=0
      DO 20 I=1,KL
      IF (I.EQ.J) GO TO 19
      IF (ABS(X1(I)-XA).GT.ZERO) GO TO 19
      IF (ABS(Y1(I)-YA).LE.ZERO) KOUNT=KOUNT+1
19    IF (ABS(X2(I)-XA).GT.ZERO) GO TO 20
      IF (ABS(Y2(I)-YA).LE.ZERO) KOUNT=KOUNT+1
20    CONTINUE
      IF (KOUNT.NE.0) GO TO 21
      IN=IN+1
      INIT(IN)=J
21    CONTINUE
      IN1=IN
      DO 24 J=1,KL
      XA=X2(J)
      YA=Y2(J)
      KOUNT=0
      DO 23 I=1,KL
      IF (I.EQ.J) GO TO 22
```

```
      IF (ABS(X2(I)-XA).GT.ZERO)  GO TO 22
      IF (ABS(Y2(I)-YA).LE.ZERO)  KOUNT=KOUNT+1
22    IF (ABS(X1(I)-XA).GT.ZERO)  GO TO 23
      IF (ABS(Y1(I)-YA).LE.ZERO)  KOUNT=KOUNT+1
23    CONTINUE
      IF (KOUNT.NE.0)  GO TO 24
      IN=IN+1
      INIT(IN)=J
24    CONTINUE
      IF (IN.NE.0)  GO TO 25
C
C     CLOSED LOOP CONTOURS
C
      WRITE (6,62)
      IN=1
      IN1=1
      INIT(1)=1
25    CONTINUE
C
C     DEFINE POINTS ON CONTOUR
C
      II=INIT(1)
      INAC=1
      NAC(1)=II
      JJ=II
      IF (IN1.NE.0)  GO TO 27
      XC(1)=X2(JJ)
      YC(1)=Y2(JJ)
      XA=X1(JJ)
      YA=Y1(JJ)
      J=1
      IF (ABS(XA-XC(J)).GT.XCOUT)  GO TO 26
      IF (ABS(YA-YC(J)).LE.XCOUT)  GO TO 29
26    CONTINUE
      XC(2)=XA
      YC(2)=YA
      J=2
      GO TO 29
27    XC(1)=X1(II)
      YC(1)=Y1(II)
      XA=X2(II)
      YA=Y2(II)
      J=1
      IF (ABS(XA-XC(J)).GT.XCOUT)  GO TO 28
      IF (ABS(YA-YC(J)).LE.XCOUT)  GO TO 29
28    CONTINUE
      XC(2)=XA
      YC(2)=YA
      J=2
29    IF (J.LT.450)  GO TO 31
      WRITE (6,63)
```

```
      DC 30 I=1,J
      WRITE (6,57) I,XC(I),YC(I)
30    CCNTINUE
      GC TO 56
31    CCNTINUE
      KCUNT=0
      DC 32 I=1,KL
      IF (I.EQ.II) GC TO 32
      IF (ABS(X1(I)-XA).GT.ZERO) GO TO 32
      IF (ABS(Y1(I)-YA).LE.ZERO) KOUNT=KOUNT+1
      IF (KOUNT.EQ.1) GC TO 33
32    CCNTINUE
      GC TC 36
33    CCNTINUE
      IF (ABS(X2(I)-XC(J)).GT.XCOUT) GO TO 34
      IF (ABS(Y2(I)-YC(J)).LE.XCOUT) GO TO 35
34    J=J+1
      XC(J)=X2(I)
      YC(J)=Y2(I)
35    CCNTINUE
      JJ=I
      II=0
      XA=X2(I)
      YA=Y2(I)
      ILAST=I
      IF (ABS(XA-XC(1)).GT.ZERO) GO TO 36
      IF (ABS(YA-YC(1)).LE.ZERO) GO TO 42
36    KNT=0
      DC 37 I=1,KL
      IF (I.EQ.JJ) GO TO 37
      IF (ABS(X2(I)-XA).GT.ZERO) GO TO 37
      IF (ABS(Y2(I)-YA).LE.ZERO) KNT=KNT+1
      IF (KNT.EG.1) GO TO 38
37    CCNTINUE
      GC TC 41
38    CCNTINUE
      IF (ABS(X1(I)-XC(J)).GT.XCOUT) GO TO 39
      IF (ABS(Y1(I)-YC(J)).LE.XCOUT) GO TO 40
39    J=J+1
      XC(J)=X1(I)
      YC(J)=Y1(I)
40    CCNTINUE
      II=I
      JJ=0
      ILAST=I
      XA=X1(I)
      YA=Y1(I)
      IF (ABS(XA-XC(1)).GT.ZERO) GO TO 41
      IF (ABS(YA-YC(1)).LE.ZERO) GO TO 42
41    IF (KOUNT.NE.0.OR.KNT.NE.0) GO TO 29
42    CCNTINUE
```

```
C
      IF (J.LE.3) GO TO 44
      JM=J-2
      XCM=XC(2)
      YCM=YC(2)
      DO 43 I=2,JM
      XCP=XC(I+1)
      YCP=YC(I+1)
      XC(I)=(XCP+XCM)/2.
      YC(I)=(YCP+YCM)/2.
      YCM=YCP
      XCM=XCP
43    CONTINUE
      JM=JM+1
      XC(JM)=XC(J)
      YC(JM)=YC(J)
      J=JM
44    IF (J.GT.2) GO TO 45
      ILAST=II
      GO TO 46
C     ONE CONTOUR COMPLETELY DEFINED
C     SMOOTH AND PLOT CONTOUR
C
45    XP=XC(1)
      YP=YC(1)
      CALL PLOT (XP,YP,3)
      CALL INTERP (XC,YC,J,XP,YP,KQQ,LAB)
C
C     CHECK FOR OTHER CONTOURS HAVING VALUE .EQ. CON
C
46    IF (ILAST.EQ.NAC(INAC)) GO TO 47
      INAC=INAC+1
      NAC(INAC)=ILAST
47    CONTINUE
      IF (INAC.GE.IN) GO TO 56
      IF (IN1.EQ.0) GO TO 51
      DO 49 I=1,IN1
      KNT=0
      DO 48 K=1,INAC
      IF (INIT(I).EQ.NAC(K)) KNT=KNT+1
48    CONTINUE
      IF (KNT.EQ.0) GO TO 50
49    CONTINUE
      GO TO 51
50    II=INIT(I)
      INAC=INAC+1
      NAC(INAC)=II
      JJ=II
      GO TO 27
51    IN11=IN1+1
      DO 53 I=IN11,IN
```

```
      KNT=0
      DO 52 K=1,INAC
      IF (INIT(I).EQ.NAC(K)) KNT=KNT+1
52    CONTINUE
      IF (KNT.EQ.0) GO TO 54
53    CONTINUE
      GO TO 56
54    JJ=INIT(I)
      INAC=INAC+1
      NAC(INAC)=JJ
      II=JJ
      XC(1)=X2(JJ)
      YC(1)=Y2(JJ)
      XA=X1(JJ)
      YA=Y1(JJ)
      J=1
      IF (ABS(XA-XC(J)).GT.XCOUT) GO TO 55
      IF (ABS(YA-YC(J)).LE.XCOUT) GO TO 29
55    CONTINUE
      XC(2)=XA
      YC(2)=YA
      J=2
      GO TO 29
56    CONTINUE
      CALL PLOT (ALEN,0.0,-3)
      WRITE (6,58)
      RETURN
C
C
C
57    FORMAT (2X,I3,2X,*XC YC*,2(2X,E12.5))
58    FORMAT (1H1)
59    FORMAT (5X,I5,3X,F10.3)
60    FORMAT (45H DIMENSION SPACE FOR X1,Y1 AND X2,Y2 EXCEEDED)
61    FORMAT (24H  CONTOUR DOES NOT EXIST)
62    FORMAT (30H CONTOUR IS CLOSED LOOP-------,//)
63    FORMAT (35H DIMENSION SPACE FOR XC,YC EXCEEDED)
      END
```

```
      SUBROUTINE INTERP (XC,YC,N,XP,YP,KQQ,LAB)
      DIMENSION XC(1), YC(1)
      DIMENSION T(500), D(500), E(500)
      COMMON /BLK2/ XMI,XMA,YMI,YMA,NI
C
C     SMOOTHING OF CONTOURS BY SPLINE METHOD AND
C     SUBSEQUENT PLOTTING
C
      ZO=1.0E-03
      XI=XMI-ZO
      YI=YMI-ZO
      XA=XMA+ZO
      YA=YMA+ZO
      NN=N-1
      GO TO (1,4), KQQ
C
C     SINGLE-VALUED CONTOURS
C
1     CALL SPLIT (N,XC,YC,D)
      DO 3 IM=1,NN
      DXX=XC(IM+1)-XC(IM)
      IDXX=DXX
      INTER=10*IABS(IDXX)
      IF (INTER.EQ.0) INTER=5
      DX=DXX/INTER
      DO 2 I=1,INTER
      XP=XP+DX
      YP=SPLINE(XC,YC,XP,IM,D)
      IF (XP.LT.XMI.OR.XP.GT.XMA) GO TO 9
      IF (YP.LT.YMI.OR.YP.GT.YMA) GO TO 9
      CALL PLOT (XP,YP,2)
2     CONTINUE
3     CONTINUE
      RETURN
C
C     MULTI-VALUED CONTOURS
C
4     T(1)=0.
      DO 5 I=2,N
      DX=XC(I)-XC(I-1)
      DY=YC(I)-YC(I-1)
      DT=SQRT(DX*DX+DY*DY)
      T(I)=T(I-1)+DT
5     CONTINUE
      CALL SPLIT (N,T,XC,D)
      CALL SPLIT (N,T,YC,E)
      DO 8 I=1,NN
      IF (LAB.EQ.0) GO TO 6
      IF (I.NE.4) GO TO 6
      ENCODE (2,12,SE) NI
      CALL LETTER (2,0.06,0.0,XXP,YYP,SE)
```

```
      CALL PLOT (XXP,YYP,3)
6     CONTINUE
      DTT=T(I+1)-T(I)
      IDTT=DTT
      INTER=10*IABS(IDTT)
      IF (INTER.EQ.0) INTER=5
      DT=DTT/INTER
      TP=T(I)
      DO 7 J=1,INTER
      TP=TP+DT
      XP=SPLINE(T,XC,TP,I,D)
      YP=SPLINE(T,YC,TP,I,E)
      IF (XP.LT.XI.OR.XP.GT.XA) GO TO 9
      IF (YP.LT.YI.OR.YP.GT.YA) GO TO 9
      XXP=XP
      YYP=YP
      CALL PLOT (XP,YP,2)
7     CONTINUE
8     CONTINUE
      RETURN
9     CONTINUE
      WRITE (6,11) XP,YP,XC(1),YC(1)
      CALL PLOT (XC(1),YC(1),3)
      DO 10 I=2,N
      CALL PLOT (XC(I),YC(I),2)
10    CONTINUE
      RETURN
C
C
11    FORMAT (30H OUT OF RANGE QUANTITIES XP,YP,2E14.4,19H FIRST COORDIN
     1ATES ,2E14.4/)
12    FORMAT (I2)
      END
```

```
      SUBROUTINE SPLIT (N,X,Y,D)
      DIMENSION X(1), Y(1), D(1)
      COMMON /BLK1/ A(3,500)
C
C     TO INITIALIZE. CALCULATES SECOND DERIVATIVES
C
      DEL=0.5
      A(1,1)=0.
      A(2,1)=2.0
      A(3,1)=-2.*DEL
      D(1)=0.
      NN=N-1
      DO 1  J=2,NN
      H1=X(J)-X(J-1)
      H2=X(J+1)-X(J)
      F2=(Y(J+1)-Y(J))/H2
      F1=(Y(J)-Y(J-1))/H1
      D(J)=6.*(F2-F1)/(H1+H2)
      AL=H2/(H1+H2)
      AU=1.-AL
      A(1,J)=AU
      A(2,J)=2.
      A(3,J)=AL
1     CONTINUE
      A(1,N)=-2.*DEL
      A(2,N)=2.0
      A(3,N)=0.
      D(N)=0.
      CALL  DIAG3 (A,D,N)
      RETURN
      END


      FUNCTION SPLINE (X,Y,XP,J,D)
      DIMENSION X(1), Y(1), D(1)
C
C     CUBIC SPLINE INTERPOLATION
C
      H=X(J+1)-X(J)
      CC=(Y(J+1)-Y(J))/H-H*(D(J+1)-D(J))/6.
      DD=Y(J)-D(J)*H*H/6.
      A=(X(J+1)-XP)**3/6./H
      B=(XP-X(J))**3/6./H
      C=(XP-X(J))
      SPLINE=D(J)*A+D(J+1)*B+CC*C+DD
      RETURN
      END
```

```
      SUBROUTINE DIAG3(A,X,N)
      DIMENSION A(3,1),X(1)
C
C     SOLUTION OF TRIDIAGONAL SYSTEM OF EQUATIONS
C
      DO 10 J=2,N
      Z=-A(1,J)/A(2,J-1)
      A(1,J)=0.
      IF(Z.EQ.0.) GO TO 10
      A(2,J)=A(2,J)+Z*A(3,J-1)
      X(J)=X(J)+Z*X(J-1)
10    CONTINUE
      JJ=N+1
      DO 20 J=1,N
      JJ=JJ-1
      IF(JJ.EQ.N) GO TO 20
      X(JJ)=X(JJ)-A(3,JJ)*X(JJ+1)
20    X(JJ)=X(JJ)/A(2,JJ)
      RETURN
      END
```

```
      PROGRAM MAIN(INPUT,OUTPUT,TAPE5=INPUT,TAPE6=OUTPUT,TAPE10)
      DIMENSION NOD(400,6), X(500), Y(500)
C
C     PLOTTING OF INPUT MESH
C     NPLOT= NUMBER OF MESHES TO BE PLOTTED
C
      CALL PLOT (0.0,0.0,3)
      CALL DATE (D1)
      CALL LETTER (8,.3,270.0,1.0,10.0,8HMOOSA    )
      CALL LETTER (10,0.3,270.0,1.0,7.6,D1)
C
      READ (5,8) NPLOT
      DO 3 NN=1,NPLOT
      READ (5,6) TITLE
      READ (5,9) NPOIN,NELEM,NCOORD,ISC,LAB,ISPOT,NEL,ALEN
      WRITE (6,7) TITLE
      CALL LETTER (10,0.2,90.0,1.0,0.1,TITLE)
      DO 1 I=1,NELEM
      READ (5,5) K,(NOD(K,J),J=1,6)
1     CONTINUE
      DO 2 I=1,NCOORD
      READ (5,4) K,X(K),Y(K)
2     CONTINUE
      CALL MESH2 (X,Y,NOD,NPOIN,NELEM,NCOORD,ISC,LAB,ISPOT,ALEN,NEL,NN)
3     CONTINUE
      CALL PLOT (10.,0.,999)
C
      STOP
C
4     FORMAT (2X,I3,2(2X,E12.5))
5     FORMAT (7(2X,I3))
6     FORMAT (A10)
7     FORMAT (*   PLOT FOR MESH *,A10)
8     FORMAT (I3)
9     FORMAT (7I3,F10.0)
      END
```

```
      SUBROUTINE MESH2 (X,Y,NOD,NPOIN,NELEM,NCOORD,ISC,LAB,ISPOT,ALEN,
     1L,ITER)
      DIMENSION NOD(400,6), X(500), Y(500)
      DIMENSION XX(7), YY(7)
C
C     PLOT OF INPUT MESH FOR FINITE ELEMENT METHOD
C
C     ALEN= AREA .LE. 10  IN WHICH PLOT DESIRED
C     ITER= PLOT NUMBER
C     OPTIONS-
C     ISC=1 PLOT IN AREA ALEN BY ALEN
C        =2  Y-LENGTH 10 IN., X-LENGTH= YSCALE*XDIF
C     LAB=1 NODES NOT LABELLED
C        =2 NODES LABELLED
C     ISPOT=1 NODES NOT SPOTTED
C          =2 NODES SPOTTED
C     NEL=1 ELEMENTS NOT LABELLED
C        =2 ELEMENTS LABELLED
C     NCOORD= NUMBER OF COORDINATES DEFINED
C     IF NCOORD=NPOIN 3 NODAL ELEMENT IS ASSUMED
C     IF NCOORD.NE.NPOIN 6 NODAL ELEMENT IS ASSUMED
C
      CALL PLOT (0.,0.,3)
      YSKIP=0.
      IF (ITER.EQ.1) YSKIP=0.1
      CALL PLOT (2.0,YSKIP,-3)
      N=NPOIN
      IF (NPOIN.EQ.NCOORD) GO TO 3
C
C     DEFINE MID-SIDE NODE COORDINATES FOR 6 NODAL ELEMENT
C
      DO 2 I=1,NELEM
      DO 1 J=1,3
      K=NOD(I,J)
      XX(J)=X(K)
      YY(J)=Y(K)
    1 CONTINUE
      K=NOD(I,5)
      X(K)=(XX(1)+XX(2))/2.
      Y(K)=(YY(1)+YY(2))/2.
      K=NOD(I,6)
      X(K)=(XX(2)+XX(3))/2.
      Y(K)=(YY(2)+YY(3))/2.
      K=NOD(I,4)
      X(K)=(XX(3)+XX(1))/2.
      Y(K)=(YY(3)+YY(1))/2.
    2 CONTINUE
C
C     SCALING
C
    3 I=1
```

```
      XMA=X(I)
      XMI=X(I)
      YMA=Y(I)
      YMI=Y(I)
      DO 4 I=1,NPOIN
      IF (X(I).GT.XMA) XMA=X(I)
      IF (X(I).LT.XMI) XMI=X(I)
      IF (Y(I).GT.YMA) YMA=Y(I)
      IF (Y(I).LT.YMI) YMI=Y(I)
4     CONTINUE
      XDIF=XMA-XMI
      YDIF=YMA-YMI
C
      GO TO (5,7), ISC
5     IF (YDIF.GT.XDIF) GO TO 6
      YW=YDIF*ALEN/XDIF
      X1=10.
      Y1=10.
      X2=X1-ALEN
      Y2=Y1-YW
      GO TO 8
6     XW=XDIF*ALEN/YDIF
      X1=10.
      Y1=10.
      X2=X1-XW
      Y2=Y1-ALEN
      GO TO 8
7     SC=YDIF/10.0
      X1=XDIF/SC
      Y1=10.0
      X2=0.0
      Y2=0.0
8     CALL FACTOR (N,X,Y,X1,Y1,X2,Y2)
C
C     DRAW MESH
C
      DO 11 I=1,NELEM
      DO 9 J=1,3
      K=NOD(I,J)
      XX(J)=X(K)
      YY(J)=Y(K)
9     CONTINUE
      XX(4)=XX(1)
      YY(4)=YY(1)
      DO 10 J=1,3
      CALL PLTLN (XX(J),YY(J),XX(J+1),YY(J+1))
10    CONTINUE
11    CONTINUE
C
C     NODE LABELLING AND SPOTTING
C
```

```
      IF (LAB.EQ.1.AND.ISPOT.EQ.1) GO TO 19
      DO 18 I=1,NPOIN
      CALL UNITTO (X(I),Y(I),XP,YP)
      GO TO (16,12), LAB
12    IF (I.LT.10) GO TO 14
      IF (I.LT.100) GO TO 13
      ENCODE (3,24,IE) I
      NN=3
      GC TO 15
13    ENCODE (2,25,IE) I
      NN=2
      GO TO 15
14    ENCODE (1,26,IE) I
      NN=1
15    ZX=XP+0.03
      ZY=YP-0.03
      CALL LETTER (NN,0.06,0.0,ZX,ZY,IE)
16    GO TO (18,17), ISPOT
17    CALL GRAF (XP,YP,0.05,1)
18    CONTINUE
19    CONTINUE
C
C     ELEMENT LABELLING
C
      GO TO (23,20), NEL
20    DO 22 I=1,NELEM
      ORX=0.
      ORY=0.
      DO 21 J=1,3
      K=NOD(I,J)
      ORX=ORX+X(K)/3.
      ORY=ORY+Y(K)/3.
21    CONTINUE
      CALL UNITTO (ORX,ORY,XP,YP)
      ENCODE (3,24,IE) I
      NN=3
      ZX=XP-0.09
      ZY=YP-0.03
      CALL LETTER (NN,0.06,0.0,ZX,ZY,IE)
22    CONTINUE
C
23    CALL PLOT (10.,0.,-3)
      RETURN
C
24    FORMAT (I3)
25    FORMAT (I2)
26    FORMAT (I1)
      END
```

APPENDIX H

The Cubic Spline

Given a set of points $x_0, x_1, \ldots, x_n$ on the interval (x_0, x_n) and a set of prescribed ordinates $f_0, f_1, \ldots, f_n$, it is possible to join each consecutive pair (x_{j-1}, f_{j-1}), (x_j, f_j) by a cubic so chosen that the resulting composite curve has continuous first and second derivatives. For small deflections from a straight configuration, it is well known that this curveis a close approximation to the configuration of a thin beam simply supported at the junctions x_j.

We begin by designating with $M_0, M_1, \ldots, M_n$ the second derivatives at the mesh locations x_j of the function $y(x)$ represented by the composite curve. The second derivative $y''(x)$ is linear between junctions and we have, for $x_{j-1} \leq x \leq x_j$,

$$y''(x) = M_{j-1} \frac{x_j - x}{h_j} + M_j \frac{x - x_{j-1}}{h_j} \quad , \quad h_j = x_j - x_{j-1} \tag{H.1}$$

Integrating twice we have

$$y'(x) = - M_{j-1} \frac{(x_j - x)^2}{2h_j} + M_j \frac{(x - x_{j-1})^2}{2h_j} + c_j \tag{H.2}$$

$$y(x) = M_{j-1} \frac{(x_j - x)^3}{6h_j} + M_j \frac{(x - x_{j-1})^3}{6h_j} + c_j(x - x_{j-1}) + D_j \tag{H.3}$$

Now $y(x_{j-1}) = f_{j-1}$, $y(x_j) = f_j$, so that we may determine c_j and D_j from

$$f_{j-1} = M_{j-1} \frac{h_j^2}{6} + D_j$$

$$f_j = M_j \frac{h_j^2}{6} + c_j h_j + D_j$$

We obtain

$$C_j = \frac{f_j - f_{j-1}}{h_j} + (M_j - M_{j-1}) \frac{h_j}{6}$$

$$D_j = f_{j-1} - M_{j-1} \frac{h_j^2}{6}$$

Thus

$$\left.\begin{aligned} y(x) = {} & M_{j-1} \frac{(x_j - x)^3}{6h_j} + M_j \frac{(x - x_{j-1})^3}{6h_j} + \left(f_{j-1} - \frac{M_{j-1} h_j^2}{6}\right) \frac{x_j - x}{h_j} \\ & + \left(f_j - \frac{M_j h_j^2}{6}\right) \frac{x - x_{j-1}}{h_j} \end{aligned}\right\} \quad (H.4)$$

$$y'(x) = -M_{j-1} \frac{(x_j - x)^2}{2h_j} + M_j \frac{(x - x_{j-1})^2}{2h_j} + \frac{f_j - f_{j-1}}{h_j} - \frac{M_j - M_{j-1}}{6} h_j \quad (H.5)$$

The quantities $M_0, M_1, \ldots, M_n$ are as yet unknown. Our choice of representation of $y''(x)$ in (H.1) has insured the overall continuity of $y''(x)$. The continuity of $y(x)$ is similarly insured by the choice of constants in (H.3). To make $y'(x)$ continuous, we require at each $j (j = 1, 2, \ldots, n-1)$ that

$$y'(x_j-) = y'(x_j+) \quad (H.6)$$

From (H.5) we have

$$\begin{aligned} y'(x_j-) &= M_j \frac{h_j}{2} + \frac{f_j - f_{j-1}}{h_j} - \frac{M_j - M_{j-1}}{6} h_j \\ &= M_j \frac{h_j}{3} + M_{j-1} \frac{h_j}{6} + \frac{f_j - f_{j-1}}{h_j} \end{aligned} \quad (H.7)$$

Using (H.4) for the $(j+1)$st interval and setting $x = x_j$ gives

$$y'(x_j+) = -M_j \frac{h_{j+1}}{2} + \frac{f_{j+1}-f_j}{h_{j+1}} - \frac{M_{j+1}-M_j}{6} h_{j+1} \tag{H.8}$$

$$= \frac{f_{j+1}-f_j}{h_{j+1}} - M_j \frac{h_{j+1}}{3} - M_{j+1} \frac{h_{j+1}}{6} .$$

Equation (H.6) now gives ($j = 1, 2, \ldots, n-1$)

$$\frac{h_j}{6} M_{j-1} + \frac{h_j+h_{j+1}}{3} M_j + \frac{h_{j+1}}{6} M_{j+1} = \frac{f_{j+1}-f_j}{h_{j+1}} - \frac{f_j-f_{j-1}}{h_j}$$

We divide by $\frac{h_j+h_{j+1}}{6}$, set $\lambda_j = \frac{h_{j+1}}{h_j+h_{j+1}}$, $\mu_j = 1 - \lambda_j$, and we obtain

$$\mu_j M_{j-1} + 2M_j + \lambda_j M_{j+1} = 6 \frac{\frac{f_{j+1}-f_j}{h_{j+1}} - \frac{f_j-f_{j-1}}{h_j}}{h_j + h_{j+1}} \tag{H.9}$$

$$= 6 \left[f_{j-1}, f_j, f_{j+1}\right]$$

We obtain in this way n-1 equations to be satisfied by the n+1 unknowns $M_0, M_1, \ldots, M_n$. Two more conditions, the <u>end conditions</u>, are to be specified. We remark that setting $M_0 = M_n = 0$ is equivalent to putting simple supports at the ends. More generally

$$M_0 - \theta M_1 = 0, \qquad 1 > \theta > 0, \tag{H.10}$$

is equivalent to placing a simple support at a location $x_{-1} = (x_0 - \theta x_1)(1-\theta)$ and requiring that the entire curve over (x_{-1}, x_1) be the arc of a cubic passing through (x_0, f_0). A common choice of θ is 1/2, in which case $x_0 - x_{-1} = x_1 - x_0$. Choosing $\theta = 1$ gives a parabolic runout of the spline to the left of $x = x_1$.

We may wish instead to specify the slope at the end of the curve. From (H.8) and (H.7),

$$\left.\begin{aligned} y'(x_0) &= \frac{f_1-f_0}{h_1} - M_0\frac{h_1}{3} - M_1\frac{h_1}{6}\ , \\ y'(x_n) &= \frac{f_n-f_{n-1}}{h_n} + M_n\frac{h_n}{3} + M_{n-1}\frac{h_n}{6}\ . \end{aligned}\right\} \qquad \text{(H.11)}$$

Thus, in general, we employ the end conditions

$$\left.\begin{aligned} 2M_0 + \lambda_0 M_1 &= d_0, \\ \mu_n M_{n-1} + 2M_n &= d_n\ , \end{aligned}\right\} \qquad \text{(H.12)}$$

where condition (H.10) is met by taking $\lambda_0 = -2\theta$, $d_0 = 0$ and (H.11) by setting $\lambda_0 = 1$, $d_0 = \frac{6}{h_1}\left(\frac{f_1-f_0}{h_1} - f_0'\right)$ (Here f_0' is used to indicate $y(x_0')$).

The condition

$$M_n = \theta M_{n-1}$$

is satisfied by taking $\mu_n = -2\theta$, $d_n = 0$ while (H.11) is satisfied with $\mu_n = 1$. $d_n = \frac{6}{h_n}\left(f_n' - \frac{f_n-f_{n-1}}{h_n}\right)$.

Once the conditions (H.12) have been chosen, we must solve the simultaneous system of equations

$$\begin{aligned}
2M_0 + \lambda_0 M_1 \qquad\qquad\qquad\qquad &= d_0 \\
\mu_1 M_0 + 2M_1 + \lambda_1 M_2 \qquad\qquad &= d_1 \\
\mu_2 M_1 + 2M_2 + \lambda_2 M_3 \qquad &= d_2 \\
&\ \ \vdots \\
\mu_{n-1} M_{n-2} + 2M_{n-1} + \lambda_{n-1} M_n &= d_{n-1} \\
\mu_n M_{n-1} + 2M_n &= d_n
\end{aligned}$$

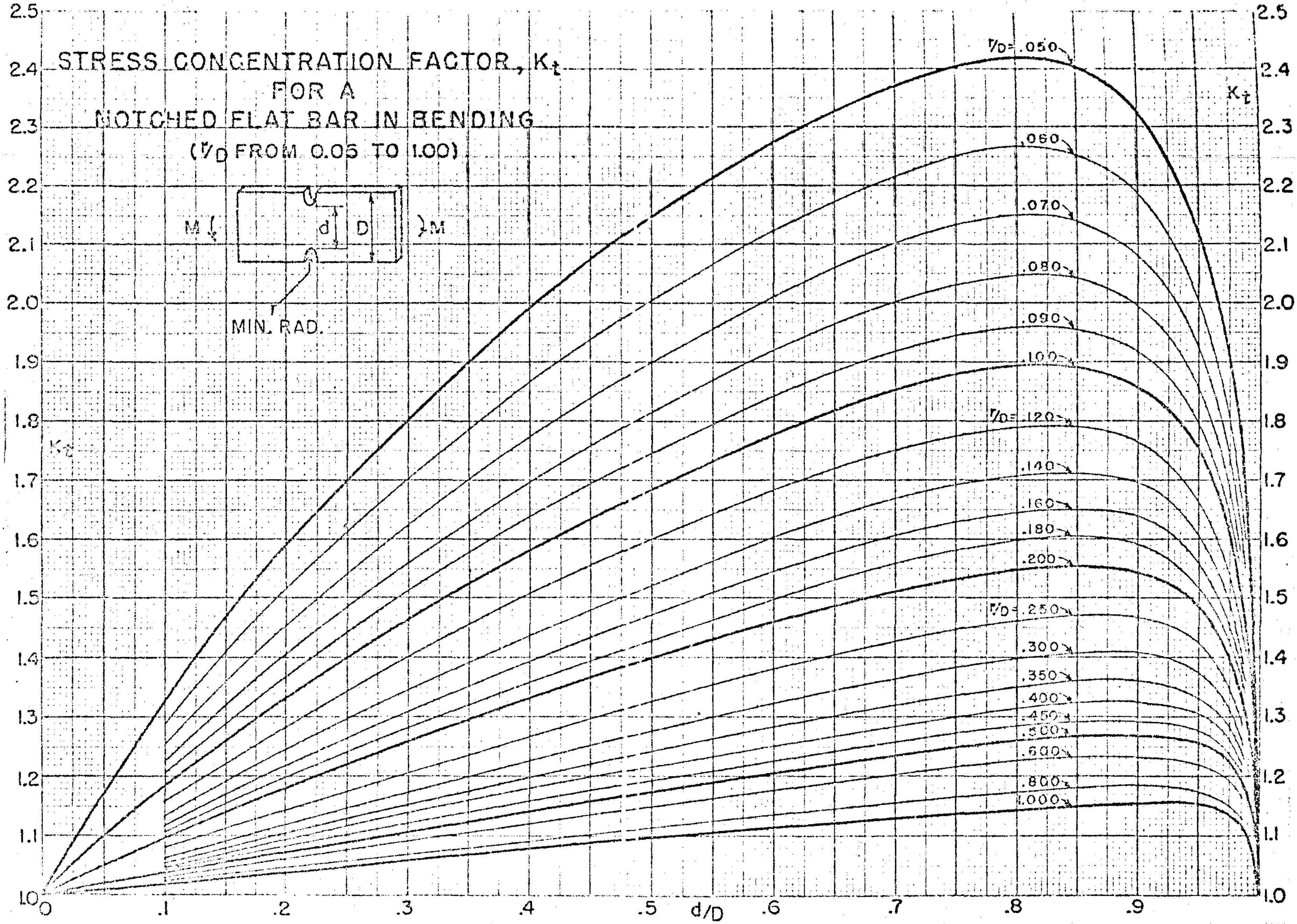
STRESS CONCENTRATION FACTOR, Kt
FOR A
NOTCHED FLAT BAR IN BENDING
(r/D FROM 0.05 TO 1.00)
M
d
D
M
r
MIN. RAD.
Kt
r/D = .050
.060
.070
.080
.090
.100
r/D = .120
.140
.160
.180
.200
r/D = .250
.300
.350
.400
.450
.500
.600
.800
1.000
d/D
0
.1
.2
.3
.4
.5
.6
.7
.8
.9
1.0
1.1
1.2
1.3
1.4
1.5
1.6
1.7
1.8
1.9
2.0
2.1
2.2
2.3
2.4
2.5

APPENDIX J

CHARACTERISTICS OF DIAMOND CIRCULAR SAW BLADES

J.1. Description of Diamond Circular Saws:

The diameters of the saw blades vary from 250 mm to about 3 metres. The hub or body of the saw is usually made of a tool steel, hardened to around 42-44 Rockwell Hardness. Radial slots are located on the periphery at equi-angular intervals. Diamond impregnated segments or tips are attached to the saw between the slots. The diamond segments are made from a variety of materials ranging from bronze to tungsten carbide. The thickness of the diamond segment is greater than the hub to maintain clearance in the cut. The relative length of segment to slot varies greatly. The saw is held firmly by large flanges or 'cheek plates' having diameters equal to 1/3 saw diameter to prevent lateral vibration of the saw.

There is no basic difference between the cutting actions of a slotted saw and a continuous periphery saw. The slots serve other important purposes:

(i) The slots aid in the removal of chips during cutting. They prevent loading of the diamond cutting edges.

(ii) The slots provide a larger cooling area and are responsible for introducing lubricant into the cutting region.

(iii) Having the slots facilitates manufacture of diamond tips. A continuous periphery saw has obvious difficulties.

(iv) The slots prevent the distortion of the hub during the brazing of the diamond tips on the hub.

At present, a narrow slot with parallel sides and a simple semi-circular base is preferred. Basically, slots should be as wide as possible, but a point is reached where rigidity is lost. Thus, where poor machines are encountered, narrow slots are preferred.

J.2. Cutting Parameters:

After choosing a blade for a stone cutting operation, the curring parameters are usually chosen according to manufacturers standards. Typical cutting speeds for some types of stone are given below,

Soft Alluvial, soft sandstone	10,000 ft/min
Medium limestone, marble	8,000 ft/min
Harder marbles, soft granite	7,000 ft/min
Harder granites and sandstones	6,000 ft/min
Basalt, quartz	5,000 ft/min

It is seen that high rotational speeds are required for soft stones.

Maximum possible depths of cut are usually taken. The limit is either flange diameter of block size except on hard stones, where cutting forces could be so high that the depth of cut has to be restricted below 3 inches. Feed rate depends on bond wear rate and machine horsepower. The trend, however, is for high cutting rates and some normally accepted figures are:

Quartz	10 sq in/min
Granite	20 sq in/min
Marble	100 sq in/min
Soft limestone	100 sq in/min

where the figures denote the product of feed rate and depth of cut.

J.3. Cutting Machine:

Circular diamond saws are used either singly or mounted in gangs. There are numerous machines on the market of all shapes and sizes, ranging from small hand operated machines (with loading through the spindle) to large multiple-blade orthogonal stone-cutting machines. Because of the high cost of diamond blades, these machines are of high quality.

J.4. Cutting Mechanism:

At this time there is no clear answer to the cutting mechanism for stone. There is no doubt, however, that a single diamond grit operating on a known area must exert an indentation force on the individual grains of the stone, greater than the crushing strength of that grain, in order to abrade the stone. The detrities or chip is then pushed away be oncoming grains. In sedimentary rocks it is usually sufficient to exert a force equal to the cementing compound strength only, which is usually considerably less than the crushing strength of individual grains. A typical example is sandstone. Here the grains remain whole after being dislodged and are particularly strong; they then act as an abrasive on both the diamond and the bond.

The maximum crushing strength encountered in rocks (quartz) is about 85,000 lb/in^2. The average area presented by one particle of 35/40 U.S. mesh diamond grit would be 0.032 mm^2 and the specific force required by this particle would be 4 lb. There would be about 1200 particles per carat or about 700 per square inch, thus giving over 1 ton/in^2 of segment contact. The crushing strength of diamond is about 1,250,000 lb/in^2, so the diamond would normally only be damaged by a specific force of 60 lb.

Grit damage on weak edges occurs much earlier and controlled breakdown of the grit when matched to the cutting rate decides grit selection.

For abrasive materials which are otherwise soft, the high strength grit is unnecessary but thermal stability is essential, whereas for high strength materials high grit strength and good shaped crystals are required.

The cutting forces increase with the diamond grit breakdown and they are proportional to power consumption. Adverse vibrations quickly change the desired conditions and are a prime cause of diamond grit failure.